Photoaging and Fibroblasts:

The Role of a Novel Dermal Fibroblast Population in Tissue Regeneration and the Response to Solar Radiation

Inaugural dissertation

for the attainment of the title of doctor
in the Faculty of Mathematics and Natural Sciences
at the Heinrich Heine University Düsseldorf

presented by

Katharina Janke

from Stuttgart

Düsseldorf, May 2022

from the IUF – Leibniz Research Institute for Environmental Medicine

at the Heinrich Heine University Düsseldorf

Published by permission of the

Faculty of Mathematics and Natural Sciences at

Heinrich Heine University Düsseldorf

Supervisor: Prof. Dr. rer. nat. Petra Boukamp

Co-supervisor: Jun.-Prof. Dr. rer. nat. Mathias Beller

Date of the oral examination: 08.08.2022

Science is part of the reality of living;

it is the what, the how, and the why

of everything in our experience.

*Rachel Carson (*1907– †1964, biologist)*

Acknowledgement

Dies ist die letzte Seite, die ich für meine Dissertation schreibe und damit das Ende einer aufregenden, lehrreichen, teilweise schwierigen und tränenreichen, aber auch schönen und inspirierenden Reise. An dieser Stelle möchte ich einigen Menschen danken, die mich in den letzten fünf Jahren auf meinem Weg begleitet haben.

Zuerst möchte ich mich bei Prof. Dr. Petra Boukamp für die Betreuung meiner Promotion bedanken. Danke Petra für dein stets offenes Ohr, die bereichernden Diskussionen, die ab und zu nötige Bestärkung und nicht zuletzt deine Leidenschaft für die Forschung, die ich sehr schätze.

Mein Dank geht außerdem an Jun.-Prof. Dr. Mathias Beller für die Bereitschaft meine Arbeit zu begutachten und die Rolle als Mentor zu übernehmen.

My heartfelt thanks go to my "inofficial" supervisor Dr. Elizabeth Pavez Loriè. Ely, thank you so much for all your support, for everything you taught me in the lab, and for our inspiring discussions about research and life. You made me a better scientist and I am grateful for having you with me during this journey, as a mentor and a friend.

Ein weiteres Dankeschön geht an unsere KAUVIR Projektpartner in Buxtehude und Darmstadt, Dr. Rüdiger Greinert, Dr. Beate Volkmer, Dr. Alexander Rapp und ihre Teams. Danke, dass ihr mich so herzlich in die „KAUVIR Familie" aufgenommen habt. Es war mir eine Freude mit euch zu arbeiten.

Besonders bedanken möchte ich mich bei Kollegen und Kooperationspartnern, die mir mit ihrer Expertise und tatkräftigen Unterstützung bei den Experimenten dieser Doktorarbeit behilflich waren: Dr. Hans-Jürgen Stark für seine Hilfe mit diversen Färbungen, Dr. Daniel Gorski für seine Unterstützung bei den Hyaluronsäure-Färbungen, Johannes Ptok für seine unschätzbare Hilfe bei der Auswertung meiner RNA-Sequenzierungsdaten und seine Geduld bei all meinen Nachfragen, Dr. Paul Hiebert für die erfolgreiche Zusammenarbeit für eine Publikation, Dr. Nadine Teichweyde für ihre Unterstützung bei der FACS Analyse, Christin Starzonek für ihre Betreuung bei meinem Besuch in Buxtehude, Dr. Sarah Degenhardt für ihre Hilfe mit der CPD Detektion und Dr. Lars Vierkotten und Nelli Blasius von der Henkel AG für die Möglichkeit die TEWL Messungen bei ihnen durchzuführen. Außerdem ein großer Dank an Prof. Dr. Jojo Händeler und PD Dr. Joachim Altschmied für die Unterstützung in Promotionsfragen.

Ein herzliches Danke geht außerdem an meine großartigen Kolleginnen und Kollegen Dr. Philipp Worst, Jessica Nagel, Ximena Riscanevo, Armin Ardeshirdavani und Mbaboh Ngah-Wanneh, die mich alle ein Stück auf meiner Reise begleitet haben. Danke für die gute Zeit im Labor oder bei Kaffee und Kuchen, thanks guys! Ganz besonders an dich, Philipp, vielen Dank, dass du mich am IUF so herzlich willkommen geheißen und mir alles gezeigt hast.

Danken möchte ich außerdem meinen Freunden außerhalb des Labors, für die schöne Ablenkung von der Arbeit und den manchmal nötigen Trost und Zuspruch. Ganz besonders dir, Sascha, vielen Dank für unzählige gemeinsame Kaffeepausen, die mir so oft den Tag verschönert haben, wenn im Labor mal wieder alles schief ging.

Mein persönlicher Dank aus tiefstem Herzen geht an meine Familie. Danke, dass ihr immer für mich da seid und ich auf euch zählen kann, in allen Höhen und Tiefen. Die Zeit mit euch ist unglaublich wertvoll für mich. Mama, du bist mein Fels in der Brandung und ohne dich hätte ich dieses Werk hier nie zu Ende gebracht – danke für alles.

Zusammenfassung

Die sonnenbedingte Hautalterung, auch Photoalterung genannt, ist ein komplexer Prozess, der trotz jahrzehntelanger Forschung immer noch nicht vollständig verstanden ist. Da Hautalterung mehr als nur ein kosmetisches Problem darstellt, sondern mit zahlreichen gesundheitlichen Risiken verbunden ist, ist das Verständnis der zugrundeliegenden Mechanismen essenziell. In den letzten Jahren wurde deutlich, dass die dermalen Fibroblasten eine entscheidende Rolle spielen und durch die Veränderung ihrer Umgebung zum Alterungsprozess beitragen.

Wir haben einen bisher unbeschriebenen Subtyp "alter" Fibroblasten identifiziert, der aus sonnenexponierter Haut älterer Spender isoliert wurde. Dieser steht in Verbindung mit chronischen Sonnenschäden (solare Elastose) und zeichnet sich durch eine sehr spezifische myochondrozyten-ähnliche Differenzierung aus. Um die Rolle dieser Fibroblasten für die Gewebemorphologie und -regeneration zu untersuchen, etablierten wir hochempfindliche organotypische Kulturmodelle (Age-SEs). Mit diesen konnte bestätigt werden, dass die alten Fibroblasten ein sehr spezifisches dermales Äquivalent bilden, das durch chondrozytenartige Matrixproteine und eine hohe Anzahl von Myofibroblasten gekennzeichnet ist. Darüber hinaus wiesen die alten Fibroblasten ein deutliches Defizit bei der Unterstützung der epidermalen Regeneration und Differenzierung auf, was zu einer beschleunigten epidermalen Atrophie führte, während die gleichen Keratinozyten von jungen Fibroblasten gut unterstützt wurden. Ein invasives Wachstum der Keratinozyten wurde nicht beobachtet, was zeigt, dass diese alten Fibroblasten nicht tumorfördernd sind.

Um die Rolle der Sonnenstrahlung für die Entwicklung und Funktion der alten Fibroblasten zu untersuchen, wurden Age-SEs einer chronischen Bestrahlung (1 MED, 3x/Woche für 2 bis 4 Wochen) mit einem neu entwickelten Bestrahlungsgerät ausgesetzt, das es ermöglichte, die SEs gleichzeitig entweder mit solarer UV-Strahlung (UVA+B) oder dem gesamten Sonnenspektrum (UVA+UVB+VIS+IRA) zu bestrahlen. Die Bestrahlung bewirkte eine transkriptionelle Herunterregulierung der Gene des Myofibroblasten-Typs in den alten Fibroblasten, verbunden mit einer signifikanten Verringerung der Anzahl der α-SMA+-Zellen. Interessanterweise korrelierte dieser Verlust mit einer Normalisierung des Gewebes und einer verbesserten epidermalen Regeneration, was darauf hindeutet, dass nicht die alten Fibroblasten an sich, sondern die Myofibroblasten die dermal-epidermale Interaktion stören, die für die epidermale Unterstützung erforderlich ist, und dass die UV-induzierte Dedifferenzierung diese Interaktion wiederherstellt. Genexpressionsanalysen sprachen für eine, wenn auch indirekte, Rolle der Strahlung auch für den chondrozyten-ähnlichen Phänotyp und die Induktion der Knorpelmatrix, allerdings wahrscheinlich durch eine indirekte Regulierung. Daher schlagen wir vor, dass die chondrogene Transdifferenzierung ein sich schrittweise entwickelnder Prozess ist, der erst durch langfristige, wiederholte Sonnenexposition und Gewebeschädigung entsteht.

In Age-SEs mit transformierten, (prä-)malignen Keratinozyten zeigte sich, dass die chronische Bestrahlung mit niedriger Dosis kein invasives Wachstum dieser Keratinozyten auslöste oder verstärkte. Zusammengenommen deuten diese Daten darauf hin, dass neben dem bekannten schädlichen Potenzial übermäßiger Sonnenexposition niedrig dosierte UV- oder Sonnenstrahlung sogar vorteilhaft sein und zu einer normalen Hautfunktion beitragen kann, insbesondere bei photogealterter Haut, ohne dabei die Tumorentstehung zu fördern.

Darüber hinaus zeigte die vergleichende Genexpressionsanalyse von Fibroblasten, die aus bestrahlten Age-SEs isoliert wurden, ein sehr unterschiedliches Reaktionsprofil der jungen und alten Fibroblasten. Dies deutet darauf hin, dass die Reaktion auf Strahlung weitgehend vom Status der Fibroblasten abhängt und dementsprechend auch in der Haut *in situ* variieren kann. Außerdem konnten wir zum ersten Mal zeigen, dass das solare UV-Spektrum allein andere Genregulationen auslöst als das kombinierte Sonnenspektrum. Diese vergleichenden Studien könnten daher möglicherweise neue Erkenntnisse darüber liefern, wie sich die Sonnenexposition im Alltag tatsächlich auf die humane Haut auswirkt, und damit zu einer besseren Grundlage für künftige Risikobewertungen und Empfehlungen für die öffentliche Gesundheit beitragen.

Summary

Sun-induced skin aging, or photoaging, is a complex process that, despite decades of research, is still not fully understood. As skin aging is more than just a cosmetic problem but associated with numerous health risks, it is important to elucidate the underlying mechanisms. In recent years, it became evident that the dermal fibroblasts play a decisive role and interest increased in how they modulate their environment during aging.

We recently identified a yet undescribed subtype of “old” fibroblasts isolated from sun-exposed skin of elderly donors that was connected to sites of chronic sun damage (solar elastosis) and characterized by a very specific myo-chondrocyte-type differentiation. To address their role for tissue morphology and regeneration, we established highly sensitive organotypic culture models (Age-SEs). With these it could be confirmed that the old fibroblasts develop a very specific dermal equivalent, characterized by chondrocyte-type matrix proteins and a high number of myofibroblasts. Moreover, the old fibroblasts exhibited a severe deficit in supporting epidermal regeneration and differentiation, leading to accelerated epidermal atrophy, whereas the same keratinocytes were well supported by young fibroblasts. Invasive growth of the keratinocytes was not observed, demonstrating that these old fibroblasts are not tumor-promoting.

To investigate the role of solar radiation for the development and function of the old fibroblasts, Age-SEs were exposed to chronic irradiation (1 MED, 3x/week for 2 to 4 weeks) with a newly developed radiation device, allowing to simultaneously irradiate the SEs with either solar UV radiation (UVA+B) or the entire solar spectrum (UVA+UVB+VIS+IRA). Irradiation caused transcriptional downregulation of the myofibroblast-type genes in the old fibroblasts, associated with a significant reduction in the number of α-SMA+ cells. Intriguingly, this loss correlated with tissue normalization and improved epidermal regeneration, suggesting that not the old fibroblasts *per se* but the myofibroblasts interfere with the dermal-epidermal interaction required for proper epidermal support and UV-induced dedifferentiation restored this interaction. Gene expression analyses argued for a role of radiation also for the chondrocyte-like phenotype and the induction of the cartilage matrix, though likely through indirect regulation. Thus, we propose that the chondrogenic transdifferentiation is a gradually developing process that emerges with long-term recurrent sun exposure and tissue damage.

Complementing Age-SEs with transformed, (pre-)malignant keratinocytes demonstrated that the low dose chronic irradiation did not provoke or increase invasion of these keratinocytes. Together, these data suggests that besides the well-established damaging potential of excessive sun exposure, low dose UV or solar radiation might even be beneficial and contribute to normal skin function, particularly in photoaged skin, without necessarily promoting tumorigenesis.

Besides that, the comparative gene expression analysis from fibroblasts isolated from irradiated Age-SEs, demonstrated a highly different response profile of young and old fibroblasts. This implies that the response to radiation is largely dependent on the status of the fibroblasts and may vary accordingly also in the skin *in situ*. Even more so and shown for the first time, the solar UV spectrum alone triggers different regulatory responses than the combined solar spectrum. Our comparative studies could therefore offer new insights into how sun exposure affects the skin in everyday life, providing a better basis for future risk assessments and public health recommendations.

Table of Content

1 Introduction

1.1 Human Skin

The skin is the largest organ of the human body, providing both protection from and sensory perception of our external environment. It helps regulate body temperature and loss of water and forms a protective barrier against mechanical insults, hazardous substances, microbial invasion, and radiation. Its complex tissue organization, with different compartments and layers (Fig. 1) that interact and communicate with each other, make it possible to fulfill all these varied tasks.

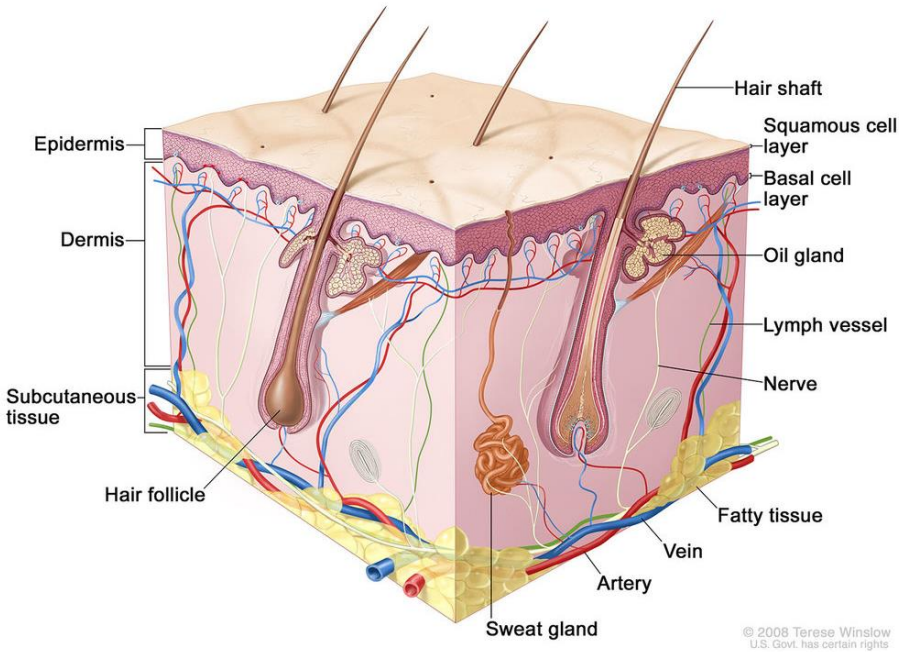

Figure 1: Anatomy of human skin
With permission from the National Cancer Institute © (2021) Terese Winslow LLC, U.S. Govt. has certain rights

1.1.1 The Epidermis

The outermost part of the skin is the epidermis, a stratified squamous epithelium that is in a constant process of regeneration and arranged in four layers: the basal layer (*stratum basale*), the spinous layer (*stratum spinosum*), the granular layer (*stratum granulosum*), and the cornified layer (*stratum corneum*), which are depicted in Figure 2 (Urmacher 1990). The epidermis contains different cell types, including melanocytes (pigment-producing cell) and Langerhans cells (skin specific immune cells), but the most abundant cell type in the epidermis is the keratinocyte, that

make up for more than 90% of epidermal cell mass (Eckert and Rorke 1989). All keratinocytes originate from epidermal stem cells residing in the basal layer. Stem cells give rise to transit amplifying cells that undergo a few rounds of cell division before they switch to terminal differentiation (Watt 2002). During this process they move upwards, from the basal layer to the cornified layer, expressing distinct proteins at each differentiation stage. On their way to the surface, they change morphology, initiate the accumulation of keratin filaments (keratinization) and finally lose their nuclei and cytoplasmic organelles and become terminally differentiated corneocytes. In corneocytes the plasma membrane is replaced by a cornified envelope, a protein shell, including loricrin, involucrin, and filaggrin. These flattened dead cells form the stratum corneum and are eventually shed from the skin's surface during desquamation. The estimated epidermal turnover time, i.e. the time it takes for the epidermis to renew itself from generating keratinocytes at the basal layer until they are sloughed off as corneocytes, is about one month (Houben, De Paepe, and Rogiers 2007). This renewal slows down with age (Grove and Kligman 1983).

The *stratum corneum* (SC) is the primary source of the skin´s barrier function and it is based on two structural components: the corneocytes and the intercellular lipids. In 1983 Elias proposed the "brick and mortar model" (Elias 1983), according to which the SC is composed of cells (bricks) surrounded by a lipid matrix (mortar), mainly composed of ceramides, free fatty acids, and cholesterols (Pouillot et al. 2008). Adhesion between corneocytes is mediated by corneodesmosomes, which are cleaved eventually to allow desquamation. The structure of the SC, especially the lipid content, provides a permeability barrier that prevents dehydration by controlling water loss to the external environment (Ananthapadmanabhan, Mukherjee, and Chandar 2013; Norlen et al. 1998).

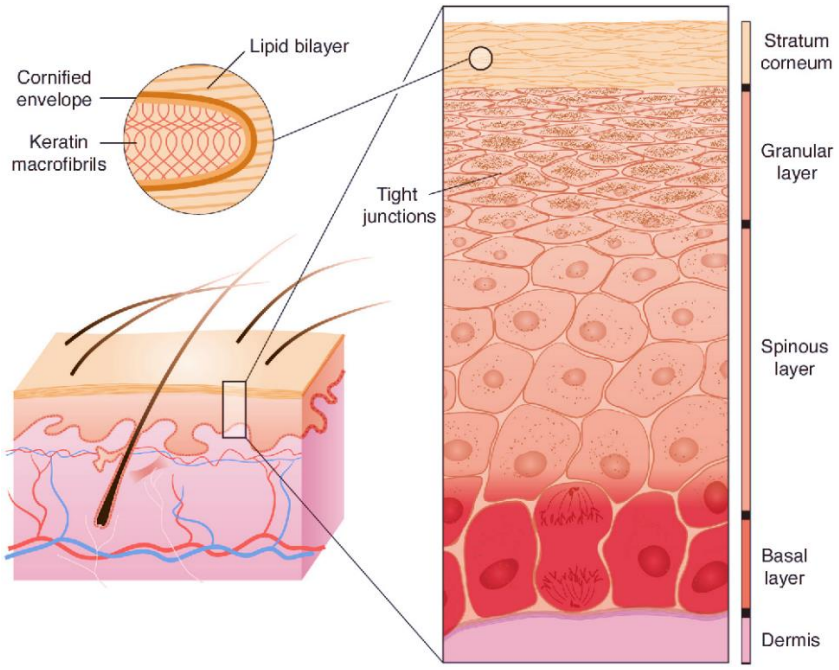

Figure 2: Schematic structure of the epidermis
Epidermal keratinocytes undergo different stages of differentiation from the mitotically active basal layer to the cornified stratum corneum. Shown in the inset are terminally differentiated corneocytes, that are to a large extent composed of keratin filaments and a cornified envelope. Encased in lipid bilayers, they provide the skin barrier. Taken from (Segre 2006).

1.1.2 The Basement Membrane

The epidermis is connected to the underlying dermis by a complex and specialized network of extracellular matrix (ECM) molecules, the dermal-epidermal junction (DEJ) or basement membrane (BM) zone (Fig.3). This zone displays a distinctive microarchitecture characterized by an undulating pattern created by epidermal extensions, the so-called rete ridges, increasing the surface area of the DEJ (Roig-Rosello and Rousselle 2020). The BM provides adhesion and resistance to shearing forces, serves as a diffusion barrier, but also allows for dermal-epidermal crosstalk. Mutation in BM-associated genes usually lead to severe or lethal blistering diseases (Aumailley et al. 2006). Ultrastructurally, the BM can be subdivided in two layers: the *lamina lucida*, made up of mainly laminins and integrins, and the *lamina densa*, consisting of a collagen type IV and VII network. The keratinocytes are attached to the BM by special multiprotein structures, the hemidesmosomes, and the underlying dermal tissue is tethered to the BM by the anchoring fibrils of collagen type VII that are connected to other collagen fibrils (including collagen type I and III) (Paulsson 1992; Breitkreutz et al. 2013).

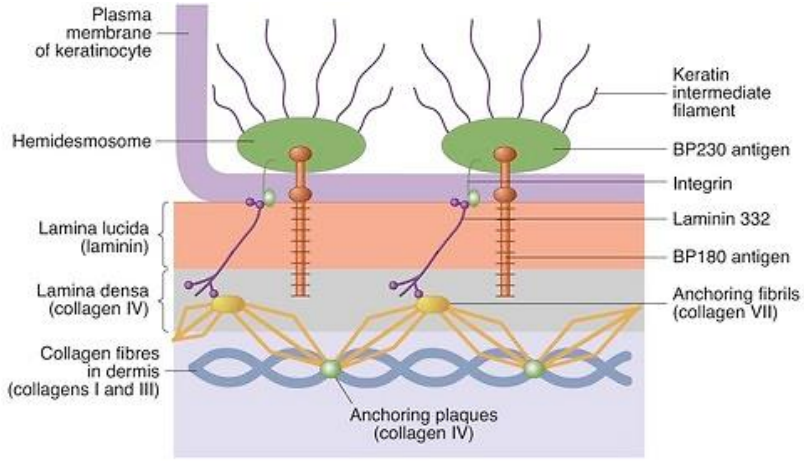

Figure 3: Detailed view of the basement membrane zone at the dermal-epidermal junction
The dermal-epidermal junction is a specialized structure which binds epidermis to dermis. The major components are illustrated in the Figure. The lamina lucida is traversed by filaments connecting the basal cells with the lamina densa, from which anchoring fibrils (collagen type VII) extend into the papillary dermis and reach the dermal fibrillar collagen meshwork (collagen type I and III). Taken from: https://plasticsurgerykey.com/microanatomy-of-the-skin

1.1.3 The Dermis

The dermis is the second layer of the skin and comprises mainly a dense connective tissue giving the skin its tensile strength and elastic properties. It is divided into two layers: the more superficial and thinner papillary dermis, which is connected to the BM, composed of loose connective tissue and highly vascularized, and the thicker underlying reticular dermis with dense irregular connective tissue. A schematic overview of the cellular and extracellular components of the dermis is given in Figure 4.

The main resident cell type of the dermis is the dermal fibroblast. Fibroblasts are essential for the function of the dermis as they produce, regulate, and maintain the dermal ECM and communicate with each other and other cell types, particularly the epidermal keratinocytes, thus also influencing processes in the epidermis. Fibroblasts play a crucial role in skin aging and cutaneous wound repair (Thulabandu, Chen, and Atit 2018; Darby et al. 2014; Tigges et al. 2014).

In the past decades, it has become more and more obvious that the dermal ECM is more than just an inactive substance providing structural support, but that the distinct network of components also plays a crucial role for the physiological function of the skin. The ECM consists of collagen, elastic fibers, glycosaminoglycans such as hyaluronic acid, proteoglycans, and glycoproteins. The major constituent is a network of collagen fibers, accounting for 90 % of the dry weight of skin,

where collagen type I (ColI) and collagen type III (ColIII) are the predominant structural components (Uitto 1986) .

Collagen is the single most abundant protein in the animal kingdom and since the discovery of the molecular structure of the first collagen in the 1930s the collagen superfamily grew to 28 members as of today (Ricard-Blum 2011). Collagen molecules are composed of three amino acid chains that are connected in a triple helix. Collagen precursor molecules (procollagen) are synthesized and secreted by dermal fibroblasts. They undergo several post-translational modifications and are ultimately arranged in fibers (fibrillar collagens e.g. ColI) or in sheets or networks (non-fibrillar collagens e.g. ColIV). Cells as well as other components of the ECM like proteoglycans and glycoproteins are able to bind to collagen molecules.

The dermis also contains other structures such as blood vessels, hair follicles, sebaceous glands, sweat glands and nerve endings, that are crucial for providing the skin with nutrients, immune response, lubricants (sebum), pH and temperature regulation and sensory stimuli like touch, pressure or pain, maintaining a healthy organ.

The underlying subcutaneous tissue, also named subcutis or hypodermis, mainly consists of fat and provides nutrient supply for the other layers, cushions and insulates the body.

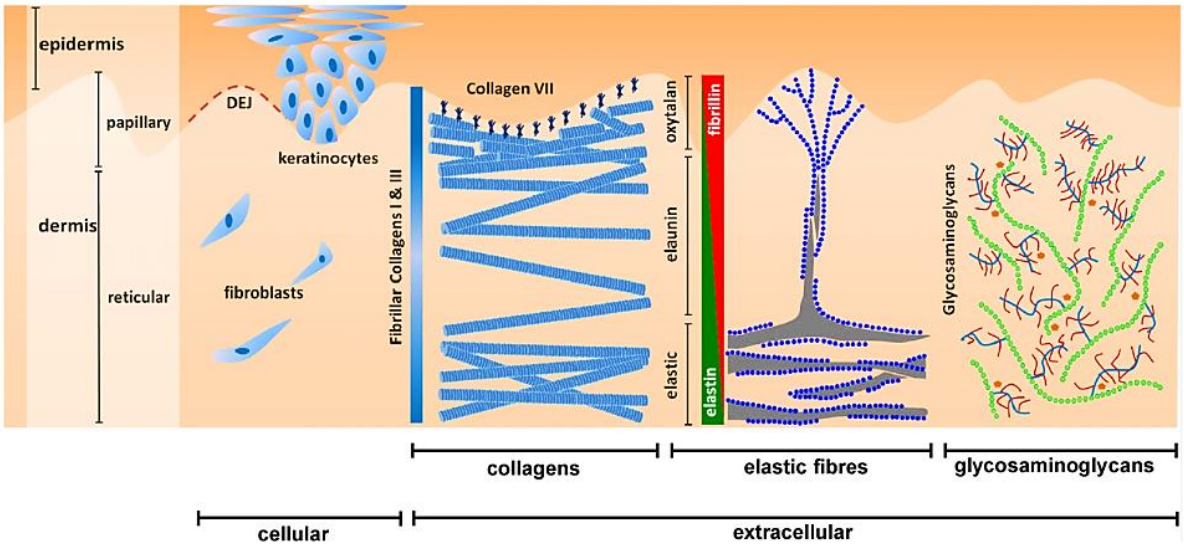

Figure 4: Schematic overview of cellular and extracellular components of the (young) dermis
The dermal fibroblasts are mainly responsible for synthesizing the ECM that is composed of collagens, elastic fibers and glycosaminoglycans. The predominant structural collagens (I and III) are particularly abundant in the papillary and deep reticular dermis. The elastic fiber system has a characteristic architecture with perpendicular oriented fibrillin microfibrils in the papillary dermis that merge with the elastin-rich elastic fibers in the reticular dermis. The skin hydration is provided by glycosaminoglycans, such as hyaluronic acid, which are distributed throughout the dermis. Taken from (Naylor, Watson, and Sherratt 2011).

1.2 Skin Aging

Aging is a complex biological process affecting all organs. Being the outmost organ of the body, the skin is exposed to numerous environmental factors that affect structure and function of the skin and influence the aging process. Skin aging is also the most visible form of the passing of years, playing an important role in our perception of health and youth. This process can be classified in two categories: intrinsic and extrinsic aging, which will be described in the following chapter.

1.2.1 Intrinsic and Extrinsic Skin Aging

Intrinsic or chronological aging is the inevitable process that naturally occurs over time and is largely determined by genetics. Gene mutations and changes in cell metabolism as well as hormonal balance (for example decline of estrogens and progesterone associated with menopause in women) are intrinsic aging factors (Makrantonaki and Zouboulis 2007). Characteristic clinical manifestations of intrinsically aged skin are for example fine wrinkles, dryness, and laxity. Histological features include flattening of the dermal-epidermal junction, i.e. the loss of rete ridge structures, and with that reduction of the contact area between epidermis and dermis (Moragas, Castells, and Sans 1993), resulting in less resistance to shearing forces, and a gradual dermal atrophy (Smith 1989; Lavker, Zheng, and Dong 1986).

Extrinsic skin aging comprises changes that are superimposed to intrinsic skin aging as a result of environmental influences. Factors driving this process are to varying degree controllable and include exposure to air pollution, smoking, nutrition, or lifestyle habits. But the most important factor is the lifelong cumulative exposure to solar ultraviolet (UV) radiation, thus it is usually referred to as photoaging (Farage et al. 2008). Consequently, extrinsically aged skin appears on normally sun-exposed parts of the body such as face, décolleté, forearm, or the back of the hands. The typical clinical picture of photoaged skin is defined by coarse wrinkles, a rough and uneven texture, mottled pigmentation and emergence of solar lentigines (age spots), telangiectasis (dilated or broken capillaries), laxity and loss of elasticity (Takema et al. 1994). In contrast to intrinsically aged skin, which shows a rather atrophic phenotype, extrinsic aging is often correlated with thickening of almost all layers of the skin, although for epidermal thickening controversial results are described (Berneburg, Plettenberg, and Krutmann 2000; Hughes et al. 2011; Yaar and Gilchrest 2001). Furthermore, this is accompanied by reduced proliferative capacity of the keratinocytes and aberrant epidermal differentiation (Yaar and Gilchrest 2001). Even more than

in intrinsically aged skin, the DEJ appears flattened and is further destabilized by a reduction in collagen type VII, the main component of the anchoring fibrils (Craven et al. 1997).

The photoaging process affects all parts of the skin, however, the most significant changes are found in the dermis, primarily in the dermal ECM. Many matrix components are very long-lived molecules and as such are predisposed to accumulate damage and modifications. For example, the half-life of fibrillar collagen is 15 to 95 years, elastin even persists for the whole life of the organism (Naylor, Watson, and Sherratt 2011). The most prominent histological feature of photoaged skin is an abnormal aggregation of amorphous elastin material, a condition termed solar elastosis (Kligman 1969; Gilchrest 1989). In these areas, the dermal collagens are found to be degraded (Bernstein and Uitto 1996). This dermal ECM disruption, especially the degradation of collagen fibrils, is a hallmark of photoaging and believed to be one of the main causes for the aged phenotype, such as the appearance of wrinkles.

1.2.2 Mechanisms of Extrinsic Skin Aging

The clinical and histological manifestations of the aging skin reflect the underlying changes in the cells and tissue. Dermal fibroblasts are long-lived cells that rarely proliferate. Thus, different from the keratinocytes that can eliminate damage through constant shedding and renewal, they accumulate damage and (mal)adaptations over time. As the fibroblasts are mainly responsible for the production of ECM components and ECM remodeling and also provide growth factors that support epidermal maintenance and differentiation, age-dependent changes in the fibroblasts consequently lead to alterations in the epidermis.

One of the most prominent alterations in photoaged skin is the degradation of the dermal matrix. Matrix metalloproteinases (MMPs), a group of zinc-containing endopeptidases are primarily responsible for this. There are at least 23 known MMPs and they can be categorized into five main subgroups: Collagenases (e.g. MMP-1); gelatinases (e.g. MMP-9); stromelysins (e.g. MMP-3); matrilysins and membrane-type MMPs (Visse and Nagase 2003; Pittayapruek et al. 2016). MMP-1 is the major protease in skin and is responsible for initiating cleavage of type I and type III collagen and therefore particularly important for degradation of the ECM. The regulation of these enzymes happens at different levels and their activity can be inhibited by tissue inhibitors of matrix metalloproteinases (TIMPs), especially TIMP-1 and TIMP-2 (Nagase, Visse, and Murphy 2006).

Both fibroblasts and keratinocytes can secrete MMPs in response to external stimuli like UV radiation. It has been shown that UV regulates MMP expression by inducing the generation of excess intracellular reactive oxygen species (ROS), a major factor in the skin aging process

(mechanisms are summarized in Fig.5). ROS in its turn activates mitogen-activated protein kinases (MAPKs) and nuclear factor-kappa B (NF-κB) leading to it transcriptionally regulating the increased synthesis of MMPs (Shin et al. 2019; Kohl et al. 2011). Previous studies have demonstrated that elevated levels of many MMPs (MMP-1, MMP-2, MMP-3, MMP-9, MMP-10, MMP-11, MMP-13, MMP-17, MMP-26, and MMP-27) can be found in aged human skin (Quan et al. 2013; Qin, Balimunkwe, and Quan 2017). Specifically, MMP-1, 2, 3 and 9 were shown to be upregulated by UV exposure (Quan et al. 2009; Dong et al. 2008; Brenneisen, Sies, and Scharffetter-Kochanek 2002) causing a cumulative degradation of existing collagen by repeated sun exposure.

In addition, it has been shown that the synthesis of new collagen fibers is reduced in photodamaged skin. Here the ROS mediated activation of the MAPK pathway which upregulates the transcription factor activator protein 1 (AP-1) and in turn inhibiting transforming growth factor beta (TGF-ß) signaling in the dermal fibroblasts, is of importance. TGF-ß is a major regulator of ECM biosynthesis and impaired TGF-ß signaling downregulates procollagen synthesis, leading to a decreased net collagen content in aged skin (Fisher et al. 1996; Shin et al. 2019). Downregulation of TGF-ß signaling appears to be a crucial event in skin aging. This molecular regulator mediates its cellular action via the Smad transcription factors. TGF-ß/Smad signaling has been implicated in being the regulatory path for 265 known ECM and ECM-related genes (Verrecchia, Chu, and Mauviel 2001). This is why it is seen as the primary regulator of ECM homeostasis, controlling for example collagen synthesis, MMP and TIMP expression.

A consequence of the reduced synthesis and fragmentation of collagen is the loss of adhesion sites between fibroblasts and intact collagen fibers. The mechanical tension that is created through this adhesion is vitally important for the fibroblasts to maintain their normal elongated shape and normal function and a loss of it was shown to lead to the formation of ROS and subsequently an induction of MMPs (Fisher et al. 2009; Qin, Balimunkwe, and Quan 2017). In addition, the reduced fibroblast spreading and defective mechanical stimulation downregulates TGF-ß signaling, leading to an inhibition of *de novo* collagen synthesis, again reducing adhesion sites (Fisher et al. 2016). Together this results in a self-perpetuating cycle that accelerates dermal aging.

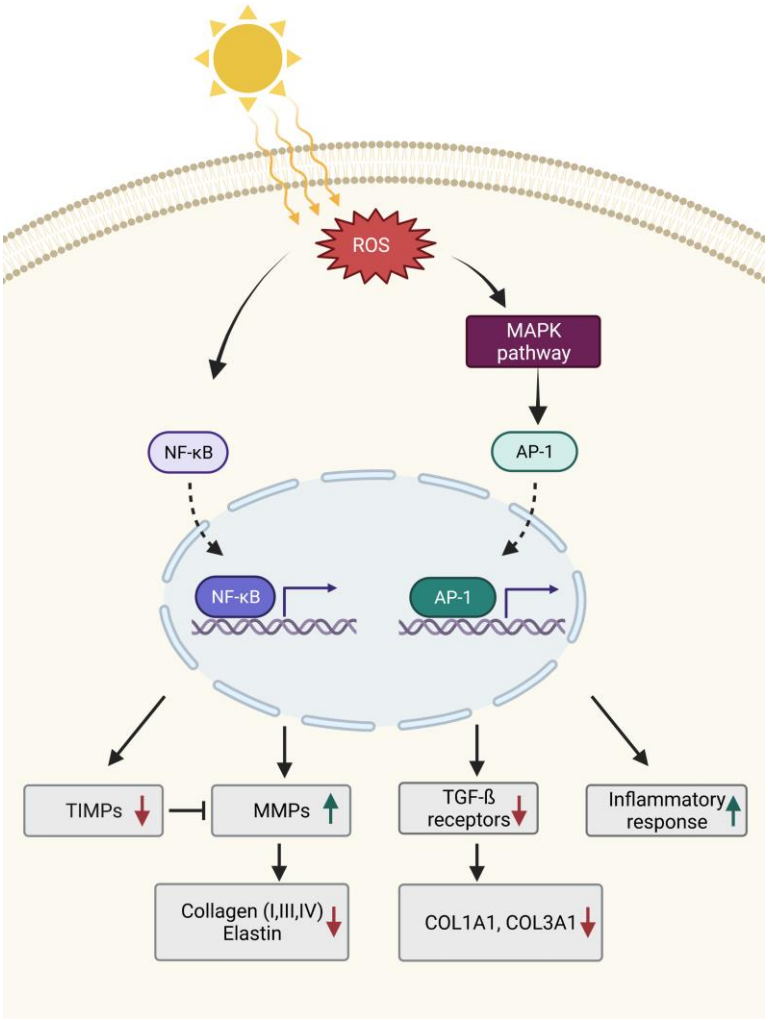

Figure 5: Schematic overview of extrinsic skin aging mechanisms
UV-induced excess intracellular reactive oxygen species (ROS) activate mitogen-activated protein kinase (MAPK) and nuclear factor kappa B (NFκB) signaling pathways, leading to the activation of AP-1 and NFκB. They transcriptionally regulate the balance between MMPs and TIMPs by activating MMPs and reducing the expression of TIMPs, resulting in degradation of the ECM (collagens and elastins). In addition, AP-1 inhibits transforming growth factor beta (TGF-β) signaling, causing a reduction in procollagen synthesis. Figure created with BioRender.com

In addition to its direct and indirect effects on the ECM turnover, TGF-ß1 is also known to induce the differentiation of fibroblasts to myofibroblasts. The transition to myofibroblasts, a cell type with contractile properties, characterized by the expression of α-smooth muscle actin (α-SMA), requires TGF-ß signaling in conjunction with a certain stiffness or mechanical tension of the ECM (Hinz et al. 2007). The transdifferentiation is usually activated in the wound healing process where myofibroblasts are responsible for tissue remodeling, wound closure, and scar formation (Tomasek et al. 2002; Hinz et al. 2012). While the controlled and transient activation of these cells is important to restore tissue integrity, their excessive persistence is associated with tissue fibrosis (Gabbiani 2003). Age-related deficits in TGF-ß1 signal transduction have been suggested as a cause for wound healing defects in elderly people (Mogford et al. 2002).

In previous work from our group (Gundermann 2012), a TGF-ß dependent transdifferentiation of fibroblasts was proposed as a model for photoaging. The *in situ* aged fibroblasts did show a "myo-chondro-fibroblastic" phenotype characterized by upregulation of genes that are typical components of cartilaginous ECM such as Aggrecan (ACAN), Hyaluronan and Proteoglycan Link

Protein (HAPLN1) and Collagen type XI (COL11A). The presence of these ECM components was also confirmed for skin *in situ* of old donors with sun damage (solar elastosis).

It has been described that in culture, human cells have a limited proliferative capacity before they withdraw from the cell cycle and enter the state of cellular senescence (Hayflick and Moorhead 1961). A potential reason for that is the "end replication problem" leading to a shortening of the chromosome ends, the telomeres, with every round of replication (Olovnikov 1973). Critical telomere shortening and other endogenous and exogenous stressors can drive cells into senescence and the resulting accumulation of senescent and functionally impaired fibroblasts would then drive the skin aging process (Campisi 2005). Senescence is coupled to multiple phenotypic changes, among these changes is the release of numerous biologically active molecules termed the senescence-associated secretory phenotype (SASP). The SASP can mediate and in part explain some of the pro-aging effects of senescent cells (Gorgoulis et al. 2019; Campisi et al. 2011). Factors secreted by senescent cells have been shown to disrupt normal tissue structure and function (Parrinello et al. 2005; Funk et al. 2000) and promote the growth of nearby premalignant cells *in vitro* and *in vivo* (Dilley, Bowden, and Chen 2003; Krtolica et al. 2001). However, senescence is not synonymous with aging and the exact mechanisms and the contribution of cellular senescence to the aging phenotype *in vivo* is still a matter of ongoing debates.

Although fibroblasts have been a model in aging research for decades there are still a lot of gaps in our knowledge about how aging affects these cells within the tissue and how in turn the aged fibroblasts influence their surroundings. We therefore proposed the establishment and use of a three-dimensional co-culture model based on primary *in situ* aged cells, which would help to overcome some of the limitations of standard cell culture, as it more closely resembles the physiological environment of the fibroblasts.

1.3 Solar Radiation and its Role in Skin Aging and Tissue Damage

Apart from the eyes, skin is the only organ directly exposed to solar radiation. The solar spectrum, depicted in Fig. 6, comprises different wavelengths, each having different and in part overlapping effects. The spectrum ranges from short wavelength, high energy, ultraviolet (UV) radiation to visible light (VIS) and to long wavelength, low energy, infrared (IR) radiation. About 2–5 % of solar radiation reaching the Earth´s surface is UV, 47 % is VIS, and 51 % is IR (Passeron et al. 2020).

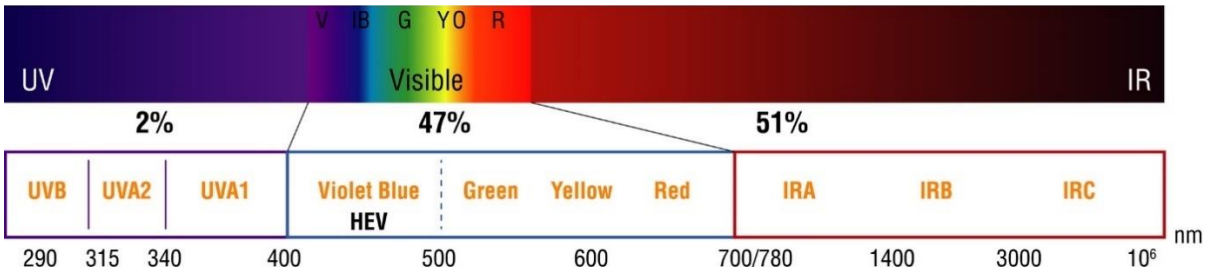

Figure 6: The solar spectrum
The solar spectrum is composed of various wavelengths, ranging from UV (shorter wavelength) to IR (longer wavelength) as depicted in the Figure. UV = ultraviolet radiation, IR = infrared. Taken from (Passeron et al. 2020)

For a long time, research focused on the UV fraction of the solar spectrum, UVB (280-315 nm) and, to a lesser extent, UVA (315-400 nm). Besides some known beneficial influences of UV light on the skin such as activation of Vitamin D synthesis and the improvement of several skin conditions, like psoriasis, atopic dermatitis, vitiligo and localized scleroderma through phototherapy (Juzeniene and Moan 2012), the adverse effects range from acute impacts (erythema, inflammation, "sunburn") to chronic consequences (photoaging, DNA damage, immunosuppression, and ultimately skin cancer).

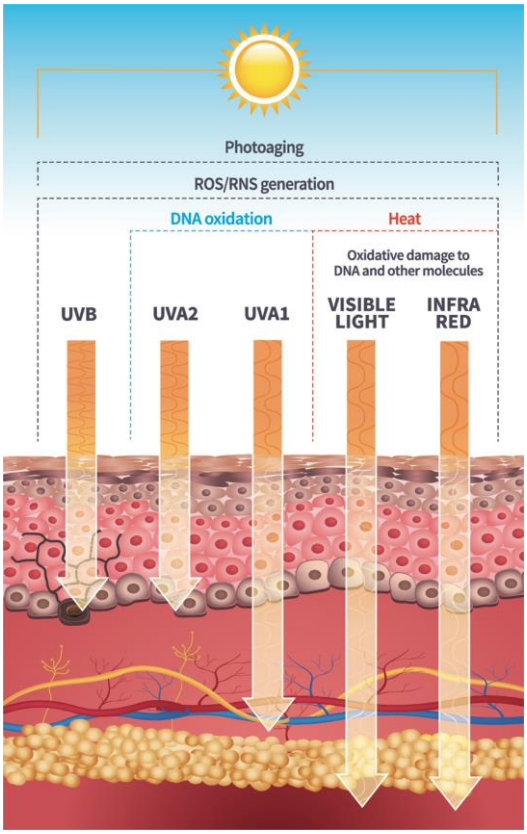

Figure 7: Penetration of solar radiation into the human skin
Solar radiation is composed of various wavelengths, which penetrate into skin at different levels. The longer the wavelength the deeper the rays penetrate the skin. Whereas UVB is mainly absorbed in the epidermis, UVA, VIS and IRA reach the dermis and directly affect the dermal fibroblasts. Taken from (Krutmann et al. 2017)

UVB with its shorter wavelength mostly affects the epidermis, whereas the longer wavelength rays of UVA, VIS and IR are able to penetrate deeply into the dermis, which is shown in Fig. 7 (Krutmann et al. 2017). The energy of UVB rays is directly absorbed by DNA, giving rise to base changes that lead to the formation of the typical bulky DNA lesions cyclobutane pyrimidine dimers (CPDs) and pyrimidine-pyrimidone (6-4) photoproducts (6-4PPs) (Cadet et al. 2012). These C→T substitutions at dipyrimidine sites, (including CC→TT double base changes) are solely induced by UV and have therefore been termed "UV signature mutations" (Brash 2015). In response to UV damage, affected keratinocytes activate DNA damage response pathways to maintain genomic integrity. If damage exceeds a threshold, keratinocytes usually will go into apoptosis and die. These apoptotic keratinocytes can be identified by their pyknotic nuclei and are termed "sunburn cells" (Young 1987; Bayerl et al. 1995). When DNA damage is left unrepaired and cells are not eliminated by apoptosis, DNA mutations can activate oncogenes or inactivate tumor suppressor genes, resulting in survival and proliferation of keratinocytes that harbor these damages and ultimately lead to skin cancer (Cadet and Douki 2018). UV exposure can also induce proliferation and differentiation of keratinocytes resulting in hyperplasia, hence increased epidermal thickness, which is thought to be a protective mechanism against further cutaneous damage (Scott et al. 2012).

On the dermal level, UV irradiation induces expression of several members of the MMP family, which degrade collagen and other extracellular matrix proteins, damaging the dermal architecture, a hallmark of photoaging (Quan et al. 2009). The contribution of UVA to the genotoxic and carcinogenic properties of UV light is not as well understood as for UVB. UVA exerts its damaging effects in a more indirect way, mainly via the generation of ROS, subsequently inducing a variety of oxidatively generated DNA lesions such as single strand breaks and oxidized bases, the most frequent being 8-oxo-7,8-dihydroguanine (8-oxoG) (Cadet and Douki 2018). CPDs have also been found in human skin exposed to UVA, but the mechanism seems to be another one than that triggered by UVB (Mouret et al. 2006). UVA was also shown to promote the degradation of collagen in the dermis and induce inflammatory responses (Wang et al. 2019).

Wavelengths beyond UV have long been thought to have no adverse effects on the skin but today we know that this assumption is not correct. A recent *in vivo* study reported that all spectral regions – UV, VIS and IR – cause the formation of free radicals and thus could promote premature skin aging (Albrecht et al. 2019). Near infrared (IRA, 750-1400 nm) was also shown to modulate the dermal ECM by upregulating MMP-1, the dominant collagen-degrading enzyme (Schieke et al. 2002), and downregulating de novo collagen synthesis (Buechner et al. 2008). This demonstrates that IRA can have similar consequences as UV in this aspect of premature aging, although the underlying mechanisms differ, in that the IRA response involves the mitochondrial electron

transport chain (Krutmann and Schroeder 2009). Besides its role in photoaging, IRA is suggested to also add to the carcinogenic potential of sun exposure by interfering with apoptotic pathways (Jantschitsch et al. 2009). Also VIS (400-750 nm) was demonstrated to induce epidermal ROS, leading to the release of proinflammatory cytokines and increased MMP-1 production in human epidermal skin equivalents (Liebel et al. 2012).

Although many molecular and cellular consequences of exposure to specific wavelengths or spectral fractions could be defined, there is still a gap of knowledge about the action of the combined solar spectrum. Only a limited number of studies recently investigated the combination of spectra (Narla et al. 2020; Tyrrell and Reeve 2006; Hudson et al. 2020). Considering that in most situations of everyday life, humans are exposed to the entire spectrum of natural sunlight, to really understand what sunlight is doing to our skin it is vitally important to study the combined and simultaneous exposure to UVA and UVB (solar UV radiation, here referred to as "UVA+B") and even more important to UVA + UVB + IRA + VIS (combined solar spectrum, here referred to as "SUN") to define the action profile of these combinations. These studies are needed to explore if the combination of different wavelengths leads to synergistic or, on the opposite, antagonistic or even new effects on the skin.

To provide the conditions for these kinds of studies, we have designed a lamp in our consortium that allows for simultaneous irradiation of cells and tissue with either individual wavelengths or the entire solar spectrum simultaneously in a highly controlled manner. With this lamp we aim at comparing the consequences of irradiation at a physiologically relevant dose (1 MED = minimal erythema dose), imitating the actual terrestrial sun exposure of human skin *in vivo*.

1.4 Skin Cancer – an Overview

One of the deleterious consequences of excessive sun exposure is the increased chance to develop skin cancer. There is strong evidence from epidemiological and molecular data linking skin cancer to UV exposure.

Skin cancer is the most frequent type of cancer worldwide and is divided in two main groups: melanoma and non-melanoma skin cancers (NMSC). Melanoma arises from the melanocytes and accounted for about 22 % of skin cancer diagnosis in 2018 (Bray et al. 2018). This leaves 78 % of the skin cancers diagnosed to be NMSCs where the most common forms in that group are basal cell carcinoma (BCC) and cutaneous squamous cell carcinoma (cSCC) that originate from epidermal keratinocytes. In 2020 NMSC was the fifth most commonly occurring cancer worldwide with almost 2 million cases, which is likely to be an underestimate due to poor diagnosis and

recording in many countries and therefore needs to be interpreted with caution. In Germany NMSC was the leading type of cancer with an incidence of more than 90.000 cases in 2020 (Sung et al. 2021). Skin cancer rates have been increasing in the last years and numbers are projected to increase in the coming decades where NMSCs represent a major public health concern. Within the scope of this work, we have therefore based parts of our studies on NMSCs and the connection to photoaging.

The causal link between UV radiation and skin cancer was established in the 1990s when UV signature mutations, described in the previous chapter, were found in the p53 tumor suppressor gene in cSCCs and BCCs. Mutations in the p53 gene are a common and probably the best studied aberration found in > 50 % of NMSCs (Brash et al. 1991; Giglia-Mari and Sarasin 2003; Pickering et al. 2014). In fact, it is estimated that 65 % of melanoma cases and 90 % of NMSCs are causally connected to UV radiation ('IARC monographs on the evaluation of carcinogenic risks to humans. Solar and ultraviolet radiation' 1992). This correlation is emphasized by the higher incidence in people who live in sunny areas or at high altitude and have fair skin and the majority of tumors arising on sun-exposed parts of the body. While BCCs seem to be correlated with intermittent UV exposure and severe sunburn in childhood and adolescence, cSCCs are more related to cumulative chronic exposure (Boukamp 2005; Rosso et al. 1996). As a logical consequence, the chance of developing NMSC, especially cSCC, increases with age. BCCs and SCCs typically appear after the age of 55 and are therefore seen as a disease of older age (Ciazynska et al. 2021).

UV radiation causes genetic and epigenetic changes not only in keratinocytes, but also in the fibroblasts, thereby altering their expression profile. This can activate the production of proteases like MMPs that are needed for the degradation of the ECM and disruption of basement membranes to allow tumor invasion. Therefore, proteolytic remodeling of the ECM has been recognized as an important event in cancer progression. Fibroblasts also secrete soluble factors like growth factors and cytokines that in turn can promote keratinocyte growth and invasion (Nissinen et al. 2016; Kerkela and Saarialho-Kere 2003).It has been described that while healthy tissue can to some degree suppress tumor development, disturbances of normal tissue homeostasis (like environmental stress) can result in a more tumor-permissive microenvironment which was shown to be required to promote premalignant lesions (Bissell and Hines 2011). Therefore, it needs to be addressed if and how changes in the skin's architecture and microenvironment that come along with aging play a role in carcinogenesis.

1.5 In vitro Skin Models to Study Skin Aging

When studying aging of the human skin, animal models, in particular mouse models as the typically used laboratory animal, are of limited value. Not only are they subject of increasing ethical concerns, but the architecture of mouse skin differs fundamentally from human skin. The differences between human and mouse range from the obvious unlike hair follicle density to a differential expression of skin-related genes (Gerber et al. 2014). This explains in part why results generated in mouse models often fail to translate into the human.

Many cellular processes can be studied in a conventional two-dimensional (2D) cell culture, which is a simple and cost-effective approach, but it also comes with limitations as it does neglect the complex multilayered structure of skin and the extra-cellular microenvironment and therefore the cell-cell and cell-matrix interactions that play a crucial role in skin health and disease.

Three-dimensional (3D) organotypic cultures (OTCs) of skin, or skin equivalents (SEs), provide a model system that allows coculture of different skin cells in a 3D matrix, mimicking key features of human skin architecture and function. With that they can help to close the gap between 2D and animal models and are currently considered the best alternative tool to study human skin aging (Nakamura et al. 2018). They also have a wide field of application from basic research to modeling of diseases, toxicological assessment, and regenerative medicine.

Pioneering work in the area of reconstructing human skin was done by Bell et al. in 1981 by seeding keratinocytes on top of collagen gels that contained dermal fibroblasts (Bell et al. 1981). Today a broad range of human skin models has been published, additionally to the collagen-based SEs, which are based on different dermal equivalent (DE) formats, such as the de-epidermized dermis approach (Regnier et al. 1988), scaffold-enforced DEs (Stark et al. 2004), and fibroblast-derived matrix DEs (Ahlfors and Billiar 2007; El Ghalbzouri et al. 2009; Berning et al. 2015). Also several SEs are now commercially available for different applications (EpiDerm™ FT (Kubilus et al. 2004), Phenion™ FT (Mewes et al. 2007), T-Skin™ (Bataillon et al. 2019)). Although more complex to produce than only epidermal models, SEs were essential to study for example the dermal-epidermal crosstalk, the penetration of drugs, wound healing and particularly aging and the effects of solar radiation (Bernerd and Asselineau 2008; Meloni, Farina, and de Servi 2010; Kuchler et al. 2010).

Despite the range of SEs that are available, there are still very few models for skin aging that reliably reproduce the characteristics of “aged skin” *in vivo*. The model developed in this study is based on previous work by Sabrina Gundermann (Gundermann 2012) in the laboratory of Prof. Boukamp, where SEs were generated with young and old fibroblasts aged *in situ*. These aged skin models were now developed further, and instead of using a scaffold to build the DE, it is self-

assembled by the fibroblasts that produce and secrete the components of the dermal ECM (fibroblast-derived matrix DE = fdmDE). The fdmDEs built by young or old primary fibroblasts that are complemented with human keratinocytes were termed Age-SEs. Fdm-based SEs closely resemble the dermal microenvironment *in vivo* (histological comparison in Fig. 8) and were shown to support epidermal differentiation and regeneration over long culture periods (up to 24 weeks) (Berning et al. 2015; El Ghalbzouri et al. 2009). This makes them suitable for long-term studies and allows investigation of phenomena like ECM remodeling. The model established here is also well connected to the extrinsic environmental factors as the fibroblasts used were isolated from sun-exposed areas and as such represent a model for photoaged skin.

Complemented with premalignant keratinocytes, fdmSEs can also provide a tool for skin cancer research, as they recapitulate the tumorigenicity and invasion phenotype of the epidermal cells (Berning et al. 2015). In this study we used HaCaT (human, adult, low calcium, high temperature, skin keratinocyte) cells, which are benign spontaneously immortalized keratinocytes, that carry UV-type specific mutations in both alleles of the p53 gene, which have likely been induced in the skin *in situ* (Boukamp et al. 1988). This cell line has been widely used as it is able to form a non-invasive epithelium and is an accepted model for early stages in skin carcinogenesis (Lehman et al. 1993). By additionally using transfected HaCaT-ras clones with different benign and malignant tumorigenic characteristics, HaCaT-ras A5 and HaCaT-ras II4, we can also model stages of skin cancer progression (Boukamp et al. 1990) and study the role of fibroblast aging in this context.

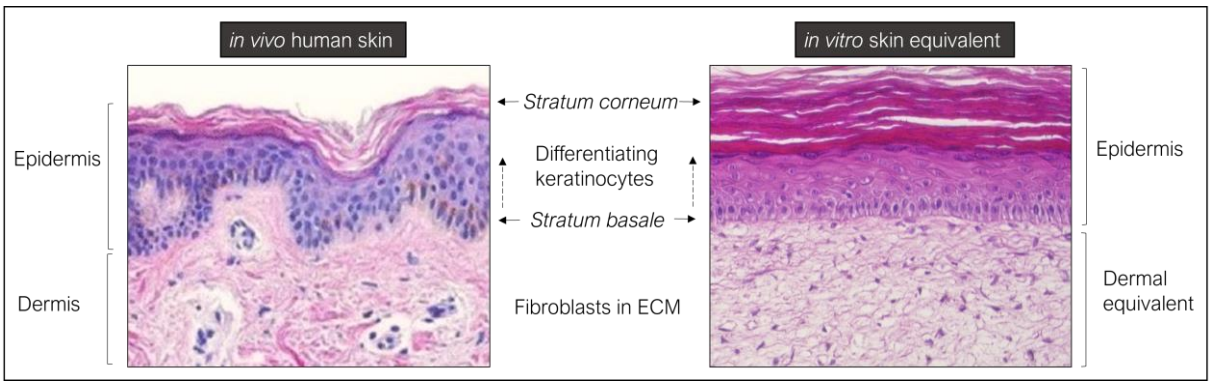

Figure 8: Histology of human skin and a reconstructed skin equivalent
H&E stainings of a human skin sample from a 25-year-old caucasian donor (left) (Roger et al. 2019) and a skin equivalent based on a fibroblast-derived matrix with fibroblasts from a 23-year-old donor (right, own picture), indicating the different layers of native skin and the corresponding parts of the skin equivalent .

1.6 Aims and Objectives

Although the multifactorial process of photoaging is still not fully understood, it is becoming increasingly clear that the dermal fibroblasts are key players in the aging process. In recent years, dermal fibroblasts were recognized as a highly heterogenous cell population and accordingly, the interest in their characterization and how they modulate their environment during aging has strongly increased. In preceding studies of our group, a novel fibroblast differentiation state was presented that is correlated with photoaging and in particular with the most severe state of photoaging – solar elastosis. Characterization of these "old" fibroblasts demonstrated a stable TGF-ß-dependent myo-chondro-fibroblastic phenotype, proven to be highly relevant also in skin *in situ*.

To study the role of this fibroblast aging phenotype for the function of the tissue and, on the other hand, the role of solar radiation for the development of this phenotype, the first objective of this project was to establish an organotypic skin model based on primary human cells, that is long-term stable and reproduces the characteristics of photoaged skin. UV radiation is well-documented to be causally related to photoaging. While most studies only focused on the effect of UVB or UVA, in real life the entire solar spectrum (UVB+UVA+VIS+IR) affects the skin. With our newly developed radiation device, it is possible to irradiate the SEs with either solar UV radiation (UVA+B) or the entire solar spectrum (SUN) simultaneously and compare their functional consequences on SEs.

With this model system the following questions should be addressed:

1. How do old fibroblasts influence tissue morphology and regeneration of the SEs compared to young fibroblasts?
2. Do old fibroblasts and the "aged ECM" induce or promote invasive growth when combined with transformed keratinocytes?
3. What is the role of solar radiation for the development of the old fibroblast phenotype (myo-chondro-fibroblasts)? And how does in turn the fibroblast age affect the response of the tissue to UVA+B or SUN irradiation?
4. Does irradiation induce or promote invasive growth of transformed keratinocytes and are SEs based on old fibroblasts more susceptible to that?
5. Are there specific differences in the tissue response to only UV radiation (UVA+B) compared to the entire solar spectrum (SUN)?

2 Material and Methods

2.1 Material

All chemicals, materials, kits and devices used for the described experiments, as well as cells, primers and antibodies are listed in the following tables.

2.1.1 Chemicals

Table 1: Chemicals

Chemical	Supplier
Acetone	Carl Roth
AKASOLV Aqua Care	Carl Roth
Annexin V (FITC-conjugated)	Biolegend
Annexin V Binding Buffer	Biolegend
Aprotinin	Carl Roth
Bovine serum albumin (BSA)	Sigma
Calcium acetate hydrate	Sigma
Calcium chloride dihydrate,	Sigma
Dispase II	Sigma
DNA AWAY®	ThermoFisher Scientific
Eosin 1 %	Morphisto
Ethanol 99.5%	Carl Roth
Fixing Agent for Anatomy and Histology	Morphisto
Glycerol	Sigma
Hematoxylin solution, Mayer‘s	Morphisto
Hoechst 33258, Pentahydrate (bis-Benzimide) - 10 mg/mL Solution in Water	Life Technologies
Hydrochloric Acid	Carl Roth
Lysis Solution RL	Analytik Jena AG
Magnesium chloride hexahydrate	Sigma
Methanol	Carl Roth
Mounting Medium, Isomount 2000 Q Path®	VWR
Phosphate Buffered Saline (PBS)	Serva
Propidium iodide	Biolegend
RNase AWAY®	ThermoFisher Scientific

Roticlear	Carl Roth
Sodium acetate	Sigma
Tissue Tek (OCT compound)	Sakura Finetek
Triton X100	Carl Roth
Trypan Blue Stain 0.4 %	Logos Biosystems
Trypsin 2.5 %	Pan Biotech
Vectashield Mounting Media with DAPI	Vector Laboratories
WesternBright ECL Substrate	Advansta
Xylole (1 l)	Carl Roth

2.1.2 Consumables

Table 2: Consumables

Item	Company
12-well ThinCert™ Cell Culture Insert, Pore Size 0,4 µm	Greiner Bio-One
12-well deep-well Plates, ThinCert™	Greiner Bio-One
Adhesive slide, HistoBond®	Marienfeld Superior
Adhesive slide, SuperFrost® Plus	Marienfeld Superior
Biopsy pads	Simport Scientific
Cell Counting Slides	Logos Biosystems
Cell Culture Dishes, Falcon®, various sizes	Corning
Cell strainer 70 µm, EASYstrainer	Greiner Bio-One
Centrifuge Tube, 15/50ml	Sarstedt
Ceramics Beads 1,4 mm	Bertin Instruments
Coverslips D 263™	Marienfeld Superior
Cryo molds	Weckert Labortechnik
Cryo Vials, CryoTubes™	Nunc
Cryostat blade Feather® C35	Feather
Embedding Cassette	Neolab
Eppendorf PCR Tubes	Eppendorf
Eppendorf Safe-Lock Tubes	Eppendorf
Filter for 5 ml pipette	Gilson
Macro tips 5000 µl	Gilson
Microtome blades Feather® R35	Feather
Nitrocellulose Membrane Amersham™ Hybond™	GE Healthcare

Pasteur pipette glass	VWR International
Pipette tips TipOne® 10/20/100/200/1000 µl	Starlab
Pipette tips filtered TipOne®	Starlab
Scalpels sterile, No 10	Swann-Morton
Serological Pipettes Stripette®	Corning
Steriflip-GP, 0.22 µm	Merck Millipore
Steritop-GP, 0.22 µm	Merck Millipore

2.1.3 Kits

Table 3: Kits

Kit	Company
AceQ qPCR SYBR® Green Master Mix	Absource Diagnostics
EnzCheckTM Gelatinase/Collagenase Assay Kit	Invitrogen
Human TIMP-1 ELISA Kit	Wuhan Fine Biotech
Human TIMP-2 ELISA Kit	Wuhan Fine Biotech
innuPREP DNA/RNA Mini Kit	Analytik Jena AG
Mykoplasmen-Kit VENOR®GEM ONE STEP	Minerva Biolabs
QuantiFast SYBR® Green PCR Kit	Qiagen
Quantikine ELISA Human MMP-3	R&D Systems
Quantikine ELISA Human Pro-MMP-1	R&D Systems
SensiFAST cDNA Synthesis Kit	Bioline
Staining kit: Picro-Sirius Red for Collagen I & III	Morphisto
Western Bright Kit	Advansta

2.1.4 Devices

Table 4: Devices

Device	Company
"My Bath", digital water bath	Biozym Scientific GmbH
CoolCell® LX freezing containers	Biozym Scientific GmbH
Cryostat CM3050S	Leica Biosystems
Electrophoresis Power supply	Pharmacia Biotech
FACSCanto Flow Cytometry System	BD Biosciences
Gilson Pipetman	Gilson

Heracell 240 CO2-Incubator, Kupfer	ThermoFisher Scientific
Heraeus Megafuge 8 230 V	ThermoFisher Scientific
Incubator CO2, compact, MIDI-40	Incubator CO2, compact, MIDI-40
Infinite M200 Pro Plate reader	TECAN
Luna II automated Cell Counter	Logos Biosystems
Microscope Axio Imager M2	Carl Zeiss AG
Microscope Axio Vert.A1	Carl Zeiss AG
Pipette Boy S1	ThermoFisher Scientific
Precellys®24 tissue homogenizer	Bertin Instruments
Rotor-Gene Q	Qiagen
Sliding Microtome	ThermoFisher Scientific
T3000 Thermocycler	Biometra
Tissue Tek VIP® 6 AI Vacuum Infiltration Processor	Sakura Finetek
Tissue-Tek Base Mold 15x15x5 mm	Miles Scientific
Tissue-Tek Cryo Console	Miles Scientific
Tissue-Tek Dispenser	Miles Scientific
Tissue-Tek Thermal Console	Miles Scientific
TRIO-Thermoblock	Biometra
Vacusafe Aspiration System	Integra Biosciences
Vornado Mini Vortexer	Biozym

2.1.5 Software

Table 5: Software

Software	Company
Adobe InDesign 2018 CC2018	Adobe Systems
Axio Imager M2	Carl Zeiss AG
Axio Vert A1	Carl Zeiss AG
EndNote 20	Clarivate Analytics
FACSDiva	BD Biosciences
GraphPad Prism 9	GraphPad Software
i-control 1.10	Tecan
ImageJ-win64 1.51h	BioVoxxel
Microsoft 365	Microsoft
Photoshop Elements 13	Adobe
ZEN 2 Pro	Zeiss

2.1.6 Cell Culture Supplements

Table 6: Cell Culture Supplements

Supplement	Company	Stock Solution
2-phospho-L-ascorbic acid trisodium salt	Sigma-Aldrich	1 M in ddH2O
Adenin	Sigma-Aldrich	24.3 mg/ml adenin in 0.2 mM HCl
Choleratoxin	Sigma-Aldrich	10-5 M choleratoxin in ddH2O
Dulbecco's Modified Eagle Medium (DMEM) w: 4,5 g/l Glucose, w: L-Glutamine, w: Sodium pyruvate, w: 3,7 g/l NaHCO3	Pan Biotech	
Dulbecco´s Modified Eagle Medium (DMEM)/F12 (1:1), w: L-Glutamine, w: 15 mM, Hepes, w: 1,2 g/l NaHCO3	Pan Biotech	
Ethylendiamintetraacetic acid (EDTA) 1% in PBS	Pan Biotech	
Fetal Bovine Serum (FBS), Lot: 0522D	Biochrom	
Hydrocortisone	Sigma-Aldrich	5 mg/ml hydrocortisone in ethanol, 400 µg/ml in ddH2O
Insulin Recombinant Human	Sigma-Aldrich	3 mg/ml insulin in culture medium, titrated with 1 M HCl
Penicillin/Streptomycin/Amphotericin B Mix	Pan Biotech	
Penicillin/Streptomycin	Pan Biotech	
Phenol Red	Sigma-Aldrich	
Recombinant Human Epidermal Growth Factor (EGF)	Life Technologies	5 µg/ml EGF in PBS with 0.1% BSA
Recombinant Human Basic Fibroblast Growth Factor (bFGF)	Life Technologies	10 µg/ml bFGF in PBS with 0.1% BSA
Recombinant Human Transforming Growth Factor (TGF) Beta 1	Life Technologies	Acidic activation, 2 µg/ml TGFß-1 in PBS with 0.1% BSA

2.1.7 Cell Culture Media and Solutions

Table 7: Cell Culture Media and Solutions

Solution	Application	Composition
D10 medium	Cultivation of HaCaT and NHDF	DMEM, 10 % (v/v) FBS, 1 % (v/v) Pen/Strep
Freezing medium	Freezing of all cell types	DMEM, 10 % (v/v) FBS, 10 % (v/v) glycerol

rFAD medium	Cultivation of SEs	DMEM and F12 (3:1), 10 % (v/v) FBS, 1% (v/v) Pen/Strep/Amp, 200 µg/ml 2-phospho-L-ascorbic acid, 0.1 nM choleratoxin, 0.4 µg/ml hydrocortisone
FADcomplete medium	Cultivation of NHEK	DMEM and F12 (3:1), 5 % (v/v) FBS, 1 % (v/v) Pen/Strep/Amp, 0.1 nM cholera toxin, 0.4 µg/ml hydrocortisone, 24 ng/ml adenine, 5 µg/ml insulin, 0.5 ng/ml EGF
CDM medium	Cultivation of dermal equivalents	DMEM and F12 (3:1), 10 % (v/v) FBS, 1 % (v/v) Pen/Strep/Amp, 200 µg/ml 2-phospho-L-ascorbic acid, 2.5 ng/ml EGF, 5 ng/ml FGFb, 1 ng/ml TGF-β1, 5 µg/ml insulin
EDTA	Removal of calcium from the cultures	PBS -/-, 0.05 % (w/v) EDTA, 0.0005 % phenol red
Trypsin 0.1 %	Detachment of NHDF	PBS -/-, 0.1 % trypsine, 0.025 % (w/v) EDTA , 0.0005% phenol red
Trypsin 0.4 %	Detachment of NHEK and HaCaT	PBS -/-, 0.4 % trypsine, 0.025 % (w/v) EDTA, 0.0005% phenol red

2.1.8 Antibodies

Table 8: Antibodies

Primary Antibodies					
Target	Origin Species	Clonality	Dilution	Company	Cat.-No.
α-smooth muscle actin	mouse	monoclonal	1:1000	Sigma	a2547
Aggrecan	mouse	monoclonal	1:100	abcam	ab3778
Collagen I	rabbit	polyclonal	1:500	Acris	R1038
Collagen IV	rabbit	polyclonal	1:1000	Progen	10760
Collagen VII (LH7.2)	mouse	monoclonal	1:100	Sigma	C6805
Collagen XI	rabbit	polyclonal	1:50	Santa Cruz	Sc-68853
CPD (TDM-2)	mouse	monoclonal	1:1000	Cosmo Bio	NMDND001
Filaggrin (FLG01)	mouse	monoclonal	1:200	Invitrogen	MA5-13440
Keratin 15	guinea pig	monoclonal	1:250	Progen	GP-CK15
Keratin 10	guinea pig	serum	1:500	Progen	GP-K10
Keratin 2	mouse	monoclonal	1:100	Progen	65191
Keratin Pan	guinea pig	serum	1:100	Progen	GP14
Ki67	rabbit	polyclonal	1:250	abcam	ab15580
Laminin (γ2 chain)	mouse	monoclonal	1:200	Merck Millipore	MAB19562

MMP-1	rabbit	polyclonal	1:200	abcam	ab38929
MMP-3	rabbit	polyclonal	1:200	Sigma	HPA007875
TGFß-1	mouse	monoclonal	1:40	abcam	ab64715
Vimentin	mouse	monoclonal	1:200	Progen	61013

Secondary Antibodies					
Target	Origin Species	Conjugate	Dilution	Company	Cat.-No.
Rabbit IgG	Goat	Cy3	1:200	Dianova	111-165-144
Mouse IgG	donkey	Cy3	1:200	Dianova	715-166-151
Guinea pig IgG	donkey	Cy3	1:200	Dianova	706-165-148
Guinea pig IgG	donkey	Alexa488	1:200	Dianova	706-546-148
Mouse IgG	sheep	Alexa488	1:200	Dianova	515-545-003
Rabbit IgG	goat	Alexa488	1:200	Dianova	111-545-003
Mouse IgG	goat	HRP	1:5000	Cell Signaling	7076P2

2.1.9 Cells

Table 9: Cells

Normal Human Dermal Fibroblasts (NHDF)			
Name	Donor age (years)	Gender	Body region
04.04.07	23	female	abdomen
08.02.96	22	female	breast
13.03.98	74	male	back
13.07.94	66	female	back
Normal Human Epidermal Keratinocytes (NHEK)			
04.04.07	23	female	abdomen
20.10.05	n/a	female	breast
17.04.07	43	female	breast
HaCaT			
Name	Modification	Reference	
HaCaT	mutant p53	Boukamp *et al.,* 1988	
HaCaT-RAS A-5	oncogenic c-Ha-Ras	Boukamp *et al*., 1990	
HaCaT-RAS II-4	oncogenic c-Ha-Ras	Boukamp *et al*., 1990	

2.1.10 qRT-PCR Primer

Table 10: qRT-PCR Primer

Gene	Sequence Forward Primer	Sequence Reverse Primer
ACAN	CCTCCCCTTCACGTGTAA AA	GCTCCGCTTCTGTAGTCTGC
ACTB	CCCCAGGCACCAGGGCGTGAT	GGTCATCTTCTCGCGGTTGGCCTTG GGGT
COL10A1	CACCTTCTGCACTGCTCATC	GGCAGCATATTCTCAGATGGA
COL11A1	TGCTCAAGCTCAGGAACCTC	CCTCTGTTACACTTTCAGCCTCTT
HPRT1	CTCATGGACTGATTATGGACAGGA C	GCAGGTCAGCAAAGAACTTATAGCC
IPO8	AGGATCAGAGGACAGCACTGCA	AGGTGAAGCCTCCCTGTTGTTC
HAPLN1	GACAGAGCTATTCACATCCAAGC	TGCCACCTCTGTGTGAAAAC
SOX9	TACCCGCACTTGCACAAC	GTAATCCGGGTGGTCCTTCT
TGFB1	TACCTGAACCCGTGTTGCTCTC	GTTGCTGAGGTATCGCCAGGAA
TGFB3	CTAAGCGGAATGAGCAGAGGATC	TCTCAACAGCCACTCACGCACA

2.2 Methods

2.2.1 Cell Culture

2.2.1.1 Cell Lines

Normal human epidermal keratinocytes (NHEK) and normal human dermal fibroblasts (NHDF) were obtained from different individual donors. Details about donor age, sex and origin of the tissue can be found in Table 9. Cells were isolated by the Boukamp laboratory at the DKFZ Heidelberg in accordance with the guidelines of the Institutional Commission of Ethics at the University of Freiburg (42/2005) and the World Medical Association Declaration of Helsinki (updated 2013). Briefly, skin samples were cut into small pieces and incubated in thermolysine (0.5 mg/ml) at 4 °C overnight to facilitate the mechanical separation of dermis and epidermis. Single cell suspensions of epidermal keratinocytes were obtained by mechanical detachment and filtration through a cell strainer. For culture conditions of NHEK see chapter 2.2.1.3. For isolation of NHDF, pieces of the dermis were cultured submersed in D20 medium in standard cell culture plates until fibroblasts grew out of the explant. When cells reached confluency, NHDF were trypsinized and propagated or frozen in liquid nitrogen for later usage as passage 1. NHEKs were used in passages 1 to 3, NHDFs in passages 6 to 9.

In addition to primary cells, dermal equivalents were complemented with the spontaneously immortalized human keratinocyte cell line HaCaT (human adult low calcium high temperature (Boukamp et al. 1988), containing UV-type specific p53 mutations. Besides the non-tumorigenic HaCaT cells, two variants (HaCaT-ras A5 and HaCaT-ras II4) were applied, that are transfected with c-Ha-ras oncogene (Boukamp et al. 1990), representing different tumorigenic states. HaCaT cells were used in passages 30 to 35.

2.2.1.2 Thawing and Cryopreservation of Cells

All cells were kept in cryo vials in liquid nitrogen tanks for long term storage. To freeze them down, cells were detached, counted and centrifuged and the resulting pellet was resuspended in freezing media (see Table 7) at a concentration of 2 x 10^6/ml. Cryo vials with the cell suspension were then put in CoolCell® cell freezing containers that ensure a standardized controlled cooling rate of -1 °C/min at -80 °C. Cells were kept in the containers in a -80 °C freezer overnight and then transferred to liquid nitrogen tanks. To thaw cells, cryo vials were taken out of the nitrogen tanks and placed in a water bath at 37 °C. When thawed, cells were seeded onto cell culture dishes in pre-warmed cell specific medium (see Table 7).

2.2.1.3 Culture and Passaging of Cells

NHDF were cultivated in D10 medium at 37°C, 5 % CO_2 and 95 % humidity. For optimal growth conditions the O_2 concentration was lowered to 10 %. Reaching confluency, fibroblasts were incubated with EDTA for 3 min followed by 2-3 min incubation with 0.1 % trypsin solution, both at 37 °C. Cells were gently detached and suspended in serum containing media to stop the enzymatic reaction. Subsequently, they were counted using an automated cell counter, pelleted to get rid of the trypsin, and resuspended in media. Fibroblasts were reseeded at densities of 0.5-1.5 x 10^6 per 15 cm cell culture dish or used for preparing dermal equivalents.

NHEKs were cultivated in $FAD_{complete}$ medium at 37 °C, 5 % CO_2 and 95 % humidity. As primary keratinocytes require a constant supply of dermal derived growth and differentiation factors, they were seeded on a layer of feeder cells, i.e. γ-irradiated fibroblasts. Feeder cells were prepared by submitting a fibroblast suspension to 60 Gy gamma rays and then reseeding them on a cell culture dish. When reaching a confluency of 90-95 %, NHEKs were incubated with EDTA for 5 min followed by 0.4 % trypsin solution for 2 min, both at 37 °C. After detachment, cells were counted, pelleted and resuspended in media as described above. The cells were then either prepared for storage in liquid nitrogen or seeded on dermal equivalents.

HaCaT cells and all HaCaT variants were cultivated in D10 medium at 37 °C, 5 % CO_2 and 95 % humidity and subcultured at a confluency of 100 %. For that, they were treated with EDTA for 8-10 min followed by 0.4 % trypsin solution for 2 min at 37 °C. Subsequently, they were suspended in media, counted and pelleted as described above. Cells were then frozen down or seeded on dermal equivalents.

Culture medium for all cell types was changed three times a week on Monday, Wednesday, and Friday. Cell growth and morphology was constantly monitored with an Axio Vert.A1 Microscope (Carl Zeiss).

2.2.1.4 Contamination Control

As a routine control, cells and organotypic cultures were regularly checked for mycoplasm contamination using the Venor®GeM OneStep Mycoplasma Detection Kit according to the manufacturer's protocol. All cells and organotypic cultures used in this work were free of mycoplasm contamination.

2.2.2 Skin Equivalent Preparation, Culture and Treatment

2.2.2.1 Preparation of Skin Equivalents (SEs)

The work described in this thesis was mainly done on 3D organotypic cultures of skin, in the following called skin equivalents (SEs), that consist of a fibroblast-derived-matrix (fdm) based dermal equivalent (DE), co-cultured with either normal human epidermal keratinocytes (NHEK) or HaCaT cells. The preparation of the SEs is based on a previously published protocol (Berning et al. 2015; Pavez Lorie and Boukamp 2020) and depicted in Figure 9. To produce Age-SEs, the dermal equivalent was built from fibroblasts of different aged donors. SEs based on a DE with young fibroblasts are further referred to as "young SEs", those based on old fibroblasts are accordingly referred to as "old SEs".

For the preparation of the dermal equivalents, fibroblasts were seeded onto ThinCert® inserts with 0.4 µm pore size in 12-well deep-well ThinCert® plates containing 5 ml of CDM medium. The seeding was done in three steps. Every 24-48 h 0.5 x 10^6 cells in passage 8 or 9 in 1 ml CDM medium were seeded dropwise into the inserts. After the last seeding, the DEs were given five weeks to mature and produce extracellular matrix. They were kept at 37 °C, 5 % CO_2 and 95 % humidity and CDM medium was changed three times a week.

24 h before seeding the keratinocytes onto the dermal equivalents, medium in both wells was exchanged to rFAD. NHEK or HaCaT cells were detached from plates and seeded dropwise on top of the CDMs at a density of 0.25 x 10^6/well in rFAD medium. After three to four days of submersed cultivation, the medium in the upper well was carefully removed ("air-lift") and cultures were subsequently cultured at the air-liquid interphase to initiate the generation of a stratified epithelium. If not stated otherwise in this thesis the co-cultures were continued for two more weeks before the start of irradiation. rFAD medium was exchanged three times a week.

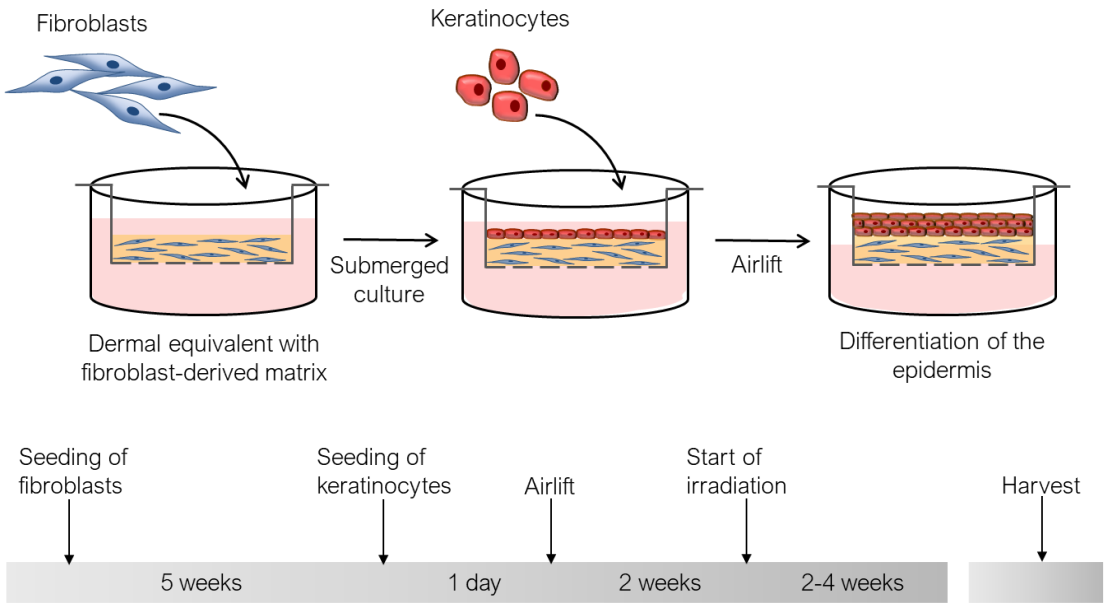

Figure 9: Schematic representation of the preparation of fdmSEs and the experimental workflow
Fibroblasts are seeded in three successive steps. After the last seeding, the dermal equivalents were given 5 weeks of submersed cultivation to mature and produce extracellular matrix. Then, keratinocytes were seeded on top of the dermal equivalents and subsequently cultured at the air-liquid interphase to initiate the generation of a stratified epithelium. Irradiation was started two weeks later on a fully developed epidermis and continued for two to four weeks before harvest.

2.2.2.2 Irradiation of SEs

Skin equivalents were irradiated three times a week, directly after exchanging the medium. An innovative light source that mimics natural sunlight, was custom-built in our consortium. The design of the irradiation device is covered by a patent application (10 2022 102 915.8) filed at the German Patent and Trade Mark Office and the description was recently submitted (Plitta-Michalak 2022). The lamp is equipped with four radiation sources, ultraviolet B (UVB, 280-315 nm), ultraviolet A (UVA, 315-400 nm), visual light (VIS, 400-750 nm) and near infrared light (IRA 750-1400 nm) that are individually controllable. This allows for an irradiation with individual wavelengths alone or any combination thereof. The radiation from the different sources is combined onto the sample with dichroic beam combiners.

The ability of UV radiation to evoke erythema in human skin strongly depends on the wavelength. Therefore, the International Commission on Illumination (CIE) proposed a standard erythema action spectrum that provides an internationally accepted representation of the erythema-inducing effectiveness of specific wavelengths (McKenzie 2014). Based on this agreement, we defined wavelength specific CIE factors to calculate the physical intensities needed to reach the desired

dose. We used the CIE scaled radiation intensity and time, that is required to elicit erythema on a person with skin type II (minimal erythema dose, MED).

For each session, SEs were exposed to the equivalent of 1 MED (UVB 0.78 kJ/m^2, UVA 51 kJ/m^2, VIS 113 kJ/m^2, IRA 300 kJ/m^2), which equaled an exposure time of ~25 min. This spectral combination and intensity can be compared to the exposure on a sunny summer day in Central Europe around noon and is further referred to as simulated solar spectrum or "SUN". During irradiation the temperature of the irradiated samples was kept constant at 37 °C by the built-in Peltier-element.

2.2.2.3 Harvest of SEs

Co-cultures were harvested 24 h after the last irradiation. With a scalpel the OTC was cut out from the insert and the filter membrane at the bottom was removed. The culture was then divided in two or three pieces with a scalpel. A quarter of the culture was put in a paraformaldehyde solution for fixation and kept there for at least 24 h to preserve the tissue structure. Further processing for histology is described in chapter 2.2.6.1. Another quarter was embedded in a plastic mold with O.C.T. compound and snap-frozen in liquid nitrogen. After some minutes, the frozen samples were transferred to -80 °C for storage until cryosectioning. Half of the culture was used to isolate DNA and RNA. As epidermis and dermis were to be analyzed individually, samples were subjected to Dispase II treatment (1 mg/ml in PBS) for 30 min at 37 °C. Dermal and epidermal parts were then separated with forceps, transferred to sterile reaction tubes and snap-frozen in liquid nitrogen. Until further processing, samples were stored at -80 °C. Additionally, 2 ml of conditioned media from each sample was taken from the wells and stored at -80 °C.

2.2.3 Apoptosis Analysis by Flow Cytometry

Apoptosis was detected by staining cells with FITC-conjugated Annexin V and Propidium Iodide (PI) and subsequent analysis by flow cytometry. Annexin V has a high binding affinity to phosphatidylserine, located at the cytoplasmic side of the plasma membrane. When cells undergo apoptosis, the membrane is flipped and phosphatidylserine is exposed on the outside of the cell, where Annexin V can bind. To distinguish apoptotic and necrotic cells, PI is used, a dye that intercalates to DNA and can only permeate late apoptotic or necrotic cells.

Fibroblasts grown on 10 cm cell culture dishes up to 80 % confluence were irradiated with UVA+B or SUN and detached 24 h after the irradiation. Cells were washed twice with cold Staining Buffer

(PBS + 2 % FBS) and then resuspended in 1x Binding Buffer (Biolegend) at a concentration of 5 x 10^6 cells/ml. 100µlof the solution, corresponding to 500 000 cells, were transferred to a 5 ml tube and stained with 3 µl FITC-Annexin V and 3 µl PI. For each cell type unstained controls, as well as single staining for either Annexin V or PI, were prepared. After gentle vortexing, cells were incubated for 15 min at room temperature (RT) in the dark. 400 µl of 1x Binding Buffer are added before analyzing the samples with a flow cytometer (FACSCanto) and the FACSDiva software.

2.2.4 Viability Assay

To measure the metabolic activity of cells in SEs and the effect that irradiation treatment has on this, the CellTiter-Blue® Cell Viability Assay (Promega) was used. It is based on the metabolic conversion of a redox dye (resazurin) into a fluorescent product (resorufin) as a marker for cell viability. After cutting the SEs out of the inserts, they were transferred to flat-bottom multi-well plates and incubated in 840 µl rFAD medium and 160 µl resazurin for 1 h under standard culture conditions. 100 µl of conditioned medium from each well were then transferred to a 96-well plate and fluorescence was measured with a microplate reader (Ex= 550 nm, Em = 610 nm, 5 positions within each well).

2.2.5 ELISA

Conditioned media of SEs was taken 24 h after the last irradiation and stored at -80 °C until further use. To determine levels of secreted proteins in the conditioned media, enzyme-linked immunosorbent assays (ELISAs) were used. Detection of MMP-1 and MMP-3 was done with the Quantikine ELISA Kits (R&D Systems), TIMP-2 was analyzed with an ELISA Kit from FineTest. Media samples were diluted and then processed as described in the manufacturer´s protocol. Optical density of each well was measured on an Infinite M200 Pro Plate reader (TECAN) at 450 nm with wavelength correction at 540 nm.

2.2.6 Paraffin-embedded Material

2.2.6.1 Histological Processing

Pieces of the SEs determined for histological analysis were harvested and fixed as described in 2.2.2.3. Dehydration and paraffin infiltration of the tissue was carried out overnight in a Tissue Tek VIP® 6 AI Vacuum Infiltration Processor. The next day, samples were embedded in molten paraffin

in steel molds and left on a cooling plate to solidify. The resulting paraffin block was cut into 7 µm thick sections with a sliding microtome, sections were collected on microscope slides, dried, and kept at RT.

2.2.6.2 Hematoxylin and Eosin (H&E) Staining

The hematoxylin and eosin (H&E) staining is a classical histological staining that provides an overview of tissue structure and morphology and is widely used in medical diagnosis. Hematoxylin stains cell nuclei in a blue-purple color, while eosin stains cytoplasm and extracellular matrix in pink. The detailed protocol is given in Table 11. Visualization was done with an Axio Vert.A1 light microscope (Carl Zeiss AG).

Table 11: Protocol for hematoxylin and eosin staining

Step	Solution	Time
Deparaffinization	Roticlear	2 x 10 min
Rehydration	Ethanol 96%	2 min
	Ethanol 70%	2 min
	Ethanol 50%	2 min
	Aqua dest.	Short dip
Nucleic staining	Mayer´s hematoxylin	6 min
Blueing	Running tap water	5 min
Counterstaining	Eosin 1% (aqu.)	3 min
Washing and Differentiation	Aqua dest.	Short dip
	Ethanol 70%	Short dip
Dehydration	Ethanol 96%	2 min
	Ethanol 99%	2 min
	Isopropanol	2 x 5 min
Mounting	Isomount	Apply coverslip

2.2.6.3 Picrosirius Red Staining

Picrosirius Red staining is a widely used tool to visualize collagen I and III fibers and study the collagen network in tissue. When analyzed under polarized light collagen fibers appear green, red, or yellow. The staining protocol is described in Table 12.

Table 12: Protocol for Picrosirius Red staining

Step	Solution	Time
Deparaffinization	Roticlear	2 x 10 min
Rehydration	Ethanol 96%	2 min
	Ethanol 70%	2 min
	Ethanol 50%	2 min
	Aqua dest.	4 min
Collagen staining	Picrosirius Red	60 min
	Acetic Acid (30%)	2 x 1 min
Dehydration	Ethanol 96%	2 min
	Ethanol 99%	2 min
	Isopropanol	2 x 5 min
Mounting	Isomount	Apply coverslip

2.2.6.4 Hyaluronic Acid Staining

A hyaluronic acid (HA) staining was performed in collaboration with Dr. Daniel Gorski from the research group of Prof. Dr. Jens Fischer at the Institute for Pharmacology at the Heinrich Heine University in Düsseldorf. It was used to visualize age-dependent or radiation induced changes in HA content and distribution within the dermal equivalents. HA was detected with a two-step streptavidin-biotin-based protocol that is described in detail in Table 13. The staining procedure was performed by Dr. Daniel Gorski and pictures were taken with an Imager M2 fluorescence microscope (Carl Zeiss AG).

Table 13: Protocol for hyaluronic acid staining

Step	Solution	Time
Deparaffinization	Roticlear	3 x 15 min
Rehydration	Ethanol 100%	2 min
	Ethanol 95%	2 min
	Ethanol 70%	2 min
	PBS $^{+/+}$	2 x 5 min
Hyaluronidase treatment	Strep Hylase in PBS$^{+/+}$, 37 °C, humid environment	1 h
	PBS $^{+/+}$	2 x 5 min
Blocking	Avidin	10 min
	Biotin	10 min
	PBS $^{+/+}$	2 x 5 min
	TBS[1] (10 % FCS, 1 % BSA)	1 h
HA labelling	Hyaluronic Acid Binding Protein (Millipore) 1:200 in PBS$^{+/+}$ (1 % BSA), 4 °C, dark wet chamber	Over night
	PBS $^{+/+}$	2 x 5 min
Biotin detection	Streptavidin (Invitrogen), 1:200 in in PBS$^{+/+}$ (1 % BSA), RT, dark wet chamber	1 h
	PBS$^{+/+}$	2 x 5 min
Mounting	Fluorocare DAPI Mounting media	Apply coverslip

[1]ddH2O (2 mM Tris, 13.7 mM NaCl)

2.2.7 Cryopreserved Tissue

2.2.7.1 Indirect Immunofluorescence

Indirect immunofluorescence (IIF) was performed on frozen sections of the SEs. Sections were fixed with cool 80 % methanol (4 °C) for 10 min, followed by cool acetone (-20 °C) for 2 min. After a blocking step with 3 % BSA in PBS$^{+/+}$ for 30 min, the primary antibody, diluted in blocking

solution, was applied to the sections (25 µl/section) and incubated over night at 4 °C in a wet chamber. Next day, the slides were rinsed with 0.1 % Triton X-100 in $PBS^{+/+}$ (5 min), followed by $PBS^{+/+}$ (3 x 10 min) and a short rinse with ddH_2O, before applying the secondary antibody diluted in blocking solution. The secondary antibody was incubated for 1 h at RT in a wet chamber and then the rinsing steps were repeated as described. Finally, the slides were left to dry and then mounted with Vectashield mounting medium with DAPI (Biozol).

Modification of standard protocol: For the primary antibodies against laminin 5 and keratin 2, an additional incubation step at 37 °C for 30 min was included before the slides were put at 4 °C over night.

When staining for MMP-1, fixation was done with 4 % formaldehyde in PBS+ for 30 min followed by a permeabilization step with 0.05 % Triton X-100 and 20 mM glycine in PBS for 15 min. Primary and secondary antibody were incubated at 37 °C for 30 min before the incubation at 4 °C over night or at RT respectively.

Antibody details and appropriate dilutions are given in Table 8.

2.2.7.2 Quantitative Assessment of Proliferation

To quantitatively assess the proliferation of epidermal cells in the SEs, frozen sections were stained for Ki67 and pan-keratin. Pan-keratin staining allowed to determine the area of the epidermal compartment. Sections were analyzed with a fluorescence microscope and images were recorded at three different areas. For the quantification, the total number of epidermal cells and the percentage of Ki67-positive cells were counted semi-automatically with a macro in ImageJ, kindly provided by Dr. Damir Krunic from the German Cancer Research Center Heidelberg (for the detailed code see Table 17 in the appendix).

2.2.7.3 Nile Red Staining

Nile Red, 9-diethylamino-5H-benzo[α]phenoxazine-5-one, is a lipophilic stain that specifically stains intracellular lipid droplets. A Nile Red stock solution (500 µg/ml) in acetone was prepared and stored at 4 °C in the dark. Staining is carried out on frozen sections that were rehydrated in PBS for 5 min. Staining solution was prepared freshly by adding 20 µl/ml of the Nile Red stock solution to a 75 % aqueous solution of glycerol. One drop of the staining solution was pipetted onto each section and incubated for 10 min at RT in the dark. After rinsing the slides with ddH_2O,

sections were mounted with Vectashield mounting medium with DAPI and directly examined with a fluorescence microscope.

2.2.7.4 Gelatinase/Collagenase Activity Assay

The gelatinase/collagenase assay is used to measure and visualize enzyme activity in the SEs. Fluorescein-labeled DQ gelatin serves as a substrate that yields a fluorescent signal when digested by enzymes. Unfixed frozen sections were covered with a collagenase buffer containing 50 µg/ml DG-gelatin and 2 µg/ml DAPI, prepared from components of the EnzCheck Gelatinase/Collagenase Assay Kit (Life Technologies) and kept in a dark chamber at RT for 60 min. Without prior washing, the sections were covered with a cover slip and immediately examined with a fluorescence microscope.

2.2.8 Gene Expression Analysis

2.2.8.1 DNA and RNA Isolation

DNA and RNA were isolated from frozen tissue, separated in dermis and epidermis. As a first step, the samples needed to be homogenized. For that, zirconium oxide beads were mixed with the sample and 450 µl lysis buffer were added. After 5 min incubation, the samples were put in a tissue homogenizer (Precellys24, Bertin Instruments) that grinds the tissue by shaking with 5000 rpm for two times 15 s. The resulting supernatant contains the nucleic acids and is further processed with the innuPREP DNA/RNA Mini Kit (Analytik Jena) according to the manufacturer´s protocol. Concentrations of purified DNA and RNA were measured with a microplate reader and samples were stored at -20 °C (DNA) or -80°C (RNA). DNA was later used for Southwestern Blot, RNA was transcribed to cDNA and used for qRT-PCR.

2.2.8.2 cDNA Synthesis

RNA extracted from the dermal and epidermal tissue was transcribed to cDNA using the SensiFAST cDNA Synthesis Kit (Bioline) as described in the protocol provided with the kit. The cDNA was stored at -20 °C until it was used for qRT-PCR.

2.2.8.3 qRT-PCR

In order to quantify mRNA expression, quantitative reverse transcription PCR (qRT-PCR) was performed using the QuantiFast SYBR Green PCR Kit (Qiagen) or the AceQ qPCR SYBR® Green Master Mix (Absource Diagnostics). Reactions were prepared with 2.5 µl of each primer (forward and reverse), 7.5 µl SYBR green mix, 4.5 µl RNAse-free ddH_2O and 3 µl cDNA in 0.1 ml tube-strips, including non-template controls with ddH_2O instead of cDNA for each primer set. Used primers are listed in Table 10. The PCR was carried out in a Rotor-GeneQ PCR cycler (Qiagen) with the following program: 95 °C for 7 min, followed by 47 cycles of 95 °C for 10 sec and 60 °C for 35 sec. The cycle threshold (Ct), the cycle number at which the fluorescence signal exceeds background level, was determined. Three reference or housekeeping genes, ß-Actin, Hypoxanthin-Guanin-Phosphoribosyl-transferase (HPRT1) and Importin 8 (IPO8) were chosen to normalize the resulting Ct values. The relative fold gene expression of the gene of interest in a sample was calculated compared to the average of the control samples using the ΔΔCt method. Statistics was done with the GraphPad Prism Software by applying Turkey's multiple comparisons test as implemented in the software function two-way ANOVA.

2.2.8.4 RNA-Sequencing

RNA sequencing (RNA-Seq) is a method to analyze the transcriptome of a biological sample at a given time by using next-generation sequencing techniques and allows quantitative comparison of gene expression between different groups or treatments.

For the RNA-Seq analysis, SEs were divided in dermal and epidermal part and RNA was isolated as described before. Quality control, library construction and sequencing were performed by BGI Genomics, Hong Kong, China. Briefly, RNA quality was measured with the Agilent 2100 Bioanalyzer or Fragment Analyzer and 26 samples that met the quality requirements were used for library construction and sequencing. After mRNA capturing, fragmentation, synthesis of cDNA, adapter ligation and library amplification, sequencing was performed on the platform BGISEQ with paired-end (PE) sequencing with 100 base pairs (bp) per read (PE100).

Further processing and analysis of the raw data was conducted in cooperation with Johannes Ptok from the working group of Prof. Heiner Schaal at the Institute for Virology at the Heinrich Heine University in Düsseldorf.

Quality control checks of the raw sequencing data (GC content, base-calling quality, adapter sequence content, read length) were done with the tools FastQC (Simon Andrews, Babraham Bioinformatics) and MultiQC (Ewels et al. 2016). Adapter sequences and bases with low base-

calling quality were trimmed from the reads with Trimmomatic (Bolger, Lohse, and Usadel 2014). To sort out reads originating from rRNA, reads were aligned to a rRNA database with the help of the SortMeRNA algorithm (Kopylova, Noe, and Touzet 2012) and the respective reads were discarded. For sequence alignment, the human reference genome GRCh38, provided by the Genome Reference Consortium, was obtained from the database Ensembl (Cunningham et al. 2015).

In order to find genes that are differentially expressed across groups of samples, the software Salmon (Patro et al. 2017) was used to quantify transcript abundance from the RNA-Seq reads and generate count matrices for the differential gene expression (DGE) analysis performed with the DESeq2 software package in R (Love, Huber, and Anders 2014). Calculated p-values of the DGE and the following gene set enrichment analysis (GSEA) analysis were adjusted following the Benjamini-Hochberg method to account for the large amount of performed statistical tests. Genes with an adjusted p-value lower than 0.05 and a significant log2-foldchange unequal 0 were considered for further analysis.

To identify sets of functionally related genes that are significantly over-represented (enriched) in a list of differentially expressed genes, GSEA was done with the R package GOseq (Young et al. 2010). Gene lists of Gene Ontology (GO) terms were analyzed, that constitute commonly used categories that link genes to biological processes, cellular components or molecular functions.

To estimate the potential biological effects of observed transcriptional changes, significantly up- or downregulated genes of a sample group comparison were tested for enrichment of genes belonging to certain GO terms. The level of significance for the adjusted p-value was set to 0.05.

To visualize common patterns in gene expression of different samples and observe if sample groups cluster together in their general gene expression, Principal Component Analysis (PCA) was performed. PCA is a statistical method to reduce dimensionality of large data sets by using linear transformation that transforms the data into a new coordinate system. Multivariate data is expressed as a set of few new variables called principal components. These new variables correspond to a linear combination of the originals. The idea is to reduce the number of variables of a data set to reduce complexity and make it easier to visualize and interpret the data, while preserving as much information as possible.

2.2.9 Southwestern Blot for CPD Detection

Cyclobutane pyrimidine dimers (CPDs) were detected with a Southwestern Slot Blot approach. DNA that was extracted from the epidermis of the SEs as described in 2.2.8.1 was diluted in

DEPC-treated water to a final concentration of 400 ng in 200 µl. In a heating block, the samples were heated up to 100 °C for 10 min and then put on ice for 5 min, while the nylon membrane (Hybond-N⁺ Amersham) was equilibrated in tap water. The membrane was placed on the support plate of a slot blotting apparatus, another plate was put on top and the assembly was connected to a vacuum pump. Samples were mixed thoroughly and 100 µl were pipetted to each slot. When vacuum is applied, samples are transferred to the membrane by suction force. As soon as the samples were completely drained from the wells, the membrane was removed from the plates, placed on a filter paper and baked in an oven at 80 °C for 30 min. As a next step, the membrane was blocked in blocking buffer (TBS-T buffer with 5 % milk powder) for 1 h on a shaker, followed by incubation with the CPD antibody (TDM-2, CosmoBio), diluted 1:1000 in the blocking buffer, at 4 °C overnight. The next day, the membrane was rinsed in TBS-T three times for 10 min each. The secondary antibody (HRP-conjugated anti-mouse) was diluted 1:5000 in blocking buffer and incubated on the membrane for 1h. Rinsing steps were repeated as before. ECL solution (Western bright Advansta) was prepared by mixing component A and B 1:1 and then pipetted onto the membrane. The chemiluminescent signal was detected with the LI-COR Odyssey Imaging System and analyzed with the Image Studio software.

2.2.10 Measurement of Transepidermal Water Loss (TEWL)

A widely used indicator of an intact or impaired skin barrier is the measurement of the transepidermal water loss (TEWL). Different devices exist to measure the amount of water evaporating from the skin´s surface. Here we used the open-chamber device Tewitro® TW24 (Courage + Khazaka electronic GmbH), especially designed for the use with skin tissue models. The measurement was conducted in cooperation with Henkel AG & Co. KGaA in Düsseldorf. Four-week-old SEs were harvested, that means cut out from the inserts and transferred to 24-well plates. Remaining liquid was aspirated from the wells. The measuring device, consisting of 24 hollow cylinders with sensor inlets inside, was placed on the plate, each cylinder covering one SE. Each sensor inlet features two sensor pairs that constantly measure temperature and relative humidity, thus measuring in an indirect way the density gradient of the water evaporating from the skin samples. The humidity gradient of water evaporating from the surface of the SEs equals the TEWL typically measured on the *in vivo* skin surface in g/m²/h. To minimize environmental influences, the 24-well plate was placed in a closed chamber and on a heating plate to ensure constant temperature of 33 °C simulating *in vivo* skin temperature. TEWL values were recorded simultaneously for all 24 samples for 10 min.

3 Results

3.1 Establishment and Characterization of 3D Human Age-SEs

A previous study from our laboratory has demonstrated different phenotypes for skin equivalents (SEs) established with either young or old human dermal fibroblasts. However, these studies were performed with a scaffold-based organotypic culture model, a model that proved inadequate for demonstrating an invasive phenotype. We, therefore, utilized an alternative organotypic culture model that is based on a scaffold-free fibroblast-derived matrix, and that was shown to adequately reproduce the normal skin and skin cancer phenotype (Berning et al., 2015).

To address whether the different fibroblasts would be of phenotypic consequence also under these new conditions, we established SEs with skin equivalents with fibroblasts from a 22- or 23-year-old donor (later on termed “young”) *versus* fibroblasts from photoaged skin of a 66- or 74-year-old donor (later on termed “old”). For each experiment the dermal equivalents (DE) generated by the different fibroblasts were complemented with the same keratinocytes (NHEK, derived from young donor) because only this would allow us to attribute the contribution of phenotypic changes in the SEs to specific fibroblast populations.

3.1.1 Morphology of SEs with Young and Old Fibroblasts

SEs were generated with young (23-year-old donor) and old (74-year-old donor) fibroblasts and complemented with NHEK from a 23-year-old donor. After a co-culture time of 4 weeks the SEs were harvested and processed for further analysis. As a first step and to get a comprehensive picture of the tissue’s morphology, we processed the tissue samples for histology and analyzed H&E- stained sections of the different SEs.

Young SEs developed a well-stratified epidermis with a clearly defined basal layer, multiple spinous layers, a distinct *stratum granulosum* and a multilayered *stratum corneum* (Fig. 10A). In SEs with old fibroblasts, the keratinocytes formed a stratified, though less organized epidermis. The basal layer lacked the typical palisade-like formation, spinous and granular layer could not be clearly defined and were loosened. The *stratum corneum* was in part parakeratotic (containing remnants of nuclei) in some cultures and compressed, leading to a wavy structure (Fig. 10B).

To exclude a cell-specific phenotype, the experiments were repeated with the same cell sets as well as a second set of fibroblasts (from a 22- and 66-year-old donor), providing a similar morphology in all experiments (representative pictures also shown in Figure 10). In addition, all experiments were performed with a different keratinocyte strain (NHEK from a 43-year-old donor).

Altogether, this clearly demonstrated that the phenotypic differences of the epidermis of SEs induced by old *versus* young fibroblasts, were highly reproducible for different experiments (little interexperimental variation), different old and young fibroblast strains, and different NHEK strains (little interpersonal variation). With that, the fdm-based Age-SEs proved as highly stable and suitable model for our further studies.

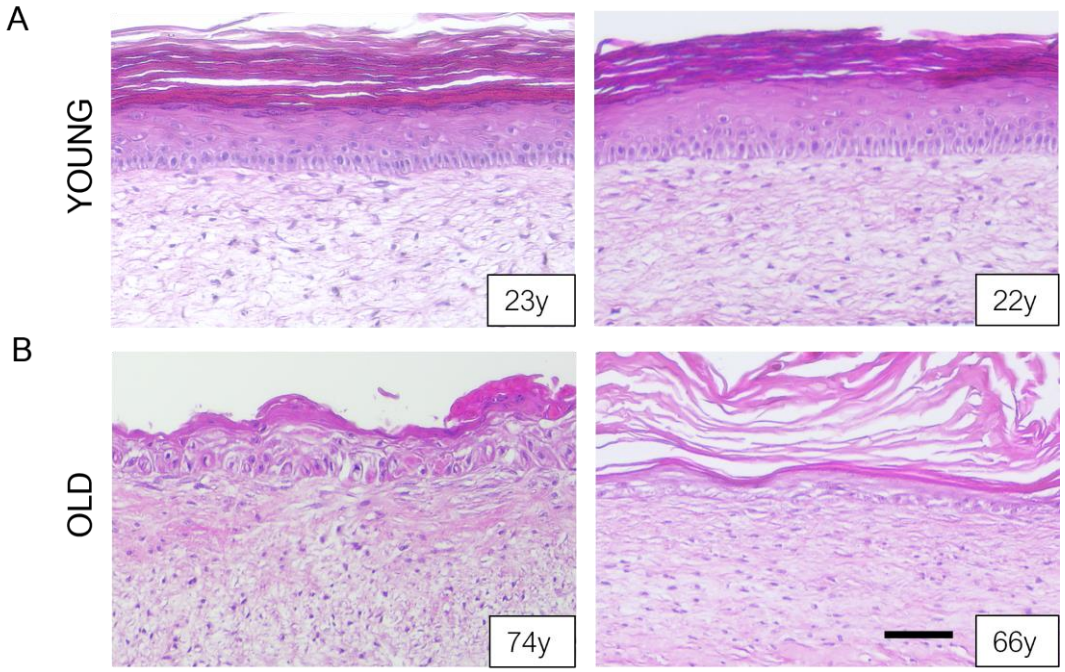

Figure 10: Histology of young and old Age-SEs
fdmSEs were established with either (**A**) young (22- or 23-year-old donor) or (**B**) old (66- or 74-year-old donor) fibroblasts and identical young keratinocytes. H&E staining was performed on paraffin sections. Displayed are representative histological images of young and old SEs after 4 weeks of co-culture, demonstrating an impaired epidermal differentiation and stratification of SEs based on old fibroblasts. The scale bar represents 100 µm.

3.1.2 Characterization of the Young and Old Phenotype

To define the phenotypic differences of the young *versus* old Age-SEs more precisely, we studied the different components of the SEs in more detail.

3.1.2.1 Epidermal Differentiation

First, we analyzed the epidermis by comparing the expression pattern of different keratins by immunofluorescence microscopy. A common marker for early epidermal differentiation is keratin

10 (K10), which is expressed in all suprabasal layers of normal human epidermis. Accordingly, young SEs showed a perfect distribution of K10 with all suprabasal layers being strongly positive while the *stratum corneum* remained unstained. In old SEs, K10 was expressed only in the upper spinous layers (delayed expression) and because of not being properly removed, was still detectable in the parakeratotic stratum corneum (Fig. 11A). Keratin 15 (K15), a marker for basal keratinocytes, was predominantly expressed by the basal keratinocytes of the young SEs, though some expression was still seen suprabasally, demonstrating that the regulation of this epidermal keratin was not yet perfect as compared to skin *in situ*. In old SEs, K15 was expressed throughout the epithelium correlating well with the delayed expression of K10 (Fig. 11B). Keratin 2 (K2), a marker for late terminal epidermal differentiation, and expressed in the *stratum granulosum* of the epidermis *in situ*, was seen in the epidermis of the young SEs also in the upper suprabasal layers and the *stratum corneum* though there was some accumulation at the transition from the vital to the cornified part of the epidermis (Fig. 11C). In old SEs, K2 was mostly absent, demonstrating a clear deficiency in epidermal differentiation due to the interaction with the old fibroblasts. This deficiency in epidermal differentiation similarly accounted for SEs with fibroblasts from the second old donor, thus excluding a "donor-specific defect" but arguing for a common impairment of the old fibroblasts in supporting epidermal differentiation.

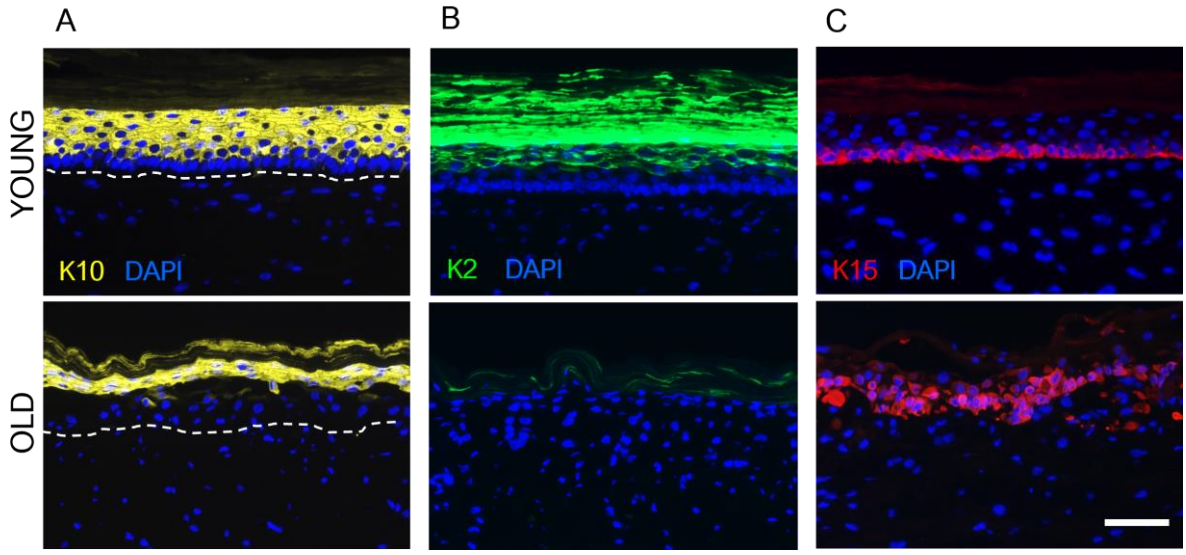

Figure 11: Epidermal differentiation of young and old Age-SEs
fdmSEs were established with either young (upper row) or old (lower row) fibroblasts and identical young keratinocytes. IIF staining for the differentiation markers (**A**) keratin 10, (**B**) keratin 2 and (**C**) keratin 15 was performed on frozen sections. Displayed are representative images of young and old SEs after 4 weeks of co-culture, demonstrating an impaired ability of old fibroblasts to support proper epidermal differentiation. Dashed white line indicates DEJ. The scale bar represents 100 µm.

3.1.2.2 Basement Membrane Composition

The dermal and epidermal compartment are connected by the basement membrane (BM), a highly specialized network of different ECM molecules. Both dermal fibroblasts and epidermal keratinocytes contribute to the formation of the BM. Three important markers are collagen type VII (ColVII), which is the major component of the anchoring fibrils, laminin-5 (=Laminin-322), a part of the *lamina densa*, important for epidermal cell adhesion and key component of the anchoring complex, and collagen type IV (ColIV), the most abundant constituent of the BM. In young SEs ColVII (Fig. 12A) and laminin-5 (Fig. 12B) were expressed as a continuous line along the dermal-epidermal junction (DEJ), which suggests a proper BM assembly. In old SEs, on the other hand, ColVII expression was reduced and more fragmented (Fig.12A). Laminin-5, unexpectedly, was rather increased (Fig. 12B). However, the expression appeared disorganized and inappropriately assembled. In several areas, we even saw duplication of the *lamina densa*, a finding which is also reported in previous studies (Amano et al. 2001). ColIV was expressed abundantly in young SEs (Fig. 12C). The strongest expression focused on the area of the DEJ but ColIV was also found in the entire DE. In old SEs the total expression of ColIV was reduced, but it still accumulated in the DEJ area (Fig. 12C). The appearance of ColIV in the entire DE instead of only at the BM is a known phenomenon in this specific model that is due to the fibroblasts permanently being in an activated state. Taken together, the expression pattern of the different BM components indicated a major impact of the fibroblast age also on the BM formation, with young fibroblasts providing an optimal support while the old fibroblasts show distinct deficits, causing an aberrant BM formation.

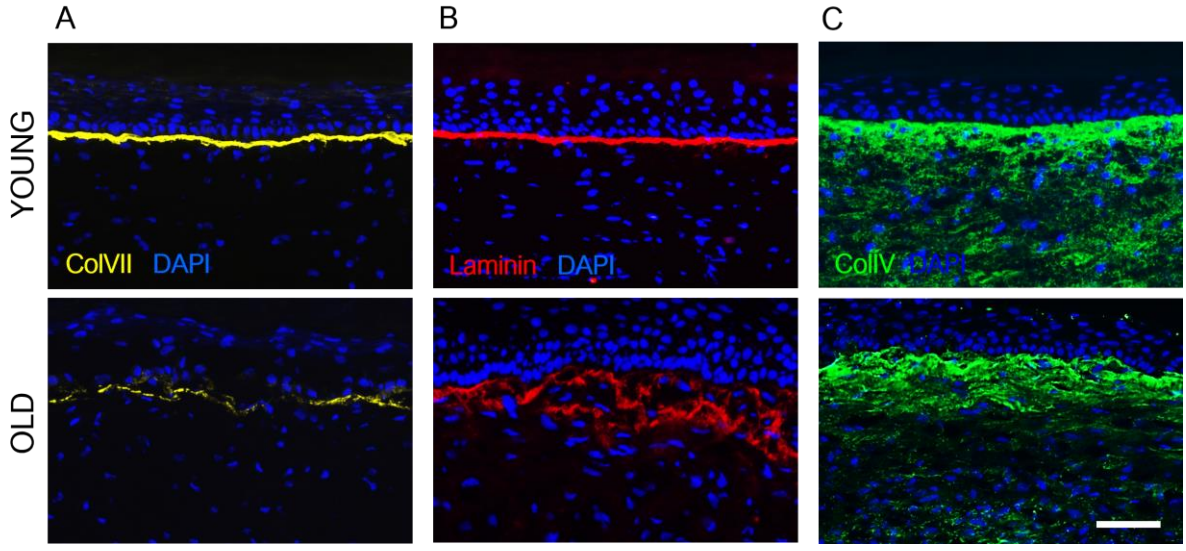

Figure 12: Basement membrane formation in young and old Age-SEs
fdmSEs were established with either young or old fibroblasts and identical young keratinocytes. IIF staining was done for the BM markers (**A**) collagen type VII, (**B**) laminin-5 and (**C**) collagen type IV. Displayed are representative images of SEs after 4 weeks of co-culture. In old SEs, the expression pattern of these markers indicates an inappropriate assembly of the BM components. Scale bar represents 100 µm.

3.1.2.3 Composition of the Dermal Equivalent

To characterize the fibroblasts as the responsible factor for forming a DE that is able to provide the basis for a proper interaction with the epidermal keratinocytes, we first stained the SEs for vimentin, the major intermediate filament component of the mesenchymal cells.

In young SEs the vimentin staining showed an even distribution of fibroblasts in the DE (Fig. 13A). In old SEs, fibroblasts were also evenly distributed but we found an increased expression and accumulation of vimentin in the individual cells (Fig. 13A). The staining also displayed changes in cell size and shape, resembling the typical morphology of myofibroblasts, also known as "activated fibroblasts". Myofibroblasts that exhibit contractile properties, generally are only present in human skin during wound healing when they are involved in remodeling of the ECM and where their persistence can result in tissue stiffening and fibrosis (Tomasek et al. 2002). To determine the nature of these cells, SEs were stained for the myofibroblast marker α-smooth muscle actin (α-SMA). While there was no α-SMA detectable in any of the young SEs, it was highly expressed in the old ones (Fig. 13B). Here, α-SMA+ cells represented about a third to a half of the dermal fibroblasts, or even more in some cultures, and were particularly concentrated in the upper half of the DE in close vicinity to the BM and epithelium. This suggested that the fibroblasts established from the old donors and characterized for a myo-chondro-fibroblast phenotype, as described previously (Gundermann 2012), maintained their specific differentiation also in the fdm-based SEs.

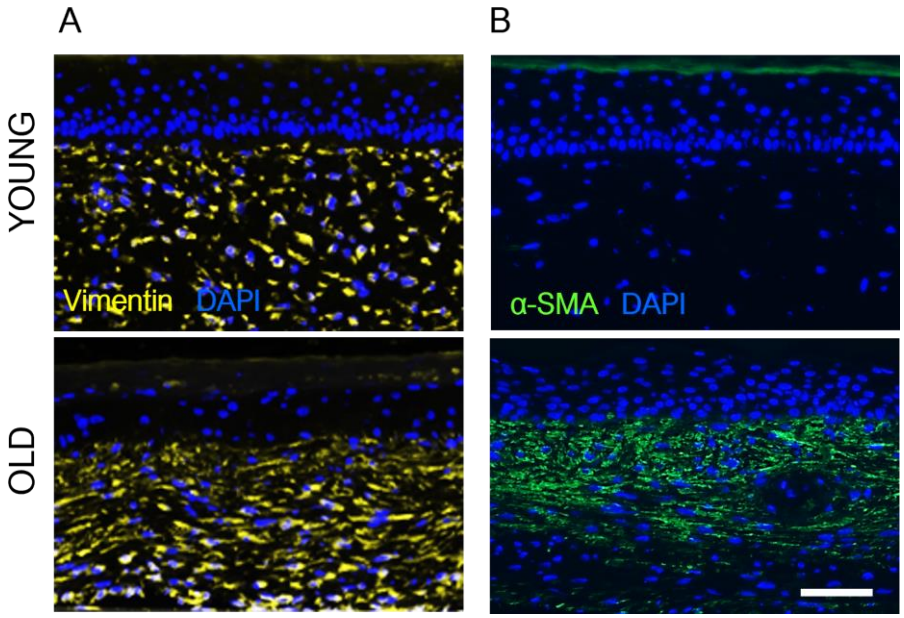

Figure 13: Fibroblast morphology and myofibroblast differentiation in young and old Age-SEs
fdmSEs were established with either young (upper row) or old (lower row) fibroblasts and identical young keratinocytes. IIF staining for (**A**) the fibroblast marker vimentin and (**B**) the myofibroblast marker a-SMA was performed on frozen sections. Displayed are representative images of young and old SEs after 4 weeks of co-culture. Vimentin staining showed differences in cell size and shape and a-SMA staining confirmed the presence of myofibroblast only in old SEs. The scale bar represents 100 µm.

To test this further, we next analyzed the SEs for a number of ECM components. In our model of fdm-based SEs, the ECM is completely cell-derived, with all components being produced by the fibroblasts. The major component of the dermal ECM is collagen, with collagen type I (ColI) being the most abundant, making up to 90% (Shin et al. 2019). Collagens, together with many other components including elastic fibers, form a dense meshwork giving skin its structure and mechanical properties. To evaluate collagen content and organization of the dermal equivalents, SEs were investigated for the expression and distribution of collagen type I and III by immunohistochemical staining of frozen sections for ColI and staining of histological (paraffin) sections with Picrosirius Red. When exposed to polarized light, this special stain enhances the natural birefringence of collagen, so collagen bundles appear yellow-red (ColI) or green (ColIII) (Junqueira, Bignolas, and Brentani 1979). It needs to be mentioned that some studies report that polarized colors are not suitable to differentiate collagen types but only reflect fiber thickness and packing (Lattouf et al. 2014).

Staining for ColI showed that this collagen was abundantly expressed in young SEs, forming a very dense meshwork of collagen fibers throughout the dermal compartment. The collagen meshwork in old SEs, on the other hand, was less dense and frequently showed gaps, particularly in the upper half of the DE, suggestive for a lack of collagen fibers in those areas (Fig. 14A).

This pattern was confirmed with Picrosirius Red staining, which similarly illustrated a higher overall collagen content in young SEs as well as the looser meshwork with larger gaps in the old SEs (Fig. 14B). Visualized under polarized light, the differences between young and old SEs became even more obvious. DEs of the young SEs showed the typical dermal collagen distribution with thinner fibers in the upper part of the DE, just beneath the epithelium, and thicker collagen bundles in the middle and lower part of the DE, representing the reticular dermis. The old SEs were characterized by a strong reduction in collagen. In the upper part of the DE, collagen fibers were present in good amounts but aligned differently than in young DEs. In the middle part of the DE, collagen was drastically reduced with only fiber fragments being scattered throughout the DE (Fig. 14C).

In addition to alterations in the collagen network, skin aging is also associated with loss of moisture content. Hyaluronic acid (HA), a glycosaminoglycan, plays a key role in binding and retaining water molecules and therefore maintaining hydration of the skin. Thus, to investigate if differences exist in the HA content of our young and old SEs, we initiated a cooperation project with Dr. Daniel Gorski from the research group of Prof. Dr. Jens Fischer at the Institute for Pharmacology at the Heinrich Heine University Düsseldorf. Staining of young SEs clearly demonstrated an even and high level of HA expressed throughout the DE. In old SEs, the amount of HA was strongly decreased. Moreover, the distribution appeared more uneven and patchy, with areas that contained almost no HA (Fig.14D).

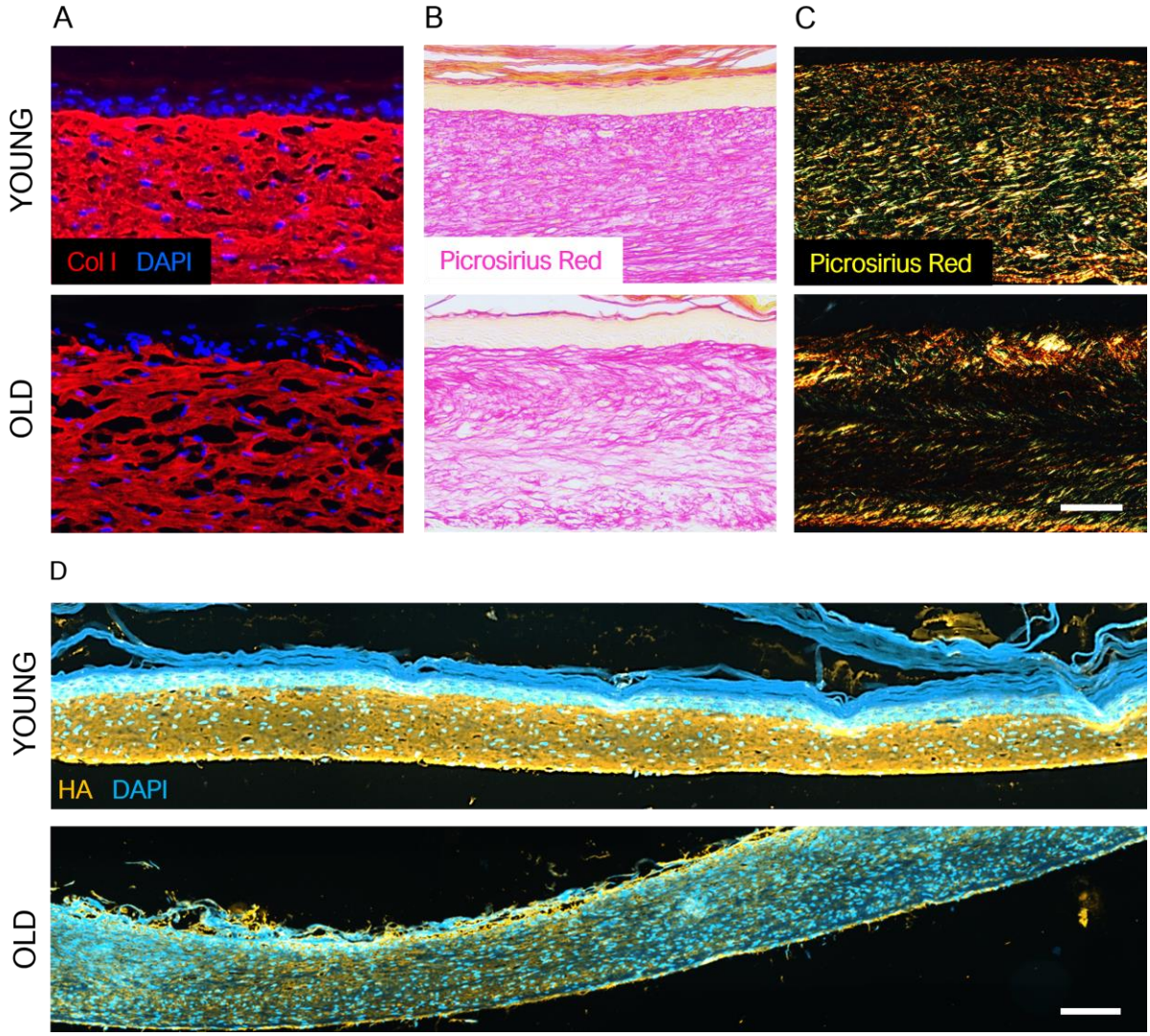

Figure 14: Composition of the dermal ECM in young and old Age-SEs
fdmSEs were established with either young or old fibroblasts and identical young keratinocytes. IIF staining for (**A**) collagen type I was performed on frozen sections, (**B,C**) Picrosirius Red staining and (**D**) IIF staining for hyaluronic acid was performed on paraffin sections. Picrosirius Red staining was analyzed under (**B**) a normal light microscope and under (**C**) polarized light. Displayed are representative images of young and old SEs after 4 weeks of co-culture. Both Col I and Picrosirius Red staining show a reduction of collagen fibers with a less dense fiber meshwork in the old SEs compared to young SEs. HA expression is drastically reduced in old SEs. The scale bar represents 100 µm in A-C and 200 µm In D.

In the primary characterization of the old fibroblasts used in this study a novel “aging phenotype” was identified, demonstrating expression of matrix proteins typical for chondrocyte differentiation (Gundermann 2012). Amongst others, this included aggrecan (ACAN) and collagen type XI (ColXI). To determine whether these specific matrix proteins were expressed also in our model of old SEs, immunofluorescence analyses was performed for the two ECM markers. Staining of the DEs with old fibroblasts highlighted a strong expression of aggrecan (Fig. 15A) as well as ColXI

(Fig. 15B). In young SEs, on the other hand, aggrecan and ColXI were not expressed or only present in minor amounts. Thus, with these studies we could confirm that the original phenotype of the respective fibroblast was maintained in the SEs and with that making these perfect models for further analyses.

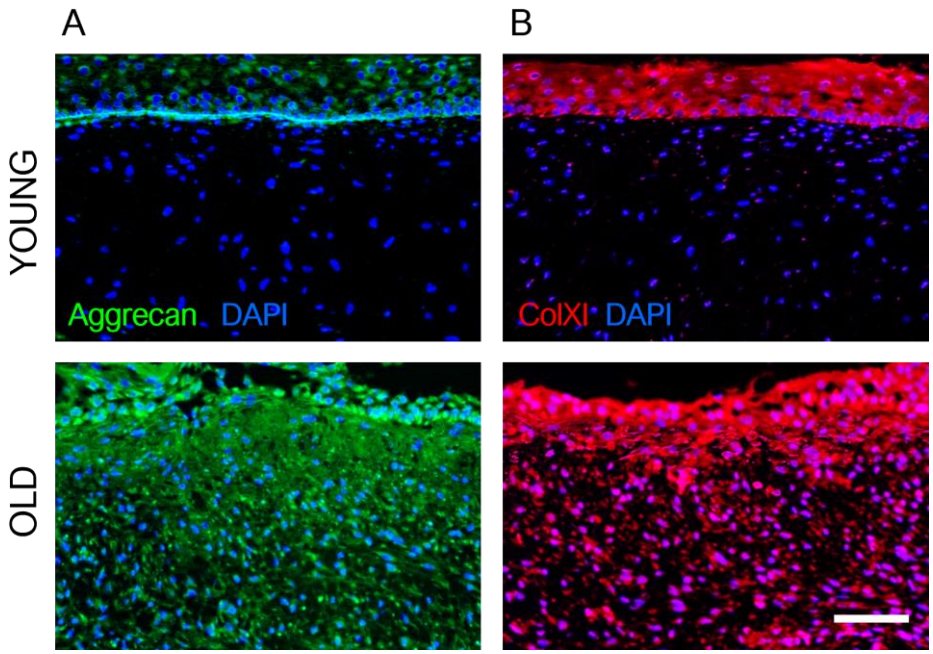

Figure 15: Chondrogenic matrix components in Age-SEs
fdmSEs were established with either young (upper row) or old (lower row) fibroblasts and identical young keratinocytes. IIF staining for the chondrogenic matrix proteins (**A**) aggrecan and (**B**) collagen type XI was performed on frozen sections. Displayed are representative images of young and old SEs after 4 weeks of co-culture. Vimentin staining showed differences in cell size and shape and a-SMA staining confirmed the presence of myofibroblast only in old SEs. The scale bar represents 100 µm.

Together, the evaluation of major ECM components clearly shows that young and old fibroblasts produce a markedly different DE. The aged ECM is characterized by a reduced collagen and HA content and instead the expression of proteins typical for chondrogenic differentiation that are not found in young SEs. Moreover, the old DE contains a large fraction of myofibroblasts which are not present in the young DE and most likely have implications for the tissue function.

3.1.3 Viability of Young and Old SEs

FdmSEs with young fibroblasts have been shown to be viable and regenerative for up to 24 weeks (Berning et al. 2015). As histological stainings demonstrated an impaired ability of the old fibroblasts to provide adequate support for the epidermis, it needed to be assessed if the viability of the old SEs is also maintained over the course of several weeks to ensure they can be used for long-term studies. Therefore, SEs were analyzed using the CellTiter-Blue® assay (Promega). The included dye resazurin is reduced to fluorescent resorufin by the mitochondrial respiratory chain in living cells and the resulting signal is proportional to the number of viable cells. Viability of young and old SEs was determined after two, three and four weeks of co-culture. At all time-points, viability was higher in the young SEs than in the old. After a slight decrease from week two to week three for both young and old SEs, viability remained stable further on until week four (Fig. 16).

These results suggests that even though old fibroblasts are not able to support epidermal regeneration the same way the young ones do, the old SEs are still viable and stable over the course of at least four weeks, making them a suitable model for the subsequent "long-term" irradiation experiments.

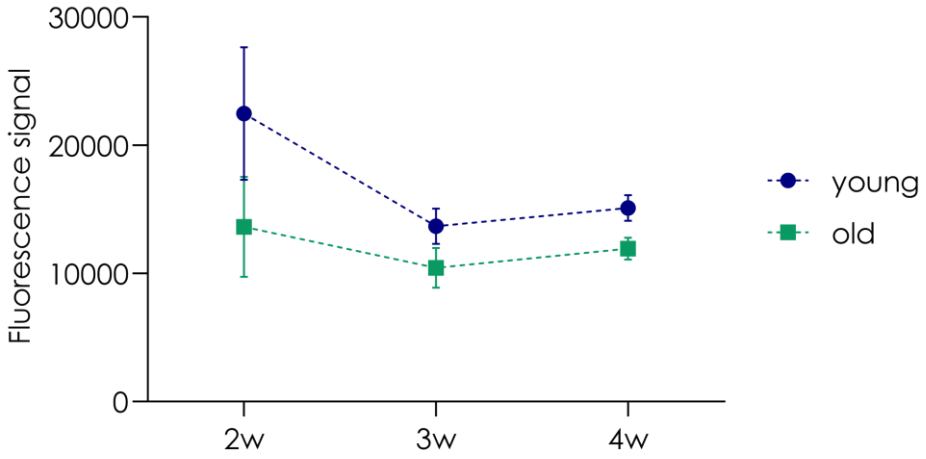

Figure 16: Viability of young and old Age-SEs over time
Viability of young and old SEs was determined by measuring metabolic activity with the CellTiter-Blue® assay after 2, 3 and 4 weeks of co-culture. Indicated values represent the measured fluorescence signal minus negative (no cell) control. N = 3 for each data point.

In essence, Age-SEs could successfully be established with young and old fibroblasts. They showed long-term viability and stable and specific "young" and "old" phenotypes, thereby reproducing many features of young and photoaged skin, respectively.

3.2 Impact of Chronic Solar Radiation and Solar UV Radiation on Young and Old Age-SEs

As seen in the previous experiments, the old fibroblasts produce a different dermal ECM than the young fibroblasts and the type of fibroblast also has functional consequences for the epidermis and BM formation. To explore the role of fibroblast age and the respective ECM they produce for the response to sun exposure, we next exposed Age-SEs to chronic (repetitive) irradiation.

The question to be addressed was if the response to solar radiation differs between young and old SEs and whether the age-dependent changes characteristic for the old SEs are of functional consequence for the epidermal and dermal damage profile upon irradiation. Assuming that solar radiation is the possible inducer of photoaging and as such responsible for the phenotype observed in the old SEs, it was similarly investigated whether chronic irradiation with the protocol used here, is able to induce such changes also in young SEs.

From experiments performed by Dr. Elizabeth Pavez Lorie in the laboratory, it has become clear that a single dose of solar UV radiation (= UVA+UVB) or the entire solar spectrum (= UVB+UVA+VIS+IRA) further on called SUN, is affecting the tissue in the SEs, however, damage is repaired immediately and does not lead to long-term changes (Pavez Lorie, personal communication). Therefore, the goal of this study was to perform chronic irradiation and thus ask for stably induced changes.

SEs were established with fibroblasts from one young and one old donor and after a co-culture time of two weeks with the same young keratinocytes, the SEs were irradiated with 1 MED (minimal erythema dose) of either UVA+B or SUN

3.2.1 Effect of Irradiation on the Viability of SEs

The dose of 1 MED was chosen for the chronic irradiation as a physiological dose, relevant for human exposure *in vivo*. Still, it needed to be assured that this dose is tolerable also for the "reconstructed skin", namely for both the young and the old SEs. Massive cell death would clearly be inappropriate to study UV-dependent regulations. To analyze whether irradiation would affect viability of the SEs, we again used the CellTiter-Blue® assay (Promega). Non-irradiated control SEs were compared to SEs irradiated repeatedly three times a week for two weeks with 1 MED of SUN. Six independent replicates were analyzed for each condition.

In young SEs, the irradiation did not lead to a reduction of mean viability. The same was found in old SEs, not suggesting a toxic effect of the irradiation in either of the SEs (Fig. 17). In controls as

well as irradiated samples viability of old SEs was lower than that of young SEs but also this trend was not statistically significant. The variance between samples was quite high in irradiated old SEs, indicating that some cultures were affected more than others and suggesting for a higher potential for instability in the old SEs.

Taken together, irradiation of both the young and old SEs does not cause a significant decline in viability. 1 MED is therefore a tolerable dose for the SEs and was accordingly used for all further chronic irradiation experiments.

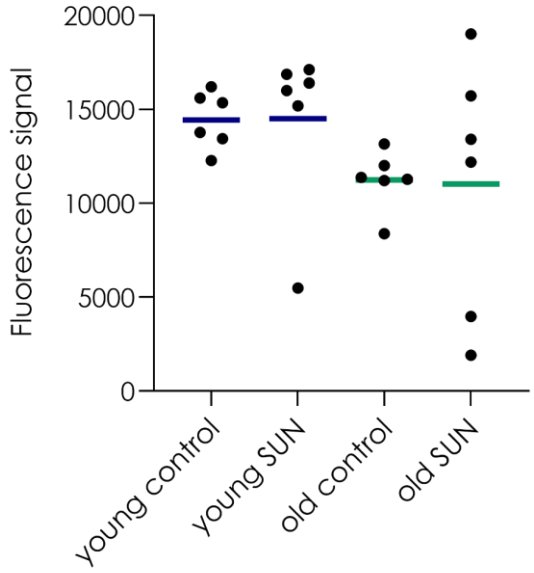

Figure 17: Influence of irradiation on viability of young and old Age-SEs
Viability of young and old SEs was determined by measuring metabolic activity with the CellTiter-Blue® assay. Non-irradiated controls were compared to cultures chronically irradiated with SUN for 2 weeks and viability was determined 24h after the last irradiation. Viability was lower in old SEs than in young, but the difference was not statistically significant. Irradiation did not affect mean viability. Indicated values represent the measured fluorescence signal minus negative (no cell) control. Black dots: fluorescence intensity of one sample (n). Blue/green line: mean fluorescence intensity of all samples, n=6. One-way ANOVA, all n.s.

3.2.2 Induction of DNA Damage (CPDs)

Exposure to solar radiation is known to cause a variety of DNA lesions, one of the predominant being cyclobutane pyrimidine dimers (CPDs) (Brash 2015). These photoproducts typically lead to cytosine (C)-to thymine (T) or CC-to-TT transition mutations that are referred to as UV signature mutations. The induction of these CPDs by irradiation with UVA+B or SUN was measured in young and old SEs.

A quantitative assessment of CPD induction was done by Southwestern Blot to compare damage induction by UVA+B and SUN in young and old SEs. Second, and to visualize the localization of the CPDs within the tissue, IIF staining with a specific antibody for CPDs was used.

Two independent experiments with three independent biological replicates for each condition were analyzed by Southwestern Blots (Fig. 18A). The two experiments comprised SEs with fibroblasts from two different young (22- and 23-year-old) and two different old donors (66- and 74-year-old). The SEs had been irradiated chronically for two weeks and the analysis was performed 24 hours after the last irradiation. As CPD induction is expected in the epidermis, the DNA was isolated from the epidermis that had been enzymatically separated from the DE. The Southwestern Blots clearly demonstrated hardly any CPDs in the non-irradiated control samples from young and old SEs. Exposure to UVA+B as well as SUN strongly induced CPD formation in young and old SEs. UVA+B treatment tended to result in higher CPD induction than irradiation with SUN. This trend was observed in both experiments and for young as well as old SEs, but the difference was only significant in one case (old, experiment II).

Staining for CPDs in tissue sections of the different SEs confirmed the above findings (Fig. 18B). While young control SEs were almost completely negative, UVA+B irradiation as well as SUN irradiation led to a clear induction of CPDs. As to be expected, positive cells were found in the basal and suprabasal layers of the epidermis. Interestingly, an induction of CPDs was also detected in the dermis. Most of the positive cells were found either in the uppermost layers of the epidermis or in the dermis. For the old SEs, the same pattern was seen. No CPDs were detected in the control samples. UVA+B as well as SUN strongly induced CPDs, especially in the upper epidermis and in the dermis. The stainings did not show clear differences in the amount or localization of induced CPDs between young and old or UVA+B or SUN exposed SEs.

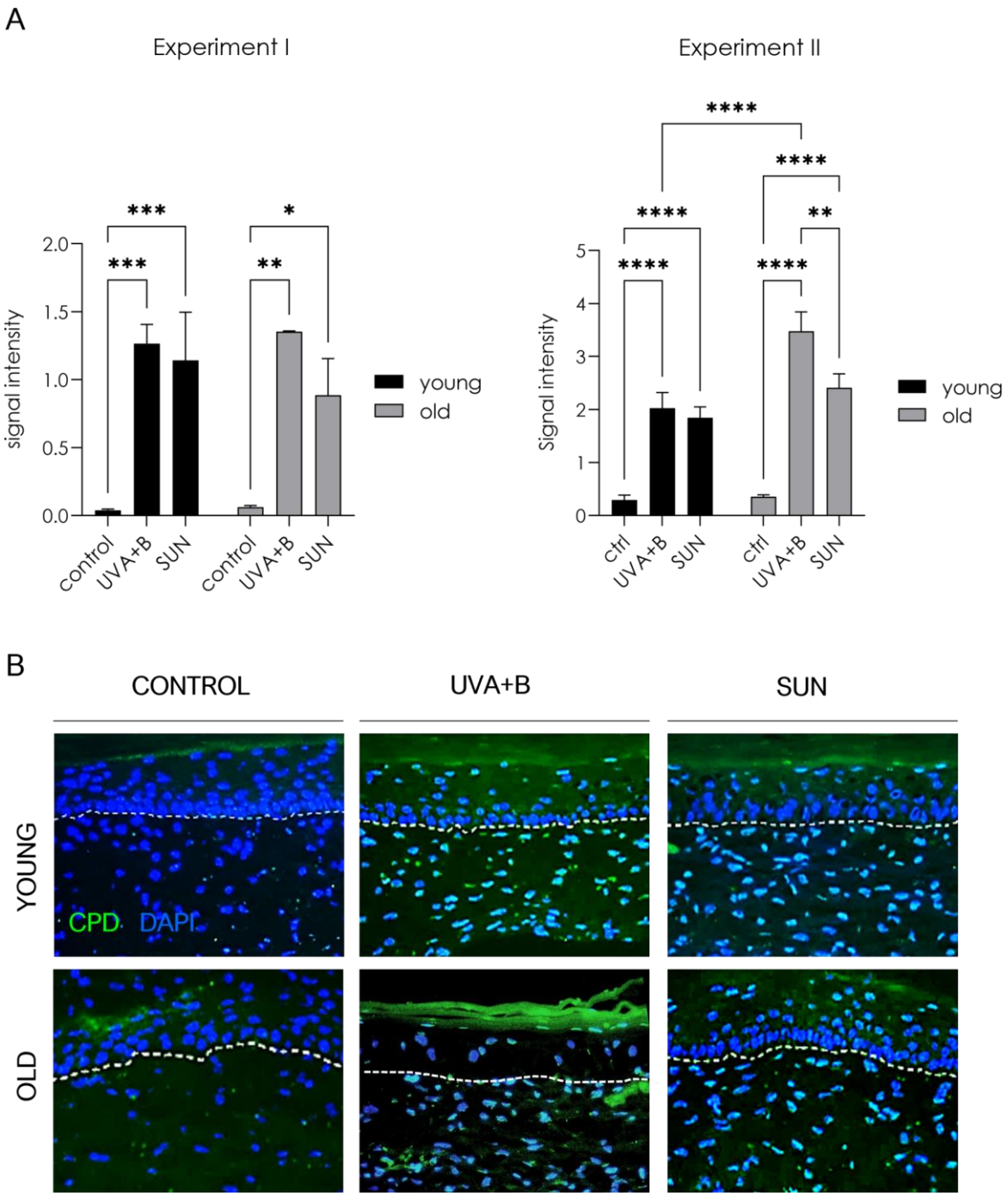

Figure 18: Induction of CPDs by irradiation in young and old Age-SEs

Young and old SEs were chronically irradiated with either the solar UV spectrum (UVA+B) or the entire solar spectrum (SUN) over the period of two weeks and compared to non-irradiated controls. Induction of CPDs was assessed 24 h after the last irradiation. (**A**) Southwestern Blot for two independent experiments. CPDs were detected in epidermal DNA by an anti-CPD antibody and the chemiluminescent signal was quantified by LI-COR Imaging System. Irradiation led to a strong induction of CPDs in young and old SEs with the trend of stronger induction with UVA+B. Error bars represent the standard error mean. Two-way ANOVA; * = p-value < 0.05; ** p-value < 0.01; *** p-value < 0.001; **** = p-value < 0.0001; n=3 (**B**) CPD formation was also evaluated by IIF staining on paraffin sections. Displayed are representative images, showing an induction of CPDs by irradiation in the epidermis, but also in the DE of young and old SEs.

3.2.3 Epidermal Proliferation Rate (Ki67)

Chronically sun-exposed skin usually shows epidermal hyperplasia, a thickening of the epidermis caused by increased proliferation of the keratinocytes. In order to assess the influence of chronic irradiation on the proliferative behavior of the cells in the SEs, the expression of the proliferation marker Ki67 was analyzed and quantitatively evaluated as described in the methods section. SEs with young and old fibroblasts (22- and 66-year-old donor) were analyzed after 2 weeks of chronic irradiation. Proliferation was quantified 24 h after the last irradiation, taking three or four replicates for each treatment and imaging three areas of each section. The total number of epidermal cells and the percentage of Ki67-positive cells was counted semi-automatically with a macro in ImageJ. To assess whether the response to irradiation would be donor specific, the analysis was repeated with a second set of cells (23- and 74-year-old donor) with very similar results. Both experiments were combined in Figure 19A.

Positive, i.e. proliferating cells were mostly found in the basal layer of the epidermis. In young SEs, the percentage of proliferating cells was quite stable at around 10 % in both analyzed experiments and was not significantly affected by the different irradiation regimes (UVA+B or SUN). In old SEs the number of proliferating cells was generally less than in the young SEs. However, the irradiation again did not affect the proliferation ratio, neither UVA+B nor SUN (Fig. 19A).

In a second experimental setup, proliferation in young SEs was followed up for six weeks (Fig. 19B). Again, proliferation ratio was assessed 24 h after the last irradiation. At all analyzed timepoints (2, 4 and 6 weeks) the rate of Ki67+ cells was around 10 % and not significantly altered neither by irradiation nor over time, indicating an ongoing regeneration of the epidermis.

The Ki67 analysis suggests that there is no significant regulation of epidermal proliferation by UVA+B or SUN in the Age-SEs. A reason for that might also be the time point of analysis 24 h after the last irradiation. In previous experiments in our group, it was observed that proliferation is reduced after one acute irradiation and then returns to baseline after 24h. That means a change in proliferative behavior could occur directly after the irradiation and is already recovered after 24 h.

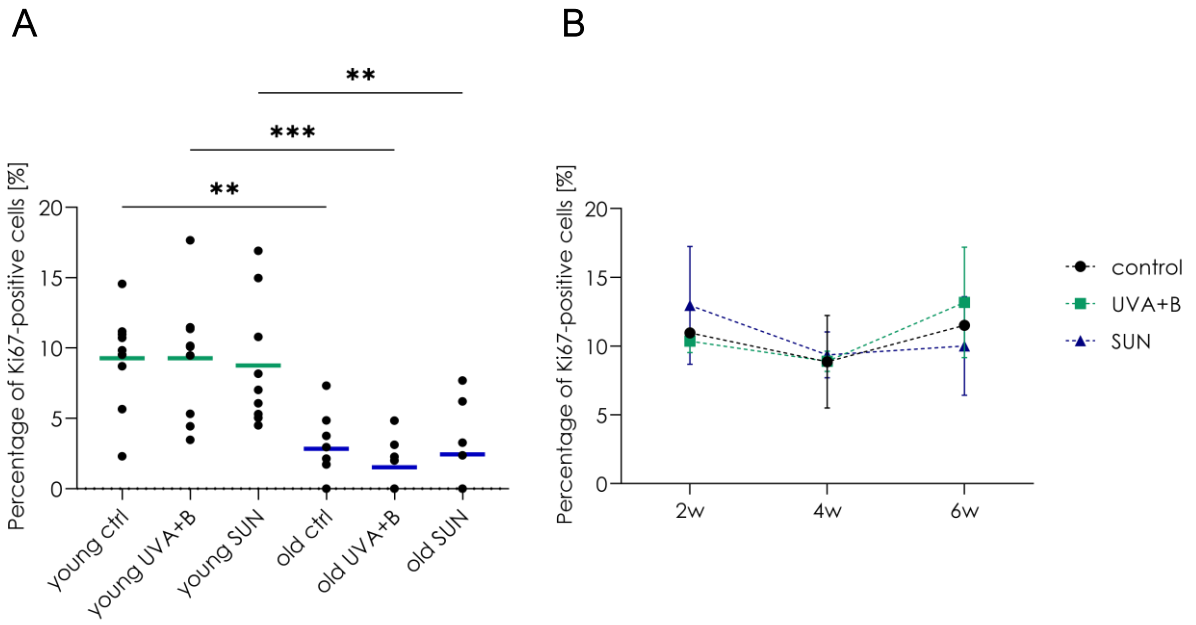

Figure 19: Proliferation rate of epidermal cells in response to irradiation
Proliferation of epidermal cells was determined in non-irradiated control SEs and SEs chronically irradiated with UVA+B or SUN for 2 weeks. The rate of proliferating cells was assessed 24h after the last irradiation by staining frozen sections for pan-keratin and Ki67 and counting all epidermal cells and Ki67+ cells with an ImageJ macro. (**A**) Proliferation rate of young versus old SEs. Black dots: percentage of Ki67+ cells of one sample (n). Blue/green line: mean of all samples. Proliferation in young SEs was higher (around 10%) than in old SEs (around 2 %), but in both cases the rate was not affected by irradiation. Depicted is the combined data of two independent experiments. young: n=9, old: n=8. (**B**) Proliferation rate of young SEs over a timecourse of 6 weeks. N=3 for each data point. Proliferation rate did not differ significantly but stayed quite stable at around 10% irrespective of the treatment. Two-way ANOVA; * = p-value < 0.05; ** p-value < 0.01; *** p-value < 0.001; **** = p-value < 0.0001.

3.2.4 Effect of Irradiation on the Morphology of Young and Old SEs

To evaluate the possible effects that irradiation with UVA+B or SUN has on the morphology of young and old Age-SEs, histological H&E stainings of tissue sections were analyzed after two and four weeks of chronic irradiation and compared to non-irradiated controls.

The well-established epidermis found in SEs with young fibroblasts was not affected by the irradiation. All cultures looked perfectly stratified after two (Fig. 20A) and four weeks (Fig. 20B) of irradiation with UVA+B or SUN and displayed clearly defined layers: The basal layer, marked by the typical palisade-like formation of cells, several layers of a *stratum spinosum*, a *stratum granulosum* that is characterized by flattened cells that contain keratohyalin granules, and several layers of a cornified *stratum corneum.*

Old SEs, as described before, produced a less organized epidermis, lacking the clearly defined layers and in many cases showing a compressed and wavy, partly parakeratotic *stratum corneum*, or, in other cases, an atrophic epithelium. Upon irradiation with UVA+B, the organization of the epidermis surprisingly seemed to slightly improve and the *stratum corneum* formation normalized (Fig. 20A). In old SEs irradiated with SUN, this improved stratification and differentiation was usually more pronounced than with UVA+B. The arrangement of the cells of the basal layer resembled the palisade-like formation in young SEs and few flattened granula-containing cells insinuated a *stratum granulosum.* These improvements were similarly observed after four weeks (Fig. 20B). This surprising finding was first observed with the first set of young and old fibroblasts (23- and 74-year-old donors). To verify this phenotype, the experiment was repeated four times with the same fibroblasts and again two times with a second set of fibroblasts (22- and 66-year-old donors). To also exclude cell-specific effects of the keratinocytes, three different keratinocyte strains were used in these experiments. All these experiments provided very similar results, indicating that the improved epidermal organization upon irradiation (especially with SUN) is a reproducible phenotype.

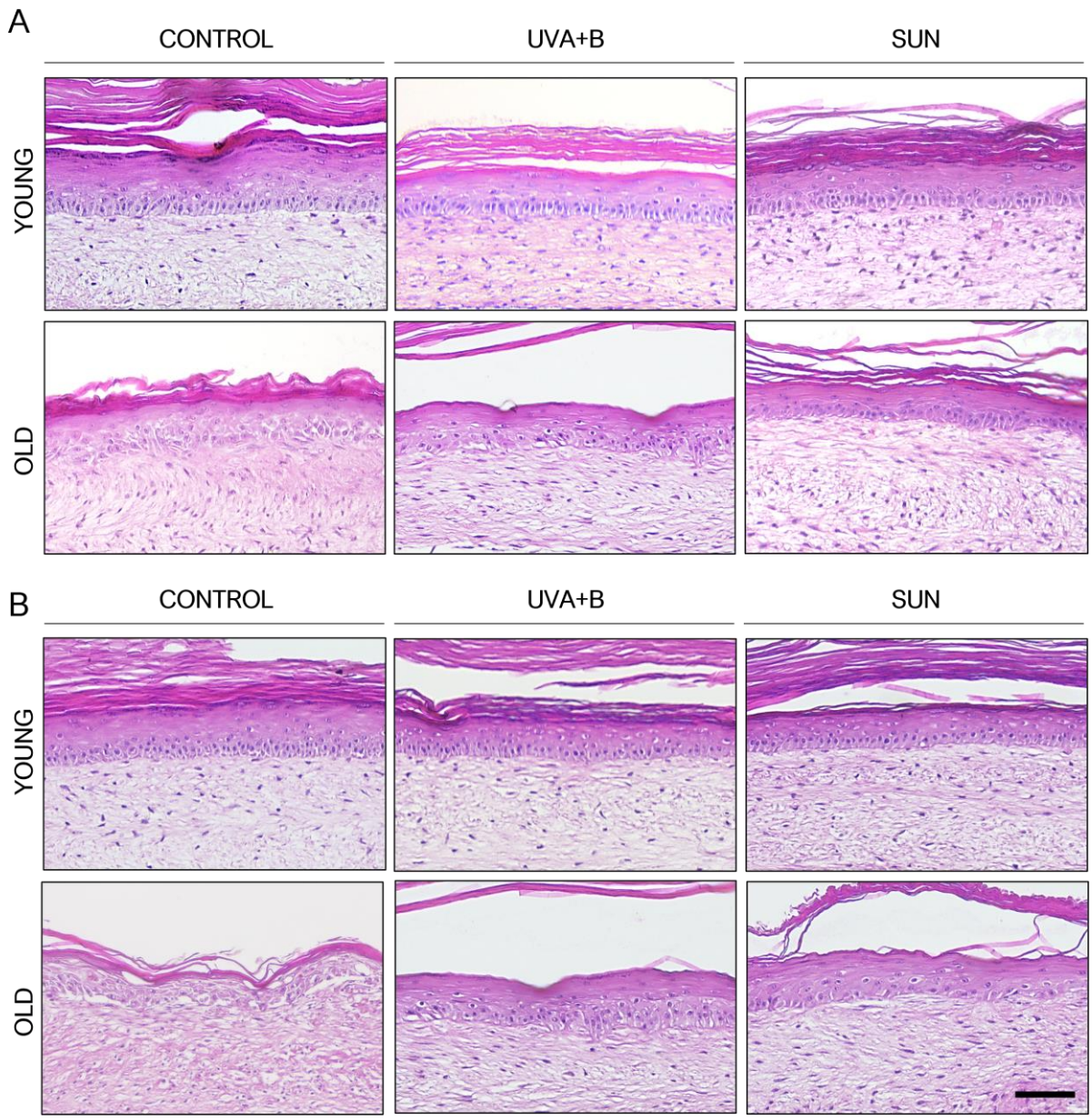

Figure 20: Effect of irradiation on histology of young and old Age-SEs
Young and old SEs were chronically irradiated with either the solar UV spectrum (UVA+B) or the entire solar spectrum (SUN) over the period of (**A**) 2 weeks or (**B**) 4 weeks. H&E staining was performed on paraffin sections. Displayed are representative images of control versus irradiated cultures. No obvious morphological changes were observed in young SEs, whereas differentiation and stratification were improved in old SEs upon irradiation. The scale bar represents 100 µm.

3.2.5 Effect of Irradiation on Epidermal Differentiation

To assess the epidermal response to irradiation, the expression of the previously described markers for early differentiation, keratin 10 (K10), late differentiation, keratin 2 (K2), and the basal keratinocytes, keratin 15 (K15), was investigated after two weeks of chronic irradiation.

In young SEs, the expression of all markers in irradiated samples recapitulated the expression pattern seen in the unirradiated controls: K15 was expressed mostly in the basal cells (Fig. 21A), K10 was strongly expressed in all suprabasal layers, excluding the *stratum corneum* (Fig. 21B) and K2 was found from the upper spinous layers up to the *stratum corneum* (Fig. 21C) This pattern was not altered by the two weeks of repeated irradiation, neither with UVA+B nor SUN, suggesting that epidermal differentiation in young SEs is not markedly affected by irradiation.

In old SEs on the other hand, the expression of all markers was highly influenced by the chronic irradiation with both UVA+B and SUN. K15 as a marker for basal keratinocytes was present throughout almost all layers of the epidermis in non-irradiated old SEs. Upon irradiation the expression was more restricted to the basal layer (Fig. 21A). K10, that was present more superficial in non-irradiated controls, indicating a delayed differentiation, was now expressed in all suprabasal layers (Fig. 21B). This correlates well with the expression of K15 that was also regulated more normally in irradiated SEs. The late differentiation marker K2 was expressed in very minor amounts or was even absent from non-irradiated old SEs. Interestingly, this expression was increased in irradiated cultures (Fig. 21C). Although K2 expression was still markedly less than in young SEs, it suggested an improvement of terminal differentiation of old SEs upon irradiation. These effects on the expression of K15, K10 and K2, were observed after irradiation with UVA+B as well as SUN, but were slightly more pronounced after irradiation with SUN.

Taken together, the expression of all three markers, K15, K10, and K2, indicated a normalization of the epidermal differentiation in old SEs induced by chronic irradiation. The described phenotype could be reproduced in six independent experiments and with cells from two different young (22- and 23-year-old) and two different old (66- and 74-year-old) donors.

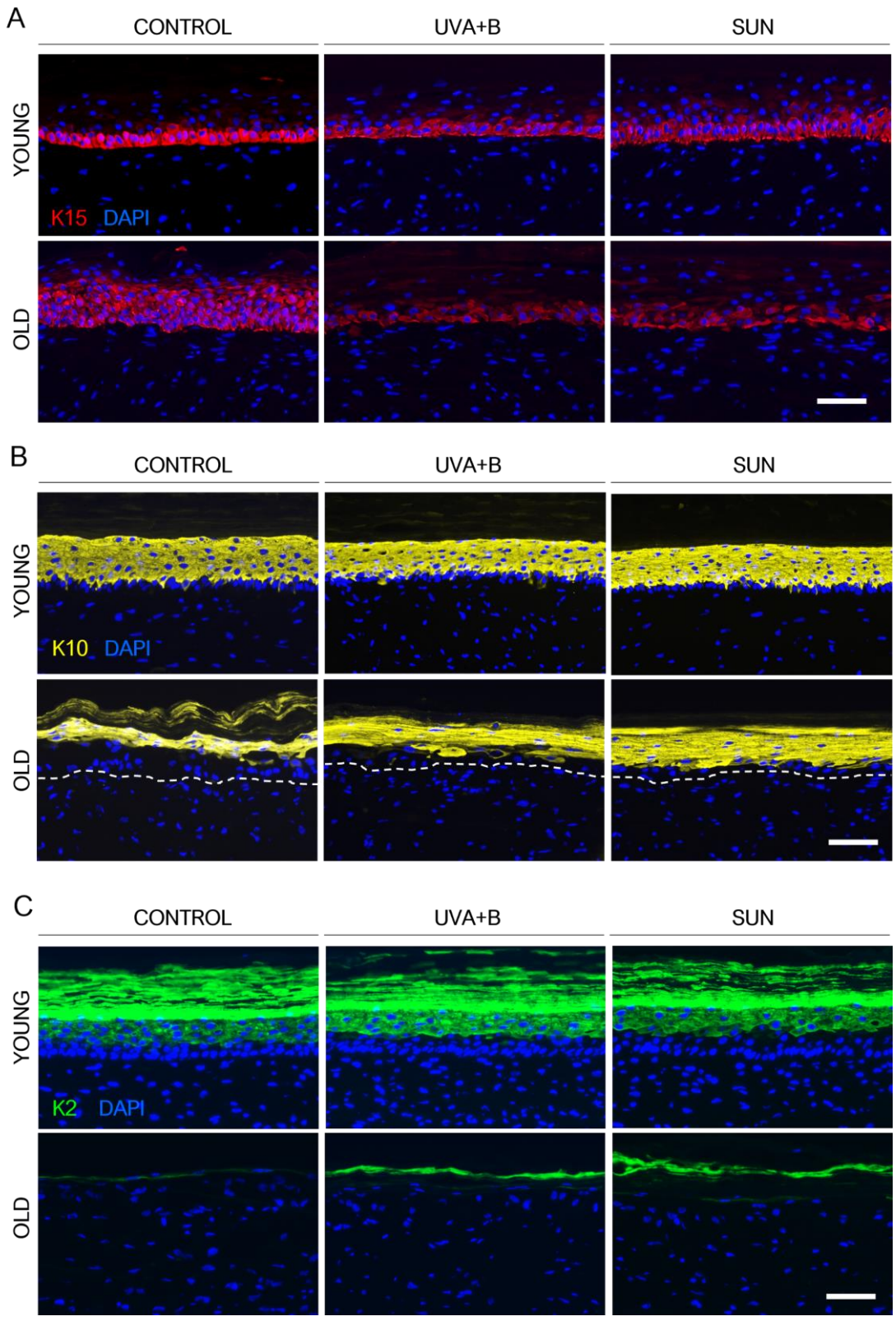

Figure 21: Effect of irradiation on epidermal differentiation of young and old Age-SEs
Young and old SEs were chronically irradiated with either UVA+B or the entire solar spectrum (SUN) for two weeks and compared to non-irradiated controls. IIF staining for the differentiation markers (**A**) keratin 15, (**B**) keratin 10 and (**C**) keratin 2 was performed on frozen sections. Displayed are representative images of young and old SEs, demonstrating an impaired ability of old fibroblasts to support proper epidermal differentiation that is in part restored after irradiation. Both treatments (UVA+B and SUN) led to an increase in K2 expression and a normalized expression pattern of K10 and K15. Young SEs did not show changes in the epidermal differentiation upon treatment. Dashed white line indicates DEJ. Scale bar represents 100 µm.

3.2.6 Evaluation of the Skin Barrier

One of the vitally important functions of the skin is to provide an effective barrier between environment and human body by preventing invasion of pathogens and fending off chemical and physical insults, but also to hinder unregulated water loss. Proper function of this barrier is dependent on the outermost layer of the epidermis, the *stratum corneum* (*stratum corneum*), which is made up of corneocytes embedded in a lipid matrix. It is known that UV exposure leads to a thickening of the horny layers of the skin (light callosity "Lichtschwiele") as a protective response. We hypothesized that the improvement in tissue differentiation that we had seen particularly in old SEs after irradiation might be part of an adaptive response of the SE to better protect against damaging UV rays by improving the skin barrier. In order to assess the integrity and function of the barrier in our SEs, three different approaches were chosen: immunohistochemical staining of Filaggrin, visualization of lipids using Nile Red and functional measurement of the transepidermal water loss (TEWL).

Filaggrin is the major structural protein in the *stratum corneum*, binding and aggregating keratin filaments. In young SEs, expression of filaggrin was found all over the *stratum corneum* and the intensity or localization was not changed by irradiation, neither with UVA+B nor SUN (Fig. 22A). In old SEs only very little filaggrin expression was seen in the unirradiated control SEs. This is in line with what was seen in histological stainings, showing that SEs produced a very thin or sometimes almost no *stratum corneum*. Interestingly, irradiation, especially irradiation with SUN, caused an increased expression of filaggrin (Fig. 22A). This increase again correlated well with the morphological changes induced by irradiation, namely the increase in *stratum corneum* thickness.

Another important contributor to the barrier function of the skin is the lipid matrix that provides a permeability barrier to prevent water loss (Elias 1983; Wertz et al. 1987). To investigate the lipid matrix, Nile Red staining was performed. Nile Red is a dye that is widely utilized for the localization and quantitation of neutral lipid droplets (Greenspan, Mayer, and Fowler 1985). In young SEs we found a clear basket weave-like structure typical for the *stratum corneum* of human skin, and the characteristic lipid lamellae being indicative for the lipid deposition in the intercellular spaces (Fig. 22B, C). The intense staining of the *stratum corneum* was similarly seen after irradiation of the SEs with UVA+B as well as SUN, suggesting for no strong radiation effect on the lipid expression and deposition.

In contrast to the well-formed *stratum corneum* in young SEs, the old SEs built only a thin, wavy *stratum corneum* and as documented in Fig. 22B the lipid layer nicely recapitulated the disorganized structure and showed more granular-like lipid aggregates. Old SEs that had been

irradiated with either UVA+B or SUN exhibited a clearly different morphology than their non-irradiated counterparts. Here the *stratum corneum* was thicker and showed densely packed lamellar sheets, making their *stratum corneum* much more compact than in the young SEs with the relaxed basket weave structure.

Next, to determine whether the differences seen in filaggrin expression and formation of the lipid matrix would also be of functional consequences for the SEs, their influence in skin barrier function was assessed. A very sensitive and widely used indicator for the function and integrity of the skin barrier is the measurement of the transepidermal water loss (TEWL). It describes the amount of water that passively diffuses across a fixed area of *stratum corneum* to the skin surface per unit time ($g/m^2/h$). Higher TEWL is usually associated with skin barrier impairments, whereas lower TEWL is related to healthy skin with an intact barrier. Here we used an open-chamber device (Tewitro®TW 24R) optimized for the measurement of *in vitro* skin models and kindly provided by Henkel AG & Co. KGaA in Düsseldorf. The detailed setup and procedure are described in the methods section. Three SEs for each condition were analyzed.

The TEWL in all cultures was around 46 $g/m^2/h$ and it did not vary significantly between young and old SEs or between controls and irradiated cultures and also did not differentiate between the old controls versus the irradiated cultures with their improved lipid layers (Fig. 22D).

Taken together, our data demonstrate that irradiation does not alter the expression of skin barrier components and in correlation with that skin barrier function in young SEs. In old SEs, the expression of filaggrin and the deposition of lipids is increased upon irradiation, both UVA+B and SUN, and this correlates with an improved organization of the *stratum corneum*. However, especially the latter did not result in functional consequences for the barrier function, at least regarding the TEWL.

Due to restrictions of the Covid-19 pandemic, this experiment could unfortunately not be repeated. Therefore, it has to remain open, how much this specific test or the technical conditions may codetermine the results and whether TEWL measurement is a sufficiently sensitive method to detect minor variations in the regulation of the barrier function.

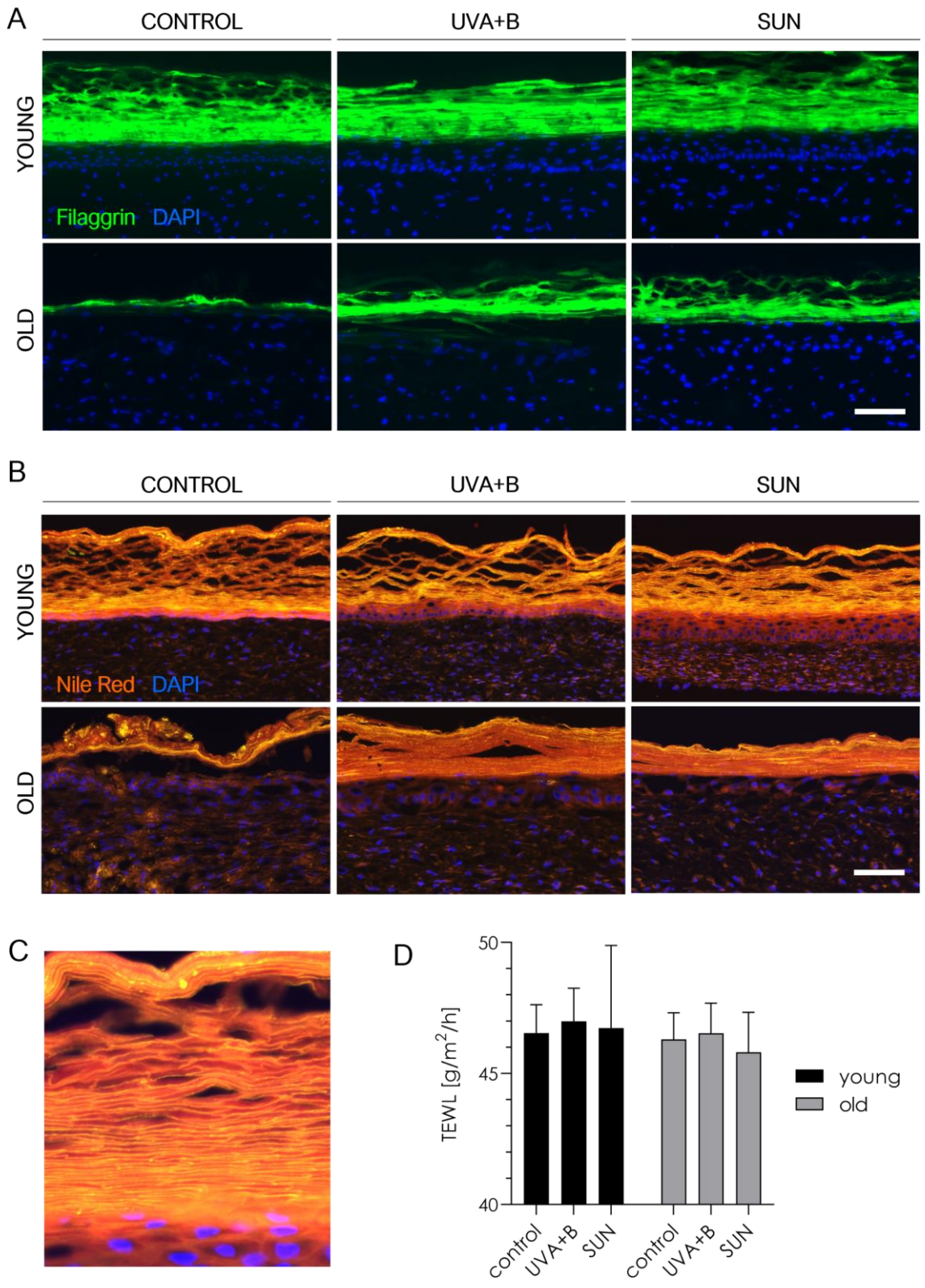

Figure 22: Evaluation of the skin barrier integrity after irradiation in young and old Age-SEs
Young and old SEs were chronically irradiated with either the solar UV spectrum (UVA+B) or the entire solar spectrum (SUN) over the period of two weeks and compared to non-irradiated controls. Integrity and function of the skin barrier were assessed by (**A**) IIF staining for filaggrin, (**B**) staining with Nile Red to visualize lipids (higher magnification of the lipid lamellae in (**C**)) and (**D**) functional analysis of the transepidermal water loss (TEWL). UVA+B and SUN led to a restoration of the reduced filaggrin expression in old SEs and to a normalization of the lipid barrier. TEWL was not altered statistically significant. Two-way ANOVA, all n.s.; n=3

3.2.7 Effect of Irradiation on the Basement Membrane

The BM components collagen type VII (ColVII), collagen type IV (ColIV) and laminin-5 were again analyzed by IIF staining in non-irradiated controls and irradiated young and old SEs. As described before, major differences in expression pattern of these markers were observed between young and old SEs that demonstrated deficits in BM formation in old SEs. In young SEs, ColVII (Fig. 23A) and laminin-5 (Fig. 23B) were both expressed in a continuous line along the BM area. ColIV (Fig. 23C) was found in the entire DE, but accumulated in the upper part, closest to the epidermis. Irradiation with UVA+B or SUN did not alter the expression of the three BM components in intensity or localization.

In old SEs, the expression of ColVII was considerably reduced compared to young SEs, and instead of a continuous line it was fragmented or partly degraded. Irradiation with UVA+B or SUN did not lead to visible alterations of that pattern (Fig. 23A). Laminin-5 expression was rather increased in old SEs but its distribution was disorganized. Upon UVA+B exposure, laminin-5 expression was slightly increased and increased even more upon exposure to SUN (Fig. 23B). The broader and chaotic distribution of laminin-5 suggested a further impaired assembly of the BM. ColIV, expressed mainly in the upper part of the DE in old SEs, was only slightly affected and rather reduced by irradiation with UVA+B (Fig. 23C).

Together these results suggests that the BM formation is highly dependent on the age of the fibroblasts, but other than epidermal differentiation, is not as much affected by radiation.

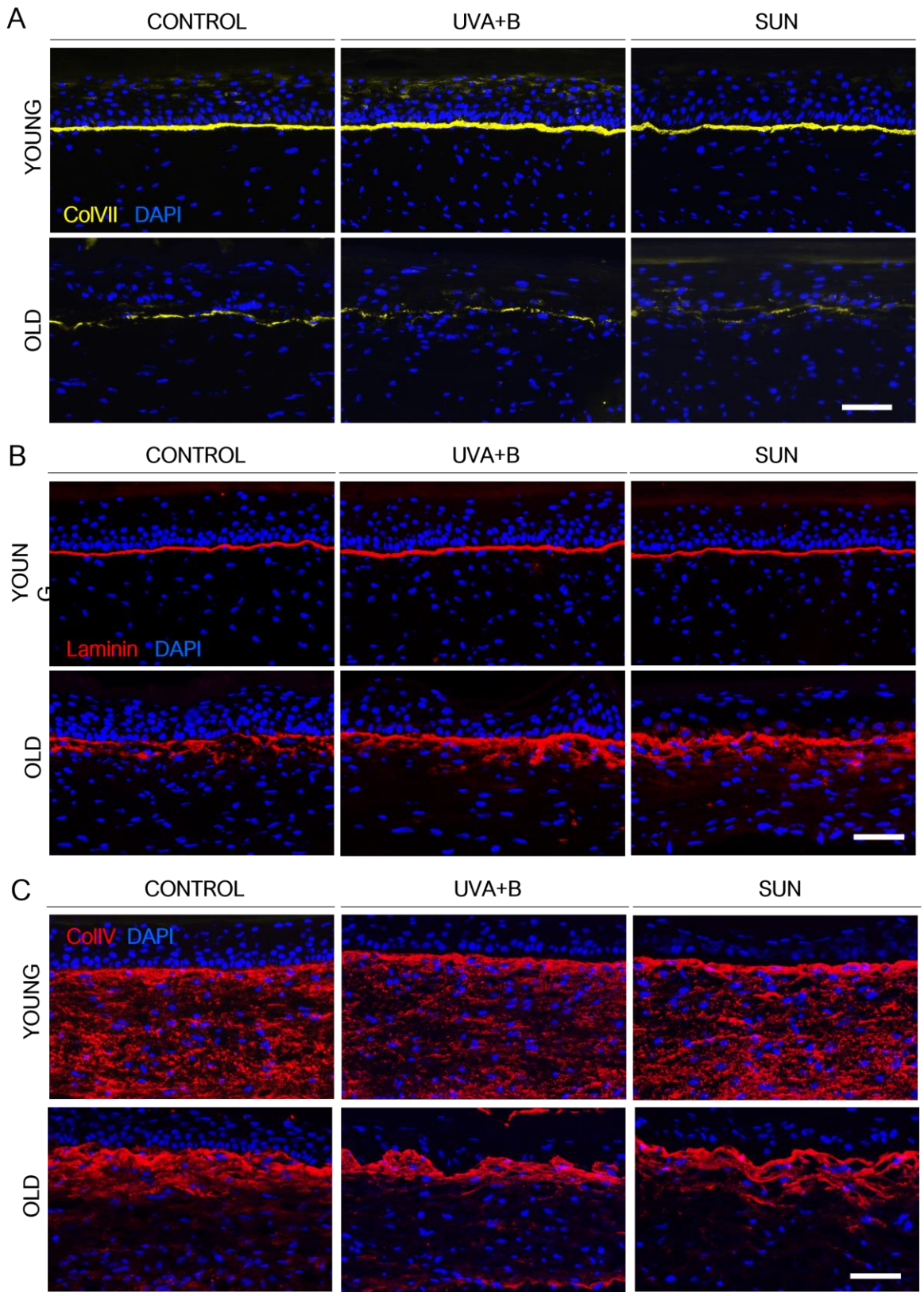

Figure 23: Effect of irradiation on basement membrane formation of young and old Age-SEs
Young and old SEs were chronically irradiated with either the solar UV spectrum (UVA+B) or the entire solar spectrum (SUN) over the period of two weeks and compared to non-irradiated controls. IIF staining for the BM markers (**A**) collagen type VII, (**B**) laminin-5 and (**C**) collagen type IV was performed on frozen sections. Displayed are representative images of young and old SEs, demonstrating a proper assembly of the BM in young SEs, that is impaired in old SEs. Irradiation did not clearly alter the expression of the BM components, neither in young nor in old SEs. Dashed white line indicates DEJ. The scale bar represents 100 µm.

3.2.8 Effects of Irradiation on the Dermal ECM

3.2.8.1 Alterations in ECM Composition

The dermal ECM as a major target of photoaging was studied by visualizing the collagen network, the hyaluronic acid (HA) content and the expression of chondrogenic matrix components in young and old SEs after irradiation with either UVA+B or SUN for two weeks.

IIF staining for collagen type I (ColI), the most abundant collagen in the dermis, demonstrated a dense meshwork of collagen fibers in the DE produced by young fibroblasts (Fig. 24A). This was not affected by the two weeks of irradiation with UVA+B or SUN. In the DE produced by old fibroblasts on the other hand, the ColI meshwork was less dense and displayed gaps and areas that lacked collagen fibers, particularly in the upper part of the DE. Exposure to UVA+B or SUN did not considerably change the ColI expression in old SEs (Fig. 24A).

Picrosirius Red staining allowed a further analysis of the collagen network. The dye visualizes collagen type I and type III (ColIII) fibers. Examined by light microscopy it confirmed what was seen in the ColI staining: an abundant expression of collagen fibers that form a very dense meshwork in young SEs, and a reduced expression in old SEs, that led to a less dense meshwork with larger gaps. Again, a change of the collagen network could not be observed after irradiation with UVA+B or SUN, neither in young nor in old SEs (Fig. 24B).

However, when examined under polarized light (Fig. 24C), the Picrosirius Red staining revealed some subtle distinctions. In both young and old SEs, the expression of collagen fibers slightly increased upon irradiation with UVA+B and also with SUN. In the DE of young SEs, irradiation particularly led to an increase in yellow-red fibers (ColI). In the DE of old SEs, both the yellow-red and green (ColIII) fibers seemed to be increased, especially in the middle part of the DE.

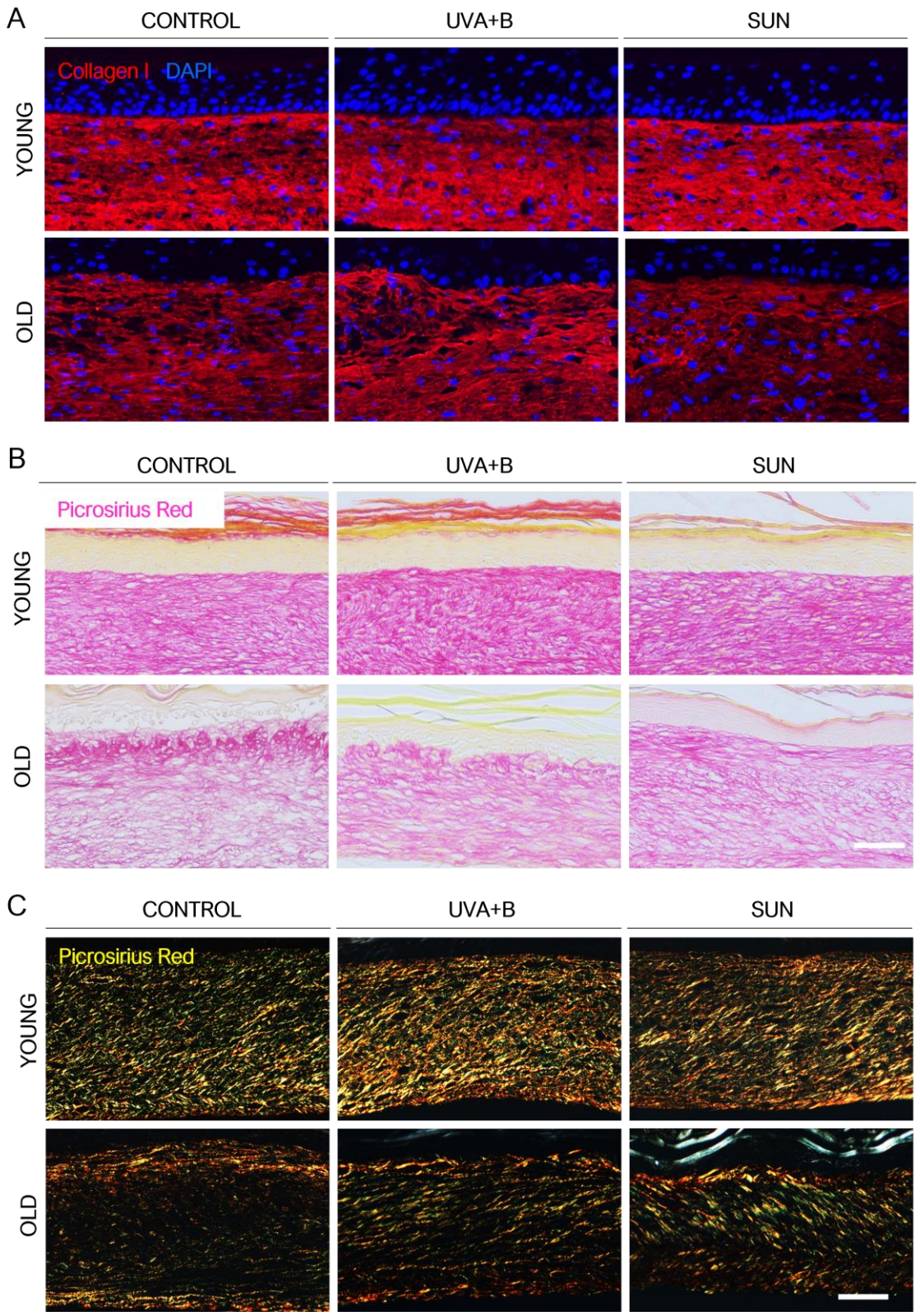

Figure 24: Effect of irradiation on the collagen network of young and old Age-SEs
Young and old SEs were chronically irradiated with either the solar UV spectrum (UVA+B) or the entire solar spectrum (SUN) over the period of two weeks and compared to non-irradiated controls. IIF staining for (**A**) collagen type I was performed on frozen sections, (**B**) Picrosirius Red staining was done on paraffin sections and (**C**) visualized under polarized light. Young SEs display a dense network of collagen fibers that was not affected by irradiation. Old SEs have a less dense collagen fiber network with larger gaps and irradiation with UVA+B or SUN led to a slight increase in collagen fibers as seen in the Picrosirius Red staining under polarized light. Displayed are representative images of young and old SEs. The scale bar represents 100 µm.

Next, the influence of irradiation on the expression pattern of HA was assessed in young and old SEs (Figure 25). In young SEs, HA was abundantly expressed and evenly distributed throughout the DE. The amount and distribution of the HA was not altered by irradiation, neither UVA+B nor SUN. In old SEs on the other hand, that displayed a markedly reduced expression of HA in unirradiated controls, exposure to UVA+B as well as SUN led to an overall increase of HA in the entire DE. Although the staining intensity was not as high as in young SEs and the HA network did not look as dense, staining intensity was drastically increased upon irradiation compared to the controls. Together this suggests that irradiation with UVA+B as well as SUN causes a strong upregulation of an otherwise obviously reduced expression (as compared to young fibroblasts) of HA in the old fibroblasts.

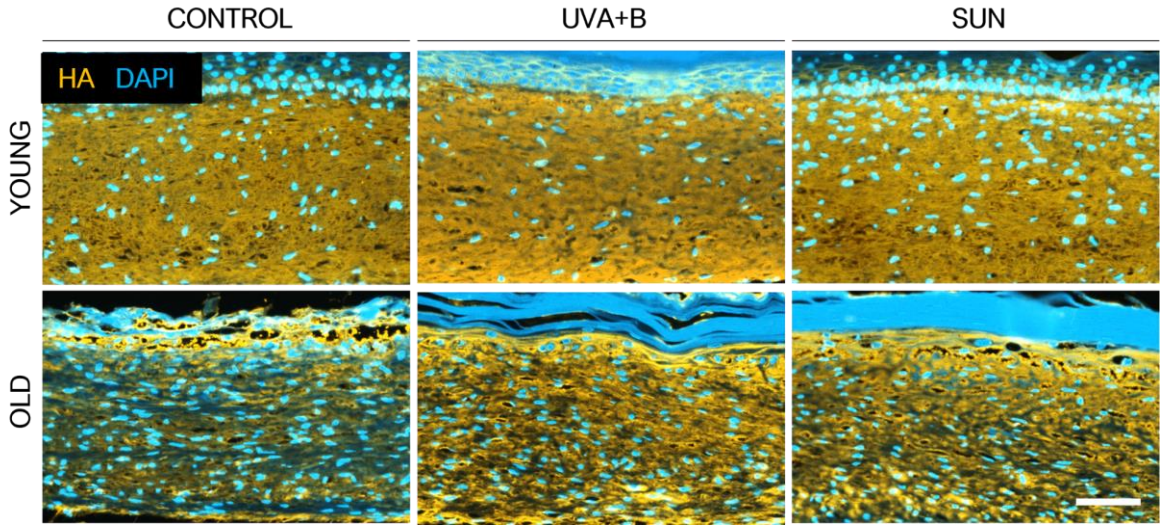

Figure 25: Effect of irradiation on the HA content of young and old Age-SEs
Young and old SEs were chronically irradiated with either the solar UV spectrum (UVA+B) or the entire solar spectrum (SUN) over the period of two weeks and compared to non-irradiated controls. IIF staining for hyaluronic acid (HA) displayed an abundant expression in the entire DE of young SEs (upper panel), that was not affected by irradiation. In old SEs that had a strongly reduced HA content in non-irradiated samples, irradiation increased HA expression (lower panel). Displayed are representative images of young and old SEs. The scale bar represents 100 µm

The proteins aggrecan and ColXI, typical components of the chondrogenic matrix, had been detected abundantly in the DE old SEs, but not in young. This pattern was not changed significantly by irradiation. The expression of both proteins was detected in the DE of irradiated as well as control old SEs. In young SEs the chondrogenic matrix proteins were not detected, or only in minor amounts (Fig. 26).

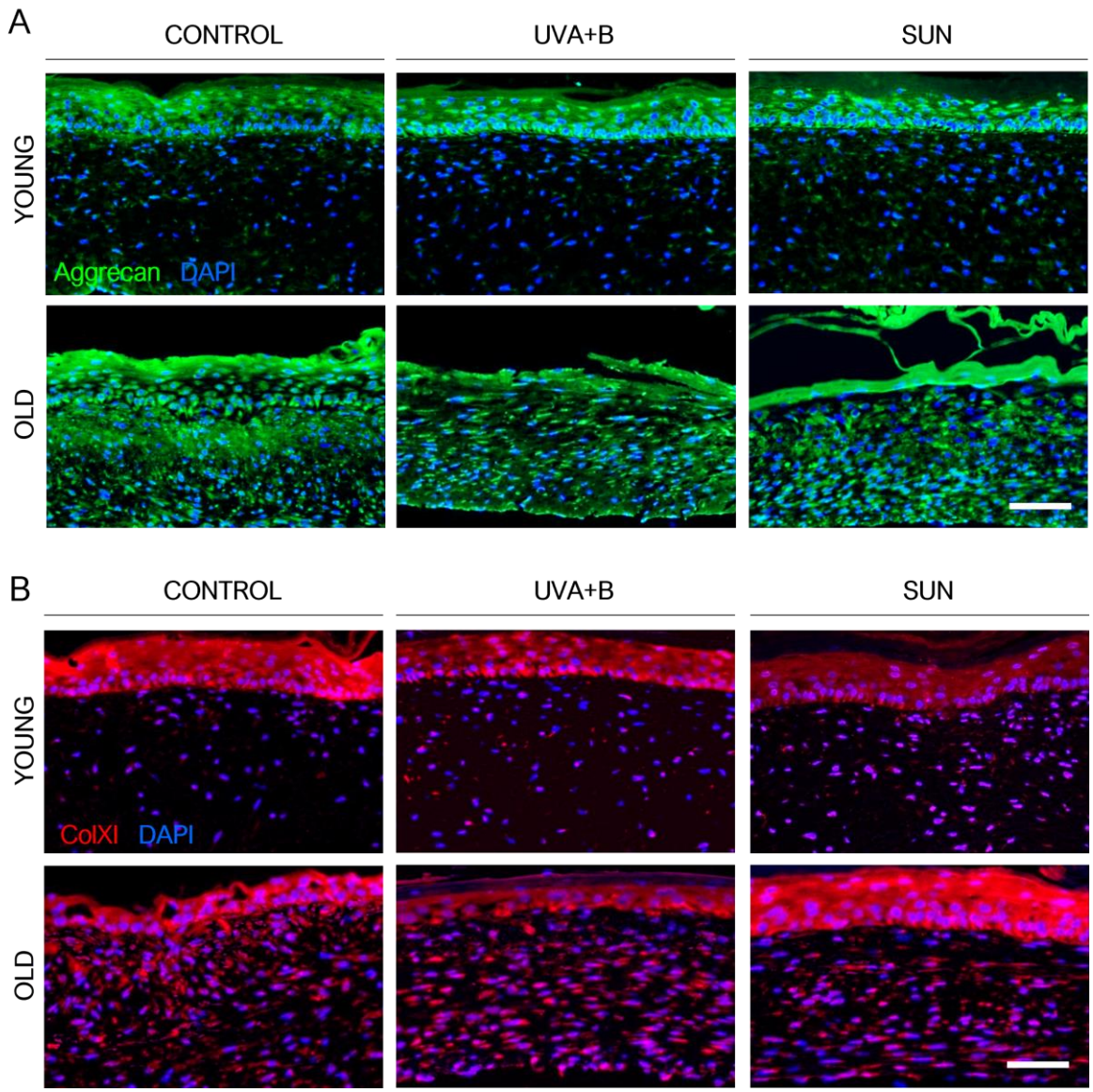

Figure 26: Expression of chondrogenic matrix components in young and old Age-SEs
Young and old SEs were chronically irradiated with either the solar UV spectrum (UVA+B) or the entire solar spectrum (SUN) over the period of two weeks and compared to non-irradiated controls. IIF staining was performed on paraffin sections for the chondrogenic matrix components (**A**) aggrecan and (**B**) collagen type XI. Both proteins were expressed abundantly in old SEs, but only in minor amounts in young SEs. Displayed are representative images of young and old SEs. The scale bar represents 100 µm.

3.2.8.2 Proteolytic Damage to the Dermal ECM

The dermal ECM is subject to constant dynamic changes. Remodeling of various components of the ECM is an important event in wound healing but also plays a major role in pathologies such as fibrosis or tumor invasion and metastasis. Disruption of the ECM, especially the degradation of collagen fibrils in the dermis, is a hallmark of aging and largely responsible for this are matrix metalloproteinases (MMPs). MMPs are regulated at different levels and their activity can be inhibited by tissue inhibitors of matrix metalloproteinases (TIMPs), especially TIMP-1 and TIMP-2.

We studied the proteolytic activity in young and old SEs with different approaches. Using a fluorometric collagenase/gelatinase assay we assessed the general activity of collagenases and gelatinases in fresh cut frozen sections of the SEs. The levels of secreted pro-MMP-1, MMP-3 and the inhibitor TIMP-2 in conditioned media were quantitatively measured by ELISA and IIF stainings gave an insight into the localization of the respective enzymes. If not stated otherwise, all assays were done with at least two independent experiments with three or four biological replicates for each condition.

The gelatinase/collagenase activity assay is based on a fluorescein-labeled DQ gelatin conjugate that yields fluorescent fragments when digested by enzymes. This assay revealed high enzymatic activity in the stratum corneum of young control SEs and a low activity in parts of the epidermis in some samples (Fig. 27A). There was no activity detectable in the dermal compartment. Irradiation with UVA+B or SUN did not alter the enzymatic activity in young SEs. In old control SEs, activity in the stratum corneum and epidermis was less than in young SEs, but a high enzymatic activity was detected in the dermal part. Irradiation (UVA+B or SUN) did not lead to noticeable alterations of that pattern.

Several studies have shown that UV radiation influences at least three MMPs, namely MMP-1, MMP-3, and MMP-9, in human skin *in vivo* (Quan et al. 2009; Brenneisen, Sies, and Scharffetter-Kochanek 2002; Fisher et al. 1997). Therefore, we focused on those three as well as the inhibitor TIMP-2 in the further analysis. Using ELISAs we detected the secreted protein in conditioned media from the SEs that was collected 24 h after the last irradiation (Fig. 27B). MMP-9 was not present in the medium or levels were too low to be detected (not shown). Pro-MMP-1 was detected in all samples, the basic value of the controls already being higher in media from the old SEs than in the young. In both cases, young and old samples, irradiation with UVA+B or SUN led to a significant increase in secreted pro-MMP-1. Absolute amount of protein was consistently higher in samples from old SEs for all conditions (Fig. 27B, left diagram). MMP-3 was found only in small amounts in media from young SEs and it was not altered significantly by irradiation. In old SEs however, irradiation with UVA+B and even more with SUN strongly increased the level of

secreted MMP-3 (Fig. 27B, middle diagram). TIMP-2 was analyzed in three different experiments. In all conditions TIMP-2 levels were higher in old SE samples than in young. Irradiation did induce a significant increase in the old samples in one of the experiments but not in the other two (Fig. 27B, right diagram).

To complement the quantitative results of the ELISA, we did IIF stainings for MMP-1 (Fig. 27C) and MMP-3 (not shown) to also localize the expression of the enzymes in the tissue. The MMP-1 staining revealed a pronounced expression in the epidermis of all cultures. In the dermal part there was almost no expression in young SEs. The dermal part of old SEs on the other hand exhibited a much stronger expression of MMP-1, distributed over the entire area. Differences between control and treated samples that were detected by ELISA could not be observed in the stainings. This does not mean that the results are invalid, but the ELISA is a more sensitive tool that provides quantitative data and also detects subtle and short-term changes, whereas the staining gives a better idea about the localization.

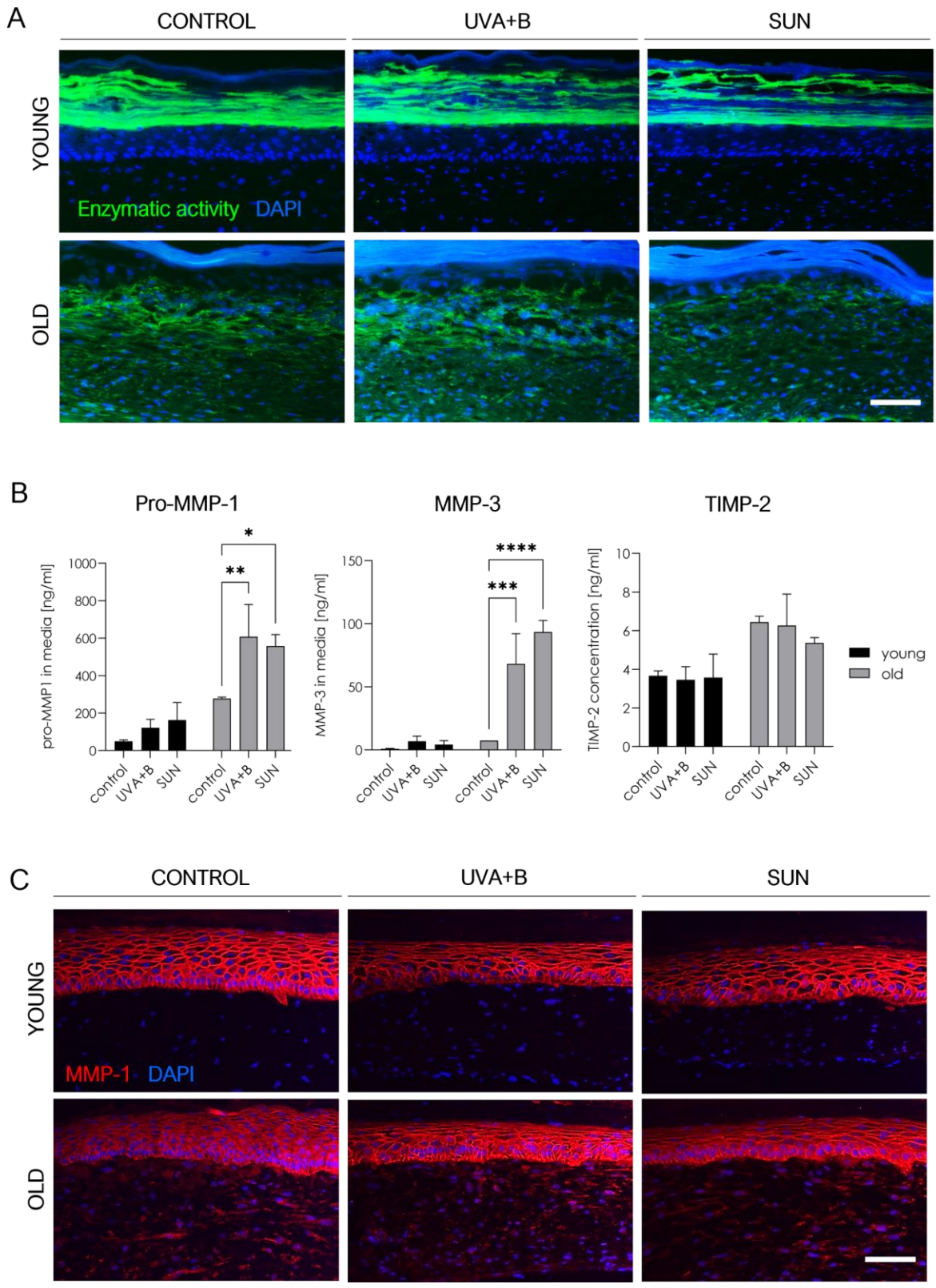

Figure 27: Modulation of the dermal ECM by proteolytic enzymes

Young and old SEs were chronically irradiated with either the solar UV spectrum (UVA+B) or the entire solar spectrum (SUN) over the period of two weeks and compared to non-irradiated controls. (**A**) A fluorescence-based collagenase/gelatinase activity assay was performed on non-fixated frozen sections. (**B**) Conditioned media was collected 24h after the last irradiation and used to detect secreted pro-MMP1, MMP-3 and TIMP-2 by ELISA. (**C**) MMP-1 expression was also analyzed by IIF staining on frozen sections. All assays show a higher proteolytic activity in old SEs. Error bars represent the standard error mean. Two-way ANOVA; * = p-value < 0.05; ** p-value < 0.01; *** p-value < 0.001; **** = p-value < 0.0001; n=3.

3.2.9 Effects of Irradiation on the Fibroblasts

Young and old Age-SEs were again stained for the mesenchymal marker vimentin and the myofibroblast marker α-SMA to determine the differentiation state of the fibroblasts in the DE and how this is affected by irradiation.

3.2.9.1 Reduction of Myofibroblasts Upon Irradiation of Old SEs

As described in 3.1.2.3 myofibroblasts represented a major part of dermal fibroblasts in old SEs, demonstrated by a positive staining for α-SMA, while young SEs comprised no myofibroblasts at all. The question was now how chronic irradiation would affect this phenotype, if myofibroblasts are induced in young SEs upon irradiation (an induction that is seen in wound healing as a response to tissue injury (Li and Wang 2011)) and if the number of myofibroblasts in old SEs is further increased. Interestingly, irradiation did not lead to an increase in myofibroblasts in old SEs (Fig. 28B). On the contrary, we found a strong decline. The reduction was apparent in UVA+B-exposed SEs and even more pronounced in those exposed to SUN. Myofibroblasts were still concentrated in the upper part of the DE. Young SEs remained completely negative for α-SMA after UVA+B or SUN exposure (Fig. 28B), suggesting that irradiation alone, at least in the dose and time it was administered here, is not enough to induce the differentiation of young fibroblasts to myofibroblasts.

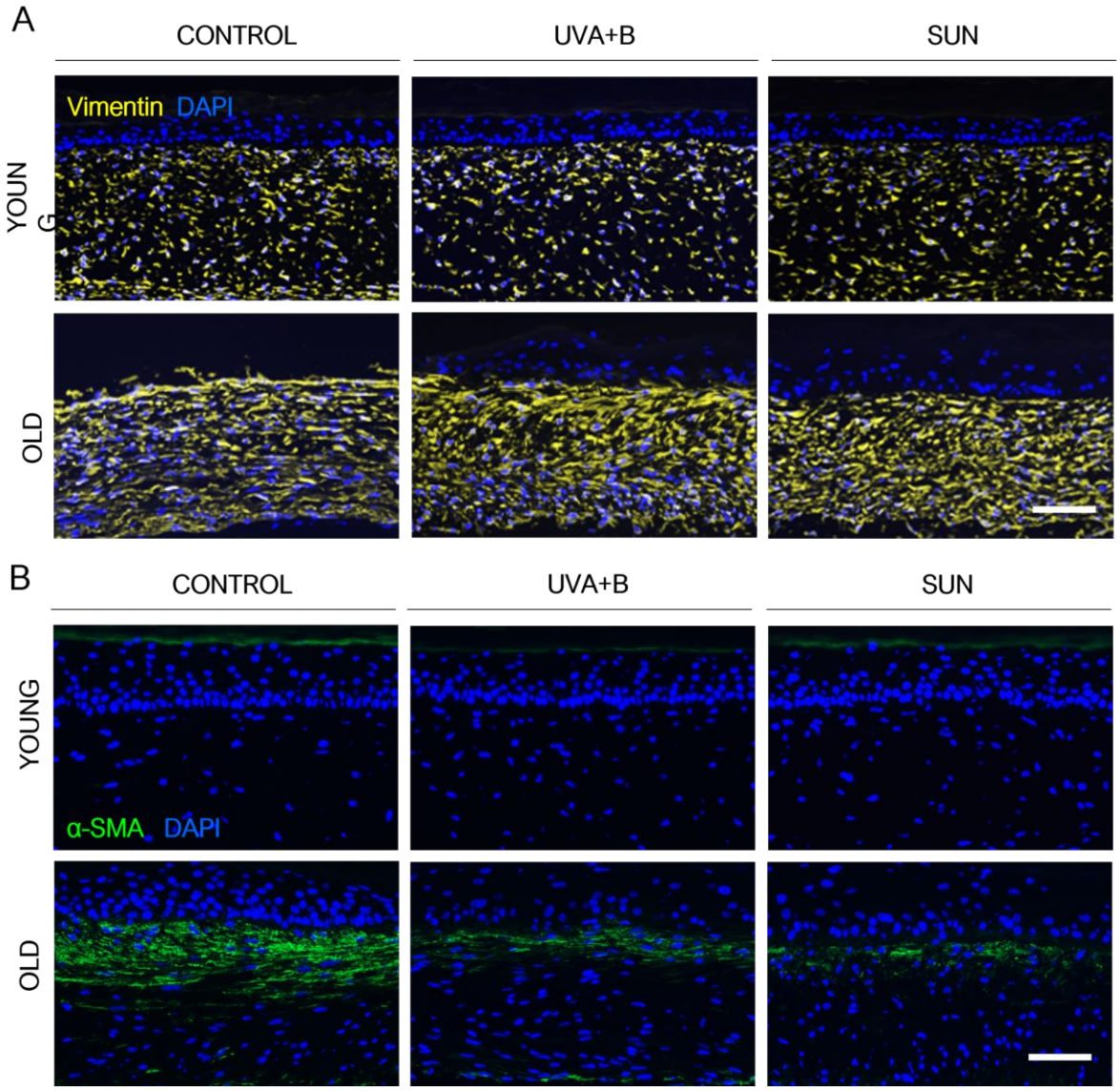

Figure 28: Effect of irradiation on young and old fibroblasts in Age-SEs
Young and old SEs were chronically irradiated with either the solar UV spectrum (UVA+B) or the entire solar spectrum (SUN) over the period of two weeks and compared to non-irradiated controls. IIF staining for the mesenchymal marker (**A**) vimentin and the myofibroblast marker (**B**) α-SMA were performed on frozen sections. Displayed are representative images of young and old SEs. The old fibroblasts displayed an enlarged morphology compared to young ones and accumulated vimentin. Myofibroblasts (α-SMA+) were only present in old SEs and markedly reduced by irradiation. The scale bar represents 100 µm.

3.2.9.2 Apoptosis analysis of young and old fibroblasts

After seeing the surprising reduction of myofibroblasts in old SEs following irradiation, the question arose if aged fibroblasts in general are more sensitive to irradiation and die as a consequence of the treatment. In this case, we would find increased rates of apoptosis or necrosis. To address this, fibroblasts of young and old donors were grown in 2D on standard cell culture plates, with three independent replicates each, and irradiated with 1 MED of SUN. To detect cell death, cells were double stained with Annexin-V-APC and PI-PE and subsequently analyzed by flow cytometry (FACS). The generated dot plots, shown in Figure 29A, can be divided in four quartiles representing the population of healthy cells in Q4 (Annexin/PI -/-), early apoptotic cells in Q3 (Annexin/PI +/-) and late apoptotic or necrotic cells in Q2 (Annexin/PI +/+). The proportion of cells undergoing apoptosis or necrosis was generally low. In the non-irradiated controls 6.3 % of the young and 8.3 % of the old fibroblasts were defined as apoptotic (Q3), 4 % of the young and 3.9 % of the old as late apoptotic or necrotic (Q2). 89.4 % and 87.2 % of young and old cells respectively were vital (Q4). The proportion of dead cells even decreased in the irradiated samples. Only 4 % of the young fibroblasts and 3.9 % of the old ones were apoptotic after irradiation. The percentage of late apoptotic/necrotic cells decreased to 1.9 % in young and 2.3 % in old fibroblasts. More than 93 % of fibroblasts, both young and old, were vital after the radiation exposure. The percentages are visualized in Figure 29B. The results show that the irradiation regime per se is not toxic and does not induce apoptosis in the fibroblasts but rather reduces it.

In addition to the FACS analysis, cultures of old fibroblasts were stained for α-SMA. Positive cells were detected in controls as well as in irradiated plates in similar amounts. This experiment clearly demonstrated that old fibroblast or aSMA+ cells do not exhibit an increased sensitivity towards irradiation triggering apoptosis. This in turn suggests, that the loss of myofibroblasts in the old SEs after irradiation is not due to their selective killing through UV or SUN.

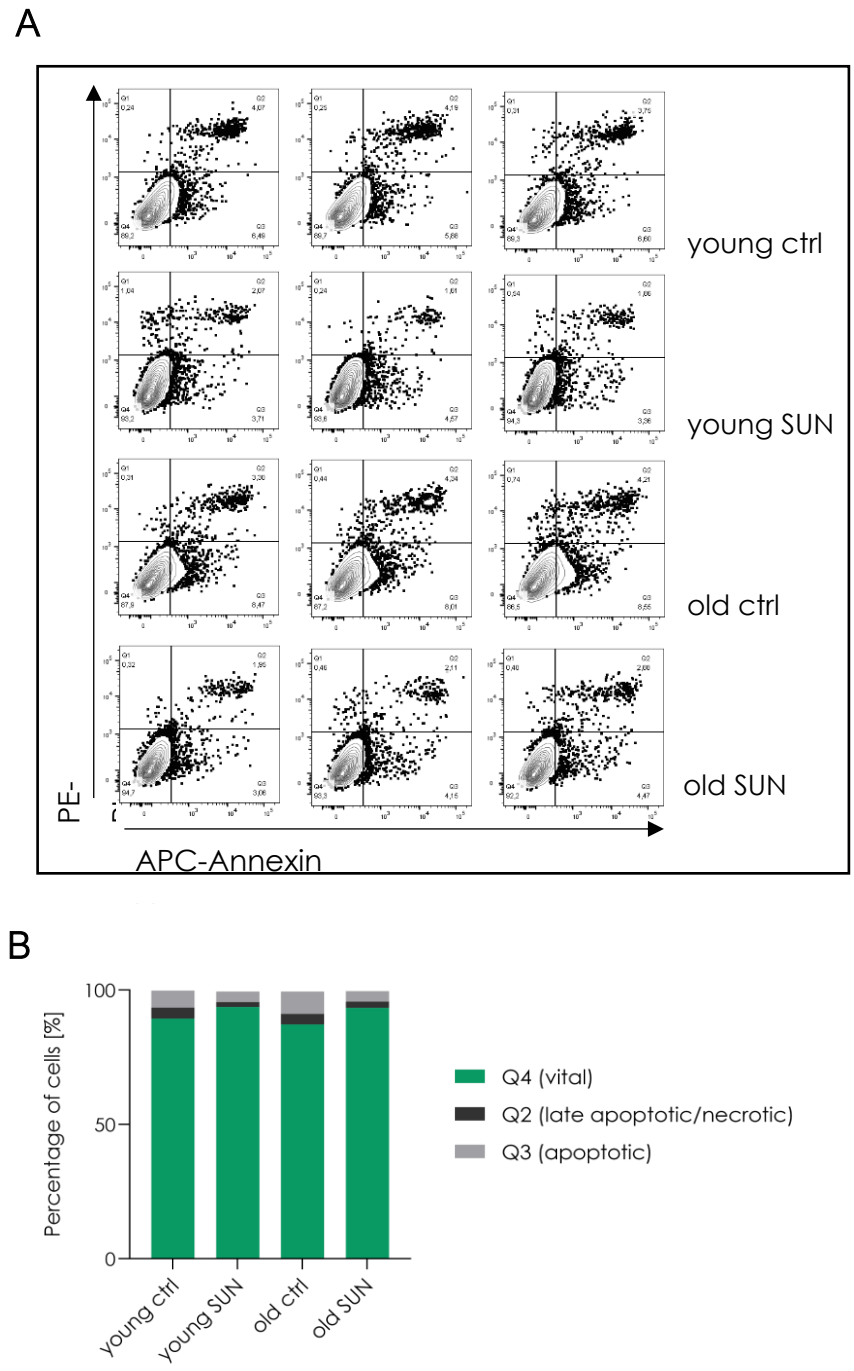

Figure 29: Flow cytometric analysis of cell death
Fibroblasts of a young and old donor were analyzed by flow cytometry after a single irradiation with 1 MED of SUN compared to non-irradiated controls. (**A**) Annexin V/Propidium iodide (PI) double staining allowed to distinguish between viable (Annexin V-/PI-, Q4), early apoptotic (Annexin V+/PI-, Q3) and late apoptotic or necrotic (Annexin V+/PI+, Q2) cells. (**B**) The percentage of apoptotic and necrotic cells did not increase upon irradiation but, on the contrary, decreased, suggesting no cell death induction by SUN. Stacked columns represent mean of n=3.

3.2.10 Gene Expression Analysis of Chondrocyte-Type Genes by qRT-PCR

Previous experiments in this study as well as the preceding characterization of the fibroblasts (Gundermann 2012) have suggested a specific differentiation of aged, sun-exposed fibroblasts to a myo-chondro-fibroblast phenotype that produce a chondrocyte-type ECM. To investigate the role of solar radiation for the development of this phenotype, i.e. to find out if it is a direct consequence of UV/sun exposure, RNA from SEs with young (23-year-old donor) and old (74-year-old donor) fibroblasts were analyzed for a panel of chondrocyte-type matrix proteins by qRT-PCR. SEs were irradiated for two weeks with UVA+B or SUN and RNA was isolated from the DE 24 h after the last irradiation.

We first asked whether radiation could induce the expression of chondrocyte-type matrix genes in SEs with young fibroblasts. To address this, the fibroblasts were analyzed for the chondrocyte-type matrix markers COL11 and HAPLN1 as well as the chondrogenic transcription factor SOX9 (SRY-Box Transcription Factor 9). Both COL11 and HAPLN1 appeared to be upregulated upon UVA+B and SUN irradiation, with only HAPLN1 being significantly increased, suggesting that irradiation might be able to induce expression of these markers. The transcription factor SOX9, on the other hand, did not seem to be regulated as yet (Fig. 30A).

To verify these findings, RNA from another experiment, based on a second set of fibroblasts (22- and 66-year-old donors), was analyzed. Of this experiment, the samples irradiated for two weeks were taken for an RNA-Seq analysis and with the samples irradiated for four weeks we performed qRT-PCR. In this analysis, the fibroblasts demonstrated a significant induction of ACAN, COL10 (for UVA+B) and CCN1 (for SUN). COL11 and HAPLN1 were only induced very slightly and non-significant (Fig. 30B). Together, this suggested that also these fibroblasts were responding to irradiation with a shift to a more chondrogenic expression phenotype, although the level of induction was rather moderate for both young fibroblast populations.

When analyzing the old fibroblasts, we found that all the genes regulated in the young fibroblasts were also regulated in the old fibroblasts, though regulation was generally delayed. After two weeks all genes were only slightly induced (Fig. 30A), while in the other experiment that was analyzed after four weeks of irradiation, HAPLN1, COL11, COL10, ACAN, and CCN1 were all strongly upregulated (Fig. 30B). SOX9, as a transcriptional regulator of the chondrogenic program, was already induced in the 2-week samples. This might suggest that SOX9 is induced first, before then leading to the induction of the chondrocyte-type matrix genes.

Expression of TGFB1 and 3 was analyzed, as they are potential regulators of the chondrogenic phenotype. TGFB1 was increased by irradiation in young and old fibroblast after two weeks, but this increase was not significant (Fig. 30A). After four weeks, TGFB1 was rather reduced upon

irradiation (significant only for young fibroblasts). TGFB3 was induced especially by UVA+B, again only being significant in young fibroblasts (Fig. 30B).

Together this suggests the irradiation with UVA+B and SUN is involved in inducing a chondrogenic expression profile in young and old fibroblasts. However, this regulation might not be direct. The delayed onset of gene expression rather points to an indirect consequence of UV-induced regulatory circuits.

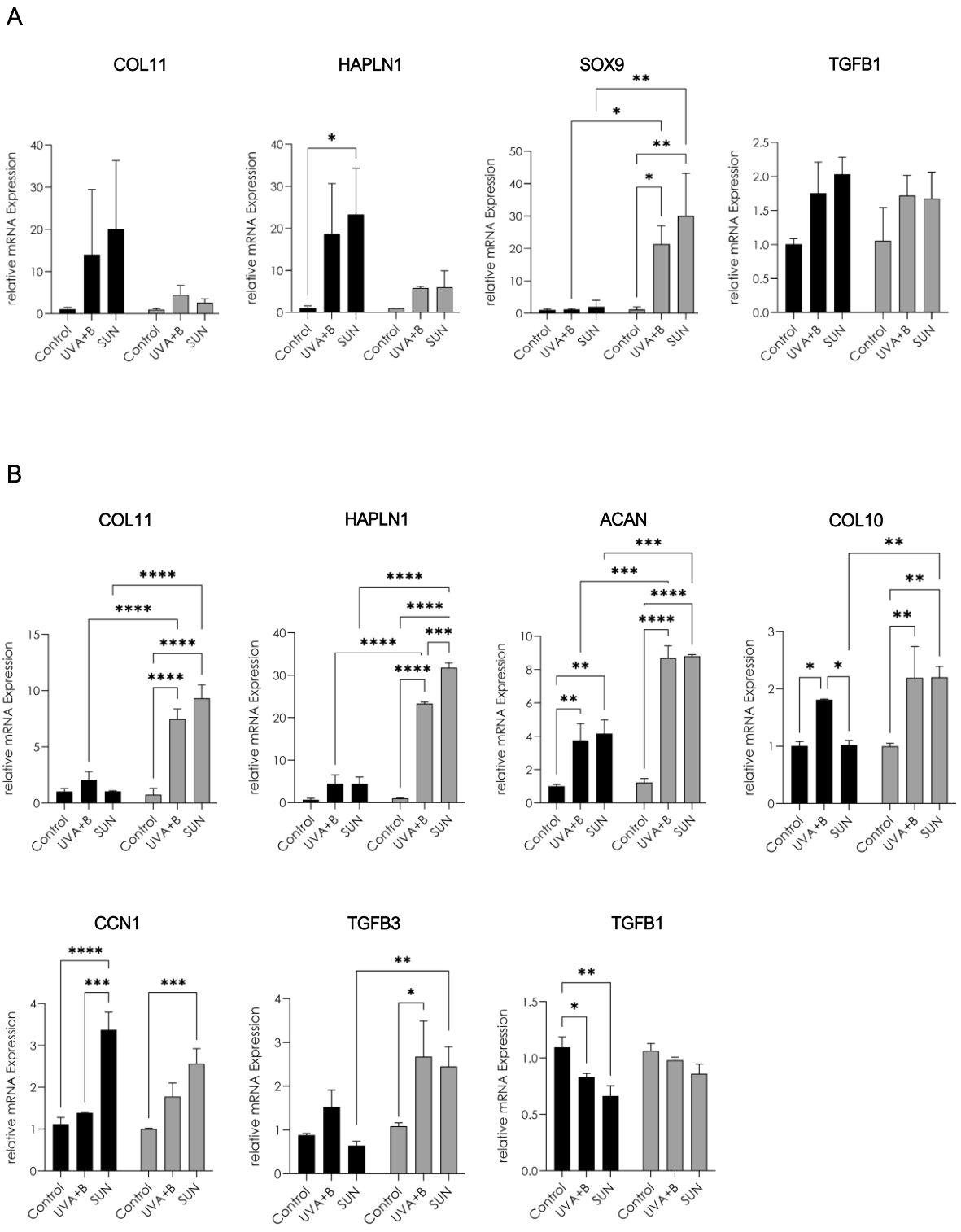

Figure 30: Relative gene expression in young and old Age-SEs

Young (black columns) and old (grey columns) SEs were chronically irradiated with either the solar UV spectrum (UVA+B) or the entire solar spectrum (SUN) over the period of two or four weeks and compared to non-irradiated controls. RNA of the DE was purified and used for qRT-PCR to determine gene expression levels of the stated genes in relation to housekeeping genes. One experiment was analyzed (**A**) after two weeks of irradiation and (**B**) another one after four weeks of irradiation. The error bars represent the standard error mean. Two-way ANOVA; * = p-value < 0.05; ** p-value < 0.01; *** p-value < 0.001; **** = p-value < 0.0001; n=3.

3.2.11 Gene Expression Analysis of Age-SEs by RNA-Sequencing

In addition to the morphological and functional analysis of young and old SEs, we were interested in their general response to irradiation on the gene expression level. In order to study the transcriptome of the SEs and compare the gene expression of the incorporated cells (fibroblasts and keratinocytes), an RNA-sequencing analysis was performed by BGI Genomics (Hong Kong, China) and the raw data was analyzed in cooperation with Johannes Ptok from the group of Prof. Heiner Schaal (Institute for Virology, Heinrich Heine University Düsseldorf). Details of the analysis are given in the Methods section. For this experiment SEs based on young (22-year-old donor) or old (66-year-old donor) fibroblasts co-cultured with young (23-year-old donor) keratinocytes were repetitively irradiated with either UVA+B or SUN for 2 weeks as described before. Dermis and epidermis were separated after the harvest and processed individually. In total, data from 26 samples (10 for epidermis, 16 for dermis) was analyzed with two or three biological replicates for each condition.

3.2.11.1 Principal Component Analysis

As a first overview, the gene expression profiles of all samples were compared and the similarity between samples was visualized by Principal Component Analysis (PCA). In the PCA, samples with a similar expression profile are positioned closer together in a two-dimensional frame, depicted in Fig. 31. The PCA clearly separated epidermis (E) samples from the dermis (D) samples in the dimension of Component 1 (x-axis). Epidermis samples from young and old SEs, irrespective of the irradiation, were located in close proximity to each other, indicating many similarities in their gene expression profile. The old and young dermis samples, on the other hand, were clearly separated along the dimension of Component 2 (y-axis), clustering together in the upper or lower left corner respectively. Interestingly, the distance between young and old dermis samples was much bigger than that between control and irradiated samples, indicating that the age of the fibroblasts accounted for more of the differences in gene regulation than the irradiation treatment.

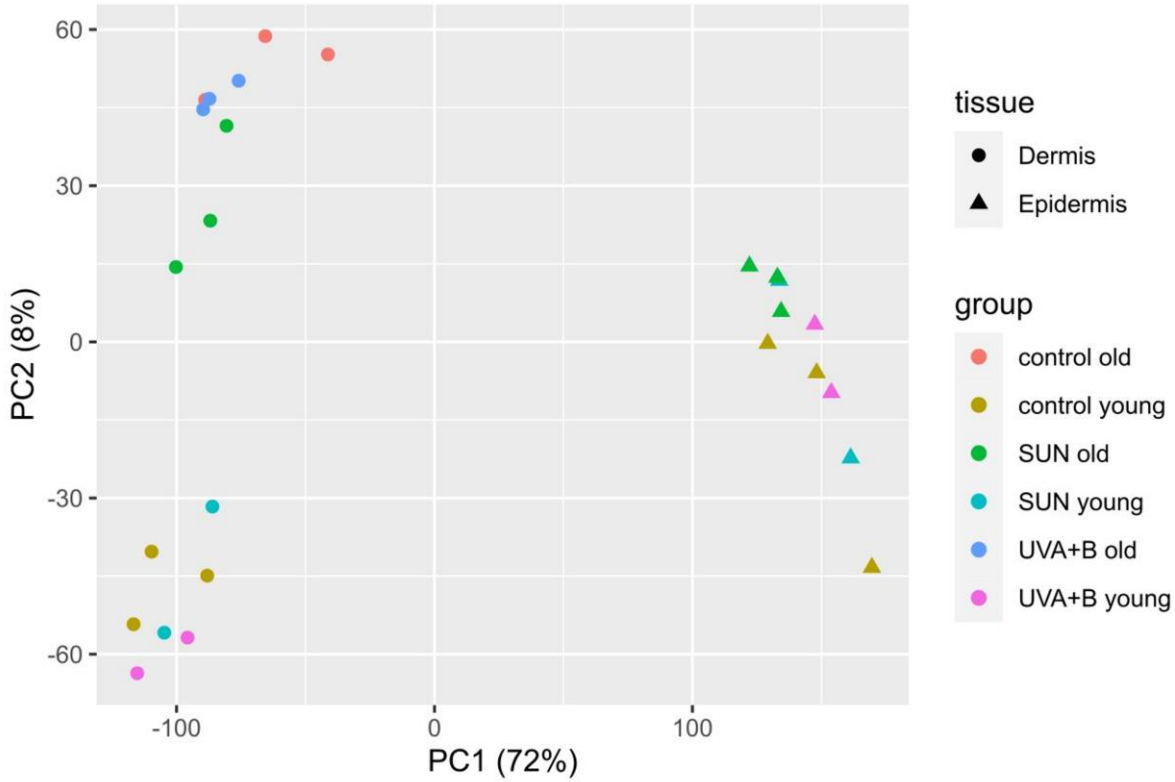

Figure 31: Principal Component Analysis (PCA)
PCA was done based on RNA-Seq data of the general gene expression Samples with a similar gene expression cluster together. The two components explain 80% of the variance between samples.

3.2.11.2 Differential Gene Expression of Young and Old Fibroblasts

To compare the transcript abundance of genes between different groups, a differential gene expression (DGE) analysis was performed with the DESeq2 software package in R (Love, Huber, and Anders 2014). Calculated p-values of the DGE were adjusted following the Benjamini-Hochberg method and only genes with an adjusted p-value lower than 0.05 and a significant log2-foldchange unequal 0 were considered for further analysis.

Venn diagrams are depicted in Fig. 32 to illustrate the number of differentially expressed genes (DEGs) in young and old fibroblasts in response to UVA+B (Fig. 32A) or SUN (Fig. 32B) treatment. In young fibroblasts from SEs irradiated with UVA+B, 185 genes were upregulated and 251 were downregulated. In old fibroblasts, the number of DEGs (both up- and downregulated) was much higher, with 641 genes being upregulated and 807 genes being downregulated in response to UVA+B irradiation. Only a small number of genes was commonly regulated in young versus old

fibroblasts (32 up and 28 down). In response to SUN, again only a small number of genes overlapped between young and old fibroblasts, 11 were commonly upregulated and 28 were downregulated. The number of genes regulated in response to SUN in young fibroblasts was nearly the same as the number regulated after UVA+B irradiation, with 187 genes being upregulated and 274 being downregulated. Interestingly and contrary to the response to UVA+B, the number of DEGs in response to SUN in old fibroblasts was much lower. Only 50 genes were up- and 71 were downregulated after SUN treatment.

The Venn diagrams in Fig. 32C and D depict the genes regulated only by UVA+B or only by SUN and the genes commonly regulated by both irradiations in young (Fig. 32C) and old (Fig. 32D) fibroblasts. These diagrams illustrate that only a part of the genes is regulated by both UVA+B and SUN (307 in young, 116 in old fibroblasts), and a large fraction of genes are uniquely regulated by either the UV spectrum or the entire solar spectrum.

This quantitative comparison of DEGs nicely demonstrated that young and old fibroblasts respond differently to irradiation and only a small number of genes was commonly regulated, showing the same response to irradiation in young and old fibroblasts (these genes are listed in Table 18 in the appendix). It also shows that the irradiation with UVA+B or SUN trigger considerably different responses on the gene expression level. The fact that a great percentage of genes was regulated only by UVA+B clearly shows that irradiation with the entire solar spectrum is not just a summation of the effects of the single wavelengths.

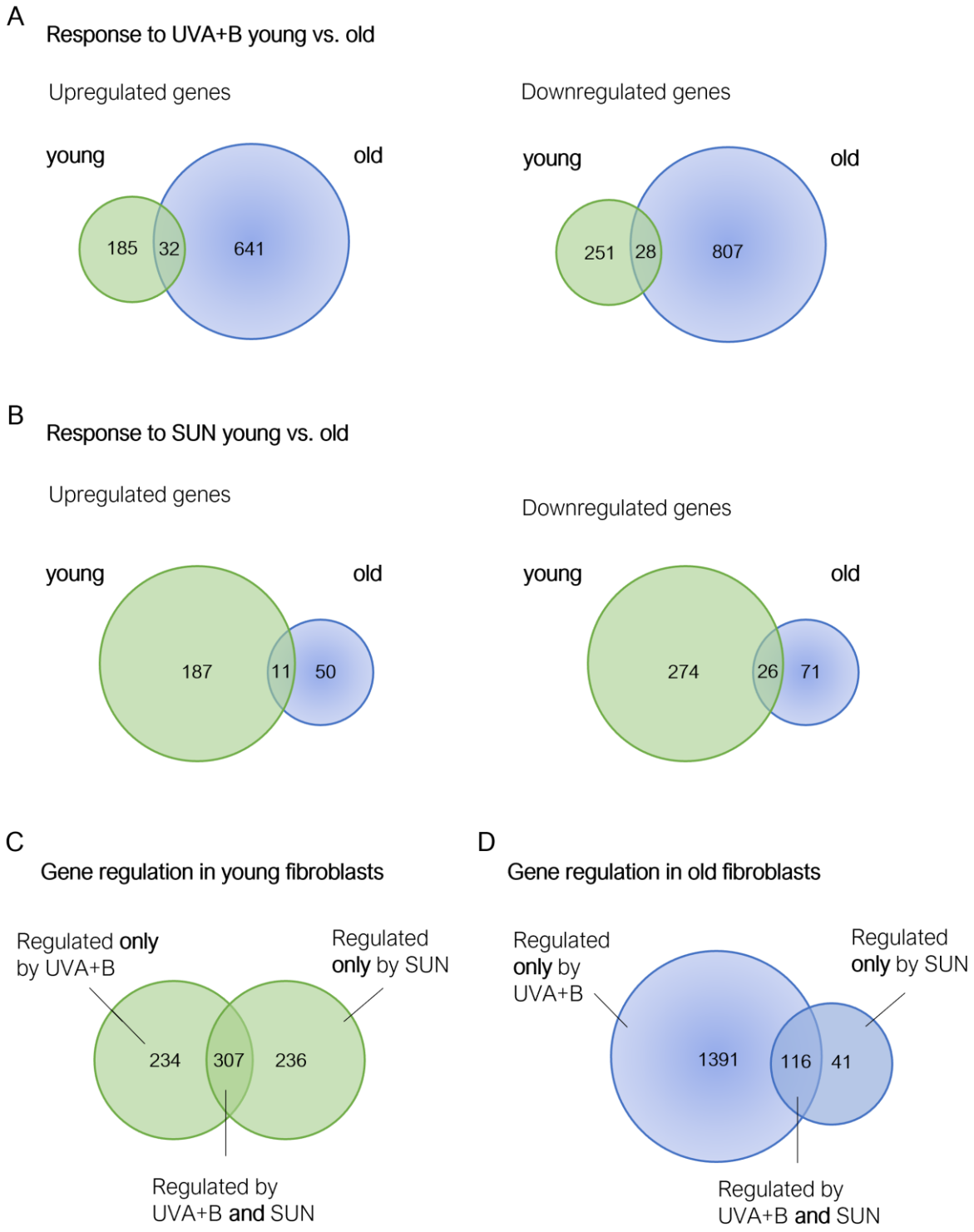

Figure 32: Regulated genes in young and old fibroblasts in response to irradiation
Venn diagrams displaying unique and shared differentially expressed genes in response to (**A**) UVA+B or (**B**) SUN irradiation. Number of genes in the green circles represent genes uniquely up- or downregulated in young fibroblasts. Number of genes in the blue circles represent genes uniquely up- or downregulated in old fibroblasts. The overlapping part represents the shared genes that are similary up- or downregulated in young and old fibroblasts. (**C**) and (**D**) display the number of genes that are uniquely regulated by UVA+B or SUN and the number of genes commonly regulated by UVA+B and SUN in **(C)** young and **(D)** old fibroblasts.

3.2.11.2.1 Differential Gene Expression of Young Fibroblasts

Lists of DEGs for the comparisons “young control” vs. “young UVA+B”, “young control” vs. “young SUN”, “old control” vs. “old UVA+B” and “old control” vs. “old SUN” were generated. Genes with an adjusted p-value lower than 0.05 and a significant log2-foldchange (L2FC) unequal 0 were considered as significantly up- or downregulated. Only relevant genes of interest are discussed here, the complete lists are provided in the supplementary digital data.

To link the regulated genes to biological processes, cellular components or molecular functions, the significantly up- or downregulated genes of a sample group comparison were submitted to Gene Set Enrichment Analysis (GSEA) and compared to categories defined in gene lists of Gene Ontology (GO). The 10 most significantly enriched gene sets, or GO terms, in up-or downregulated genes are summarized in Fig. 33.

Many of the GO categories that stood out in the young fibroblast in response to irradiation (both UVA+B and SUN) were connected to the extracellular matrix. Importantly, that accounted especially for the downregulated genes. Elastin (ELN) as well as several collagens (see Table 14) were downregulated. COL1A1, encoding the main structural component of the dermis, Collagen type I, had the highest expression level in the group of genes downregulated after UVA+B and SUN exposure, followed by COL3A1, encoding collagen type III.

Also connected to the ECM and its remodeling are the MMPs. Among the significant DEGs we found five MMPs (MMP-1, 3, 9, 11 and 19) and, in the case of UVA+B exposure, also the inhibitor TIMP2. MMP-1 was upregulated after UVA+B or SUN exposure. This upregulation was confirmed by the pro-MMP-1 ELISA, that also showed an (non-significant) increase of secreted pro-MMP-1 in the conditioned media of young SEs irradiated with UVA+B or SUN. MMP-3 and MMP-9 were both found to be upregulated in the DGE analysis, but both had a very low expression level. This was again reflected in the ELISAs, where MMP-3 was only present in small amounts and MMP-9 could not be detected at all in the conditioned media. MMP-11 and MMP-19 were downregulated in response to UVA+B and SUN in the DGE analysis. The MMP-inhibitor TIMP-2 was slightly downregulated (L2FC -0.5) after UVA+B exposure. This downregulation did not seem to be prominent enough to alter the protein content as measured by ELISA in the conditioned media of the SEs. Rather, the level of TIMP2 remained largely unaltered (see Fig. 27B).

Among the significant DEGs regulated upon UVA+B as well as SUN exposure, several genes came up that are connected to the MAPK and the NFκB signaling pathway (Table 14). As both signaling pathways are known to be involved in the process of photoaging (Choi et al. 2016; Fisher and Voorhees 1998; Shin et al. 2019), our data highlights their relevance also for our model of irradiating SEs with young fibroblasts.

Interestingly, the Cartilage Intermediate Layer Protein (CILP) was among the top 3 most significantly regulated genes. It was downregulated in both UVA+B and SUN-treated samples. As CILP is associated with the cartilage ECM and thought to inhibit TGFB1-mediated induction of cartilage matrix genes via its interaction with TGFB1 (Gross and Thum 2020), this further points to a role for UV/SUN in regulating cartilage-specific genes.

Taken together, the RNA-Seq analysis of the young fibroblasts isolated from non-irradiated and irradiated SEs, demonstrated that especially the dermal ECM is affected by chronic irradiation. Most importantly, the most essential structural component, collagen type I, described to be downregulated in several studies of acute UV irradiation (Quan et al. 2004; Fisher et al. 1997), were also downregulated in response to both chronic UVA+B and SUN thereby confirming this regulation but also highlighting the relevance of our model of young fibroblasts for these studies.

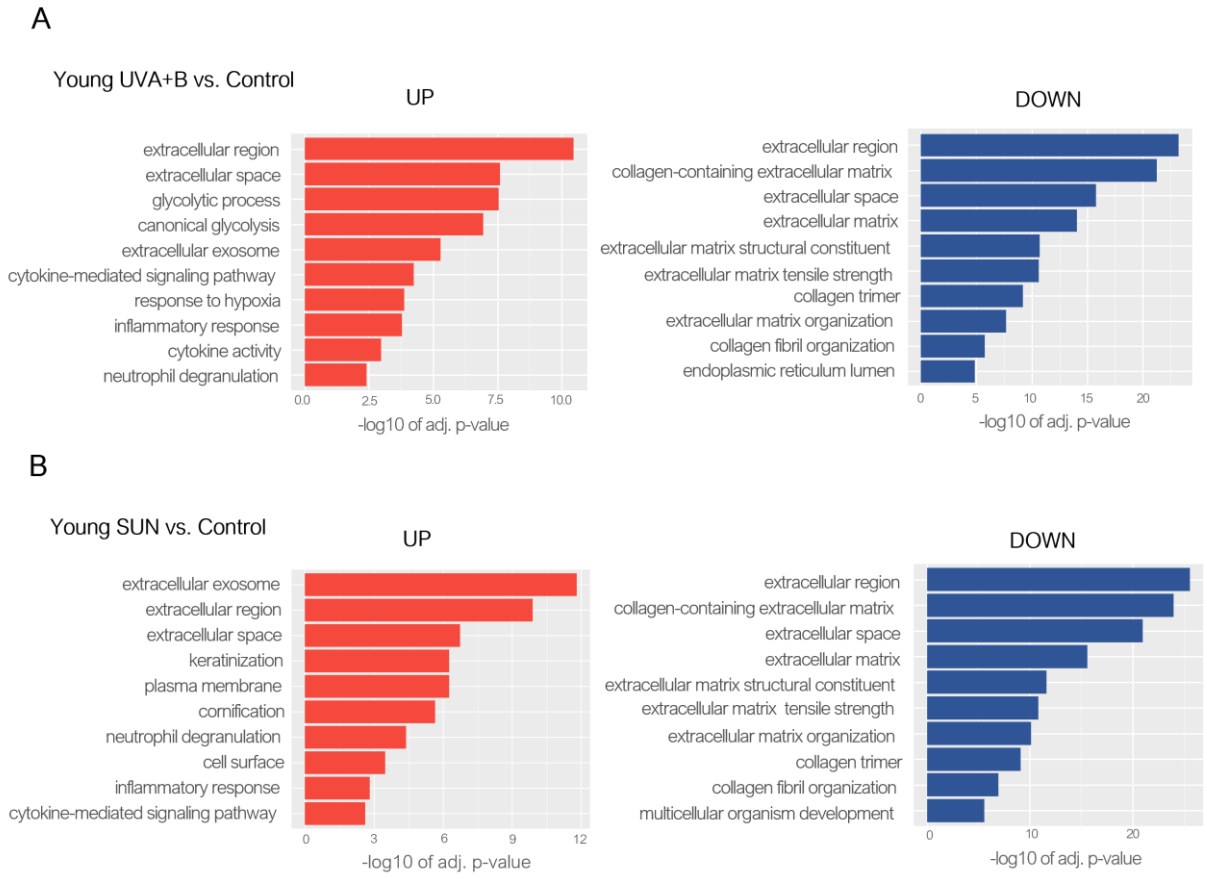

Figure 33: Results of Gene Set Enrichment Analysis (GSEA) of young dermal fibroblasts
Shown are the 10 most significantly enriched gene sets in differentially regulated genes (adj. $p < 0.05$) in the comparison between (**A**) control vs. UVA+B and (**B**) control vs. SUN, using gene ontology (GO) categories. On the left, upregulated gene sets are displayed in red, on the right downregulated gene sets are displayed in blue.

Table 14: Differentially expressed genes in young fibroblasts

Young Dermis UVA+B			
Gene		L2FC	adj. p-value
ECM			
CILP	Cartilage Intermediate Layer Protein	-2,75	3,16E-26
COL14A1	Collagen Type XIV Alpha 1 Chain	-3,21	6,92E-42
COL1A1	Collagen Type I Alpha 1 Chain	-1,20	1,46E-07
COL21A1	Collagen Type XXI Alpha 1 Chain	-2,34	8,18E-09
COL3A1	Collagen Type III Alpha 1 Chain	-0,87	9,37E-05
COL18A1	Collagen Type XVIII Alpha 1 Chain	0,72	5,87E-04
COL15A1	Collagen Type XV Alpha 1 Chain	-1,56	7,44E-04
COL5A3	Collagen Type V Alpha 3 Chain	-0,71	1,29E-03
COL5A2	Collagen Type V Alpha 2 Chain	-0,87	2,28E-03
COL12A1	Collagen Type XII Apha 1 Chain	-0,82	3,64E-02
COL5A1	Collagen Type V Alpha 1 Chain	-0,62	4,70E-02
ELN	Elastin	-2,39	2,32E-15
MMPs			
MMP1	Matrix Metalloproteinase 1	3,19	0,001
MMP11	Matrix Metalloproteinase 11	-1,42	0,002
MMP19	Matrix Metalloproteinase 19	-0,80	0,006
MMP9	Matrix Metalloproteinase 9	3,27	0,027
MMP3	Matrix Metalloproteinase 3	2,09	0,038
TIMP2	Tissue Inhibitor of Metalloproteinases 2	-0,50	0,050
Pathways			
TGFBI	Transforming Growth Factor Beta Induced	2,25	1,15E-26
MAP3K2	Mitogen-Activated Protein Kinase Kinase Kinase 2	-9,94	3,91E-07
MAP3K5	Mitogen-Activated Protein Kinase Kinase Kinase 5	1,52	5,69E-04
JUNB	JunB Proto-Oncogene, AP-1 Transcription Factor Subunit	0,56	1,30E-02
MAPKAPK2	MAPK Activated Protein Kinase 2	0,79	9,36E-03
NFKB2	Nuclear Factor Kappa B Subunit 2	1,16	7,21E-04
NFKBIA	NFKB Inhibitor Alpha	-0,66	1,99E-03
RELB	RELB Proto-Oncogene, NF-KB Subunit	2,21	8,42E-05

Young Dermis SUN			
Gene		**L2FC**	**adj. p-value**
ECM			
CILP	Cartilage Intermediate Layer Protein	-3,08	1,52E-39
COL14A1	Collagen Type XIV Alpha 1 Chain	-3,21	9,23E-28
COL1A1	Collagen Type I Alpha 1 Chain	-1,56	6,53E-15
COL3A1	Collagen Type III Alpha 1 Chain	-1,07	3,13E-10
COL15A1	Collagen Type XV Alpha 1 Chain	-1,51	3,94E-10
COL1A2	Collagen Type I Alpha 2 Chain	-0,79	1,60E-05
COL5A1	Collagen Type V Alpha 1 Chain	-0,79	8,96E-05
COL21A1	Collagen Type XXI Alpha 1 Chain	-1,65	3,35E-03
ELN	Elastin	-2,07	4,20E-20
MMPs			
MMP1	Matrix Metalloproteinase 1	3,19	1,70E-20
MMP3	Matrix Metalloproteinase 3	3,10	2,25E-05
MMP11	Matrix Metalloproteinase 11	-1,31	1,59E-04
MMP19	Matrix Metalloproteinase 19	-1,00	3,48E-04
MMP9	Matrix Metalloproteinase 9	3,43	1,27E-03
Pathways			
TGFBI	Transforming Growth Factor Beta Induced	2,19	1,80E-24
NFKBIA	NFKB Inhibitor Alpha	-1,61	3,02E-12
FOS	Fos Proto-Oncogene, AP-1 Transcription Factor Subunit	-1,24	1,51E-06
FOSB	FosB Proto-Oncogene, AP-1 Transcription Factor Subunit	-1,83	6,33E-06
NFKBIZ	NFKB Inhibitor Zeta	-1,71	1,18E-05
TGFB3	Transforming Growth Factor Beta 3	-5,38	2,33E-03
RELB	RELB Proto-Oncogene, NF-KB Subunit	1,19	7,12E-03
MAPKAPK2	MAPK Activated Protein Kinase 2	0,81	1,02E-02
JUND	JunD Proto-Oncogene, AP-1 Transcription Factor Subunit	-0,85	3,45E-02

3.2.11.2.2 Differential Gene Expression of Old Fibroblasts

Analyzing the old fibroblasts in more detail, DGE and GSEA were performed as described before. Again, the most significantly up- or downregulated GO categories in response to UVA+B (Fig. 34A) or SUN (Fig. 34B) exposure were connected to the extracellular region/ extracellular matrix organization. Differentially expressed genes of interest are summarized in Table 15.

Upon irradiation with UVA+B, elastin (ELN) was downregulated, as well as collagen type I (COL1A1) and the BM-type collagen, collagen type IV (COL4A1, COL4A2, COL4A4, COL4A5). In agreement with that, a slight reduction of ColIV protein was also found in the IIF staining of UVA+B exposed SEs. The irradiation with SUN similarly led to a downregulation of elastin, but not a significant downregulation of COL1 or COL4, demonstrating differences in the regulation upon solar UV (UVA+B) *versus* the entire solar spectrum (SUN).

Similar upregulation was seen for two ECM components, DCN (decorin), that plays a role in the assembly of collagen fibrils, and FBN2 (Fibrillin 2), involved in elastic fiber assembly. Likewise, HAS2, which encodes the enzyme hyaluronan synthase 2, was upregulated upon UVA+B and SUN irradiation, being in good agreement with the increased HA content that was detected by IIF staining of irradiated SEs with old fibroblasts.

Concerning the regulation of cartilage-related genes, interestingly, COL11 and HAPLN1 were found to be significantly downregulated in response to UVA+B irradiation while exposure to SUN did not induce significant downregulation of these genes. In both scenarios, UVA+B and SUN irradiation, however, we found several other genes related to chondrocytes and the regulation of cartilage matrix. These included SOX9 and COMP (Cartilage Oligomeric Matrix Protein), also known as thrombospondin-5, MMP13, and the collagens COL9A2 and COL22A1, that are both associated with the ECM of cartilage. Importantly, all those cartilage-related genes were downregulated in response to UVA+B and SUN. The only one upregulated was GDF5 (Growth Differentiation Factor 5) also called Cartilage-Derived Morphogenetic Protein 1 (CDMP1), a growth factor involved in bone and cartilage formation, that regulates differentiation of chondrogenic tissues via TGF-ß signaling.

The most significant DEG in both UVA+B and SUN exposed samples was MYH11 (Myosin heavy chain), a major component of smooth muscle myosin, that was strongly downregulated. Several other genes that are connected to the smooth muscle contractile fibers or the myofibroblast phenotype also stood out in the response to both UVA+B and SUN (specified in Table 15). These included TPM1 (tropomyosin 1), ACTG2 (Actin Gamma 2, Smooth Muscle) and ACTA2 (Actin Alpha 2, Smooth Muscle), encoding the myofibroblast marker α-SMA. All the mentioned genes in this group were downregulated, thus correlating well with the results from the IIF staining for α-

SMA in old SEs and strongly supporting our finding that upon irradiation the number of myofibroblasts declines. It further suggests that UV or solar radiation is regulating α-SMA at the transcriptional level.

Together, the gene expression analysis for the old fibroblasts isolated from irradiated and non-irradiated SEs demonstrated that the dermal ECM is an important target of irradiation and that both UVA+B and SUN exposure lead to a regulation of ECM-related genes. Several cartilage-related genes were found to be downregulated, arguing against the hypothesis that the irradiation with UVA+B or SUN directly induces the expression of the aberrant, cartilage-like matrix components. Another important result of the analysis was the downregulation of myofibroblast markers, suggesting either a loss or a redifferentiation of the myofibroblast phenotype.

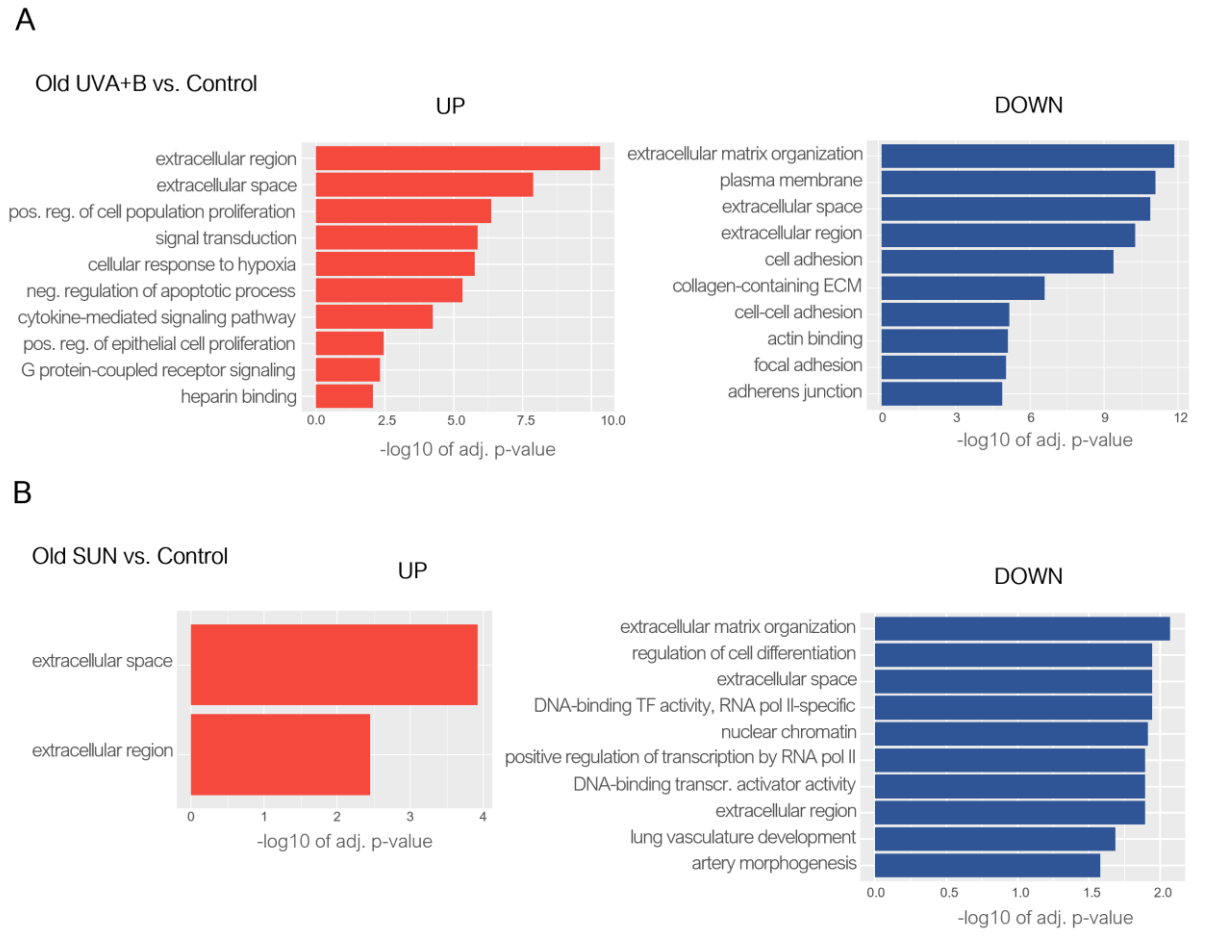

Figure 34: Results of Gene Set Enrichment Analysis (GSEA) of old dermal fibroblasts
Shown are the 10 most significantly enriched gene sets in differentially regulated genes (adj. $p < 0.05$) in the comparison between (A) control vs. UVA+B and (B) control vs. SUN, using gene ontology (GO) categories. On the left, upregulated gene sets are displayed in red, on the right downregulated gene sets are displayed in blue.

Table 15: Differentially expressed genes in old fibroblasts

Old Dermis UVA+B			
Gene	Gene Name	L2FC	adjusted p-value
ECM			
HAS2	Hyaluronan Synthase 2	1,92	2,39E-29
FBN2	Fibrillin 2	1,26	9,02E-15
DCN	Decorin	1,07	1,01E-06
COL4A4	Collagen Type IV Alpha 4 Chain	1,67	1,13E-04
COL4A1	Collagen Type IV Alpha 1 Chain	-0,72	1,37E-03
ELN	Elastin	-0,68	2,76E-03
COL1A1	Collagen Type I Alpha 1 Chain	-0,83	3,04E-03
COL4A5	Collagen Type IV Alpha 5 Chain	-1,61	6,50E-03
COL4A2	Collagen Type IV Alpha 2 Chain	-0,71	8,75E-03
FBN1	Fibrillin 1	1,06	1,94E-02
Myofibroblast phenotype			
MYH11	Myosin Heavy Chain 11	-4,02	1,04E-50
ACTG2	Actin Gamma 2, Smooth Muscle	-2,64	1,12E-16
TPM1	Tropomyosin 1	-1,40	1,79E-21
ACTA2	Actin Alpha 2, Smooth Muscle	-1,86	1,01E-12
MYLK	Myosin Light Chain Kinase	-1,15	1,45E-11
MYH14	Myosin Heavy Chain 14	-3,33	6,91E-06
ACTG1	Actin Gamma 1, Smooth Muscle	-0,59	1,58E-05
MYH9	Myosin Heavy Chain 9	-0,88	2,52E-04
Chondrocyte/Cartilage-related phenotype			
COL22A1	Collagen Type XXII Alpha 1 Chain	-3,26	3,18E-08
COL9A2	Collagen Type IX Alpha 2 Chain	-2,26	3,90E-10
MMP13	Matrix Metallopeptidase 13	-5,59	1,76E-27
SOX9	SRY-Box Transcription Factor 9	-2,94	4,62E-15
COMP	Cartilage Oligomeric Matrix Protein (Thrombospondin-5)	-1,11	4,46E-11
GDF5	Growth Differentiation Factor 5	2,78	4,07E-22

COL11A1	Collagen Type XI Alpha 1 Chain	-0,94	1,20E-04
HAPLN1	Hyaluronan And Proteoglycan Link Protein 1	-1,10	2,93E-03
HAPLN3	Hyaluronan And Proteoglycan Link Protein 3	-0,99	4,94E-02
CILP	Cartilage Intermediate Layer Protein	-0,91	2,00E-02
CILP2	Cartilage Intermediate Layer Protein 2	-0,65	3,48E-03

Old Dermis SUN			
ECM			
HAS2	Hyaluronan Synthase 2	1,66	1,09E-03
DCN	Decorin	1,22	4,24E-02
FBN2	Fibrillin 2	1,23	5,00E-02
Myofibroblast phenotype			
MYH11	Myosin Heavy Chain 11	-6,13	8,79E-21
CNN1	Calponin 1	-2,61	5,94E-05
TPM1	Tropomyosin 1	-1,46	9,68E-05
ACTA2	Actin Alpha 2, Smooth Muscle	-1,60	1,25E-02
ACTG2	Actin Gamma 2, Smooth Muscle	-1,87	1,77E-02
TAGLN	Transgelin	-1,65	2,28E-03
Chondrocyte/Cartilage-related phenotype			
COL22A1	Collagen Type XXII Alpha 1 Chain	-4,20	1,98E-02
COL9A2	Collagen Type IX Alpha 2 Chain	-2,50	3,51E-02
MMP13	Matrix Metallopeptidase 13	-4,76	4,41E-06
SOX9	SRY-Box Transcription Factor 9	-3,28	1,10E-04
COMP	Cartilage Oligomeric Matrix Protein (Thrombospondin-5)	-1,08	2,17E-02
GDF5	Growth Differentiation Factor 5	2,46	1,52E-03

3.2.11.3 Differential Gene Expression in the Epidermis

As described earlier, RNA from the epidermis was processed separate from the dermal equivalent in order to be able to analyze the gene expression pattern in both compartments individually.

Similar to the dermal samples, lists of DEGs were prepared and analyzed for enrichment of gene sets belonging to a certain GO category. Comparisons were done for “young control” vs. “young UVA+B” and “young control” vs. “young SUN”.

The most significantly enriched gene sets in response to UVA+B were “keratinization”, “epidermis development”, “cornified envelope” and “desmosomes” (Fig. 35A). In response to SUN, we also found “keratinization” and “epidermis development”, together with “cornification” (Fig. 35B).

Accordingly, in the lists of DEGs (Table 16), genes connected to late terminal differentiation of keratinocytes and formation of the cornified envelope were among the most significantly regulated ones. Two protein families were particularly present in the list of DEGs: SPPRs (small proline-rich proteins) and LCE (late cornified envelope) proteins. All of the SPRR and LCE genes, specified in Table 16, were upregulated, with the exception of SPPR3, which was downregulated in both scenarios, UVA+B and SUN treatment.

The GSEA and DGE analysis of the epidermis of young SEs suggested a late differentiation/cornification-inducing effect of UVA+B and SUN exposure. Although the epidermis of old SEs could not be analyzed in the RNA-seq due to technical reasons it could be speculated that this is a general phenomenon, as the results from the IIF stainings of several differentiation markers on old SEs clearly demonstrate that improved differentiation particularly accounts for the epidermis on old fibroblasts.

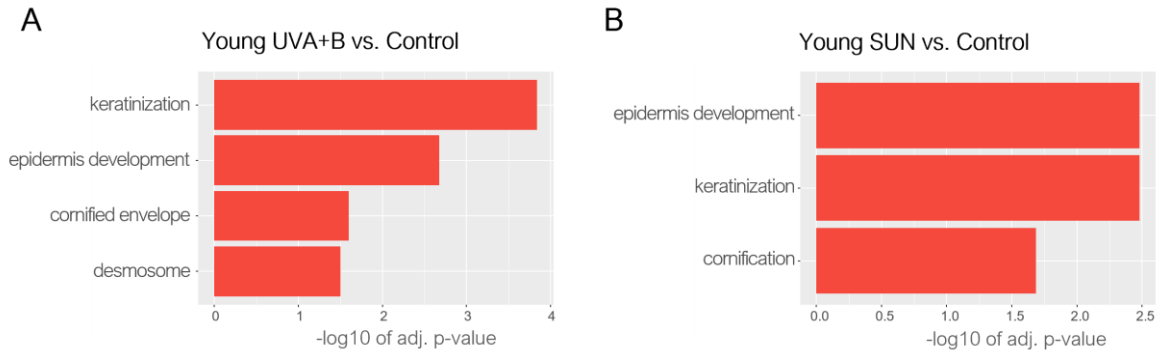

Figure 35: Results of Gene Set Enrichment Analysis (GSEA) of epidermal samples
Shown are the 10 most signficantly enriched gene sets in differentially upregulated genes (adj. $p < 0.05$) in the comparison between (**A**) control vs. UVA+B and (**B**) control vs. SUN, using gene ontology (GO) categories.

Table 16: Differentially expressed genes in young epidermis

Young Epidermis			
Gene		L2FC	adj. p-value
UVA+B			
ELF3	E74 Like ETS Transcription Factor 3	-1,20	2,20E-01
ELF5	E74 Like ETS Transcription Factor 5	1,93	4,37E-03
LCE2A	Late Cornified Envelope 2A	1,41	7,35E-04
LCE3D	Late Cornified Envelope 3D	2,16	1,14E-09
LCE3E	Late Cornified Envelope 3E	1,31	4,52E-03
LCE6A	Late Cornified Envelope 6A	1,31	4,97E-03
SPRR2B	Small Proline Rich Protein 2B	3,45	5,39E-16
SPRR2D	Small Proline Rich Protein 2D	1,93	9,94E-08
SPRR2E	Small Proline Rich Protein 2E	2,59	2,13E-15
SPRR3	Small Proline Rich Protein 3	-4,42	3,37E-21
SPRR5	Small Proline Rich Protein 5	2,05	6,24E-06
SUN			
ELF3	E74 Like ETS Transcription Factor 3	-2,06	3,24E-04
LCE3A	Late Cornified Envelope 3A	3,08	3,28E-02
LCE3D	Late Cornified Envelope 3D	1,78	1,94E-06
SPRR2B	Small Proline Rich Protein 2B	3,04	4,93E-12
SPRR2D	Small Proline Rich Protein 2D	1,41	7,02E-04
SPRR2E	Small Proline Rich Protein 2E	1,86	1,95E-07
SPRR2F	Small Proline Rich Protein 2F	3,43	2,54E-04
SPRR3	Small Proline Rich Protein 3	-5,07	2,96E-27

3.3 The Effect of Fibroblast Aging on SEs with Transformed Keratinocytes

Skin cancer, especially non-melanoma skin cancer (NMSC), is a disease of the skin that highly correlates with age as a result of lifelong sun exposure. Aged (senescent) fibroblasts that accumulate with aging, are discussed as a tumor-promoting factor (Campisi et al. 2011; Fitsiou et al. 2021). To identify the role of our old fibroblasts in the development of skin cancer, we complemented young and old SEs with HaCaT cells, a spontaneously immortalized human keratinocyte cell line containing UV-type specific p53 mutations and thus representing an early stage in the multistep process of skin carcinogenesis (Boukamp et al. 1988). To account for different stages of malignancy, we also produced models with HaCaT-ras A5, benign tumorigenic cells that can gain invasive potential upon challenge and thus are a paradigm of premalignant skin keratinocytes; and HaCaT-ras II4, as an example of a malignant tumorigenic cell line that is highly invasive (Boukamp et al. 1990). As shown before (Berning et al. 2015) the cell-derived matrix skin equivalents are perfectly suited models to study the invasion behavior of cells. With the HaCaT models we aimed at elucidating whether and how an “old environment”, i.e., a matrix produced by aged fibroblasts, affects (pre)malignant keratinocytes.

3.3.1 Morphology of Young and Old SEs with Transformed Keratinocytes

The HaCaT-based models show a different morphology than the NHEK-based models with a rather aberrantly organized epithelium consisting of only few vital cell layers and a thick parakeratotic stratum corneum (Fig. 36). This phenotype was characteristic for the HaCaT-SEs irrespective of being cocultured with young or old fibroblasts.

SEs with HaCaT-A5 present a similar morphology, but with a beginning invasion of epidermal cells in some cultures. This manifested more as invaginations, only partly breaking through the BM. These invaginations were only present in some cultures and found in young as well as old SEs, but slightly more frequent in old SEs.

In SEs with HaCaT-II4, we found massive invasion of epidermal cells, reaching deep into the dermal part, irrespective of the age of the fibroblasts forming the DE. In addition, all HaCaT-II4 cultures displayed so called acantholysis in suprabasal areas, which describes the loss of intercellular connections and cohesion between keratinocytes, a histological feature seen in diseases such as *pemphigus vulgaris.*

Taken together, we were able to establish completely cell-derived skin equivalents that represent different stages of carcinogenesis and reproduce the invasive behavior of the transformed cells as seen in *in vivo* experiments (Boukamp et al. 1990). The histological analysis indicated that the

different HaCaT cell lines are more independent from the fibroblasts they are co-cultured with and probably less sensitive to regulatory factors provided by the fibroblasts than the NHEK.

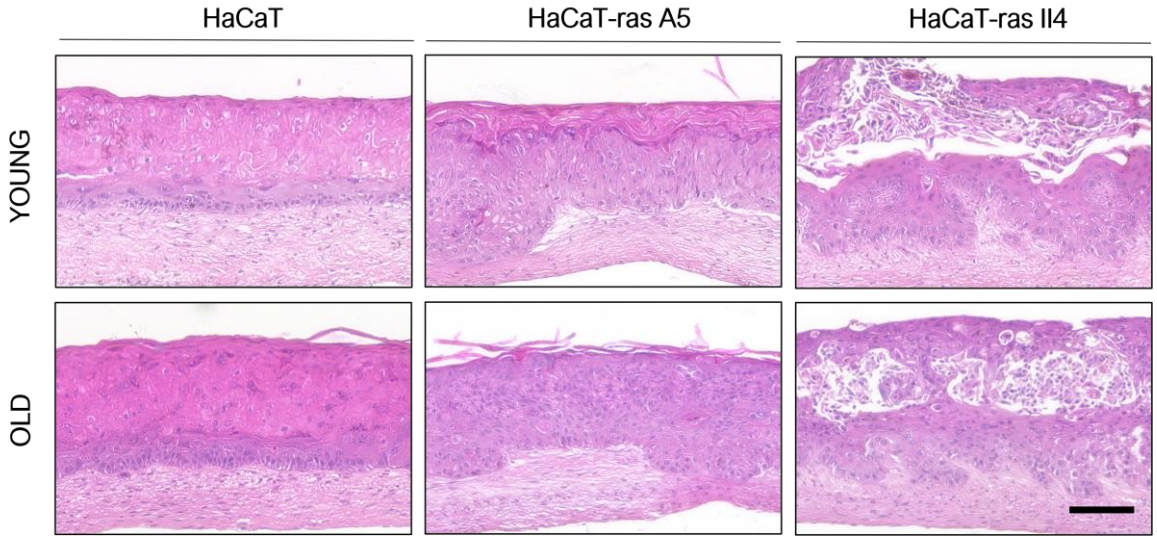

Figure 36: Histology of young and old Age-SEs complemented with transformed keratinocytes
fdmSEs were established with either young or old fibroblasts and the transformed keratinocyte cell lines HaCaT, HaCaT-ras A5 or HaCaT-ras II4. H&E staining was performed on paraffin sections. Displayed are representative histological images of young and old SEs after 4 weeks of co-culture. The different keratinocytes show a distinct invasion behavior: HaCaT are non-tumorigenic keratinocytes that produce a parakeratotic *stratum corneum*, HaCaT-ras A5 are benign tumorigenic and form invaginations, HaCaT-ras II4 are malignant keratinocytes that massively invade the DE.The scale bar represents 100 µm.

3.3.2 Evaluation of Epidermal Differentiation, Basement Membrane and Dermal ECM of Young and Old SEs with Transformed Keratinocytes

To assess the differentiation status as well as the BM formation and the collagen network of the DE, we stained for several markers that were already used and described for the NHEK models: K10 and K2 for early and late epidermal differentiation, ColVII as marker for BM integrity and ColI as the main structural component of the dermal equivalent (depicted in Fig. 37).

Other than in NHEK-SEs, the epidermal differentiation in HaCaT models, visualized by K10 (Fig. 37A) and K2 (Fig. 37B), did not display obvious differences between models based on young or old fibroblasts. In HaCaT- as well as HaCaT-A5-SES, K10 was expressed in all suprabasal layers and K2 was only sparsely expressed and not restricted to the uppermost layer but scattered all over the epidermal part, again showing the disorganized differentiation pattern of HaCaT epithelia. In HaCaT-II4 cultures, not all suprabasal cells expressed K10, leaving larger areas with undifferentiated cells. K2 was not present at all in HaCaT-II4 epithelia. This indicates that early differentiation is not induced in all cells and late differentiation is not induced at all in these malignant cells. Expression of ColVII, a major component of the BM, was similar in intensity and distribution in young and old SEs (Fig. 37A). It was displayed as a more or less continuous line

between epidermal and dermal part in HaCaT- and HaCaT-A5-SEs, as seen in NHEK-SEs as well. Models complemented with HaCaT-II4 did not show this typical linear pattern but a rather chaotic expression, indicating an erosion of the basement membrane or an incorrect assembly of its components. ColI expression displayed major differences between young and old SEs (Fig. 37B). The collagen meshwork appeared much denser in young cultures whereas the old DE showed bigger holes and a looser structure. This was true for all HaCaT variants, also A5 and II4.

These findings support the hypothesis that the different HaCaT cell lines (HaCaT, A5 and II4) are more independent of the age of the fibroblasts included in the DE than NHEK, also in respect to epithelial differentiation and BM assembly.

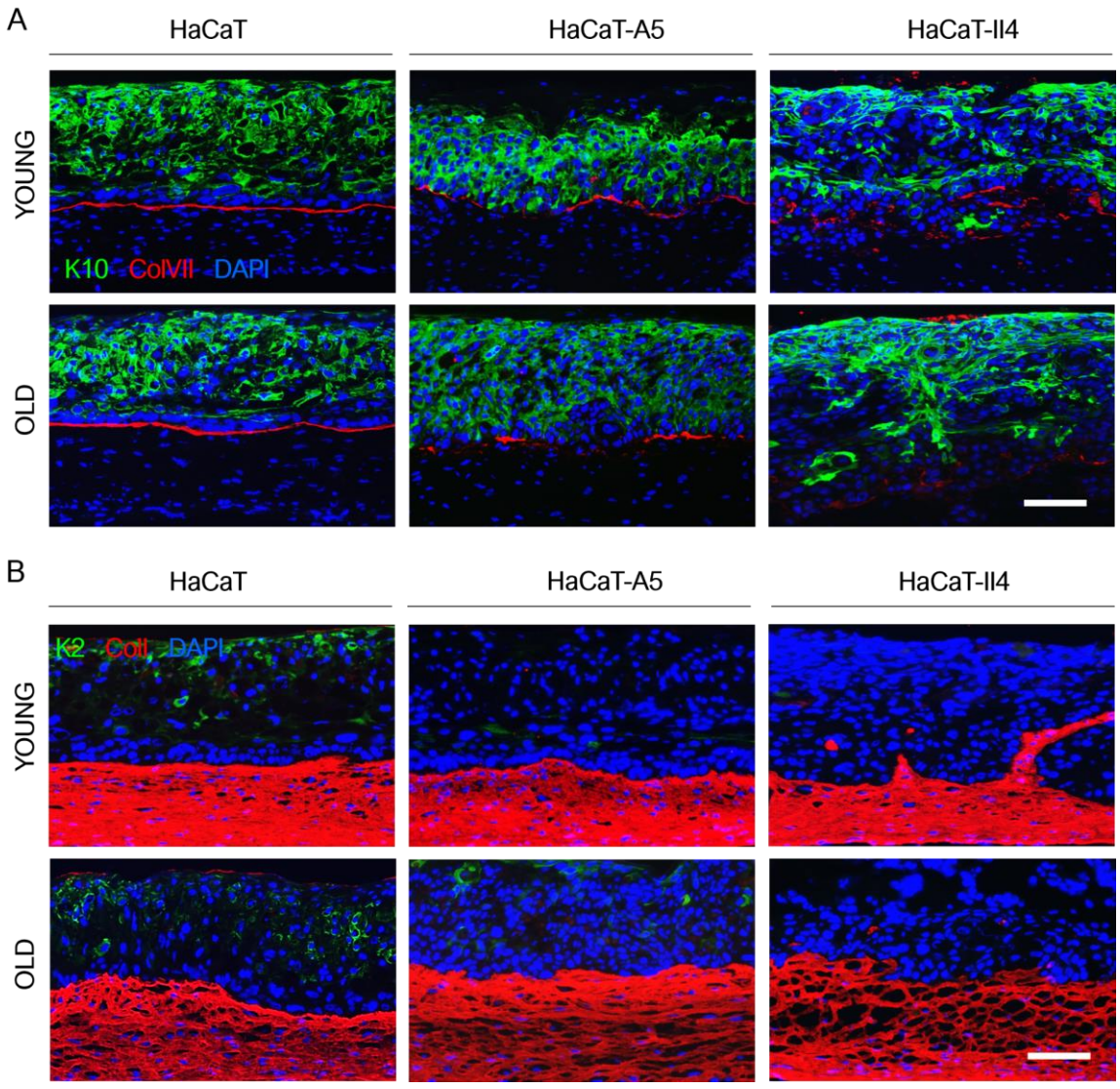

Figure 37: Epidermal differentiation, BM and DE in HaCaT-, HaCaT-A5- and HaCaT-II4-SEs
fdmSEs were established with either young or old fibroblasts and transformed keratinocytes. IIF stainings for (**A**) keratin 10 (K10, green) and collagen type VII (ColVII, red) and (**B**) keratin 2 (K2, green) and collagen type I (ColI, red) were performed on frozen sections. Displayed are representative images of SEs after 4 weeks of co-culture. With increasing malignancy of the epidermal cells, the differentiation and BM formation were more dysregulated. The ColI network was less dense in old DEs. Scale bar represents 100 µm.

3.4 Radiation Response of Young and Old Age-SEs With Transformed Keratinocytes

Young and old Age-SEs with transformed keratinocytes (HaCaT, HaCaT-A5 and HaCaT-II4) were subjected to the same irradiation regime as the NHEK-based SEs before, namely chronic irradiation for two weeks three times a week with 1 MED of either the solar UV spectrum (UVA+B) or the entire solar spectrum (SUN). With this we wanted to address the question how irradiation affects transformed keratinocytes and if the treatment is promoting tumorigenic transformation i.e. inducing an invasive phenotype even in non-tumorigenic HaCaT cells. Furthermore, we wanted to investigate if the altered matrix of aged fibroblasts is more permissive for invasive growth and thus adds to UV-dependent carcinogenesis.

3.4.1 Morphology and Invasion

The morphology of irradiated and non-irradiated young and old SEs complemented with HaCaT variants are depicted in Figure 38. Upon chronic irradiation of young HaCaT-SEs, we found a slightly more stratified epithelium with a more condensed though still parakeratotic stratum corneum. So, irradiation seemed to rather improve the skin status towards a more normally organized epithelium, as seen in NHEK-SEs. This was not the case in HaCaT-SEs with old fibroblasts.

HaCaT-A5-SEs, as described in the previous chapter, displayed invasive buds or invaginations. This was found in young as well as old SEs, but more often in old SEs. Irradiation with UVA+B or SUN did not increase the appearance of these invaginations, neither in young nor in old HaCaT-A5-SEs. Figure 39 depicts examples of invasive sites in HaCaT-A5-SEs, where epidermal cells were breaking through the BM, indicated by disrupted ColVII staining. The invading cells partly lose their keratin expression (indicated by pan-keratin staining), which is one hallmark for epithelial mesenchymal transition (EMT) (Barriere et al. 2015; Fortier, Asselin, and Cadrin 2013).

In HaCaT-II4-SEs the age of the fibroblasts did not obviously influence the morphology of the SE or invasive behavior of the epithelial cells (Fig. 38). Irrespective of the young or old DE, the HaCaT-II4 were highly invasive. Remarkably, irradiation (both UVA+B and SUN) did not induce or aggravate invasion in any case, on the contrary, invasion was rather reduced.

These findings demonstrate that a chronic irradiation regime of two weeks is clearly not sufficient to induce tumorigenic conversion of premalignant cells or to further push invasive behavior of already malignant cells.

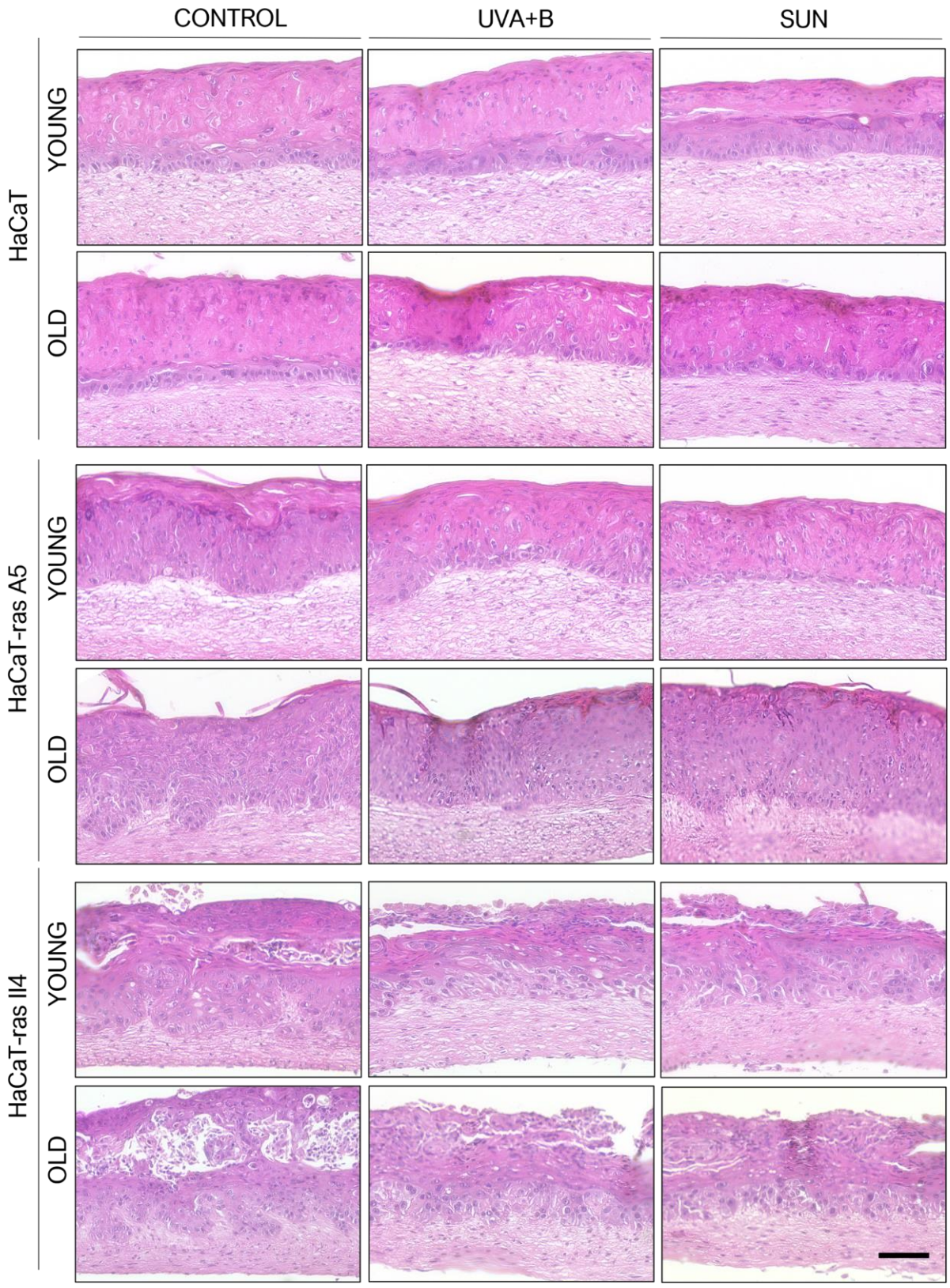

Figure 38: Effect of irradiation on the histology of young and old HaCaT-, HaCaT-A5- and HaCaT-II4-SEs
Young and old SEs complemented with HaCaT (upper panel), HaCaT-ras A5 (middle panel) or HaCaT-ras II4 (lower panel) keratinocytes were chronically irradiated with either the solar UV spectrum (UVA+B) or the entire solar spectrum (SUN) over the period of two weeks and compared to non-irradiated controls. H&E staining was performed on paraffin sections. Displayed are representative histological images of young and old SEs. Irradiation did not induce or increase invasive growth of epidermal cells, neither in young nor old SEs, but rather reduced the massive invasion of HaCaT-ras II4. The scale bar represents 100 µm.

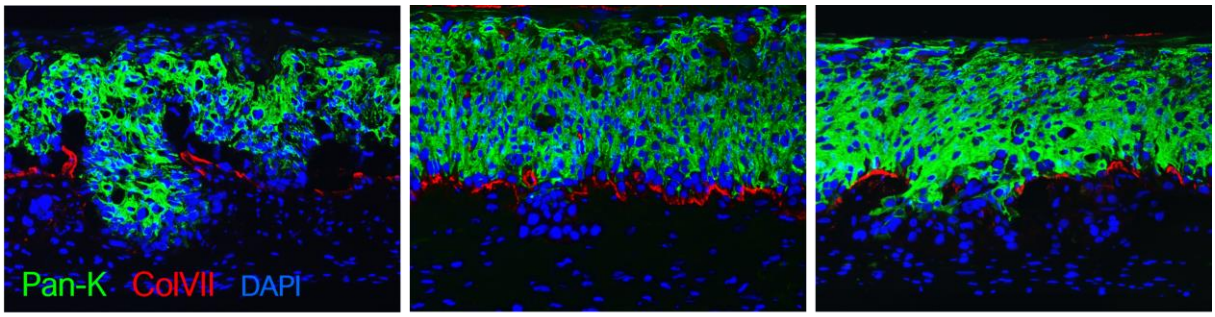

Figure 39: Examples of invasion sites
Shown are exemplary pictures of invasion sites in HaCaT-A5 SEs (from left to right: young UVA+B, old UVA+B, old SUN), where epidermal cells are breaking through the BM. Collagen type VII (ColVII, red) is disrupted at the invasion sites and keratinocytes are losing the pan-keratin (Pan-K, green) staining. The scale bar represents 100 µm.

3.4.2 Effect of Irradiation on Differentiation, Basement Membrane and Dermal ECM

The differentiation, BM formation and collagen content of the DE in the HaCaT models were evaluated after irradiation with UVA+B and SUN by staining for the known markers K10, K2, ColVII and ColI (Fig. 40).

The expression pattern of the markers in the different models (HaCaT, HaCaT-A5 and HaCat-II4) has been described in 3.3.2. Other than for the NHEK-SEs, the early and late differentiation as well as the BM formation of HaCaT/A5/II4-SEs seemed to be not so much dependent on the DE and the age of the fibroblasts included and therefore looked similar in young and old SEs.

In HaCaT-SEs, the early differentiation, represented by K10 (Fig. 40A), and the late differentiation, represented by K2 (Fig. 40B), were not altered by irradiation with UVA+B or SUN, neither in young nor old SEs. ColVII expression was slightly reduced by irradiation (both UVA+B and SUN) and showed more interruptions (Fig. 40A). The collagen network in the DE, visualized by ColI staining (Fig. 40B), was very dense in the young HaCaT-SEs and appeared looser with more holes in the old SEs. Irradiation did not further alter that phenotype.

In HaCaT-A5-SEs, similar to the observations in the HaCaT-SEs, the differentiation and ColI network were not altered by irradiation. ColVII in young and old HaCaT-A5-SEs was not expressed in a continuous line like in HaCaT models but interrupted. Expression was again slightly reduced by irradiation with UVA+B or SUN (Fig. 40A). This suggests a degradation of the BM, which is one necessary step for the invasion of epithelial cells into the dermal compartment.

Young and old HaCaT-II4-SEs displayed a chaotic and reduced K10 expression that was further reduced by UVA+B and SUN irradiation (Fig. 40A). K2 was completely missing in all HaCaT-II4-SEs (Fig. 40B), which again supports the finding of a dysregulated terminal differentiation of these

malignant cells. ColVII was not expressed in the typical linear pattern but disrupted and chaotic (Fig. 40A). In both young and old SEs, irradiation (UVA+B and SUN) did further reduce ColVII and expression was scattered over the entire epithelium, showing a defective BM assembly in HaCaT-II4-SEs. ColI expression again was not altered by irradiation (Fig. 40B).

Taken together, the SEs with transformed keratinocytes displayed clear differences dependent on the keratinocyte variant (HaCaT, -A5, or II4) with an increasing deregulation of differentiation and BM formation with increasing malignancy of the keratinocytes. The age of the fibroblasts however did not significantly affect the epithelium and the response to irradiation. The strongest effect of the irradiation was found on ColVII which was reduced.

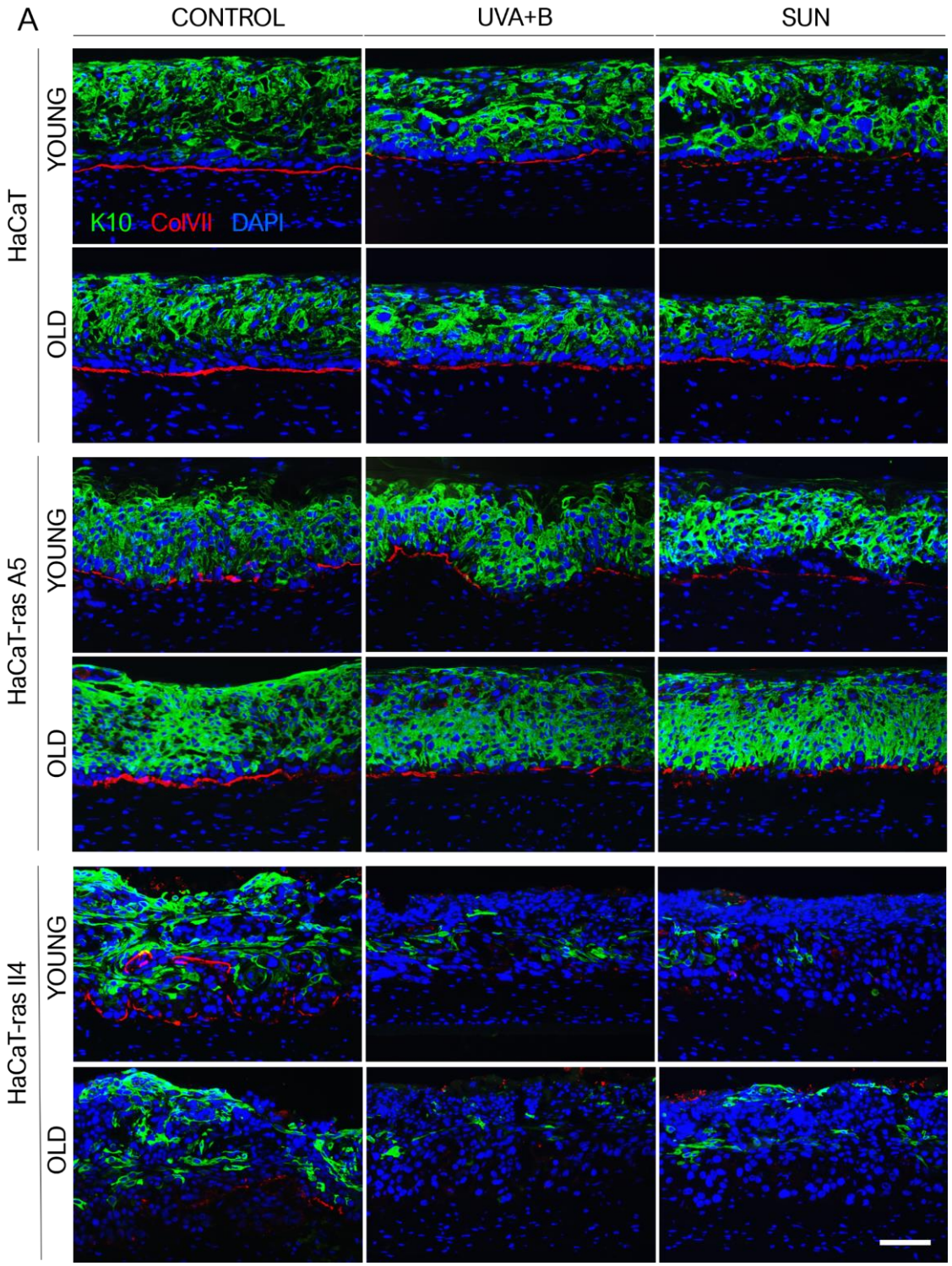
A
CONTROL
UVA+B
SUN
HaCaT
HaCaT-ras A5
HaCaT-ras II4
YOUNG
OLD
K10 ColVII DAPI

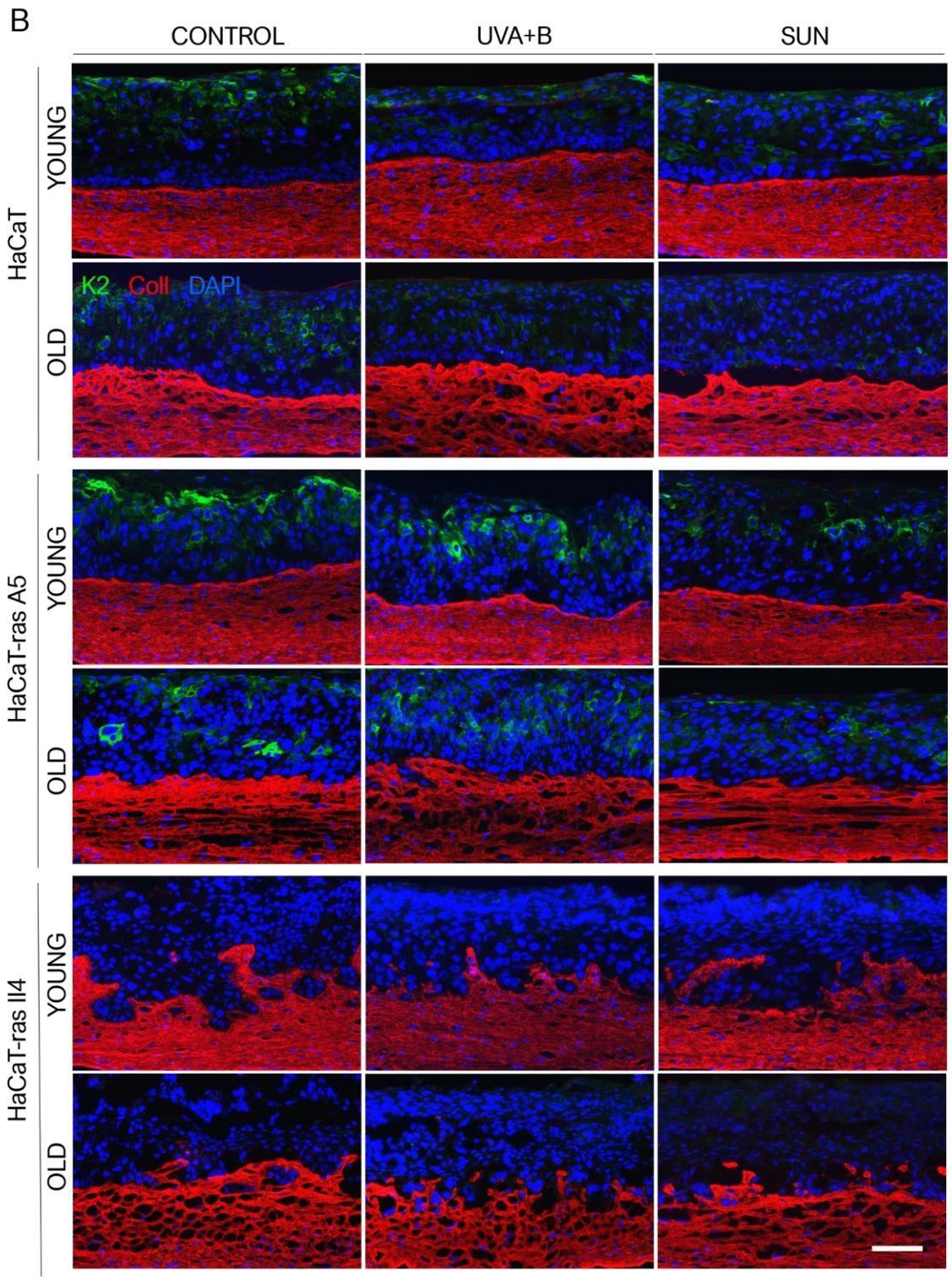

Figure 40: Effect of irradiation on differentiation, BM and DE of young and old HaCaT-, HaCaT-A5- and HaCaT-II4-SEs

Young and old SEs complemented with HaCaT (upper panel), HaCaT-ras A5 (middle panel) or HaCaT-ras II4 (lower panel) keratinocytes were chronically irradiated with either the solar UV spectrum (UVA+B) or the entire solar spectrum (SUN) over the period of two weeks and compared to non-irradiated controls. IIF staining for (**A**) keratin 10 (K10, green) and collagen type VII (ColVII, red) and (**B**) keratin 2 (K2, green) and collagen type I (ColI, red) was performed on frozen sections. Displayed are representative images of young and old SEs. ColVII expression was slightly more disrupted in irradiated SEs compared to controls in HaCaT- and HaCaT-A5-SEs. In HaCaT-II4-SEs differentiation and BM assembly were completely disturbed and this was even aggravated by irradiation. K2 was slightly decreased by irradiation and not present at all in HaCaT-II4 SEs. ColI network was less dense in old SEs. The scale bar represents 100 µm.

3.4.3 MMP-1 Induction by Irradiation

An essential step in tumorigenesis is the degradation of the BM and ECM that allows tumor cells to migrate and invade the surrounding tissue. Especially MMP-1 has been shown to be connected to tumor progression in cSCCs (Lederle et al. 2011). Thus, we measured the level of secreted pro-MMP-1 in the conditioned media of young and old HaCaT, HaCaT-A5 and HaCaT-II4-SEs, that was collected 24 h after the last irradiation (Fig. 41). The irradiation with UVA+B and SUN led to a significant increase of pro-MMP-1 in young and old HaCaT-SEs, in young HaCaT-A5-SEs and in young HaCaT-II4-SEs. In old HaCaT-A5 and -II4-SEs no induction of pro-MMP-1 was observed. Interestingly, the strong induction of pro-MMP-1 in all HaCaT models with young fibroblast was the opposite of what was seen in NHEK-SEs, where pro-MMP-1 was only induced in SEs with old fibroblasts (see 3.2.8.2).

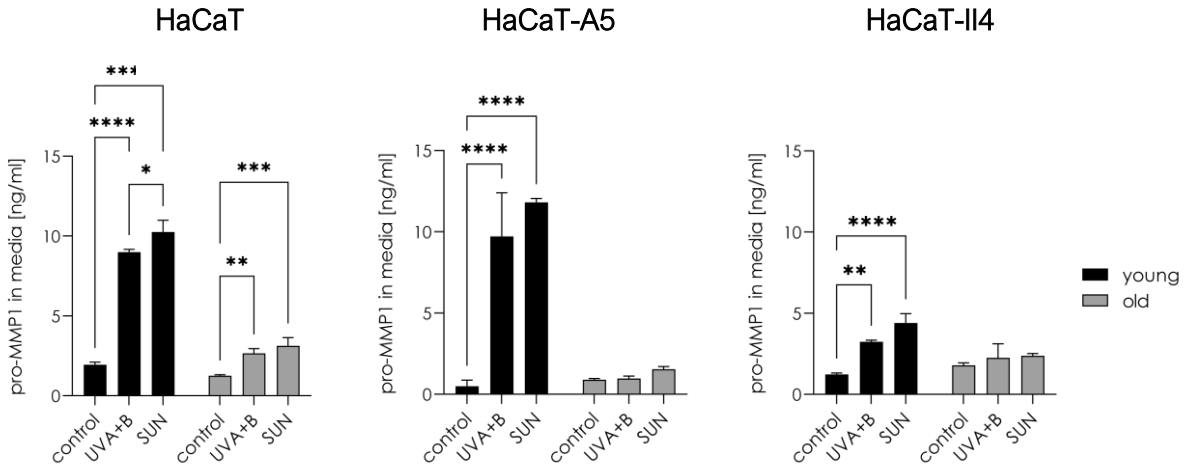

Figure 41: Levels of secreted pro-MMP1 in HaCaT-, HaCaT-A5- and HaCaT-II4-SEs
Young and old SEs were chronically irradiated with either the solar UV spectrum (UVA+B) or the entire solar spectrum (SUN) over the period of two weeks and compared to non-irradiated controls. Conditioned media was collected 24h after the last irradiation and used to detect secreted pro-MMP1 in HaCaT-SEs (left), HaCaT-A5-SEs (middle) and HaCaT-II4-SEs (right) by ELISA. Irradiation induced increased pro-MMP-1 secretion in young SEs. In old SEs a significant induction was only seen in HaCaT-SEs. Error bars represent the standard error mean. Two-way-ANOVA; * = $p < 0.05$; ** $p < 0.01$; *** $p < 0.001$; **** = $p < 0.0001$; n=3.

3.4.4 Analysis of Desmosomes in HaCaT-Il4-SEs

As described in chapter 3.4.1, we found a loss of adhesion between keratinocytes, so called acantholysis, in the epidermis of HaCaT-Il4-SEs. This phenomenon is known from several diseases and caused by defects in desmosomal components. Desmosomes are intercellular junctions, mediating cell-cell adhesion in the epidermis. By staining for different desmosomal proteins, the cadherins desmoglein 1 (Dsg1) and 3 (Dsg3) and desmoplakin (Dsp), we investigated if the age of the DE or the irradiation treatment would affect the integrity of the desmosomes in HaCaT-Il4-SEs.

In normal human skin, Dsg3 is predominantly distributed throughout the lower layers of the epidermis, while Dsg1 is mainly expressed in the upper layers. Both are targets in the autoimmune blistering diseases *pemphigus vulgaris* and *pemphigus foliaceus* (Payne et al. 2004). Desmoplakin tethers the desmosomal cadherins to the intermediate filament cytoskeleton and is normally expressed throughout the epidermis (Delva, Tucker, and Kowalczyk 2009).

In the HaCaT-Il4-SEs, both young and old, Dsg1 was only expressed in minor amounts and expression was not changed with irradiation (UVA+B or SUN), as depicted in Figure 42C. Dsg3 (Fig. 42A) and Dsp (Fig. 42B) showed a similar expression pattern and similar changes after irradiation. In young and old control SEs, both proteins were expressed abundantly all over the epidermis, up to the most superficial layers. Exposing the SEs to either UVA+B or SUN led to a more restricted expression in the lower and middle part of the epidermis. No major differences were observed between young and old SEs.

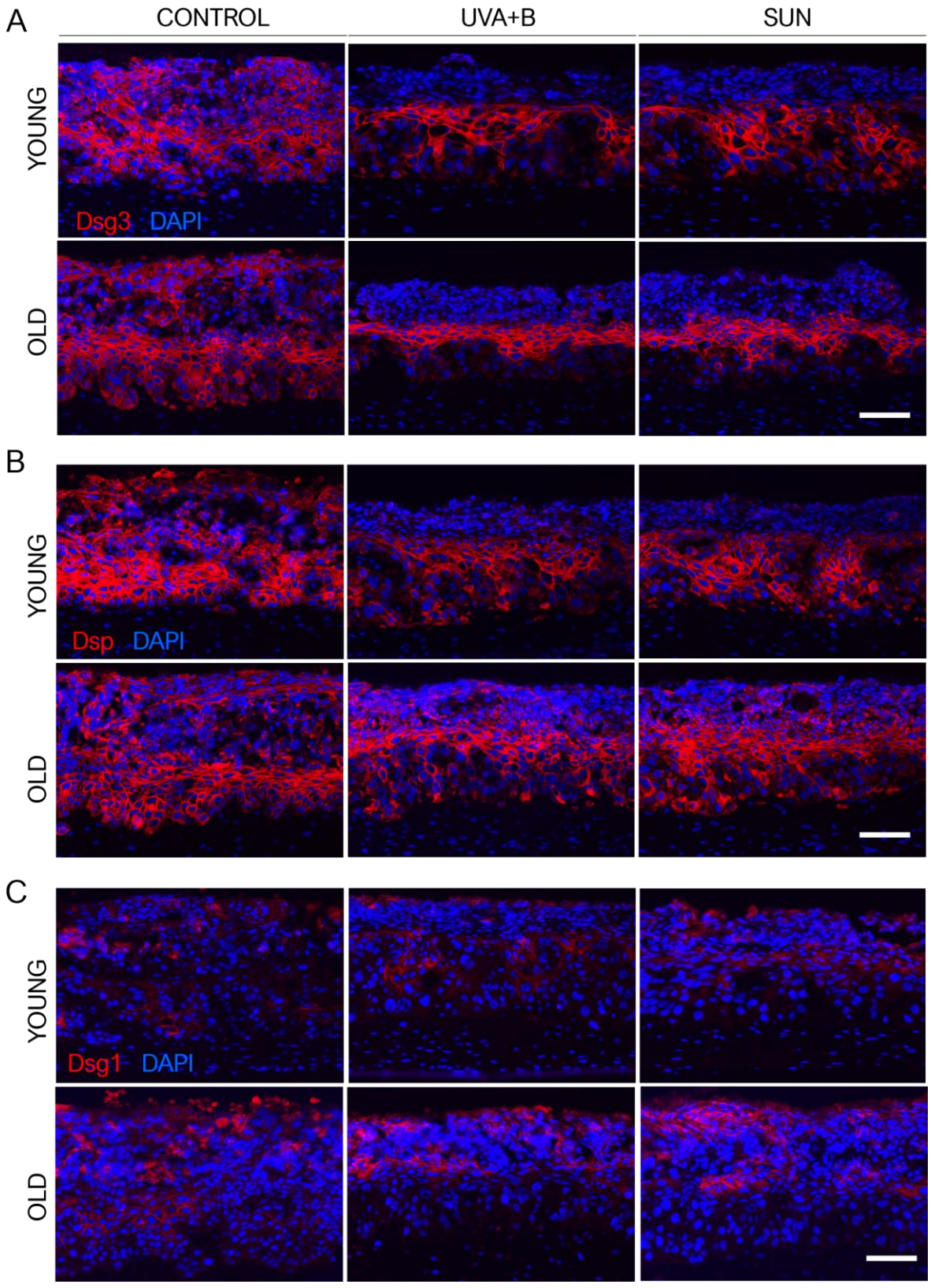

Figure 42: Effect of irradiation on desmosome components in HaCaT-II4-SEs
The integrity of desmosomes was assessed in young and old HaCaT-II4-SEs by IIF staining for the desmosome components **(A)** desmoglein 3, **(B)** desmoplakin and **(C)** desmoglein 1. Desmoglein 3 as well as desmoplakin expression was found up to the uppermost layers of the control SEs but was reduced and more restricted to the middle part of the epithelium after irradiation. Desmoglein 1 was only expressed in minor amounts in controls and irradiated SEs. The scale bar represents 100 µm.

3.4.5 Effect of Irradiation on the Proliferation of SEs with Transformed Keratinocytes

To evaluate the influence of irradiation on the proliferative behavior of the different SEs, they were stained for Ki67, and the proliferation index was quantitatively determined by half-automated cell counting as described before. In addition, IIF staining illustrated the localization of proliferating cells within the tissue. Three replicates of each treatment were analyzed, and pictures were taken from three different areas of the section. All cultures were harvested 24 h after the last irradiation.

Looking at the immunofluorescent staining (Fig. 43A), the distribution of proliferating cells differed considerably between the different cell lines. In HaCaT-SEs Ki67-positive cells were almost only present in the basal layer or near the basal layer, while in HaCaT-A5-SEs positive cells were also found in suprabasal areas of the epithelium and particularly focused on those regions that showed invaginations or starting invasion. In HaCaT-II4-SEs proliferating cells were randomly spread all over the entire epidermal part, not restricted to any specific area.

By counting Ki67+ cells, the proliferation rate was determined (Fig. 43B). In HaCaT-SEs, neither the age of the fibroblasts nor the irradiation with UVA+B or SUN did have a significant impact on the proliferation. In young SEs, irradiation slightly increased the percentage of proliferating cells (from 12.75 ± 2.66 % to 14.04 ± 1.63 % with UVA+B and 15.06 ± 4.85 % with SUN), in old SEs irradiation it slightly reduced it (from 16.15 ± 4.35 % to 11.87 ± 1.89 % with UVA+B and 10.65 ± 3.23 % with SUN), but both trends were not statistically significant.

In HaCaT-A5-SEs, proliferation rates of controls were similar to HaCaT-SEs. Irradiation with UVA+B as well as SUN decreased proliferation rate in both young (from 11.81 ± 4.24 % to 7.72 ± 2.43 % with UVA+B and 7.20 ± 6.80 with SUN) and old (from 15.72 ± 7.35 % to 7.53 ± 1.93 % with UVA+B and 6.88 ± 3.07 % with SUN) HaCaT-A5-SEs. This decrease was only statistically significant for the old samples

Epithelia with HaCaT-II4 cells had the highest proliferation rates, with a percentage of around 28 % of proliferating cells in young and old controls. Irradiation with UVA+B or SUN did significantly reduce proliferation in young SEs (from 28.51 ± 2.27 % to 17.72 ± 1.80 % with UVA+B and 18.60 ± 2.70 % with SUN). In old SEs, there was no significant reduction (from 27.98 ± 7.71 % in controls to 28.18 ± 0.73 % with UVA+B and 25.43 ± 2.73 % with SUN). Taken together, proliferation in HaCaT epithelia seemed to be less dependent on the underlying DE than it was seen in NHEK epithelia. The effect of irradiation was only statistically significant in two cases (HaCaT-A5 old and HaCaT-II4 young), but the overall tendency was rather a reduction than an induction of proliferation. There was no difference between irradiation with UVA+B or SUN. To account for inter-experimental variations, we analyzed another independent experiment with similar results.

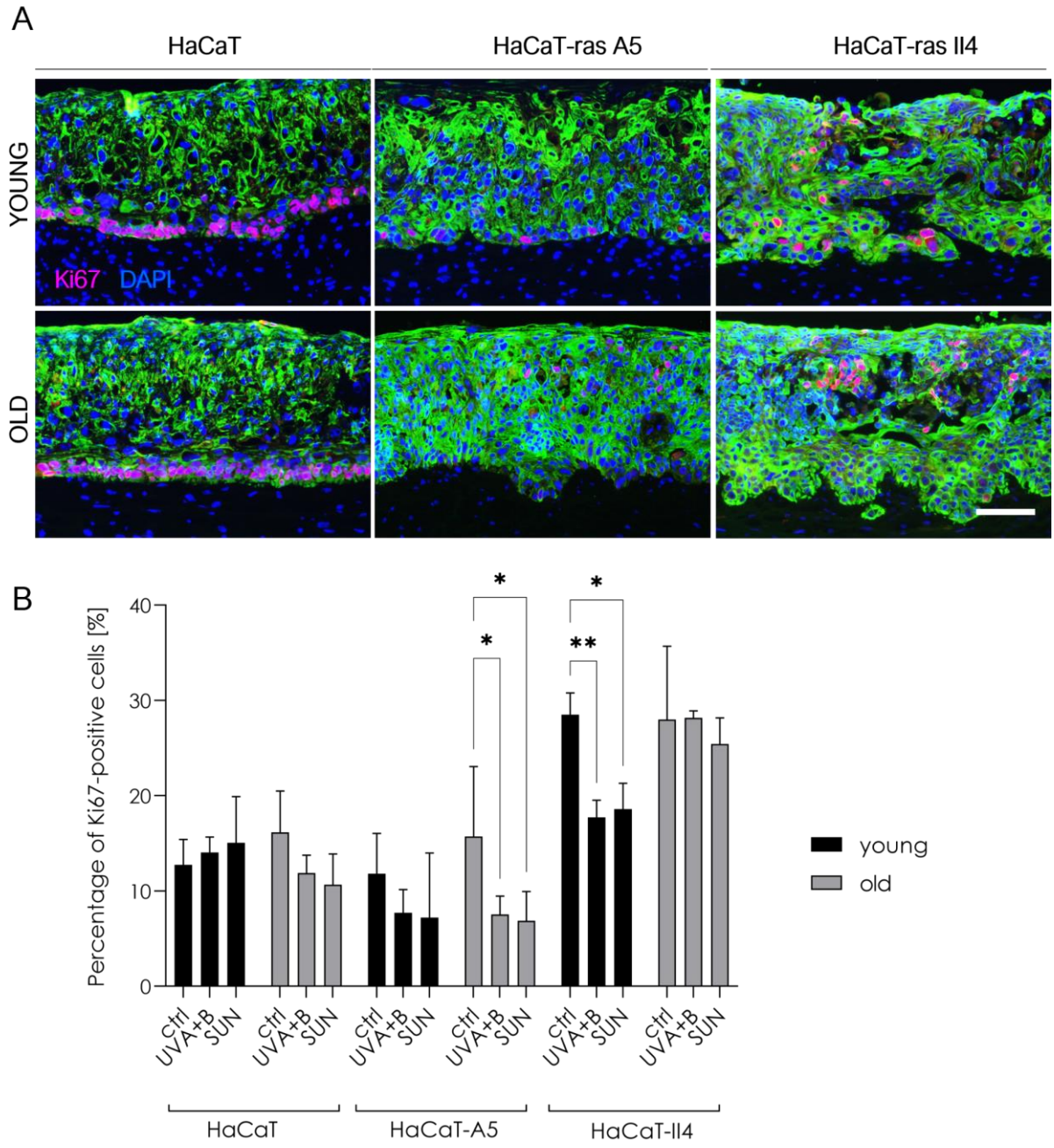

Figure 43: Proliferation of epidermal cells in HaCaT-, HaCaT-A5- and HaCaT-II4-SEs
Proliferation of epidermal cells was determined in non-irradiated control SEs and SEs irradiated with UVA+B or SUN for 2 weeks. The rate of proliferating cells was assessed 24 h after the last irradiation by **(A)** staining for pan-keratin and Ki67 and **(B)** counting all epidermal cells and Ki67+ cells with an ImageJ macro. **(A)** displays the localization of proliferating cells within the epithelia. Scale bar =100 µm. **(B)** Quantification of Ki67+ cells. One-way ANOVA (comparison within one cell type); * = p-value < 0.05; ** p-value < 0.01; n=3 (with 3 analyzed sections each).

3.4.6 Evaluation of the Skin Barrier in SEs with Transformed Keratinocytes

The slightly improved stratification and *stratum corneum* formation of HaCaT-SEs seen in the H&E staining together with results from previous studies of our group that showed an upregulation of genes connected to the skin barrier in HaCaT-SEs (Schardt 2017), led to the idea that this might be part of an adaptive response of the skin to form a protective shield against UV radiation. Therefore, we performed the assessment of skin barrier components as described before for the NHEK models also for the models with the transformed cells by staining for filaggrin and with Nile Red and subsequently measuring the transepidermal water loss (TEWL). Results are depicted in Figure 44.

Nile Red staining was performed for the visualization of the lipid content (Fig. 44A). In HaCaT epithelia (Fig. 44A upper panel), lipid deposition was found all over the thick parakeratotic stratum corneum and the pattern differed significantly from what was observed in NHEK epithelia. Other than the lamellar structure that was found in NHEK-SEs, lipid deposition in HaCaT-SEs appeared more droplet-like, especially in the lower parts of the SC. HaCaT-SEs did not display major differences between young and old or irradiated and control samples.

In HaCaT-A5-SEs (Fig. 44A, middle panel) the amount of lipids differed between young and old controls. HaCaT-A5 epithelia based on old DEs contained considerably less lipids than the young counterparts. Irradiation seemed to slightly increase lipid deposition in both young and old HaCaT-A5-SEs. This increase was particularly evident in the young HaCaT-A5-SEs where irradiation led to a massive accumulation of lipid droplets in the lower part of the SC.

A similar tendency could be observed in HaCaT-II4-SEs (Fig. 44A, lower panel). In both young and old SEs, the irradiation caused an increase in lipid content and the formation of a more compact lipid layer on top.

Distribution of filaggrin in the HaCaT epithelium differed from that in the NHEK epidermis (Fig. 44B, upper panel). It was not only present in the upper layers of the *stratum corneum*, but also in areas closer to the basal layer. All HaCaT samples looked quite similar, irrespective of the age of the fibroblasts or the irradiation treatment (UVA+B or SUN).

In HaCaT-A5-SEs (Fig. 44B, middle panel), filaggrin was restricted to the more superficial layers of the epithelium in SEs based on young DEs. In SEs based on old DEs, this localization was similar, but the expression was clearly reduced. However, irradiation with UVA+B and SUN caused an upregulation of filaggrin in old SEs that was not observed with young SEs.

In SEs with HaCaT-II4 (Fig. 44B, lower panel) we found very little filaggrin and expression was mainly focused near the basal layer in young SEs. Irradiation with UVA+B and SUN slightly

increased filaggrin expression in those young SEs, but the localization remained the same. In HaCaT-II4-SEs based on old DEs, filaggrin was hardly expressed and only found in small, scattered patches. Irradiation with UVA+B or SUN did not lead to noticeable changes. The reduced filaggrin expression and the localization in lower parts of the epithelium, especially of HaCaT-II4-SEs, suggests a disturbed differentiation and barrier formation that correlates well with the previous analysis of differentiation markers.

To assess the functional consequences of the differences found in skin barrier components, we again determined the amount of transepidermal water loss (Fig. 44C). As described before, the TEWL was measured in cooperation with Henkel AG & Co. KGaA in Düsseldorf with the open chamber device Tewitro®TW 24R. We analyzed three independent replicates for each condition. The differences in TEWL between the samples were small and not statistically significant. However, we observed two tendencies that were found in all models (HaCaT, HaCaT A5 and HaCaT II4): the TEWL of cultures based on old fibroblasts was slightly higher than of that with young fibroblasts, indicating a slightly higher water loss in old cultures; and the TEWL did not increase with irradiation with UVA+B or SUN but rather decreased. This tendency might argue for the hypothesis that exposure to solar radiation could improve the skin barrier but as the differences were only small and not statistically significant, this experiment would need to be repeated to draw conclusions. It might also well be that the timeframe of two weeks of irradiation is not long enough to induce major functional improvements of the skin barrier that can be measured by TEWL or that the method used is not sensitive enough to detect the subtle changes.

HaCaT-II4 models had the highest TEWL values which is in line with the results from histological and immunohistochemical stainings that revealed an impaired stratum corneum and the almost complete loss of filaggrin as a fundamental component of the skin barrier.

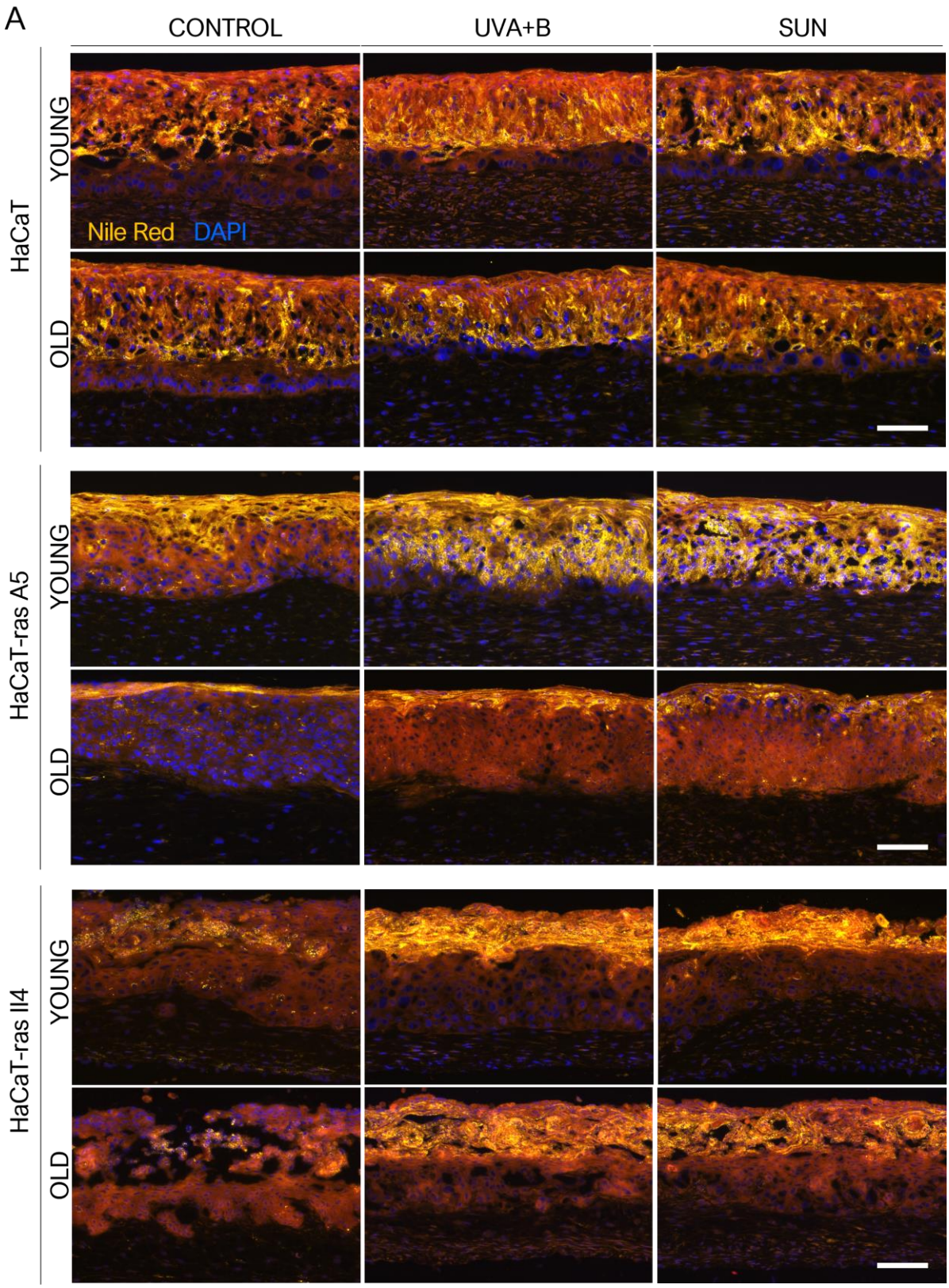
A
CONTROL
UVA+B
SUN
HaCaT
HaCaT-ras A5
HaCaT-ras II4
YOUNG
OLD
Nile Red DAPI

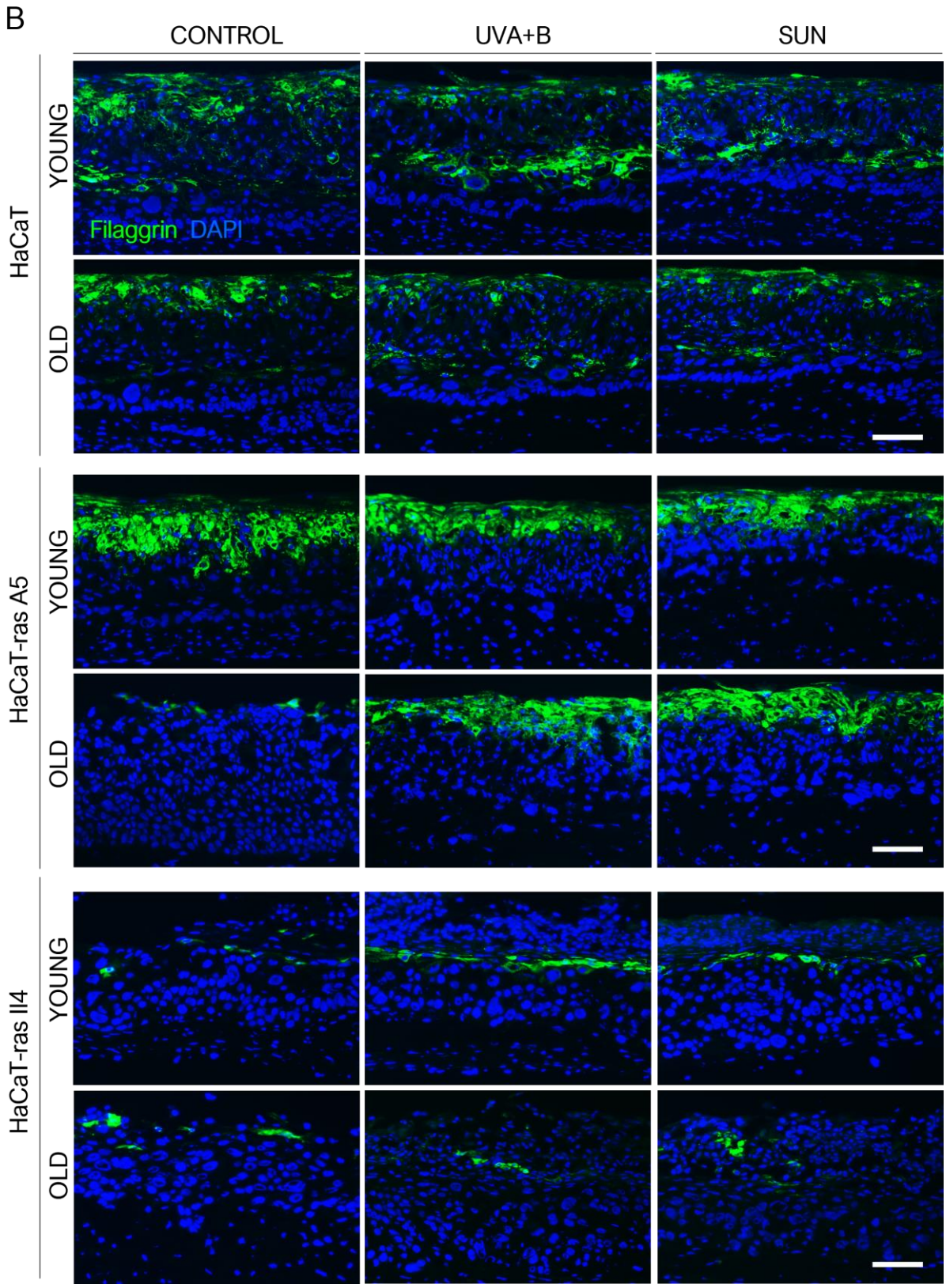
B
CONTROL
UVA+B
SUN
HaCaT
HaCaT-ras A5
HaCaT-ras II4
YOUNG
OLD
Filaggrin DAPI

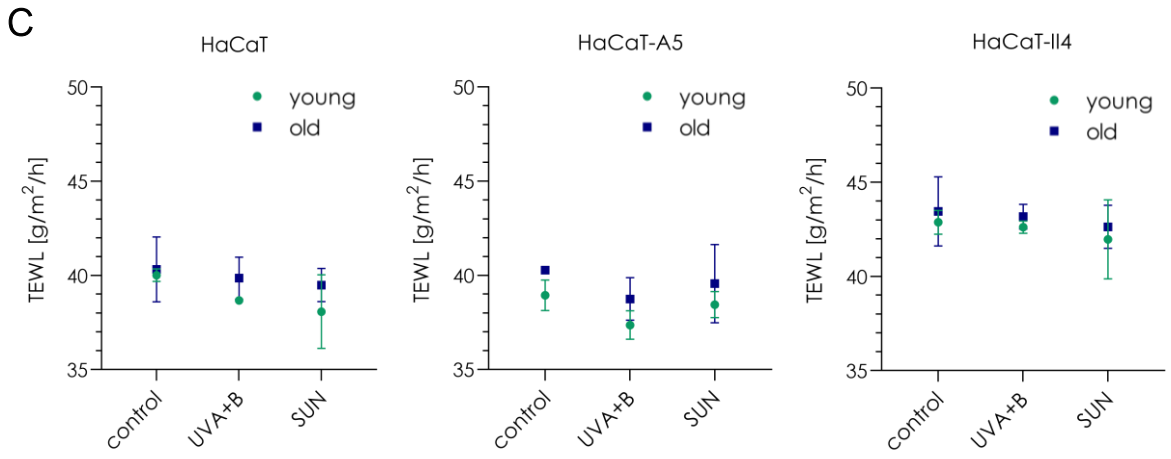

Figure 44: Evaluation of the skin barrier in HaCaT-, HaCaT-A5- and HaCaT-Il4-SEs
Integrity and function of the skin barrier was assessed in non-irradiated control SEs and SEs chronically irradiated with UVA+B or SUN for 2 weeks by (**A**) staining with Nile Red to visualize lipids, (**B**) IIF staining for filaggrin and (**C**) functional analysis of the transepidermal water loss (TEWL). The scale bar represents 100 µm. Two-way ANOVA, all n.s.; n=3.

4 Discussion

4.1 Establishment of a Skin Aging Model

When studying skin aging, it is crucial to choose an appropriate model in which the relevant processes can be observed. For the scope of this work, the model needed to be of human origin as well as stable and regenerating over several weeks to enable chronic irradiation studies. To particularly investigate the role of the fibroblasts and the dermal ECM, the model should resemble the three-dimensional architecture of skin and allow the interaction between keratinocytes and fibroblasts as well as potential invasion of epithelial cells.

Thus, 3D skin equivalents were the most suitable option. The first step in establishing an SE is to generate a DE with fibroblasts. Keratinocytes are then seeded on top and epidermal differentiation is initiated by exposing the cultures to an air-liquid interphase. Especially the DE needs to be chosen with care as different dermal compositions come with different advantages and limitations and the DE strongly influences epidermal regeneration (Boehnke et al. 2007; Thakoersing et al. 2012).

Collagen hydrogels are widely used for SEs and keratinocytes can initially form an intact epidermis on them. However, collagen based DEs lack stability and have a relatively short lifespan making them unsuitable for long-term studies. The natural dermal ECM composition and properties, which play an important role in processes such as ECM remodeling and migration of cells, for example the stiffness, (Tschumperlin 2013; Friedl et al. 2012), are not well reflected by collagen gels. Stability of the models can be improved by adding different kinds of scaffolds (Stark et al. 2004; Berthod et al. 1996; Cooper et al. 1991). In a scaffold based model with hyaluronic acid fibers, the use of fibrin gels improved colonization of the scaffold and this provisional matrix was remodeled by the fibroblasts to produce an authentical dermal matrix which improved epidermal architecture and supported epidermal regeneration for 15 weeks and longer (Boehnke et al. 2007).

These scaffold-based SEs were shown to be well-suited for aging studies in the preceding work of Sabrina Bauer (Gundermann 2012), however, they proved to be inadequate to study invasion and tumor growth (Kollar and Boukamp, personal communication). As one of the questions we wanted to answer in this study, was if irradiation would lead to tumorigenic conversion of the epithelial cells, fdmSEs present a reasonable alternative that also allows to investigate invasion. Cell migration behavior is highly dependent on the surrounding matrix (Even-Ram and Yamada 2005; Wolf et al. 2009) and fdmSEs, complemented with transformed keratinocytes or skin cancer cell lines, were demonstrated to recapitulate a broad range of histological and molecular features

of skin cancer (cSCC), including hyperplasia, acantholysis and particularly cell-specific invasion behavior (Berning et al. 2015).

A range of different techniques have been developed to produce fibroblast-derived matrices, from dish-based (Chen et al. 2009) to transfer (Ng et al. 2012) and transwell (Pouyani et al. 2009; Ahlfors and Billiar 2007; El Ghalbzouri et al. 2009) approaches. The transwell approach chosen here was shown to display remarkable similarities to the human dermis in biochemical composition and mechanical properties. FdmDEs were also shown to support epidermal differentiation and regeneration over long culture periods (Berning et al. 2015; El Ghalbzouri et al. 2009) which makes them a suitable model for long-term studies. This is important when studying the effects of repetitive UV and sunlight exposure over several weeks.

Compared to collagen- or scaffold-based SEs, the fdmSEs established here comprise a higher number of fibroblasts. Studies in our laboratory showed that this accelerated and augmented the establishment of the aging phenotype, providing us with a highly sensitive model to study relevant processes in a shorter timeframe.

Currently there are very few models for “aged skin” that reliably reproduce the phenotype of older skin *in vivo*. An important consideration for the development of a relevant skin aging model is what kind of fibroblasts should be used. Several skin equivalents have been developed with senescent fibroblasts as a model for aging, either generated by prolonged serial passaging (Janson et al. 2013), by applying mitomycin-C resulting in drug-induced accelerated senescence (Diekmann et al. 2016) or by exposing cells to H_2O_2 to activate stress-induced premature senescence (Weinmullner et al. 2020). Human SEs generated with these fibroblasts show several of the characteristics of aged skin *in vivo.* Senescence is one cellular defense mechanism, driven by intrinsic (e.g., telomere shortening, ROS) and extrinsic (e.g., UV exposure) influences and as damage accumulates with aging, the prevalence of senescent cells in different tissues increases with chronological age, also in skin (Dimri et al. 1995; Ressler et al. 2006; Lewis et al. 2011). Senescent cells are defined by a permanent cell cycle arrest and undergo phenotypic and functional alterations. They influence their microenvironment through their specific senescence-associated secretory phenotype (SASP) and are thought to play a major role in driving the aging process, which has been covered in many recent reviews (Low et al. 2021; Fitsiou et al. 2021; Gorgoulis et al. 2019; Cavinato and Jansen-Durr 2017). At the same time the connection between senescence and aging is still not fully understood and there is an ongoing debate to which extent senescence contributes to skin aging. Although clinical intervention trials have been less conclusive so far (reviewed in (Low et al. 2021)), there is increasing evidence for a highly important role of senescent cells and recently there has been a surge of interest in targeting senescence through therapeutic interventions, known as senotherapy, to improve healthy aging and age-

related diseases. (Gorgoulis et al. 2019; Velarde and Demaria 2016; Toutfaire, Bauwens, and Debacq-Chainiaux 2017).

However, *in vitro* aged fibroblasts were shown to differ from *in situ* aged fibroblasts in several aspects (Tigges et al. 2014). Therefore, it remains questionable to which extent *in vitro* aged fibroblasts represent a fibroblast population that reflects the aging process *in vivo*.

For the establishment of our Age-SEs, we therefore chose to use primary fibroblasts that were isolated from patients of different age and as such by definition are aged *in situ.* In comparison to cell lines, primary cells also account for the heterogeneity of human donors. Taken from sun-exposed areas of the body, the old fibroblasts represent a relevant model for photoaged human skin. The old fibroblasts displayed a morphology associated with senescence (enlarged, flattened cells) but the analysis of several senescence-associated markers (increased ß-galactosidase activity, expression of p21 and 16, shorter telomeres) indicated that these cells are not senescent (Gundermann 2012). Instead, characterization of these cells identified a novel fibroblast differentiation state shown to be related to the most advanced state of photoaging, solar elastosis. This argues for the hypothesis, that senescent fibroblasts may not be the only fibroblast population relevant for the establishment of an “aging phenotype” in human skin.

Using the primary *in situ* aged “young” and “old” fibroblasts to establish fdmSEs, they were successfully developed further to the Age-SEs presented here. Histological and IIF stainings demonstrated that the Age-SEs nicely recapitulate major characteristics of young or photoaged skin, depending on the incorporated young or old fibroblasts. The experiments were repeated with different sets of fibroblasts and different keratinocytes to exclude cell-specific effects, thereby demonstrating that the described phenotypes of the SEs induced by old or young fibroblasts are highly reproducible. Thus, the Age-SEs proved to represent robust and suitable models to study the role of fibroblast aging in the tissue context.

4.2 Fibroblast Age Influences Tissue Homeostasis, Epidermal Differentiation, and Basement Membrane Formation

With the Age-SEs it was possible to show that the age of the fibroblasts has a major impact on the epidermal differentiation, the formation of the BM and the composition of the dermal ECM. Age-SEs with young fibroblasts form a well-stratified and cornified epidermis, closely resembling normal human interfollicular epidermis. Histological stainings demonstrated clearly defined basal, spinous, and granular layers and a multilayered *stratum corneum*. The different layers are characterized by the sequential expression of differentiation-specific keratins (Houben, De Paepe,

and Rogiers 2007). Keratinocytes of the basal layer are mitotically active and express K5, K14 and K15. When they commit to differentiation and start moving upwards, they express K1 and K10 (early differentiation marker). In the upper spinous and granular layer, where cells flatten and accumulate keratohyalin granules, they express K2 (late differentiation marker) (Wang, Zieman, and Coulombe 2016). This differentiation pattern was well reflected by the epidermis of young Age-SEs. Incorporating old fibroblasts in the Age-SEs strongly affected the epidermal differentiation. The epidermis was stratified but less organized and the basal layer did not show the typical palisade-like formation. The expression profile of the keratin markers, in particular the little or missing K2 expression suggested an impaired differentiation.

In a recently published skin culture model constructed with senescent cells (Weinmullner et al. 2020), Weinmüllner et al. presented very similar results regarding the differentiation. They also found a reduced expression of K10 and filaggrin, suggesting a modulation of the keratinocyte differentiation also by senescent fibroblasts. Changes in the differentiation of epidermal keratinocytes and epidermal morphology have also been documented in aging human skin (Charruyer et al. 2021; Kurban and Bhawan 1990).

Late terminal differentiation includes the formation of the cornified envelope (CE) and the CE protein filaggrin is accordingly deposited in the *stratum granulosum* and upwards in young skin (Kanitakis et al. 1988). This was well reflected in the young Age-SEs, while old Age-SEs showed a drastically reduced filaggrin expression. An intact CE is crucial for the integrity of the skin and its barrier function. Rinnerthaler et al. (Rinnerthaler et al. 2013) described drastic changes in the formation of the CE during aging, including a significant downregulation of filaggrin. The expression of filaggrin is dependent on a calcium peak specific for the *stratum granulosum* and Rinnerthaler et al. found a redistribution of calcium in aged human skin to be causal for the reduced synthesis of CE components. Another study (Takahashi and Tezuka 2004) also found filaggrin to be reduced in aged versus young skin, which matches the results from our Age-SEs. As the filaggrin mRNA levels in aged skin were not reduced compared to young skin, the authors suggested that the decrease in filaggrin protein is due to an increased proteolysis in the aged skin.

Apart from the cellular components, also the “mortar”, the intercellular lipids which are aligned in lipid lamellae, are vitally important for the integrity of the *stratum corneum* and with that the skin barrier (Elias 1983; Wertz et al. 1987). In old Age-SEs, the lipid lamellae were reduced and did not show the basket-weave-like structure displayed in young Age-SEs. Similarly, skin *in vivo* is characterized by an age-related decline of all major *stratum corneum* lipids and a reduced number of lipid lamellae in aged skin (Ghadially et al. 1995; Rogers et al. 1996; Sahle et al. 2015).

Although important components of the skin barrier were reduced in old Age-SEs, this did not result in a significantly increased transepidermal water loss (TEWL), which is the most widely used objective measurement for assessing skin barrier integrity (Fluhr, Feingold, and Elias 2006; Alexander et al. 2018). However, Ghadially et al. reported that assessment of TEWL in aged epidermis under basal conditions might anyhow be misleading. They found an even lower baseline TEWL in aged humans than in young, as similarly described by other studies (Kottner, Lichterfeld, and Blume-Peytavi 2013; Thune et al. 1988), but the aged barrier was perturbed more easily and recovered more slowly after skin irritation (Ghadially et al. 1995; Seyfarth et al. 2011). To test if there are age-dependent or irradiation-induced differences in the regeneration of the skin barrier, methods like tape stripping (Olesen et al. 2019) or other irritation tests could be applied.

A continuous regeneration of the epidermis of young Age-SEs was demonstrated by Ki67 staining, suggesting an ongoing proliferation for up to six weeks. In old Age-SEs, the proliferation rate was strongly reduced (from 9.2% to 2.5% proliferating cells) but still showed a stable low-level proliferation for at least four weeks. Reduced epidermal proliferation rates were similarly reported in skin of old versus young patients (Engelke et al. 1997; Gilhar et al. 2004; Rube et al. 2021). Engelke et al. observed a decrease of 29% in old skin, Gilhar et. al found the proliferation rate in old skin to be half of that of young skin. Connected to the decreasing proliferation, the epidermal turnover rate is known to slow down during aging. Grove and Kligman reported a *stratum corneum* transit time of 20 days in young adults, that extended to 30 days or more in older adults (Grove and Kligman 1983). The prolonged turnover contributes to delayed and impaired wound healing and less effective desquamation in older people (Eaglstein 1989).

Importantly, young Age-SEs also assembled an intact BM, characterized by the presence of laminin-5, and type IV and VII collagens. The BM is an essential structure that connects the epidermis to the dermis and controls dermal-epidermal interaction, thereby also regulating epidermal homeostasis. In old Age-SEs the BM assembly was disturbed. ColVII, that forms the anchoring fibrils, was found to be reduced and fragmented, indicating either an impaired BM formation or degradation of this component. As we found increased levels of secreted MMP-1 in old Age-SEs, degradation of ColVII might well have been the result of a higher proteolytic activity. Accordingly, higher proteolytic activity and increased levels of MMP-1 were confirmed in the DE of old Age-SEs by IIF staining. Amano et. al (Amano 2009) demonstrated an increase in BM components including ColVII and a reconstitution of the BM after treating SEs with MMP inhibitors. This suggests that increased degradation of the BM components might well be the cause for the disrupted BM.

The reduction of ColVII in the old Age-SEs is well-reflecting the *in vivo* situation. In patients with chronically sun-exposed skin, the number of anchoring fibrils was found to be significantly lower

than in sun-protected controls (Craven et al. 1997) and loss of ColVII was most prominent in areas with wrinkles (Contet-Audonneau, Jeanmaire, and Pauly 1999), suggesting that the weakened connection of dermis and epidermis is involved in wrinkle formation. The role of ColVII for the dermal-epidermal adhesion is also reinforced by the fact that mutations in the COL7A1 gene lead to skin fragility and the blistering disease epidermolysis bullosa (Christiano et al. 1993).

Expression of laminin-5, another BM component, was increased in old Age-SEs, but looked disorganized and even showed signs of duplication. This duplication of the *lamina densa* was reported in sun-exposed skin of aged adults (Lavker 1979) and even in the sun-exposed cheek skin of a 30-year-old woman, but not in young sun-protected skin and only very little in old sun-protected skin (Amano et al. 2001). So, it is thought to be a result of sun damage. The disrupted and multilayered BM structure probably also impairs dermal-epidermal adhesion and might contribute to the fragility and weaker resistance to shearing forces in aged skin that is observed clinically (Farage et al. 2009).

The importance of the BM for the epidermal homeostasis by providing signals that regulate keratinocyte adhesion, polarity, survival, and differentiation, has been demonstrated in several studies (Lee and Cho 2005; Marionnet et al. 2006; Roig-Rosello and Rousselle 2020). If BM components are not synthesized and assembled properly, the basal keratinocytes lack information about cell polarity and about when to exit the cell cycle and differentiate (Jevtic et al. 2020; Simpson, Patel, and Green 2011). Hence, the impaired BM formation found in old Age-SEs might well be causal for the deficiency of the old fibroblasts to support epidermal long-term regeneration in SEs.

An important feature of the Age-SEs is the fibroblast-derived matrix. During five weeks of culture, the young fibroblasts established an ECM that consisted of a dense meshwork of collagen fibers and comprised a ground substance including hyaluronic acid (HA), as confirmed by IIF stainings. The ECM produced by old fibroblasts was characterized by a drastically reduced amount of HA and a looser collagen meshwork with larger gaps, as visualized by staining for ColI and with Picrosirius Red.

Loss and fragmentation of collagen is one of the most characteristic findings in photoaged skin *in vivo* (Kohl et al. 2011). The reduction in net collagen content in aged skin is the result of a reduced *de novo* synthesis on the one hand and an increased degradation on the other hand. Fibroblasts isolated from aged skin have been shown to have a reduced capacity of collagen synthesis, which is mediated mainly by ROS-dependent impaired TGF-ß signaling (Quan et al. 2004; Varani et al. 2006). The degradation of collagen is mainly driven by increased MMP activity (Fisher et al. 1996), that is induced by UV-dependent activation of the MAPK signaling pathway (Fisher and Voorhees

1998). Concordantly, we detected a higher enzymatic activity in the DE of old Age-SEs compared to young Age-SEs, which is likely causal for the degradation of the collagen fibers in the DE.

Skin aging is also associated with loss of skin moisture. HA with its unique capacity to bind and retain water is a key molecule for the maintenance of skin hydration. There are conflicting reports about age-related changes in the level of HA *in vivo*. One study found HA to be reduced in photo-aged skin (Ghersetich et al. 1994), while another found no changes in the amount of HA (Meyer and Stern 1994). Tzellos et al. reported an increase of dermal HA of low molecular mass and a decrease of hyaluronan synthase 1 (HAS1) in sun-damaged skin (Tzellos et al. 2009). Simpson et al. described an age-related impairment of HA synthesis and HAS2 induction in *in vitro* aged fibroblasts (Simpson et al. 2009). In our Age-SEs, dermal HA was strongly reduced in old *versus* young SEs, which might be the result of a reduced expression of HA synthases as it was found by Tzellos et al. or Simpson et al.

Taken together, the Age-SEs established with young fibroblasts largely resemble normal human skin and the Age-SEs established with old fibroblasts reproduce a broad range of characteristics of aged skin *in vivo*. Age-SEs therefore represent a highly relevant model to study age-dependent differences.

Characterization of the epidermal differentiation, proliferation, and BM formation clearly emphasize the importance of the dermal fibroblasts and the dermal microenvironment for the epidermal phenotype and thus for the aging process. Our results suggest that many of the age-related changes that are characteristic for the epidermis of older people may not be due to age-related changes in the epidermis itself but may rather be the consequence of an impaired interaction with the dermal fibroblasts. These obviously accumulate age-related changes that modulate their phenotype and function and thereby drive the aging process.

4.3 Old Fibroblasts Display a Myo-Chondro-Fibroblast Phenotype

Fibroblasts isolated from old donors were shown (Gundermann 2012) to upregulate matrix genes which are characteristic components of cartilage ECM such as Aggrecan (ACAN), Matrix Gla Potein (MGP), Hyaluronan and Proteoglycan Link Protein (HAPLN1), and Collagen type XI (COL11A1). Furthermore, genes connected to chondrogenic differentiation and the cartilage-specific transcriptional regulators SOX9 and ATF5 were upregulated. The fibroblasts maintained this chondrogenic phenotype in the 3D context of scaffold-based SEs and produced a cartilaginous ECM. In the Age-SEs we could now confirm the expression of the chondrogenic

matrix proteins aggrecan and ColXI by old fibroblasts, while young fibroblasts did not express ColXI and only very minor amounts of aggrecan.

The physiological relevance of this chondrogenic phenotype was demonstrated in skin samples from different aged donors, detecting the chondrocyte-type matrix genes predominantly or exclusively in skin from old donors. Even more, stainings demonstrated that the chondrocyte-type matrix was associated with sites of solar elastosis, where it replaced the "normal" collagen matrix (Gundermann 2012). Therefore, the chondrogenic phenotype described here for the old fibroblasts most likely is not a general aging phenotype, but rather a phenotype related to solar elastosis, that developed at sites of extensive damage.

In recent years, fibroblasts were increasingly appreciated as a highly dynamic and heterogenous cell type, with various subpopulations or differentiation states (LeBleu and Neilson 2020). Different fibroblast subpopulations, which reside in the papillary (Fp) and reticular (Fr) dermis, were shown to differ in their gene expression (Janson et al. 2012) and also differ in their capacity to support epidermal morphology and homeostasis in reconstructed skin models (Pageon, Zucchi, and Asselineau 2012), strengthening the importance of the dermal-epidermal crosstalk for skin regeneration. Mine et al. characterized Fp and Fr subpopulations for their specific functional properties and changes during aging and found that particularly the Fp population is altered with aging, which has consequences for the epidermal morphogenesis (Mine et al. 2008). Sequencing studies by Haydont et al. could generate specific gene expression profiles for the different fibroblast subpopulations (Haydont et al. 2019). Interestingly, they detected the expression of ACAN and COL11A1 in the aged fibroblasts and the expression level correlated with the elastosis grades in biopsies of photodamaged skin. Together, this suggests that the fibroblasts from old donors we present here, might be closely related to the aged papillary fibroblasts. However, the fibroblast population that we describe does not only express the mentioned genes connected to cartilage, but a much more complex chondrogenic expression profile, assuming that they might represent a different subpopulation or differentiation state.

In addition to the chondrogenic expression profile, one of the most striking differences between young and old Age-SEs was the presence of myofibroblasts in old Age-SEs, a fibroblast phenotype never observed in young Age-SEs. Myofibroblasts, identified by the expression of α-SMA, are an "activated" differentiation state of fibroblasts, characterized by the acquisition of smooth muscle features, most notably the gain of contractile properties by rearrangement of the actin cytoskeleton. First described by Gabbiani et. al in 1971 (Gabbiani, Ryan, and Majne 1971), in recent years, myofibroblasts attracted increasing interest and a lot of research has been done to uncover their origin, phenotype and diverse functions in physiological and pathological situations. It is now well documented that he fibroblast - myofibroblast differentiation is regulated by the

activation of the TGF-ß/Smad signaling pathway (Desmouliere et al. 1993) and recently reviewed in (Frangogiannis 2020)) and mechanical tension arising from the cell-ECM interaction and maintained by different modulators such as fibronectin and HAS2-synthesized HA (Webber et al. 2009).

Myofibroblasts are activated upon tissue trauma and their appearance is beneficial for tissue repair processes, as they are essential for ECM-production and -remodeling during wound healing. Myofibroblasts produce ECM components such as collagen type I and III, HA, fibronectin (FN), and extra domain A fibronectin (EDA-FN), an alternative splicing variant of fibronectin, expressed in tissue repair and fibrosis (Klingberg, Hinz, and White 2013; Serini et al. 1998) to repair lost or damaged ECM. In normal wound healing, this process ends with apoptosis of the myofibroblasts (Desmouliere et al. 1995). However, dysregulation of the repair process leads to persistence of the myofibroblast and an excessive accumulation of ECM, finally resulting in tissue stiffening and fibrosis (Tomasek et al. 2002; Hinz 2016).

Preceding work has demonstrated that the phenotype of the old fibroblasts is correlated with an upregulation of genes connected to actin remodeling, e.g. ACTG2, ACTA2, and ACTC1, as well as contractile proteins such as MYH11, MYLK, CNN1 and the potential inducer of this phenotype, TGFB3 (Gundermann 2012). I could now show that the old fibroblasts maintain this phenotype also in the context of the Age-SEs. As the early stage of SEs is in many respects a “wound-healing-like” situation, one would expect to see myofibroblasts in young as well as old Age-SEs. However, in the experiments performed here, myofibroblasts only established in old Age SEs where they were maintained throughout the entire culture period, while never been observed in young Age-SEs at any given time. The question is if this is an intrinsic and stable differentiation state of the old fibroblasts or if external factors are required to induce this differentiation. Worth mentioning, the myofibroblasts always concentrated in the upper part of the DE, in close vicinity to the epidermis. This might argue for an epidermis-induced regulation. However, old fibroblasts seem to react more “sensitive” to this regulation than young fibroblasts.

IIF stainings for the chondrogenic and myofibroblast markers demonstrated that the chondrogenic markers were expressed in the entire DE, while expression of myofibroblast markers were only detected in the upper half. This raises the question if the myo-chondro-fibroblast differentiation is a common regulation or if these are distinct processes or differentiation states.

The myo-chondro-fibroblast phenotype we present was not described for fibroblasts isolated from human skin before but, interestingly, in 2018 Fu et al. presented a model of differentiation states of cardiac fibroblasts after myocardial infarction in the mouse heart (Fu et al. 2018), that shares several similarities with the fibroblast differentiation we describe. The authors show that after

infarction, the resident fibroblasts are activated and differentiate to α-SMA-expressing myofibroblasts that secrete ECM proteins as commonly seen in wound healing processes. As the scar fully matured, however, they observed that the fibroblasts were not cleared by apoptosis as expected, but persisted within the scar, and instead differentiated into a stable state they termed "matrifibrocytes". These cells were characterized by the expression of genes connected to cartilage and chondrocytes (including COMP and CILP2), much like what we observed for the old dermal fibroblasts. As the matrifibrocytes share several characteristics with chondrocytes, the authors suggested that they might be better adapted to highly collagenous environments and are specialized cells to support the mature scar.

Since the old fibroblasts described here, were likely derived from sites of solar elastosis, which are sites of extensive and chronic tissue damage, it might be presumed that a similar differentiation program as in the myocardial fibroblasts was activated in the dermal fibroblasts. The differentiation to the myo-chondro-fibroblasts might therefore be a response to sun-induced tissue damage and the accompanying collapse of the normal tissue architecture, which could be compared to the infarct situation of the mouse heart. This differentiation has considerable functional consequences for the tissue, as demonstrated by the deficit of the old fibroblasts to support epidermal regeneration.

4.4 Experimental Setup to Simulate Sun Exposure

As the old fibroblasts were isolated from sun-exposed skin and the myo-chondro-fibroblast phenotype was associated with sun-induced tissue damage (solar elastosis), we reasoned that UV/solar radiation plays a role in the development of this phenotype.

Most of the studies performed focus on acute effects caused by UV radiation. We had experienced that effects induced in SEs by acute (a single MED) irradiation were rather transient and reverted back to normal within hours (Pavez Lorie et al., personal communication). In line with that, we expected acute irradiation to be insufficient to induce long-term functional consequences in the keratinocytes and fibroblasts. We, therefore, focused on repetitive "chronic" irradiation in our study. This was possible because the long-term stability and viability of our model system enabled us to expose the Age-SEs to two or even four weeks of irradiation. By seeding the keratinocytes on top of the DEs two weeks before starting the irradiation, we could ensure that the irradiation would not interfere with the early phase of epidermal development. Instead, irradiation could be performed on a fully developed and homeostatic epidermis. Thereby we expected to gain relevant information on tissue regulation as it is expected for skin *in situ*. This is worth mentioning, as skin

equivalents in other studies are often restricted to early tissue development due to their shorter lifespan.

Different from most previous radiation studies that use single high doses of UV radiation, we have chosen an irradiation dose of 1 MED (UVB 0.78 kJ/m^2, UVA 51 kJ/m^2, VIS 113 kJ/m^2, IRA 300 kJ/m^2), that represents a physiologically relevant dose, comparable to what skin is exposed to on a summer day in Germany. This dose was applied 3 times a week for two or four weeks and we demonstrated that this irradiation regime did not significantly reduce viability of the Age-SEs. We therefore can conclude that we have a quite robust model, that can tolerate the irradiation, as human skin does, and that the effects we are seeing are not the result of massive cell death or tissue destruction. Our system can rather provide more insights into the response of skin to a chronic low-dose irradiation.

Most of the present knowledge about radiation effects is derived from irradiation studies with keratinocytes and/or fibroblasts in conventional monolayer cultures. However, it is without doubt, that the response to radiation is dependent on the organization of a tissue. In a tissue context, not all cells are hit by the same intensity of the radiation and different wavelengths reach different parts of the tissue (Dupont, Gomez, and Bilodeau 2013; Svobodova and Vostalova 2010). Thus, irradiating a tissue leads to other consequences than irradiating cells in monolayer culture and the three-dimensional architecture of the SEs mimics the *in vivo* situation much better than a monolayer cell culture and can provide more relevant information to elucidate the effects of UV on skin physiology and aging. So far, only few studies were described to use OTCs for irradiation (Bernerd and Asselineau 2008; Fernandez et al. 2014; Marionnet, Tricaud, and Bernerd 2014) and most of them only used UV radiation.

With our novel, purpose-built radiation device, we had the unique possibility to simultaneously irradiate the Age-SEs with either the solar UV spectrum (UVA+B) or the entire solar spectrum (SUN) using the same device. The KAUVIR lamp combines the emission of four individual lamps (UVB, UVA, VIS and IRA) to achieve a solar-like exposure from 280-1500 nm with individual controllable spectral components. This is quite different from other studies that predominantly irradiate with individual spectral components, mostly UVB or UVA and if they also include other wavelengths of the solar spectrum, they usually use different lamps or irradiate with different wavelengths sequentially instead of simultaneously (Burren et al. 1998; Bernerd and Asselineau 2008; Schieke et al. 2005). With our irradiation setup we come quite close to resemble natural sunlight and this spectral resemblance is, to the best of our knowledge, not met by many other study´s irradiation setup.

4.5 Differential Gene Regulation in Young and Old Fibroblasts in Response to Irradiation with UV or SUN

Our experimental setup, the SEs with young and old fibroblasts, irradiated with solar UV radiation or the entire solar spectrum, now allowed to directly compare the effects of the different irradiations on a tissue built by young or old fibroblasts. Accordingly, we analyzed the differential gene expression of cells from young and old Age-SEs by RNA-Sequencing. With that analysis we found major differences in the response to irradiation between young and old Age-SEs.

Only a small number of genes was regulated the same way in young and old fibroblasts. This indicates that the young and old fibroblasts react differently to the irradiation. Hence, the old fibroblasts do not only differ from the young in their phenotype, but also in their gene regulation in response to irradiation. The small percentage of commonly regulated genes suggests that these differences are quite substantial, and that irradiation probably induces completely different regulatory pathways in old fibroblasts than in young fibroblasts. This is a very important finding, and it suggests that we might need to question if gene expression profiles derived from normal/young fibroblasts can simply be extrapolated to other age groups.

There are several studies analyzing the gene expression changes induced by UV radiation in normal/young fibroblasts. Marionnet et al. characterized the modulation of gene expression in fibroblasts and keratinocytes in an SE model irradiated with UVA+UVB irradiation and described several changes that we also verified for the young fibroblasts and keratinocytes, such as downregulation of collagens, upregulation of several MMPs and upregulation of epidermal differentiation markers (LCE, SPRR genes) (Marionnet, Tricaud, and Bernerd 2014). Others compared the gene expression of young and old fibroblasts, like Haydont et al., that identified differential gene expression profiles for dermal fibroblasts from young vs. old donors and for intrinsically aged vs. photoaged fibroblasts (Haydont et al. 2019). Another study compared gene expression profiles of cultured dermal fibroblasts from young and old donors and from sun-exposed and sun-protected body sites and did not find age-related differences (Kaisers et al. 2017). A recent study also compared the expression profiles of fibroblasts from young and old donors, which were "*in vitro* aged" by accelerated proliferation or UVB irradiation and, different than Kaisers et. al, found several differences in gene expression related to aging (Lago and Puzzi 2019). None of the studies did directly compare the response of young and old fibroblasts to irradiation as we present here. Therefore, our results could be of great value to understand how young and aged skin responds differently to sun exposure.

In addition to the age-related differences, our RNA-Seq analysis also demonstrated that the entire solar spectrum triggers a clearly different response than only the UV fraction (UVA+B). While a

part of the genes was regulated by both UVA+B and SUN, a large fraction was only regulated by UVA+B or only by SUN. Particularly in old fibroblasts the number of genes regulated by UVA+B only was much higher than the number of genes regulated by SUN. These results do not support the common idea that the irradiation with the entire solar spectrum causes a summation of the effects of the individual wavelengths. They rather argue for a modulating effect of the additional wavelengths (VIS, IRA) or a completely different regulatory response induced by the combination of wavelengths than by single wavelengths. While UV-induced effects on the skin have been studied extensively, much less is known about the IRA and VIS spectrum of solar radiation and, in particular, their interaction with UV. Only recently, evidence is increasing that the combination of spectra (e.g., UVA+VIS or UVB+IRA) leads to different biological consequences that are not just additive (Narla et al. 2020; Hudson et al. 2020; Grandi and D'Ovidio 2020). Our study emphasizes that it is crucial for further research to not only focus on the effect of specific wavelengths, but rather the combined solar spectrum, as this is what humans are exposed to in their everyday life, to provide a better basis for risk assessment.

4.6 The Role of Radiation for the Fibroblast Phenotype

Suggesting a role for solar radiation in the establishment of the myo-chondro-fibroblast phenotype that we described in old Age-SEs, we analyzed the expression profile of young and old Age-SEs, asking the question if irradiation can induce the phenotype in young or alter it in old fibroblasts.

From the literature there is evidence that dermal fibroblasts are in principle capable to directly transdifferentiate to a chondrogenic lineage. A chondrogenic differentiation of dermal fibroblasts *in vitro* was shown after pretreatment with insulin growth factor 1 (IGF-1) and a culture on aggrecan (French et al. 2004), by addition of demineralized bone powder (Mizuno and Glowacki 1996) or by the forced expression of Sox5, Sox6 and Sox9 (Ikeda et al. 2004). Yin et. al described a chondrogenic transdifferentiation *in vitro* by stimulation with cartilage-derived morphogenetic protein 1 (CDMP1), also called GDF5 (Growth Differentiation Factor 5) (Yin et al. 2010). Interestingly, CDMP1 was upregulated in our RNA-Seq analysis in young fibroblasts upon SUN irradiation and in old fibroblasts upon UVA+B and SUN irradiation. This growth factor is involved in bone and cartilage formation and regulates differentiation of chondrogenic tissues via TGF-ß signaling (Bai et al. 2004; Francis-West et al. 1999). It might therefore be one factor contributing to the development of a chondrogenic phenotype that should be investigated further. In our RNA-Seq analysis though we did not find an induction of other chondrocyte-specific genes, e.g. the cartilage matrix genes, neither in young nor old fibroblasts. Some genes connected to cartilage were rather downregulated in old fibroblasts. However, gene expression analysis by qRT-PCR of

the same fibroblasts after 4 weeks of irradiation showed an induction of several cartilage matrix genes (HAPLN1, ACAN, COLX, COLXI), especially in old fibroblasts. In another experiment with different fibroblast strains, we saw only a slight upregulation of some genes (HAPLN1 in young, SOX9 in old fibroblasts) already after 2 weeks. This suggests that UV irradiation might contribute to the regulation of the chondrogenic phenotype and the induction of the cartilage matrix, but this is rather a delayed response and therefore unlikely a direct regulation but rather an indirect consequence of other regulatory circuits.

TGF-β has been proven to be an essential factor in chondrogenesis and is commonly used in chondrogenic differentiation of mesenchymal stem cells (MSCs) (Johnstone et al. 1998; Cassiede et al. 1996). Previous work suggested an important role of TGF-ß for the development of the chondrogenic phenotype in our fibroblasts and the age-dependent presence of TGFß-1 and 3 was also demonstrated in skin samples (Gundermann 2012). TGF-ß is expressed in its latent form and sequestered by matrix components such as fibrillin (Zilberberg et al. 2012), decorin (Hildebrand et al. 1994), or thrombospondin-1 (Schultz-Cherry et al. 1994). Decorin and fibrillin were both upregulated in old fibroblasts in response to UVA+B and SUN in our analysis. This might have an impact on the sequestration and activation of TGF-ß and thereby influence the chondrogenic differentiation via TGF-ß signaling.

In young fibroblasts, the Cartilage Intermediate Layer Protein (CILP) was among the top 3 most significantly regulated genes and was downregulated after UVA+B and SUN exposure. CILP is thought to inhibit TGF-ß-mediated induction of cartilage matrix genes via its interaction with TGFß-1 (Gross and Thum 2020). A member of the TGF-ß family, TGFβ-induced protein (TGFBI), was upregulated in young fibroblasts upon UVA+B and SUN exposure. Ruiz et al. described that TGFBI plays a role in early stages of chondrogenesis (Ruiz et al. 2019). Thus, the specific regulation of these two genes may further support that irradiation has an influence on the TGF-ß-dependent regulation of cartilage-specific genes.

Another factor for the age-dependent alterations in the dermal matrix induced by UV and a further connection to TGF-ß might be cysteine-rich protein 61 (CCN1), which was upregulated, as shown by qRT-PCR, by UVA+B and even more prominent by SUN in young and old fibroblasts. CCN1 is found to be elevated in aged human skin *in vivo* (Quan et al. 2006) and it is also elevated by acute UV irradiation in skin and in UV-irradiated fibroblasts (Quan et al. 2010). Increased CCN1 in dermal fibroblasts was shown to alter the expression of several proteins in a pattern that closely resembled that observed in aged dermis, such as reduction of collagens type I and III via inhibition of TGF-ß signaling, increased secretion of multiple MMPs and proinflammatory cytokines. Quan et al. therefore proposed that CCN1 plays a key role in creating a tissue microenvironment that contributes to age-related decline of skin function (Quan and Fisher 2015).

Despite some direct regulations in the epidermal keratinocytes and the dermal fibroblasts, most of our data argues for a more indirect regulation by irradiation. Our results indicate that the irradiation regime in this study was not sufficient to directly induce the full chondrogenic transdifferentiation in young fibroblasts. However, although we did not find the chondrogenic matrix proteins upregulated in the RNA-Seq analysis, there are several hints that point to a role for UV or SUN in regulating the chondrogenic phenotype indirectly, e.g. by altering TGF-ß signaling. It might be that the transdifferentiation process needs further regulatory influences that do not establish after 2 weeks of irradiation but after long term chronic damage from sun exposure. One of these influences that develop gradually over long time could be the stiffness or mechanical property of the ECM. ECM stiffness is known to efficiently alter the TGF-ß response and promote chondrocyte differentiation (Allen, Cooke, and Alliston 2012; Park et al. 2011). The altered matrix composition in old skin, and particularly in the areas of solar elastoses, probably affects the mechanical properties and might play a role in the chondrogenic differentiation of the fibroblasts.

Other than the chondrocytic phenotype, the myofibroblast phenotype was strongly altered by irradiation in old Age-SEs. Both UVA+B and SUN irradiation caused a downregulation of numerous myofibroblast-related genes, including ACTA2, ACTG2 and, as the most significantly regulated gene, MYH11. This argued for a UV-dependent transcriptional regulation of the myofibroblast phenotype. This correlated with a decrease of α-SMA-positive cells in the irradiated SEs. It is generally thought that myofibroblast are eliminated e.g. from sites of wound healing by apoptosis and it might be suggested that the loss of α-SMA staining is indicative of UV-induced cell death of the myofibroblasts. However, the upper part of the DEs, where the myofibroblasts were found, was not depleted of cells, as indicated by nucleic staining. To further exclude the possibility that the old fibroblasts react more sensitive to the irradiation, cell death rates of young and old fibroblasts in irradiated and non-irradiated cultures were determined by flow cytometry. The rate of apoptotic and necrotic cells was generally very low and was not increased by irradiation, neither in young nor old fibroblasts, arguing against the hypothesis that the myofibroblasts are cleared by cell death. Since there were still cells in the areas where myofibroblasts were located before and those cells were still positive for aggrecan or ColXI, it might be reasoned that the myofibroblasts are not lost but only lose their myofibroblast phenotype and dedifferentiate to the chondro-fibroblast phenotype. This could involve a similar process as the one described by Fu et al. in the infarcted mouse heart, where the myofibroblasts were also not eliminated by apoptosis but instead lost their α-SMA expression and differentiated to a stable state with a chondrogenic expression profile. The authors proposed that in other studies, which were not based on lineage tracing of the cells, the loss of α-SMA expression might have been incorrectly interpreted as cell loss (Fu et al. 2018).

4.7 Irradiation Improves Epidermal Differentiation of Old Age-SEs

An unexpected and interesting observation in my studies was that irradiation with UVA+B or SUN led to an improved regeneration and epidermal differentiation of old SEs, demonstrated by prominent alterations in the expression of the differentiation markers K15, K10, K2 and filaggrin.

It is known that a proper morphogenesis and function of the epidermis and the dermal-epidermal junction is highly dependent on the crosstalk between fibroblasts and keratinocytes and that fibroblasts regulate the epidermal differentiation processes (Boehnke et al. 2007; Marionnet et al. 2006; El Ghalbzouri, Lamme, and Ponec 2002; Jevtic et al. 2020). The paracrine signaling between keratinocytes and fibroblasts is mediated through different soluble factors, including interleukins and growth factors, that regulate cell proliferation, adhesion, migration, or differentiation. Different subpopulations of dermal fibroblasts have been shown to not only produce a distinct ECM but also have different secretory profiles (Mine et al. 2008; Driskell et al. 2013).

In this context it is important to note that we found myofibroblasts mainly in the upper dermis of unirradiated old SEs and an irradiation-dependent reduction of those myofibroblasts. This reduction or loss of myofibroblasts correlated with the improved differentiation and regeneration of the SEs. Thus, it is tempting to speculate that the presence of myofibroblasts in close vicinity to the epidermis in old SEs, somehow disturbs the dermal support for the epidermis and that dedifferentiation of the myofibroblasts allows for a normalization of the dermal-epidermal interaction. The fact that the cells in this area maintained their chondrogenic phenotype suggests that not the old fibroblasts *per se* but the myofibroblasts blocked the support for keratinocyte growth and differentiation. One reason for that could be that the differentiation to the myo-chondro-fibroblast phenotype and also the dedifferentiation alters the secretory profile of the cells and therefore the secretion of factors that are required for the epidermal support. In the RNA-Seq analysis, the GO category “cytokine-mediated signaling pathways” was found within the 10 most significantly regulated gene sets in young and old fibroblasts. A thorough analysis of the cytokine profile of the young and old fibroblasts and further quantitative investigation of secreted cytokines, e.g. by ELISAs would be very useful to clarify if this hypothesis holds true.

Cytokines can either be secreted and act directly or are sequestered in the surrounding ECM that can serve as a reservoir for these factors. Several interactions between specific ECM proteins and cytokines or growth factors, including TGF-ß, have been described (Wijelath et al. 2006; Goetz and Mohammadi 2013; ten Dijke and Arthur 2007). In the case of TGF-ß it is suggested that also the mechanical stiffness of the ECM plays a critical role in the storage and activation and therefore the bioavailability of TGF-ß (Hinz 2015). Thus, it could be hypothesized that the myofibroblast-derived matrix or the resulting changes in mechanical forces, might alter the storage and release

of factors, that influence the epidermal homeostasis and as soon as the obstruction is diminished or abolished, the interaction normalizes. This hypothesis, of course, needs further extensive investigation.

Another hypothesis that would explain the increased or improved epidermal differentiation we observed in old SEs upon irradiation, apart from the reduction of myofibroblasts, was that this is part of an adaptive response of the SE and an attempt to protect against damaging irradiation by improving the skin barrier.

It is known that UV exposure leads to a thickening of the horny layers of the skin (Pearse, Gaskell, and Marks 1987). In studies by Lehmann et al., UVA- and UVB-irradiated areas proved to be more resistant to damage than unirradiated skin in different irritation models. They also found an increase in lipid content in the *stratum corneum* of irradiated skin, both findings indicating an improvement of the barrier function after UV irradiation (Lehmann et al. 1991).

In agreement with this idea, we found an increased filaggrin expression as well as a strong improvement of the lipid matrix in the *stratum corneum* of irradiated old SEs, both components being essential for an intact skin barrier. In addition, the RNA-Seq analysis of epidermal samples from young SEs revealed the GO categories “cornification”, “cornified envelope” and “keratinization” within the most significantly upregulated gene sets. Accordingly, in the lists of DEGs, several SPPRs (small proline-rich proteins) and LCE (late cornified envelope) proteins, connected to late terminal differentiation of keratinocytes and formation of the cornified envelope (CE) (Jackson et al. 2005; Tesfaigzi and Carlson 1999) were among the most significantly regulated ones. Modulation of these genes by UV has been confirmed in other *in vitro* studies as well (Marionnet, Tricaud, and Bernerd 2014). The importance of the CE for skin barrier integrity is strengthened by a number of diseases which display defective epidermal barrier function as a result of defects in or loss of CE proteins, like filaggrin in atopic dermatitis (Kezic and Jakasa 2016) or LCE3 in psoriasis (de Cid et al. 2009).

The epidermal morphology of young SEs is already quite “perfect”, so the immunofluorescence stainings of differentiation markers or the lipid matrix did not display marked changes after irradiation. The upregulation of genes connected to keratinization and CE formation upon irradiation nevertheless argues for an increase in late differentiation and skin barrier formation also in young SEs.

Interestingly, the improved differentiation, including the upregulated expression of important components of the skin barrier, by UV or SUN exposure did not result in a functional improvement of the TEWL in our SEs with young or old fibroblasts. There are different reports about the effects of UV exposure on TEWL. Single, high doses of UVB are known to perturb the skin barrier function,

indicated by an increase in TEWL (Jiang et al. 2007; Meguro et al. 1999; Haratake et al. 1997). Others reported an increase in TEWL in a dose-dependent manner and that the barrier recovery time extended with higher irradiation doses (Liu et al. 2010; Lim et al. 2008). Frodin et al. found an increase in TEWL after irradiation with 3 MED, but not with 0.5 or 1 MED (Frodin, Molin, and Skogh 1988). Interestingly, 3 days of exposure to low dose (0.5 MED) of UVB were described by Hong et al. to even accelerate barrier recovery and increase the expression of filaggrin in hairless mice (Hong et al. 2008). The different results indicate that the effect of UV exposure on TEWL is highly dependent on the dose and that low-dose UVB can be beneficial for the skin barrier. This effect is also utilized in the treatment of atopic dermatitis, which is characterized by a defective skin barrier (Wulf and Bech-Thomsen 1998). It is important to note that all mentioned studies were done with UVB alone and it needs to be investigated further if low dose exposure to the spectral combination as we applied it in our experiments has different consequences for the skin barrier than UVB alone.

The improved growth and differentiation seen in the old SEs in response to irradiation, as well as the hyperplasia observed in some of the young SEs, both require an increase in proliferation of epidermal cells. However, the proliferation rates determined in the Age-SEs 24 h after the last irradiation of the 2-week irradiation regime, were not significantly changed by irradiation. Even irradiation for 4 or 6 weeks did not affect the proliferation rates of young SEs. This suggests that an increased proliferation, needed to establish the observed phenotypes, is not maintained throughout the period of chronic irradiation. We rather expect an initial peak of proliferation that goes back to baseline.

Lee at al. determined the proliferation of basal keratinocytes from human biopsies after irradiation with 1 MED of UVB and found a significant increase in proliferation after 48 h (but not after 24 h) that fell to control level again after 72 h (Lee et al. 2002). Similar results were described by El-Abaseri et al. who exposed mice to UV irradiation and found a peak in proliferation after 48 h whereas after 24 h and after 72 h the proliferation rate was not significantly increased (El-Abaseri, Putta, and Hansen 2006). So, it might well be, that at 24 h after the irradiation we do not see the proliferative peak, that is only an acute response in a short time frame before the tissue reaches again a homeostatic state and it might be necessary to check the proliferation rate 48 h after the irradiation.

It is well established that high doses of UV are genotoxic and trigger apoptosis of damaged keratinocytes (Kulms et al. 2002; Batista et al. 2009). The dose applied here did not induce massive cell death, as demonstrated by viability assays and a flow cytometric apoptosis analysis. Nevertheless, we observed the induction of CPDs, the typical DNA lesion indicative of UV-induced damage (Brash 2015) after irradiation with UVA+B and SUN in young and old Age-SEs. If DNA

damage cannot be repaired, cells undergo apoptosis. These apoptotic keratinocytes are known as sunburn cells and are identified by their pyknotic nuclei (Bayerl et al. 1995; Young 1987; Murphy et al. 2001). We did not find evidence for sunburn cells in the epidermis of irradiated Age-SE. The reason for the appearance of sunburn cells and massive cell death in other studies could be that they often use high doses of UVB. Bayerl et al. for example observed sunburn cells in skin biopsies after treating the skin with 4 MED (Bayerl et al. 1995), which is approximately four times the dose applied in our study. Wolf et al. found a significant induction of sunburn cells *in vivo* 6 h after irradiation with 2 MED.

In everyday life, skin is usually not exposed to such high doses at once, but rather repeatedly exposed to low or moderate doses of UV. De Pedro et. al studied the response of human keratinocytes to different doses of UVB and while acute high levels of UVB (1.5-3 kJ/m^2) caused apoptosis, moderate levels of UVB (0.1-0.25 kJ/m^2) triggered terminal differentiation of the keratinocytes. They propose this increased differentiation with the consequence of cell shedding as a self-protective alternative approach of the skin to get rid of potentially pre-cancerous cells (de Pedro et al. 2018). This is also supported by other studies that report differentiation-inducing effects of sub erythemal UVB doses (Del Bino et al. 2004; Bertrand-Vallery et al. 2010). This mechanism probably contributes to the beneficial therapeutic effects of moderate sun exposure or UV treatment (phototherapy) for the treatment of skin disorders like psoriasis (Armstrong and Read 2020).

The positive effect of low dose irradiation on keratinocyte differentiation could in part explain the improved growth and differentiation that we observed in the irradiated old Age-SEs. However, it is not sufficient to explain the significant differences in epidermal regeneration between young and old Age-SEs. Given that the keratinocytes in each experiment were derived from the same young donor, the improved differentiation and stratification of the epidermis on old DEs can most likely largely be attributed to influences of the fibroblasts. As discussed before, the presence or reduction of myofibroblasts may be the decisive factor for the regeneration of the epidermis.

The different responses of skin cells to high and low doses of UVB also emphasize that the irradiation regime is of high importance when comparing outcomes of different studies as beneficial or detrimental effects of UV exposure might often be dose dependent. In addition, most of the irradiation studies only use UVB. As we could show in our direct comparison of gene expression analysis in response to UVA+B and SUN, irradiation with the entire solar spectrum induces significantly different regulations than the UV spectrum alone. To the best of our knowledge there are no studies using comparable experimental parameters (entire solar spectrum, physiological dose, chronic exposure, tissue context), highlighting the importance and relevance of our study to understand the effects of sun exposure on human skin.

4.8 Transformed Keratinocytes are Less Dependent on The Fibroblasts

Skin cancer predominantly affects the elderly population. It is therefore vitally important to understand how age-dependent changes in the skin might contribute to cancer progression. The complex crosstalk between cells and their surrounding ECM regulates tissue function and also plays an important role in cancer development (Nelson and Bissell 2006; Parrinello et al. 2005). In turn, tumors modify their ECM to form a cancer-permissive environment, promoting tumor progression and cell migration (Winkler et al. 2020). Age-dependent alterations in the organization of the ECM were shown to influence the way tumor cells move and melanoma cells were more invasive in *in vitro* skin models built with aged fibroblasts (Kaur et al. 2019). Senescent fibroblasts and the secreted factors they produce, the senescence-associated secretory phenotype (SASP), are discussed to promote malignant phenotypes and tumor growth (Campisi et al. 2011). Therefore, we wanted to elucidate the role of our old fibroblasts and their altered ECM for the tumorigenicity of different transformed epithelial cells. We complemented young and old Age-SEs with HaCaT cells, which represent the typical population of cells with UV-type specific p53 mutations preexisting in sun-exposed human skin (Boukamp et al. 1988). In addition, we produced models with HaCaT-ras A5, which contain p53 mutations and the c-Ha-ras oncogene. These cells form benign cysts upon injection into nude mice (Boukamp et al. 1990) and grow as surface epithelia that can gain invasive growth potential upon challenge (Tham et al. 2022). As an example of malignant tumorigenic cells, the HaCaT-ras II4 were included. This HaCaT variant also developed upon introduction of the c-Ha-ras oncogene but gained the ability to form cutaneous squamous cell carcinomas (cSCC) in nude mice and to grow invasively in fdm-based SEs (Boukamp et al. 1990; Berning et al. 2015). The fdmSEs perfectly recapitulated the respective phenotypes and the cell-specific invasion behavior, making them well suited models to study the influence of the dermal microenvironment on the development of cSCCs.

Age-SEs with HaCaT cells formed a stratified epithelium that was rather aberrantly organized, consisting of only few vital cell layers and a thick parakeratotic stratum corneum, but displayed no invasive behavior. With HaCaT-A5 we observed invaginations indicative of beginning invasion in some cultures, that were partly breaking through the BM. HaCaT-II4 built a completely disorganized epithelium and massively invaded the dermal part. Differentiation markers and BM components were progressively disorganized or reduced with increasing malignancy of the epidermal cells.

In the epithelia of the malignant HaCaT-II4-SEs we observed acantholysis, a histological feature characteristic for several skin diseases, e.g. *pemphigus vulgaris* (Payne et al. 2004), but also for cSCCs (Cassarino, Derienzo, and Barr 2006), which is the result of a loss of cohesion between

keratinocytes. Stable adherens junctions and desmosomes are essential for cell-cell adhesion and tissue integrity and the loss or reduction of one or more desmosome components, including desmoglein 1-3 (Dsg1-3) and desmoplakin (Dsp), was reported during the development, progression and metastasis of human skin cancer (Tada et al. 2000; Harada et al. 1992; Kocher et al. 1981).

In our Age-SEs, we observed known alterations connected to tumor development, like loss of differentiation, loss of BM components, and loss of intercellular adhesion with increasing tumorigenicity of the HaCaT variants. Importantly, these phenotypes were largely independent from the fibroblasts the epidermal cells were co-cultured with, suggesting that the transformed keratinocytes, different than the NHEK, react less sensitive to changes in the DE and the regulatory factors provided by the fibroblasts. This might be due to one of the hallmarks of cancer, which is self-sufficiency in growth factors (Hanahan and Weinberg 2000), meaning that malignant cells gain independence from stimulatory signals from their surroundings. Therefore, the transformed keratinocytes might be less dependent on their microenvironment and with that less sensitive to age-dependent changes in the microenvironment, allowing them to adapt well on supportive as well as non-supportive environments.

4.9 Irradiation Did Not Induce Invasion in SEs with Transformed Keratinocytes

The causal role for UV radiation in induction and progression of skin cancer is well established (Brash et al. 1991; Pfeifer 2020; Leiter, Keim, and Garbe 2020). Therefore, we exposed the HaCaT models to the chronic irradiation regime with UVA+B or SUN to see if this would lead to an induction or increase of invasion in irradiated SEs compared to controls. Interestingly, we did not observe an increased invasion in any of the SEs (HaCaT, -A5 and -II4), neither with young nor old fibroblasts. On the contrary, invasion was rather reduced.

Prerequisites for tumorigenic growth and invasion are an increased proliferation of the epidermal cells and a degradation of the BM and ECM. This degradation as an essential step in tumorigenesis that allows the epithelial tumor cells to migrate, break through the BM, and invade the connective tissue, is mainly mediated by MMPs (reviewed in (Kerkela and Saarialho-Kere 2003; Quintero-Fabian et al. 2019; Pittayapruek et al. 2016)). MMP-1 is one of the best studied proteolytic factors, known to be involved in skin cancer and induced by UV radiation (Dong et al. 2008; Quan et al. 2009). Expression of MMP-1 was reported to be associated with the initial steps of tumor growth in cSCCs *in vitro* and *in vivo* (Lederle et al. 2011). Ramos et al. reported an induction of MMP-1

in a squamous carcinoma cell line by UV radiation (Ramos et al. 2004). This is in line with our results. Irradiation with UVA+B or SUN increased pro-MMP-1 levels in Age-SEs with HaCaT, HaCaT-A5 and HaCaT-II4, at least in those with young fibroblasts. This shows that the irradiation can trigger MMP activity that enables tissue degradation. However, this did not lead to increasing invasion of epithelial cells in the SEs.

Another way that UV exposure contributes to skin cancer development is by deregulating cell proliferation and survival. Normally, the skin responds to UV-induced damage with cell cycle arrest to allow for the repair or induce apoptosis of damaged cells. If these mechanisms fail, it can lead to expansion of damaged (mutated) cells that finally can contribute to tumor development (Matsumura and Ananthaswamy 2002; El-Abaseri, Putta, and Hansen 2006; Rodust et al. 2009). In human skin samples from normal skin, sun-damaged skin, and cSCCs, proliferation was significantly increased in the progression from normal skin to cSCC (Einspahr et al. 1999). Accordingly, we found the highest proliferation rates in the SEs with the malignant HaCaT-II4 cells. Other than in NHEK-SEs, in the SEs with the different HaCaT variants there were no significant differences in proliferation between SEs with young or old fibroblasts, again indicating that transformed keratinocytes are more independent from dermal influences, like growth factors, for their survival and proliferation. Interestingly, irradiation did not induce increased proliferation. As discussed for NHEK, it cannot be excluded that irradiation may have induced an early proliferation response also in the transformed keratinocytes. If so, this proliferation stimulus was not maintained throughout the irradiation period.

Taken together, these findings demonstrated that different from previous suggestions (Campisi et al. 2011; Krtolica et al. 2001), our old fibroblasts with their altered ECM do not exhibit tumor promoting activity in the Age-SEs. Even more so, the chronic irradiation regime is not sufficient to induce tumorigenic conversion of the immortal (HaCaT) and premalignant (HaCaT-A5) cells or to further increase invasion of the malignant (HaCaT-II4) cells. This further adds to the idea that besides the well described damaging potential of UV radiation, chronic low doses of solar radiation do not seem to provoke tumorigenic conversion but may rather exert beneficial effects by contributing to improved tissue organization.

4.10 Conclusion

In this study we successfully established fdm-based SEs with young and old fibroblasts that we termed Age-SEs. With these we could verify and further characterize a novel differentiation state of old fibroblasts derived from sun-damaged skin, the myo-chondro-fibroblast. The Age-SEs demonstrated the influence of the fibroblast phenotype on the tissue morphology and function.

Interestingly, irradiation with 1 MED of the solar UV spectrum or the entire solar spectrum led to a normalization of the tissue structure and improved the epidermal differentiation and regeneration of old Age-SEs. These improvements correlated with a dedifferentiation of the myofibroblast phenotype, showing that this phenotype is reversible, and this might allow for a better dermal-epidermal communication. Our results also argued for a role of UV irradiation in the regulation of the chondrocyte-like phenotype and the induction of the cartilage matrix. However, this is most likely not a direct effect. Instead, we propose that long term recurrent sun exposure, that leads to tissue damage and the appearance of solar elastosis, triggers the differentiation of the fibroblasts as an indirect consequence.

Analyzing the gene expression profiles of the fibroblasts we could prove that young and old fibroblasts respond differently to irradiation and that the solar UV spectrum alone triggers different regulatory responses than the entire solar spectrum. This needs to be taken into account when results from irradiation studies are used for risk assessment.

In addition, by complementing Age-SEs with transformed keratinocytes, we could show that the old fibroblasts are not *per se* tumor promoting and that the low dose irradiation did not provoke or increase invasion of the keratinocytes.

In summary, our results suggest that, besides the known detrimental effects of excessive sun exposure, low dose UV or solar radiation might have beneficial effects and contribute to the normal skin function, without necessarily inducing tumorigenesis. In analogy to phototherapy used for the treatment of a number of skin diseases, it might be speculated that a controlled phototherapy for solar elastoses may help to stimulate renormalization of skin physiology.

References

Ahlfors, J. E., and K. L. Billiar. 2007. 'Biomechanical and biochemical characteristics of a human fibroblast-produced and remodeled matrix', *Biomaterials*, 28: 2183-91.

Albrecht, S., S. Jung, R. Muller, J. Lademann, T. Zuberbier, L. Zastrow, C. Reble, I. Beckers, and M. C. Meinke. 2019. 'Skin type differences in solar-simulated radiation-induced oxidative stress', *Br J Dermatol*, 180: 597-603.

Alexander, H., S. Brown, S. Danby, and C. Flohr. 2018. 'Research Techniques Made Simple: Transepidermal Water Loss Measurement as a Research Tool', *J Invest Dermatol*, 138: 2295-300 e1.

Allen, J. L., M. E. Cooke, and T. Alliston. 2012. 'ECM stiffness primes the TGFbeta pathway to promote chondrocyte differentiation', *Mol Biol Cell*, 23: 3731-42.

Amano, S. 2009. 'Possible involvement of basement membrane damage in skin photoaging', *J Investig Dermatol Symp Proc*, 14: 2-7.

Amano, S., N. Akutsu, Y. Matsunaga, T. Nishiyama, M. F. Champliaud, R. E. Burgeson, and E. Adachi. 2001. 'Importance of balance between extracellular matrix synthesis and degradation in basement membrane formation', *Exp Cell Res*, 271: 249-62.

Ananthapadmanabhan, K. P., S. Mukherjee, and P. Chandar. 2013. 'Stratum corneum fatty acids: their critical role in preserving barrier integrity during cleansing', *Int J Cosmet Sci*, 35: 337-45.

Armstrong, A. W., and C. Read. 2020. 'Pathophysiology, Clinical Presentation, and Treatment of Psoriasis: A Review', *JAMA*, 323: 1945-60.

Aumailley, M., C. Has, L. Tunggal, and L. Bruckner-Tuderman. 2006. 'Molecular basis of inherited skin-blistering disorders, and therapeutic implications', *Expert Rev Mol Med*, 8: 1-21.

Bai, X., Z. Xiao, Y. Pan, J. Hu, J. Pohl, J. Wen, and L. Li. 2004. 'Cartilage-derived morphogenetic protein-1 promotes the differentiation of mesenchymal stem cells into chondrocytes', *Biochem Biophys Res Commun*, 325: 453-60.

Barriere, G., P. Fici, G. Gallerani, F. Fabbri, and M. Rigaud. 2015. 'Epithelial Mesenchymal Transition: a double-edged sword', *Clin Transl Med*, 4: 14.

Bataillon, M., D. Lelievre, A. Chapuis, F. Thillou, J. B. Autourde, S. Durand, N. Boyera, A. S. Rigaudeau, I. Besne, and C. Pellevoisin. 2019. 'Characterization of a New Reconstructed Full Thickness Skin Model, T-Skin, and its Application for Investigations of Anti-Aging Compounds', *Int J Mol Sci*, 20.

Batista, L. F. Z., B. Kaina, R. Meneghini, and C. F. M. Menck. 2009. 'How DNA lesions are turned into powerful killing structures: insights from UV-induced apoptosis', *Mutat Res*, 681: 197-208.

Bayerl, C., S. Taake, I. Moll, and E. G. Jung. 1995. 'Characterization of sunburn cells after exposure to ultraviolet light', *Photodermatol Photoimmunol Photomed*, 11: 149-54.

Bell, E., H. P. Ehrlich, D. J. Buttle, and T. Nakatsuji. 1981. 'Living tissue formed in vitro and accepted as skin-equivalent tissue of full thickness', *Science*, 211: 1052-4.

Berneburg, M., H. Plettenberg, and J. Krutmann. 2000. 'Photoaging of human skin', *Photodermatol Photoimmunol Photomed*, 16: 239-44.

Bernerd, F., and D. Asselineau. 2008. 'An organotypic model of skin to study photodamage and photoprotection in vitro', *J Am Acad Dermatol*, 58: S155-9.

Berning, M., S. Pratzel-Wunder, J. R. Bickenbach, and P. Boukamp. 2015. 'Three-Dimensional In Vitro Skin and Skin Cancer Models Based on Human Fibroblast-Derived Matrix', *Tissue Eng Part C Methods*, 21: 958-70.

Bernstein, E. F., and J. Uitto. 1996. 'The effect of photodamage on dermal extracellular matrix', *Clin Dermatol*, 14: 143-51.

Berthod, F., F. Sahuc, D. Hayek, O. Damour, and C. Collombel. 1996. 'Deposition of collagen fibril bundles by long-term culture of fibroblasts in a collagen sponge', *J Biomed Mater Res*, 32: 87-93.

Bertrand-Vallery, V., E. Boilan, N. Ninane, C. Demazy, B. Friguet, O. Toussaint, Y. Poumay, and F. Debacq-Chainiaux. 2010. 'Repeated exposures to UVB induce differentiation rather than senescence of human keratinocytes lacking p16(INK-4A)', *Biogerontology*, 11: 167-81.

Bissell, M. J., and W. C. Hines. 2011. 'Why don't we get more cancer? A proposed role of the microenvironment in restraining cancer progression', *Nat Med*, 17: 320-9.

Boehnke, K., N. Mirancea, A. Pavesio, N. E. Fusenig, P. Boukamp, and H. J. Stark. 2007. 'Effects of fibroblasts and microenvironment on epidermal regeneration and tissue function in long-term skin equivalents', *Eur J Cell Biol*, 86: 731-46.

Bolger, A. M., M. Lohse, and B. Usadel. 2014. 'Trimmomatic: a flexible trimmer for Illumina sequence data', *Bioinformatics*, 30: 2114-20.

Boukamp, P. 2005. 'UV-induced skin cancer: similarities--variations', *J Dtsch Dermatol Ges*, 3: 493-503.

Boukamp, P., R. T. Petrussevska, D. Breitkreutz, J. Hornung, A. Markham, and N. E. Fusenig. 1988. 'Normal keratinization in a spontaneously immortalized aneuploid human keratinocyte cell line', *J Cell Biol*, 106: 761-71.

Boukamp, P., E. J. Stanbridge, D. Y. Foo, P. A. Cerutti, and N. E. Fusenig. 1990. 'c-Ha-ras oncogene expression in immortalized human keratinocytes (HaCaT) alters growth potential in vivo but lacks correlation with malignancy', *Cancer Res*, 50: 2840-7.

Brash, D. E. 2015. 'UV signature mutations', *Photochem Photobiol*, 91: 15-26.

Brash, D. E., J. A. Rudolph, J. A. Simon, A. Lin, G. J. McKenna, H. P. Baden, A. J. Halperin, and J. Ponten. 1991. 'A role for sunlight in skin cancer: UV-induced p53 mutations in squamous cell carcinoma', *Proc Natl Acad Sci U S A*, 88: 10124-8.

Bray, F., J. Ferlay, I. Soerjomataram, R. L. Siegel, L. A. Torre, and A. Jemal. 2018. 'Global cancer statistics 2018: GLOBOCAN estimates of incidence and mortality worldwide for 36 cancers in 185 countries', *CA Cancer J Clin*, 68: 394-424.

Breitkreutz, D., I. Koxholt, K. Thiemann, and R. Nischt. 2013. 'Skin basement membrane: the foundation of epidermal integrity--BM functions and diverse roles of bridging molecules nidogen and perlecan', *Biomed Res Int*, 2013: 179784.

Brenneisen, P., H. Sies, and K. Scharffetter-Kochanek. 2002. 'Ultraviolet-B irradiation and matrix metalloproteinases: from induction via signaling to initial events', *Ann N Y Acad Sci*, 973: 31-43.

Buechner, N., P. Schroeder, S. Jakob, K. Kunze, T. Maresch, C. Calles, J. Krutmann, and J. Haendeler. 2008. 'Changes of MMP-1 and collagen type Ialpha1 by UVA, UVB and IRA are differentially regulated by Trx-1', *Exp Gerontol*, 43: 633-7.

Burren, R., C. Scaletta, E. Frenk, R. G. Panizzon, and L. A. Applegate. 1998. 'Sunlight and carcinogenesis: expression of p53 and pyrimidine dimers in human skin following UVA I, UVA I + II and solar simulating radiations', *Int J Cancer*, 76: 201-6.

Cadet, J., and T. Douki. 2018. 'Formation of UV-induced DNA damage contributing to skin cancer development', *Photochem Photobiol Sci*, 17: 1816-41.

Cadet, J., S. Mouret, J. L. Ravanat, and T. Douki. 2012. 'Photoinduced damage to cellular DNA: direct and photosensitized reactions', *Photochem Photobiol*, 88: 1048-65.

Campisi, J. 2005. 'Senescent cells, tumor suppression, and organismal aging: good citizens, bad neighbors', *Cell*, 120: 513-22.

Campisi, J., J. K. Andersen, P. Kapahi, and S. Melov. 2011. 'Cellular senescence: a link between cancer and age-related degenerative disease?', *Semin Cancer Biol*, 21: 354-9.

Cassarino, D. S., D. P. Derienzo, and R. J. Barr. 2006. 'Cutaneous squamous cell carcinoma: a comprehensive clinicopathologic classification. Part one', *J Cutan Pathol*, 33: 191-206.

Cassiede, P., J. E. Dennis, F. Ma, and A. I. Caplan. 1996. 'Osteochondrogenic potential of marrow mesenchymal progenitor cells exposed to TGF-beta 1 or PDGF-BB as assayed in vivo and in vitro', *J Bone Miner Res*, 11: 1264-73.

Cavinato, M., and P. Jansen-Durr. 2017. 'Molecular mechanisms of UVB-induced senescence of dermal fibroblasts and its relevance for photoaging of the human skin', *Exp Gerontol*, 94: 78-82.

Charruyer, A., T. Weisenberger, H. Li, A. Khalifa, A. W. Schroeder, A. Belzer, and R. Ghadially. 2021. 'Decreased p53 is associated with a decline in asymmetric stem cell self-renewal in aged human epidermis', *Aging Cell*, 20: e13310.

Chen, C. Z., Y. X. Peng, Z. B. Wang, P. V. Fish, J. L. Kaar, R. R. Koepsel, A. J. Russell, R. R. Lareu, and M. Raghunath. 2009. 'The Scar-in-a-Jar: studying potential antifibrotic compounds from the epigenetic to extracellular level in a single well', *Br J Pharmacol*, 158: 1196-209.

Choi, Y. J., K. M. Moon, K. W. Chung, J. W. Jeong, D. Park, D. H. Kim, B. P. Yu, and H. Y. Chung. 2016. 'The underlying mechanism of proinflammatory NF-kappaB activation by the mTORC2/Akt/IKKalpha pathway during skin aging', *Oncotarget*, 7: 52685-94.

Christiano, A. M., D. S. Greenspan, G. G. Hoffman, X. Zhang, Y. Tamai, A. N. Lin, H. C. Dietz, A. Hovnanian, and J. Uitto. 1993. 'A missense mutation in type VII collagen in two affected siblings with recessive dystrophic epidermolysis bullosa', *Nat Genet*, 4: 62-6.

Ciazynska, M., G. Kaminska-Winciorek, D. Lange, B. Lewandowski, A. Reich, M. Slawinska, M. Pabianek, K. Szczepaniak, A. Hankiewicz, M. Ulanska, J. Morawiec, M. Blasinska-Morawiec, Z. Morawiec, J. Piekarski, D. Nejc, R. Brodowski, A. Zaryczanska, M. Sobjanek, R. J. Nowicki, W. Owczarek, M. Slowinska, K. Wrobel, A. Bieniek, A. Wozniacka, M. Skibinska, J. Narbutt, W. Niemczyk, K. Ciazynski, and A. Lesiak. 2021. 'The incidence and clinical analysis of non-melanoma skin cancer', *Sci Rep*, 11: 4337.

Contet-Audonneau, J. L., C. Jeanmaire, and G. Pauly. 1999. 'A histological study of human wrinkle structures: comparison between sun-exposed areas of the face, with or without wrinkles, and sun-protected areas', *Br J Dermatol*, 140: 1038-47.

Cooper, M. L., J. F. Hansbrough, R. L. Spielvogel, R. Cohen, R. L. Bartel, and G. Naughton. 1991. 'In vivo optimization of a living dermal substitute employing cultured human fibroblasts on a biodegradable polyglycolic acid or polyglactin mesh', *Biomaterials*, 12: 243-8.

Craven, N. M., R. E. Watson, C. J. Jones, C. A. Shuttleworth, C. M. Kielty, and C. E. Griffiths. 1997. 'Clinical features of photodamaged human skin are associated with a reduction in collagen VII', *Br J Dermatol*, 137: 344-50.

Cunningham, F., M. R. Amode, D. Barrell, K. Beal, K. Billis, S. Brent, D. Carvalho-Silva, P. Clapham, G. Coates, S. Fitzgerald, L. Gil, C. G. Giron, L. Gordon, T. Hourlier, S. E. Hunt, S. H. Janacek, N. Johnson, T. Juettemann, A. K. Kahari, S. Keenan, F. J. Martin, T. Maurel, W. McLaren, D. N. Murphy, R. Nag, B. Overduin, A. Parker, M. Patricio, E. Perry, M. Pignatelli, H. S. Riat, D. Sheppard, K. Taylor, A. Thormann, A. Vullo, S. P. Wilder, A. Zadissa, B. L. Aken, E. Birney, J. Harrow, R. Kinsella, M. Muffato, M. Ruffier, S. M. Searle, G. Spudich, S. J. Trevanion, A. Yates, D. R. Zerbino, and P. Flicek. 2015. 'Ensembl 2015', *Nucleic Acids Res*, 43: D662-9.

Darby, I. A., B. Laverdet, F. Bonte, and A. Desmouliere. 2014. 'Fibroblasts and myofibroblasts in wound healing', *Clin Cosmet Investig Dermatol*, 7: 301-11.

de Cid, R., E. Riveira-Munoz, P. L. Zeeuwen, J. Robarge, W. Liao, E. N. Dannhauser, E. Giardina, P. E. Stuart, R. Nair, C. Helms, G. Escaramis, E. Ballana, G. Martin-Ezquerra, M. den Heijer, M. Kamsteeg, I. Joosten, E. E. Eichler, C. Lazaro, R. M. Pujol, L. Armengol, G. Abecasis, J. T. Elder, G. Novelli, J. A. Armour, P. Y. Kwok, A. Bowcock, J. Schalkwijk, and X. Estivill. 2009. 'Deletion of the late cornified envelope LCE3B and LCE3C genes as a susceptibility factor for psoriasis', *Nat Genet*, 41: 211-5.

de Pedro, I., P. Alonso-Lecue, N. Sanz-Gomez, A. Freije, and A. Gandarillas. 2018. 'Sublethal UV irradiation induces squamous differentiation via a p53-independent, DNA damage-mitosis checkpoint', *Cell Death Dis*, 9: 1094.

Del Bino, S., C. Vioux, P. Rossio-Pasquier, A. Jomard, M. Demarchez, D. Asselineau, and F. Bernerd. 2004. 'Ultraviolet B induces hyperproliferation and modification of epidermal differentiation in normal human skin grafted on to nude mice', *Br J Dermatol*, 150: 658-67.

Delva, E., D. K. Tucker, and A. P. Kowalczyk. 2009. 'The desmosome', *Cold Spring Harb Perspect Biol*, 1: a002543.

Desmouliere, A., A. Geinoz, F. Gabbiani, and G. Gabbiani. 1993. 'Transforming growth factor-beta 1 induces alpha-smooth muscle actin expression in granulation tissue myofibroblasts and in quiescent and growing cultured fibroblasts', *J Cell Biol*, 122: 103-11.

Desmouliere, A., M. Redard, I. Darby, and G. Gabbiani. 1995. 'Apoptosis mediates the decrease in cellularity during the transition between granulation tissue and scar', *Am J Pathol*, 146: 56-66.

Diekmann, J., L. Alili, O. Scholz, M. Giesen, O. Holtkotter, and P. Brenneisen. 2016. 'A three-dimensional skin equivalent reflecting some aspects of in vivo aged skin', *Exp Dermatol*, 25: 56-61.

Dilley, T. K., G. T. Bowden, and Q. M. Chen. 2003. 'Novel mechanisms of sublethal oxidant toxicity: induction of premature senescence in human fibroblasts confers tumor promoter activity', *Exp Cell Res*, 290: 38-48.

Dimri, G. P., X. Lee, G. Basile, M. Acosta, G. Scott, C. Roskelley, E. E. Medrano, M. Linskens, I. Rubelj, O. Pereira-Smith, and et al. 1995. 'A biomarker that identifies senescent human cells in culture and in aging skin in vivo', *Proc Natl Acad Sci U S A*, 92: 9363-7.

Dong, K. K., N. Damaghi, S. D. Picart, N. G. Markova, K. Obayashi, Y. Okano, H. Masaki, S. Grether-Beck, J. Krutmann, K. A. Smiles, and D. B. Yarosh. 2008. 'UV-induced DNA damage initiates release of MMP-1 in human skin', *Exp Dermatol*, 17: 1037-44.

Driskell, R. R., B. M. Lichtenberger, E. Hoste, K. Kretzschmar, B. D. Simons, M. Charalambous, S. R. Ferron, Y. Herault, G. Pavlovic, A. C. Ferguson-Smith, and F. M. Watt. 2013. 'Distinct fibroblast lineages determine dermal architecture in skin development and repair', *Nature*, 504: 277-81.

Dupont, E., J. Gomez, and D. Bilodeau. 2013. 'Beyond UV radiation: a skin under challenge', *Int J Cosmet Sci*, 35: 224-32.

Eaglstein, W. H. 1989. 'Wound healing and aging', *Clin Geriatr Med*, 5: 183-8.

Eckert, R. L., and E. A. Rorke. 1989. 'Molecular biology of keratinocyte differentiation', *Environ Health Perspect*, 80: 109-16.

Einspahr, J. G., D. S. Alberts, J. A. Warneke, P. Bozzo, J. Basye, T. M. Grogan, M. A. Nelson, and G. T. Bowden. 1999. 'Relationship of p53 mutations to epidermal cell proliferation and apoptosis in human UV-induced skin carcinogenesis', *Neoplasia*, 1: 468-75.

El-Abaseri, T. B., S. Putta, and L. A. Hansen. 2006. 'Ultraviolet irradiation induces keratinocyte proliferation and epidermal hyperplasia through the activation of the epidermal growth factor receptor', *Carcinogenesis*, 27: 225-31.

El Ghalbzouri, A., S. Commandeur, M. H. Rietveld, A. A. Mulder, and R. Willemze. 2009. 'Replacement of animal-derived collagen matrix by human fibroblast-derived dermal matrix for human skin equivalent products', *Biomaterials*, 30: 71-8.

El Ghalbzouri, A., E. Lamme, and M. Ponec. 2002. 'Crucial role of fibroblasts in regulating epidermal morphogenesis', *Cell Tissue Res*, 310: 189-99.

Elias, P. M. 1983. 'Epidermal lipids, barrier function, and desquamation', *J Invest Dermatol*, 80: 44s-9s.

Engelke, M., J. M. Jensen, S. Ekanayake-Mudiyanselage, and E. Proksch. 1997. 'Effects of xerosis and ageing on epidermal proliferation and differentiation', *Br J Dermatol*, 137: 219-25.

Even-Ram, S., and K. M. Yamada. 2005. 'Cell migration in 3D matrix', *Curr Opin Cell Biol*, 17: 524-32.

Ewels, P., M. Magnusson, S. Lundin, and M. Kaller. 2016. 'MultiQC: summarize analysis results for multiple tools and samples in a single report', *Bioinformatics*, 32: 3047-8.

Farage, M. A., K. W. Miller, E. Berardesca, and H. I. Maibach. 2009. 'Clinical implications of aging skin: cutaneous disorders in the elderly', *Am J Clin Dermatol*, 10: 73-86.

Farage, M. A., K. W. Miller, P. Elsner, and H. I. Maibach. 2008. 'Intrinsic and extrinsic factors in skin ageing: a review', *Int J Cosmet Sci*, 30: 87-95.

Fernandez, T. L., D. R. Van Lonkhuyzen, R. A. Dawson, M. G. Kimlin, and Z. Upton. 2014. 'Characterization of a human skin equivalent model to study the effects of ultraviolet B radiation on keratinocytes', *Tissue Eng Part C Methods*, 20: 588-98.

Fisher, G. J., S. C. Datta, H. S. Talwar, Z. Q. Wang, J. Varani, S. Kang, and J. J. Voorhees. 1996. 'Molecular basis of sun-induced premature skin ageing and retinoid antagonism', *Nature*, 379: 335-9.

Fisher, G. J., T. Quan, T. Purohit, Y. Shao, M. K. Cho, T. He, J. Varani, S. Kang, and J. J. Voorhees. 2009. 'Collagen fragmentation promotes oxidative stress and elevates matrix metalloproteinase-1 in fibroblasts in aged human skin', *Am J Pathol*, 174: 101-14.

Fisher, G. J., Y. Shao, T. He, Z. Qin, D. Perry, J. J. Voorhees, and T. Quan. 2016. 'Reduction of fibroblast size/mechanical force down-regulates TGF-beta type II receptor: implications for human skin aging', *Aging Cell*, 15: 67-76.

Fisher, G. J., and J. J. Voorhees. 1998. 'Molecular mechanisms of photoaging and its prevention by retinoic acid: ultraviolet irradiation induces MAP kinase signal transduction cascades that induce Ap-1-regulated matrix metalloproteinases that degrade human skin in vivo', *J Investig Dermatol Symp Proc*, 3: 61-8.

Fisher, G. J., Z. Q. Wang, S. C. Datta, J. Varani, S. Kang, and J. J. Voorhees. 1997. 'Pathophysiology of premature skin aging induced by ultraviolet light', *N Engl J Med*, 337: 1419-28.

Fitsiou, E., T. Pulido, J. Campisi, F. Alimirah, and M. Demaria. 2021. 'Cellular Senescence and the Senescence-Associated Secretory Phenotype as Drivers of Skin Photoaging', *J Invest Dermatol*, 141: 1119-26.

Fluhr, J. W., K. R. Feingold, and P. M. Elias. 2006. 'Transepidermal water loss reflects permeability barrier status: validation in human and rodent in vivo and ex vivo models', *Exp Dermatol*, 15: 483-92.

Fortier, A. M., E. Asselin, and M. Cadrin. 2013. 'Keratin 8 and 18 loss in epithelial cancer cells increases collective cell migration and cisplatin sensitivity through claudin1 up-regulation', *J Biol Chem*, 288: 11555-71.

Francis-West, P. H., J. Parish, K. Lee, and C. W. Archer. 1999. 'BMP/GDF-signalling interactions during synovial joint development', *Cell Tissue Res*, 296: 111-9.

Frangogiannis, N. 2020. 'Transforming growth factor-beta in tissue fibrosis', *J Exp Med*, 217: e20190103.

French, M. M., S. Rose, J. Canseco, and K. A. Athanasiou. 2004. 'Chondrogenic differentiation of adult dermal fibroblasts', *Ann Biomed Eng*, 32: 50-6.

Friedl, P., E. Sahai, S. Weiss, and K. M. Yamada. 2012. 'New dimensions in cell migration', *Nat Rev Mol Cell Biol*, 13: 743-7.

Frodin, T., L. Molin, and M. Skogh. 1988. 'Effects of single doses of UVA, UVB, and UVC on skin blood flow, water content, and barrier function measured by laser-Doppler flowmetry, optothermal infrared spectrometry, and evaporimetry', *Photodermatol*, 5: 187-95.

Fu, X., H. Khalil, O. Kanisicak, J. G. Boyer, R. J. Vagnozzi, B. D. Maliken, M. A. Sargent, V. Prasad, I. Valiente-Alandi, B. C. Blaxall, and J. D. Molkentin. 2018. 'Specialized fibroblast differentiated states underlie scar formation in the infarcted mouse heart', *J Clin Invest*, 128: 2127-43.

Funk, W. D., C. K. Wang, D. N. Shelton, C. B. Harley, G. D. Pagon, and W. K. Hoeffler. 2000. 'Telomerase expression restores dermal integrity to in vitro-aged fibroblasts in a reconstituted skin model', *Exp Cell Res*, 258: 270-8.

Gabbiani, G. 2003. 'The myofibroblast in wound healing and fibrocontractive diseases', *J Pathol*, 200: 500-3.

Gabbiani, G., G. B. Ryan, and G. Majne. 1971. 'Presence of modified fibroblasts in granulation tissue and their possible role in wound contraction', *Experientia*, 27: 549-50.

Gerber, P. A., B. A. Buhren, H. Schrumpf, B. Homey, A. Zlotnik, and P. Hevezi. 2014. 'The top skin-associated genes: a comparative analysis of human and mouse skin transcriptomes', *Biol Chem*, 395: 577-91.

Ghadially, R., B. E. Brown, S. M. Sequeira-Martin, K. R. Feingold, and P. M. Elias. 1995. 'The aged epidermal permeability barrier. Structural, functional, and lipid biochemical abnormalities in humans and a senescent murine model', *J Clin Invest*, 95: 2281-90.

Ghersetich, I., T. Lotti, G. Campanile, C. Grappone, and G. Dini. 1994. 'Hyaluronic acid in cutaneous intrinsic aging', *Int J Dermatol*, 33: 119-22.

Giglia-Mari, G., and A. Sarasin. 2003. 'TP53 mutations in human skin cancers', *Hum Mutat*, 21: 217-28.

Gilchrest, B. A. 1989. 'Skin aging and photoaging: an overview', *J Am Acad Dermatol*, 21: 610-3.

Gilhar, A., Y. Ullmann, R. Karry, R. Shalaginov, B. Assy, S. Serafimovich, and R. S. Kalish. 2004. 'Ageing of human epidermis: the role of apoptosis, Fas and telomerase', *Br J Dermatol*, 150: 56-63.

Goetz, R., and M. Mohammadi. 2013. 'Exploring mechanisms of FGF signalling through the lens of structural biology', *Nat Rev Mol Cell Biol*, 14: 166-80.

Gorgoulis, V., P. D. Adams, A. Alimonti, D. C. Bennett, O. Bischof, C. Bishop, J. Campisi, M. Collado, K. Evangelou, G. Ferbeyre, J. Gil, E. Hara, V. Krizhanovsky, D. Jurk, A. B. Maier, M. Narita, L. Niedernhofer, J. F. Passos, P. D. Robbins, C. A. Schmitt, J. Sedivy, K. Vougas, T. von Zglinicki, D. Zhou, M. Serrano, and M. Demaria. 2019. 'Cellular Senescence: Defining a Path Forward', *Cell*, 179: 813-27.

Grandi, C., and M. C. D'Ovidio. 2020. 'Balance between Health Risks and Benefits for Outdoor Workers Exposed to Solar Radiation: An Overview on the Role of Near Infrared Radiation Alone and in Combination with Other Solar Spectral Bands', *Int J Environ Res Public Health*, 17.

Greenspan, P., E. P. Mayer, and S. D. Fowler. 1985. 'Nile red: a selective fluorescent stain for intracellular lipid droplets', *J Cell Biol*, 100: 965-73.

Gross, S., and T. Thum. 2020. 'TGF-beta Inhibitor CILP as a Novel Biomarker for Cardiac Fibrosis', *JACC Basic Transl Sci*, 5: 444-46.

Grove, G. L., and A. M. Kligman. 1983. 'Age-associated changes in human epidermal cell renewal', *J Gerontol*, 38: 137-42.

Gundermann, Sabrina. 2012. 'TGFß-abhängige Transdifferenzierung zu einem chondrozytenähnlichen Phänotyp: ein neuer Mechanismus zur Fibroblasten-involvierten Hautalterung', Dissertation, Ruprecht-Karls-Universität Heidelberg.

Hanahan, D., and R. A. Weinberg. 2000. 'The hallmarks of cancer', *Cell*, 100: 57-70.

Harada, T., M. Shinohara, S. Nakamura, M. Shimada, and M. Oka. 1992. 'Immunohistochemical detection of desmosomes in oral squamous cell carcinomas: correlation with differentiation, mode of invasion, and metastatic potential', *Int J Oral Maxillofac Surg*, 21: 346-9.

Haratake, A., Y. Uchida, M. Schmuth, O. Tanno, R. Yasuda, J. H. Epstein, P. M. Elias, and W. M. Holleran. 1997. 'UVB-induced alterations in permeability barrier function: roles for epidermal hyperproliferation and thymocyte-mediated response', *J Invest Dermatol*, 108: 769-75.

Haydont, V., V. Neiveyans, H. Zucchi, N. O. Fortunel, and D. Asselineau. 2019. 'Genome-wide profiling of adult human papillary and reticular fibroblasts identifies ACAN, Col XI alpha1,

and PSG1 as general biomarkers of dermis ageing, and KANK4 as an exemplary effector of papillary fibroblast ageing, related to contractility', *Mech Ageing Dev*, 177: 157-81.

Hayflick, L., and P. S. Moorhead. 1961. 'The serial cultivation of human diploid cell strains', *Exp Cell Res*, 25: 585-621.

Hildebrand, A., M. Romaris, L. M. Rasmussen, D. Heinegard, D. R. Twardzik, W. A. Border, and E. Ruoslahti. 1994. 'Interaction of the small interstitial proteoglycans biglycan, decorin and fibromodulin with transforming growth factor beta', *Biochem J*, 302 (Pt 2): 527-34.

Hinz, B. 2015. 'The extracellular matrix and transforming growth factor-beta1: Tale of a strained relationship', *Matrix Biol*, 47: 54-65.

———. 2016. 'The role of myofibroblasts in wound healing', *Curr Res Transl Med*, 64: 171-77.

Hinz, B., S. H. Phan, V. J. Thannickal, A. Galli, M. L. Bochaton-Piallat, and G. Gabbiani. 2007. 'The myofibroblast: one function, multiple origins', *Am J Pathol*, 170: 1807-16.

Hinz, B., S. H. Phan, V. J. Thannickal, M. Prunotto, A. Desmouliere, J. Varga, O. De Wever, M. Mareel, and G. Gabbiani. 2012. 'Recent developments in myofibroblast biology: paradigms for connective tissue remodeling', *Am J Pathol*, 180: 1340-55.

Hong, S. P., M. J. Kim, M. Y. Jung, H. Jeon, J. Goo, S. K. Ahn, S. H. Lee, P. M. Elias, and E. H. Choi. 2008. 'Biopositive effects of low-dose UVB on epidermis: coordinate upregulation of antimicrobial peptides and permeability barrier reinforcement', *J Invest Dermatol*, 128: 2880-7.

Houben, E., K. De Paepe, and V. Rogiers. 2007. 'A keratinocyte's course of life', *Skin Pharmacol Physiol*, 20: 122-32.

Hudson, L., E. Rashdan, C. A. Bonn, B. Chavan, D. Rawlings, and M. A. Birch-Machin. 2020. 'Individual and combined effects of the infrared, visible, and ultraviolet light components of solar radiation on damage biomarkers in human skin cells', *FASEB J*, 34: 3874-83.

Hughes, M. C., C. Bredoux, F. Salas, D. Lombard, G. M. Strutton, A. Fourtanier, and A. C. Green. 2011. 'Comparison of histological measures of skin photoaging', *Dermatology*, 223: 140-51.

'IARC monographs on the evaluation of carcinogenic risks to humans. Solar and ultraviolet radiation'. 1992. *IARC Monogr Eval Carcinog Risks Hum*, 55: 1-316.

Ikeda, T., S. Kamekura, A. Mabuchi, I. Kou, S. Seki, T. Takato, K. Nakamura, H. Kawaguchi, S. Ikegawa, and U. I. Chung. 2004. 'The combination of SOX5, SOX6, and SOX9 (the SOX trio) provides signals sufficient for induction of permanent cartilage', *Arthritis Rheum*, 50: 3561-73.

Jackson, B., C. M. Tilli, M. J. Hardman, A. A. Avilion, M. C. MacLeod, G. S. Ashcroft, and C. Byrne. 2005. 'Late cornified envelope family in differentiating epithelia--response to calcium and ultraviolet irradiation', *J Invest Dermatol*, 124: 1062-70.

Janson, D. G., G. Saintigny, A. van Adrichem, C. Mahe, and A. El Ghalbzouri. 2012. 'Different gene expression patterns in human papillary and reticular fibroblasts', *J Invest Dermatol*, 132: 2565-72.

Janson, D., M. Rietveld, R. Willemze, and A. El Ghalbzouri. 2013. 'Effects of serially passaged fibroblasts on dermal and epidermal morphogenesis in human skin equivalents', *Biogerontology*, 14: 131-40.

Jantschitsch, C., S. Majewski, A. Maeda, T. Schwarz, and A. Schwarz. 2009. 'Infrared radiation confers resistance to UV-induced apoptosis via reduction of DNA damage and upregulation of antiapoptotic proteins', *J Invest Dermatol*, 129: 1271-9.

Jevtic, M., A. Lowa, A. Novackova, A. Kovacik, S. Kaessmeyer, G. Erdmann, K. Vavrova, and S. Hedtrich. 2020. 'Impact of intercellular crosstalk between epidermal keratinocytes and dermal fibroblasts on skin homeostasis', *Biochim Biophys Acta Mol Cell Res*, 1867: 118722.

Jiang, S. J., A. W. Chu, Z. F. Lu, M. H. Pan, D. F. Che, and X. J. Zhou. 2007. 'Ultraviolet B-induced alterations of the skin barrier and epidermal calcium gradient', *Exp Dermatol*, 16: 985-92.

Johnstone, B., T. M. Hering, A. I. Caplan, V. M. Goldberg, and J. U. Yoo. 1998. 'In vitro chondrogenesis of bone marrow-derived mesenchymal progenitor cells', *Exp Cell Res*, 238: 265-72.

Junqueira, L. C., G. Bignolas, and R. R. Brentani. 1979. 'Picrosirius staining plus polarization microscopy, a specific method for collagen detection in tissue sections', *Histochem J*, 11: 447-55.

Juzeniene, A., and J. Moan. 2012. 'Beneficial effects of UV radiation other than via vitamin D production', *Dermatoendocrinol*, 4: 109-17.

Kaisers, W., P. Boukamp, H. J. Stark, H. Schwender, J. Tigges, J. Krutmann, and H. Schaal. 2017. 'Age, gender and UV-exposition related effects on gene expression in in vivo aged short term cultivated human dermal fibroblasts', *PLoS One*, 12: e0175657.

Kanitakis, J., A. Ramirez-Bosca, A. Reano, J. Viac, P. Roche, and J. Thivolet. 1988. 'Filaggrin expression in normal and pathological skin. A marker of keratinocyte differentiation', *Virchows Arch A Pathol Anat Histopathol*, 412: 375-82.

Kaur, A., B. L. Ecker, S. M. Douglass, C. H. Kugel, 3rd, M. R. Webster, F. V. Almeida, R. Somasundaram, J. Hayden, E. Ban, H. Ahmadzadeh, J. Franco-Barraza, N. Shah, I. A. Mellis, F. Keeney, A. Kossenkov, H. Y. Tang, X. Yin, Q. Liu, X. Xu, M. Fane, P. Brafford, M. Herlyn, D. W. Speicher, J. A. Wargo, M. T. Tetzlaff, L. E. Haydu, A. Raj, V. Shenoy, E. Cukierman, and A. T. Weeraratna. 2019. 'Remodeling of the Collagen Matrix in Aging Skin Promotes Melanoma Metastasis and Affects Immune Cell Motility', *Cancer Discov*, 9: 64-81.

Kerkela, E., and U. Saarialho-Kere. 2003. 'Matrix metalloproteinases in tumor progression: focus on basal and squamous cell skin cancer', *Exp Dermatol*, 12: 109-25.

Kezic, S., and I. Jakasa. 2016. 'Filaggrin and Skin Barrier Function', *Curr Probl Dermatol*, 49: 1-7.

Kligman, A. M. 1969. 'Early destructive effect of sunlight on human skin', *JAMA*, 210: 2377-80.

Klingberg, F., B. Hinz, and E. S. White. 2013. 'The myofibroblast matrix: implications for tissue repair and fibrosis', *J Pathol*, 229: 298-309.

Kocher, O., M. Amaudruz, A. M. Schindler, and G. Gabbiani. 1981. 'Desmosomes and gap junctions in precarcinomatous and carcinomatous conditions of squamous epithelia. An electron microscopic and morphometrical study', *J Submicrosc Cytol*, 13: 267-81.

Kohl, E., J. Steinbauer, M. Landthaler, and R. M. Szeimies. 2011. 'Skin ageing', *J Eur Acad Dermatol Venereol*, 25: 873-84.

Kopylova, E., L. Noe, and H. Touzet. 2012. 'SortMeRNA: fast and accurate filtering of ribosomal RNAs in metatranscriptomic data', *Bioinformatics*, 28: 3211-7.

Kottner, J., A. Lichterfeld, and U. Blume-Peytavi. 2013. 'Transepidermal water loss in young and aged healthy humans: a systematic review and meta-analysis', *Arch Dermatol Res*, 305: 315-23.

Krtolica, A., S. Parrinello, S. Lockett, P. Y. Desprez, and J. Campisi. 2001. 'Senescent fibroblasts promote epithelial cell growth and tumorigenesis: a link between cancer and aging', *Proc Natl Acad Sci U S A*, 98: 12072-7.

Krutmann, J., A. Bouloc, G. Sore, B. A. Bernard, and T. Passeron. 2017. 'The skin aging exposome', *J Dermatol Sci*, 85: 152-61.

Krutmann, J., and P. Schroeder. 2009. 'Role of mitochondria in photoaging of human skin: the defective powerhouse model', *J Investig Dermatol Symp Proc*, 14: 44-9.

Kubilus, J., P. J. Hayden, S. Ayehunie, S. D. Lamore, C. Servattalab, K. L. Bellavance, J. E. Sheasgreen, and M. Klausner. 2004. 'Full Thickness EpiDerm: a dermal-epidermal skin model to study epithelial-mesenchymal interactions', *Altern Lab Anim*, 32 Suppl 1A: 75-82.

Kuchler, S., N. B. Wolf, S. Heilmann, G. Weindl, J. Helfmann, M. M. Yahya, C. Stein, and M. Schafer-Korting. 2010. '3D-wound healing model: influence of morphine and solid lipid nanoparticles', *J Biotechnol*, 148: 24-30.

Kulms, D., E. Zeise, B. Poppelmann, and T. Schwarz. 2002. 'DNA damage, death receptor activation and reactive oxygen species contribute to ultraviolet radiation-induced apoptosis in an essential and independent way', *Oncogene*, 21: 5844-51.

Kurban, R. S., and J. Bhawan. 1990. 'Histologic changes in skin associated with aging', *J Dermatol Surg Oncol*, 16: 908-14.

Lago, J. C., and M. B. Puzzi. 2019. 'The effect of aging in primary human dermal fibroblasts', *PLoS One*, 14: e0219165.

Lattouf, R., R. Younes, D. Lutomski, N. Naaman, G. Godeau, K. Senni, and S. Changotade. 2014. 'Picrosirius red staining: a useful tool to appraise collagen networks in normal and pathological tissues', *J Histochem Cytochem*, 62: 751-8.

Lavker, R. M. 1979. 'Structural alterations in exposed and unexposed aged skin', *J Invest Dermatol*, 73: 59-66.

Lavker, R. M., P. S. Zheng, and G. Dong. 1986. 'Morphology of aged skin', *Dermatol Clin*, 4: 379-89.

LeBleu, V. S., and E. G. Neilson. 2020. 'Origin and functional heterogeneity of fibroblasts', *FASEB J*, 34: 3519-36.

Lederle, W., S. Depner, S. Schnur, E. Obermueller, N. Catone, A. Just, N. E. Fusenig, and M. M. Mueller. 2011. 'IL-6 promotes malignant growth of skin SCCs by regulating a network of autocrine and paracrine cytokines', *Int J Cancer*, 128: 2803-14.

Lee, D. Y., and K. H. Cho. 2005. 'The effects of epidermal keratinocytes and dermal fibroblasts on the formation of cutaneous basement membrane in three-dimensional culture systems', *Arch Dermatol Res*, 296: 296-302.

Lee, J. H., H. T. An, J. H. Chung, K. H. Kim, H. C. Eun, and K. H. Cho. 2002. 'Acute effects of UVB radiation on the proliferation and differentiation of keratinocytes', *Photodermatol Photoimmunol Photomed*, 18: 253-61.

Lehman, T. A., R. Modali, P. Boukamp, J. Stanek, W. P. Bennett, J. A. Welsh, R. A. Metcalf, M. R. Stampfer, N. Fusenig, E. M. Rogan, and et al. 1993. 'p53 mutations in human immortalized epithelial cell lines', *Carcinogenesis*, 14: 833-9.

Lehmann, P., E. Holzle, B. Melnik, and G. Plewig. 1991. 'Effects of ultraviolet A and B on the skin barrier: a functional, electron microscopic and lipid biochemical study', *Photodermatol Photoimmunol Photomed*, 8: 129-34.

Leiter, U., U. Keim, and C. Garbe. 2020. 'Epidemiology of Skin Cancer: Update 2019', *Adv Exp Med Biol*, 1268: 123-39.

Lewis, D. A., J. B. Travers, C. Machado, A. K. Somani, and D. F. Spandau. 2011. 'Reversing the aging stromal phenotype prevents carcinoma initiation', *Aging (Albany NY)*, 3: 407-16.

Li, B., and J. H. Wang. 2011. 'Fibroblasts and myofibroblasts in wound healing: force generation and measurement', *J Tissue Viability*, 20: 108-20.

Liebel, F., S. Kaur, E. Ruvolo, N. Kollias, and M. D. Southall. 2012. 'Irradiation of skin with visible light induces reactive oxygen species and matrix-degrading enzymes', *J Invest Dermatol*, 132: 1901-7.

Lim, S. H., S. M. Kim, Y. W. Lee, K. J. Ahn, and Y. B. Choe. 2008. 'Change of biophysical properties of the skin caused by ultraviolet radiation-induced photodamage in Koreans', *Skin Res Technol*, 14: 93-102.

Liu, Z., J. W. Fluhr, S. P. Song, Z. Sun, H. Wang, Y. J. Shi, P. M. Elias, and M. Q. Man. 2010. 'Sun-induced changes in stratum corneum function are gender and dose dependent in a Chinese population', *Skin Pharmacol Physiol*, 23: 313-9.

Love, M. I., W. Huber, and S. Anders. 2014. 'Moderated estimation of fold change and dispersion for RNA-seq data with DESeq2', *Genome Biol*, 15: 550.

Low, E., G. Alimohammadiha, L. A. Smith, L. F. Costello, S. A. Przyborski, T. von Zglinicki, and S. Miwa. 2021. 'How good is the evidence that cellular senescence causes skin ageing?', *Ageing Res Rev*, 71: 101456.

Makrantonaki, E., and C. C. Zouboulis. 2007. 'Molecular mechanisms of skin aging: state of the art', *Ann N Y Acad Sci*, 1119: 40-50.

Marionnet, C., C. Pierrard, C. Vioux-Chagnoleau, J. Sok, D. Asselineau, and F. Bernerd. 2006. 'Interactions between fibroblasts and keratinocytes in morphogenesis of dermal epidermal junction in a model of reconstructed skin', *J Invest Dermatol*, 126: 971-9.

Marionnet, C., C. Tricaud, and F. Bernerd. 2014. 'Exposure to non-extreme solar UV daylight: spectral characterization, effects on skin and photoprotection', *Int J Mol Sci*, 16: 68-90.

Matsumura, Y., and H. N. Ananthaswamy. 2002. 'Molecular mechanisms of photocarcinogenesis', *Front Biosci*, 7: d765-83.

McKenzie, R., Blumthaler, M., Diaz, S., Fioletov, V., Herman, J., Seckmeyer, G., Smedley, A., and Webb, A. . 2014. "Rationalizing Nomenclature for UV Doses and Effects on Humans." In.

Meguro, S., Y. Arai, K. Masukawa, K. Uie, and I. Tokimitsu. 1999. 'Stratum corneum lipid abnormalities in UVB-irradiated skin', *Photochem Photobiol*, 69: 317-21.

Meloni, M., A. Farina, and B. de Servi. 2010. 'Molecular modifications of dermal and epidermal biomarkers following UVA exposures on reconstructed full-thickness human skin', *Photochem Photobiol Sci*, 9: 439-47.

Mewes, K. R., M. Raus, A. Bernd, N. N. Zoller, A. Sattler, and R. Graf. 2007. 'Elastin expression in a newly developed full-thickness skin equivalent', *Skin Pharmacol Physiol*, 20: 85-95.

Meyer, L. J., and R. Stern. 1994. 'Age-dependent changes of hyaluronan in human skin', *J Invest Dermatol*, 102: 385-9.

Mine, S., N. O. Fortunel, H. Pageon, and D. Asselineau. 2008. 'Aging alters functionally human dermal papillary fibroblasts but not reticular fibroblasts: a new view of skin morphogenesis and aging', *PLoS One*, 3: e4066.

Mizuno, S., and J. Glowacki. 1996. 'Chondroinduction of human dermal fibroblasts by demineralized bone in three-dimensional culture', *Exp Cell Res*, 227: 89-97.

Mogford, J. E., N. Tawil, A. Chen, D. Gies, Y. Xia, and T. A. Mustoe. 2002. 'Effect of age and hypoxia on TGFbeta1 receptor expression and signal transduction in human dermal fibroblasts: impact on cell migration', *J Cell Physiol*, 190: 259-65.

Moragas, A., C. Castells, and M. Sans. 1993. 'Mathematical morphologic analysis of aging-related epidermal changes', *Anal Quant Cytol Histol*, 15: 75-82.

Mouret, S., C. Baudouin, M. Charveron, A. Favier, J. Cadet, and T. Douki. 2006. 'Cyclobutane pyrimidine dimers are predominant DNA lesions in whole human skin exposed to UVA radiation', *Proc Natl Acad Sci U S A*, 103: 13765-70.

Murphy, G., A. R. Young, H. C. Wulf, D. Kulms, and T. Schwarz. 2001. 'The molecular determinants of sunburn cell formation', *Exp Dermatol*, 10: 155-60.

Nagase, H., R. Visse, and G. Murphy. 2006. 'Structure and function of matrix metalloproteinases and TIMPs', *Cardiovasc Res*, 69: 562-73.

Nakamura, M., T. Haarmann-Stemmann, J. Krutmann, and A. Morita. 2018. 'Alternative test models for skin ageing research', *Exp Dermatol*, 27: 495-500.

Narla, S., I. Kohli, I. H. Hamzavi, and H. W. Lim. 2020. 'Visible light in photodermatology', *Photochem Photobiol Sci*, 19: 99-104.

Naylor, E. C., R. E. Watson, and M. J. Sherratt. 2011. 'Molecular aspects of skin ageing', *Maturitas*, 69: 249-56.

Nelson, C. M., and M. J. Bissell. 2006. 'Of extracellular matrix, scaffolds, and signaling: tissue architecture regulates development, homeostasis, and cancer', *Annu Rev Cell Dev Biol*, 22: 287-309.

Ng, Y. Z., C. Pourreyron, J. C. Salas-Alanis, J. H. Dayal, R. Cepeda-Valdes, W. Yan, S. Wright, M. Chen, J. D. Fine, F. J. Hogg, J. A. McGrath, D. F. Murrell, I. M. Leigh, E. B. Lane, and A. P. South. 2012. 'Fibroblast-derived dermal matrix drives development of aggressive cutaneous squamous cell carcinoma in patients with recessive dystrophic epidermolysis bullosa', *Cancer Res*, 72: 3522-34.

Nissinen, L., M. Farshchian, P. Riihila, and V. M. Kahari. 2016. 'New perspectives on role of tumor microenvironment in progression of cutaneous squamous cell carcinoma', *Cell Tissue Res*, 365: 691-702.

Norlen, L., I. Nicander, A. Lundsjo, T. Cronholm, and B. Forslind. 1998. 'A new HPLC-based method for the quantitative analysis of inner stratum corneum lipids with special reference to the free fatty acid fraction', *Arch Dermatol Res*, 290: 508-16.

Olesen, C. M., C. S. K. Fuchs, P. A. Philipsen, M. Haedersdal, T. Agner, and M. L. Clausen. 2019. 'Advancement through epidermis using tape stripping technique and Reflectance Confocal Microscopy', *Sci Rep*, 9: 12217.

Olovnikov, A. M. 1973. 'A theory of marginotomy. The incomplete copying of template margin in enzymic synthesis of polynucleotides and biological significance of the phenomenon', *J Theor Biol*, 41: 181-90.

Pageon, H., H. Zucchi, and D. Asselineau. 2012. 'Distinct and complementary roles of papillary and reticular fibroblasts in skin morphogenesis and homeostasis', *Eur J Dermatol*, 22: 324-32.

Park, J. S., J. S. Chu, A. D. Tsou, R. Diop, Z. Tang, A. Wang, and S. Li. 2011. 'The effect of matrix stiffness on the differentiation of mesenchymal stem cells in response to TGF-beta', *Biomaterials*, 32: 3921-30.

Parrinello, S., J. P. Coppe, A. Krtolica, and J. Campisi. 2005. 'Stromal-epithelial interactions in aging and cancer: senescent fibroblasts alter epithelial cell differentiation', *J Cell Sci*, 118: 485-96.

Passeron, T., J. Krutmann, M. L. Andersen, R. Katta, and C. C. Zouboulis. 2020. 'Clinical and biological impact of the exposome on the skin', *J Eur Acad Dermatol Venereol*, 34 Suppl 4: 4-25.

Patro, R., G. Duggal, M. I. Love, R. A. Irizarry, and C. Kingsford. 2017. 'Salmon provides fast and bias-aware quantification of transcript expression', *Nat Methods*, 14: 417-19.

Paulsson, M. 1992. 'Basement membrane proteins: structure, assembly, and cellular interactions', *Crit Rev Biochem Mol Biol*, 27: 93-127.

Pavez Lorie, E., and P. Boukamp. 2020. 'Methods in cell biology: Cell-derived matrices', *Methods Cell Biol*, 156: 309-32.

Payne, A. S., Y. Hanakawa, M. Amagai, and J. R. Stanley. 2004. 'Desmosomes and disease: pemphigus and bullous impetigo', *Curr Opin Cell Biol*, 16: 536-43.

Pearse, A. D., S. A. Gaskell, and R. Marks. 1987. 'Epidermal changes in human skin following irradiation with either UVB or UVA', *J Invest Dermatol*, 88: 83-7.

Pfeifer, G. P. 2020. 'Mechanisms of UV-induced mutations and skin cancer', *Genome Instab Dis*, 1: 99-113.

Pickering, C. R., J. H. Zhou, J. J. Lee, J. A. Drummond, S. A. Peng, R. E. Saade, K. Y. Tsai, J. L. Curry, M. T. Tetzlaff, S. Y. Lai, J. Yu, D. M. Muzny, H. Doddapaneni, E. Shinbrot, K. R. Covington, J. Zhang, S. Seth, C. Caulin, G. L. Clayman, A. K. El-Naggar, R. A. Gibbs, R. S. Weber, J. N. Myers, D. A. Wheeler, and M. J. Frederick. 2014. 'Mutational landscape of aggressive cutaneous squamous cell carcinoma', *Clin Cancer Res*, 20: 6582-92.

Pittayapruek, P., J. Meephansan, O. Prapapan, M. Komine, and M. Ohtsuki. 2016. 'Role of Matrix Metalloproteinases in Photoaging and Photocarcinogenesis', *Int J Mol Sci*, 17.

Plitta-Michalak, B., Stricker, N., Pavez Lorie, E., Chen, I., Pollet, M., Krutmann, J., Volkmer, B., Greinert, R., Boukamp, P., Rapp, A. 2022. 'Development and characterisation of an irradiation device for biomedical studies covering the solar spectrum with individual regulated spectral bands'.

Pouillot, A., N. Dayan, A. S. Polla, L. L. Polla, and B. S. Polla. 2008. 'The stratum corneum: a double paradox', *J Cosmet Dermatol*, 7: 143-8.

Pouyani, T., V. Ronfard, P. G. Scott, C. M. Dodd, A. Ahmed, R. L. Gallo, and N. L. Parenteau. 2009. 'De novo synthesis of human dermis in vitro in the absence of a three-dimensional scaffold', *In Vitro Cell Dev Biol Anim*, 45: 430-41.

Qin, Z., R. M. Balimunkwe, and T. Quan. 2017. 'Age-related reduction of dermal fibroblast size upregulates multiple matrix metalloproteinases as observed in aged human skin in vivo', *Br J Dermatol*, 177: 1337-48.

Quan, T., and G. J. Fisher. 2015. 'Role of Age-Associated Alterations of the Dermal Extracellular Matrix Microenvironment in Human Skin Aging: A Mini-Review', *Gerontology*, 61: 427-34.

Quan, T., T. He, S. Kang, J. J. Voorhees, and G. J. Fisher. 2004. 'Solar ultraviolet irradiation reduces collagen in photoaged human skin by blocking transforming growth factor-beta type II receptor/Smad signaling', *Am J Pathol*, 165: 741-51.

Quan, T., T. He, Y. Shao, L. Lin, S. Kang, J. J. Voorhees, and G. J. Fisher. 2006. 'Elevated cysteine-rich 61 mediates aberrant collagen homeostasis in chronologically aged and photoaged human skin', *Am J Pathol*, 169: 482-90.

Quan, T., E. Little, H. Quan, Z. Qin, J. J. Voorhees, and G. J. Fisher. 2013. 'Elevated matrix metalloproteinases and collagen fragmentation in photodamaged human skin: impact of altered extracellular matrix microenvironment on dermal fibroblast function', *J Invest Dermatol*, 133: 1362-6.

Quan, T., Z. Qin, W. Xia, Y. Shao, J. J. Voorhees, and G. J. Fisher. 2009. 'Matrix-degrading metalloproteinases in photoaging', *J Investig Dermatol Symp Proc*, 14: 20-4.

Quan, T., Z. Qin, Y. Xu, T. He, S. Kang, J. J. Voorhees, and G. J. Fisher. 2010. 'Ultraviolet irradiation induces CYR61/CCN1, a mediator of collagen homeostasis, through activation of transcription factor AP-1 in human skin fibroblasts', *J Invest Dermatol*, 130: 1697-706.

Quintero-Fabian, S., R. Arreola, E. Becerril-Villanueva, J. C. Torres-Romero, V. Arana-Argaez, J. Lara-Riegos, M. A. Ramirez-Camacho, and M. E. Alvarez-Sanchez. 2019. 'Role of Matrix Metalloproteinases in Angiogenesis and Cancer', *Front Oncol*, 9: 1370.

Ramos, M. C., H. Steinbrenner, D. Stuhlmann, H. Sies, and P. Brenneisen. 2004. 'Induction of MMP-10 and MMP-1 in a squamous cell carcinoma cell line by ultraviolet radiation', *Biol Chem*, 385: 75-86.

Regnier, M., C. Desbas, C. Bailly, and M. Darmon. 1988. 'Differentiation of normal and tumoral human keratinocytes cultured on dermis: reconstruction of either normal or tumoral architecture', *In Vitro Cell Dev Biol*, 24: 625-32.

Ressler, S., J. Bartkova, H. Niederegger, J. Bartek, K. Scharffetter-Kochanek, P. Jansen-Durr, and M. Wlaschek. 2006. 'p16INK4A is a robust in vivo biomarker of cellular aging in human skin', *Aging Cell*, 5: 379-89.

Ricard-Blum, S. 2011. 'The collagen family', *Cold Spring Harb Perspect Biol*, 3: a004978.

Rinnerthaler, M., J. Duschl, P. Steinbacher, M. Salzmann, J. Bischof, M. Schuller, H. Wimmer, T. Peer, J. W. Bauer, and K. Richter. 2013. 'Age-related changes in the composition of the cornified envelope in human skin', *Exp Dermatol*, 22: 329-35.

Rodust, P. M., E. Stockfleth, C. Ulrich, M. Leverkus, and J. Eberle. 2009. 'UV-induced squamous cell carcinoma--a role for antiapoptotic signalling pathways', *Br J Dermatol*, 161 Suppl 3: 107-15.

Roger, M., N. Fullard, L. Costello, S. Bradbury, E. Markiewicz, S. O'Reilly, N. Darling, P. Ritchie, A. Maatta, I. Karakesisoglou, G. Nelson, T. von Zglinicki, T. Dicolandrea, R. Isfort, C. Bascom, and S. Przyborski. 2019. 'Bioengineering the microanatomy of human skin', *J Anat*, 234: 438-55.

Rogers, J., C. Harding, A. Mayo, J. Banks, and A. Rawlings. 1996. 'Stratum corneum lipids: the effect of ageing and the seasons', *Arch Dermatol Res*, 288: 765-70.

Roig-Rosello, E., and P. Rousselle. 2020. 'The Human Epidermal Basement Membrane: A Shaped and Cell Instructive Platform That Aging Slowly Alters', *Biomolecules*, 10.

Rosso, S., R. Zanetti, C. Martinez, M. J. Tormo, S. Schraub, H. Sancho-Garnier, S. Franceschi, L. Gafa, E. Perea, C. Navarro, R. Laurent, C. Schrameck, R. Talamini, R. Tumino, and J. Wechsler. 1996. 'The multicentre south European study 'Helios'. II: Different sun exposure patterns in the aetiology of basal cell and squamous cell carcinomas of the skin', *Br J Cancer*, 73: 1447-54.

Rube, C. E., C. Baumert, N. Schuler, A. Isermann, Z. Schmal, M. Glanemann, C. Mann, and H. Scherthan. 2021. 'Human skin aging is associated with increased expression of the histone variant H2A.J in the epidermis', *NPJ Aging Mech Dis*, 7: 7.

Ruiz, M., M. Maumus, G. Fonteneau, Y. M. Pers, R. Ferreira, L. Dagneaux, C. Delfour, X. Houard, F. Berenbaum, F. Rannou, C. Jorgensen, and D. Noel. 2019. 'TGFbetai is involved in the chondrogenic differentiation of mesenchymal stem cells and is dysregulated in osteoarthritis', *Osteoarthritis Cartilage*, 27: 493-503.

Sahle, F. F., T. Gebre-Mariam, B. Dobner, J. Wohlrab, and R. H. Neubert. 2015. 'Skin diseases associated with the depletion of stratum corneum lipids and stratum corneum lipid substitution therapy', *Skin Pharmacol Physiol*, 28: 42-55.

Schardt, Lisa. 2017. 'The impact of Cyclosporine A on human epidermal keratinocytes', Dissertation, Ruprecht-Karls-Universität Heidelberg.

Schieke, S. M., K. Ruwiedel, H. Gers-Barlag, S. Grether-Beck, and J. Krutmann. 2005. 'Molecular crosstalk of the ultraviolet a and ultraviolet B signaling responses at the level of mitogen-activated protein kinases', *J Invest Dermatol*, 124: 857-9.

Schieke, S., H. Stege, V. Kurten, S. Grether-Beck, H. Sies, and J. Krutmann. 2002. 'Infrared-A radiation-induced matrix metalloproteinase 1 expression is mediated through extracellular signal-regulated kinase 1/2 activation in human dermal fibroblasts', *J Invest Dermatol*, 119: 1323-9.

Schultz-Cherry, S., S. Ribeiro, L. Gentry, and J. E. Murphy-Ullrich. 1994. 'Thrombospondin binds and activates the small and large forms of latent transforming growth factor-beta in a chemically defined system', *J Biol Chem*, 269: 26775-82.

Scott, T. L., P. A. Christian, M. V. Kesler, K. M. Donohue, B. Shelton, K. Wakamatsu, S. Ito, and J. D'Orazio. 2012. 'Pigment-independent cAMP-mediated epidermal thickening protects against cutaneous UV injury by keratinocyte proliferation', *Exp Dermatol*, 21: 771-7.

Segre, J. A. 2006. 'Epidermal barrier formation and recovery in skin disorders', *J Clin Invest*, 116: 1150-8.

Serini, G., M. L. Bochaton-Piallat, P. Ropraz, A. Geinoz, L. Borsi, L. Zardi, and G. Gabbiani. 1998. 'The fibronectin domain ED-A is crucial for myofibroblastic phenotype induction by transforming growth factor-beta1', *J Cell Biol*, 142: 873-81.

Seyfarth, F., S. Schliemann, D. Antonov, and P. Elsner. 2011. 'Dry skin, barrier function, and irritant contact dermatitis in the elderly', *Clin Dermatol*, 29: 31-6.

Shin, J. W., S. H. Kwon, J. Y. Choi, J. I. Na, C. H. Huh, H. R. Choi, and K. C. Park. 2019. 'Molecular Mechanisms of Dermal Aging and Antiaging Approaches', *Int J Mol Sci*, 20.

Simpson, C. L., D. M. Patel, and K. J. Green. 2011. 'Deconstructing the skin: cytoarchitectural determinants of epidermal morphogenesis', *Nat Rev Mol Cell Biol*, 12: 565-80.

Simpson, R. M., S. Meran, D. Thomas, P. Stephens, T. Bowen, R. Steadman, and A. Phillips. 2009. 'Age-related changes in pericellular hyaluronan organization leads to impaired dermal fibroblast to myofibroblast differentiation', *Am J Pathol*, 175: 1915-28.

Smith, L. 1989. 'Histopathologic characteristics and ultrastructure of aging skin', *Cutis*, 43: 414-24.

Stark, H. J., M. J. Willhauck, N. Mirancea, K. Boehnke, I. Nord, D. Breitkreutz, A. Pavesio, P. Boukamp, and N. E. Fusenig. 2004. 'Authentic fibroblast matrix in dermal equivalents normalises epidermal histogenesis and dermoepidermal junction in organotypic co-culture', *Eur J Cell Biol*, 83: 631-45.

Sung, H., J. Ferlay, R. L. Siegel, M. Laversanne, I. Soerjomataram, A. Jemal, and F. Bray. 2021. 'Global Cancer Statistics 2020: GLOBOCAN Estimates of Incidence and Mortality Worldwide for 36 Cancers in 185 Countries', *CA Cancer J Clin*, 71: 209-49.

Svobodova, A., and J. Vostalova. 2010. 'Solar radiation induced skin damage: review of protective and preventive options', *Int J Radiat Biol*, 86: 999-1030.

Tada, H., M. Hatoko, A. Tanaka, M. Kuwahara, and T. Muramatsu. 2000. 'Expression of desmoglein I and plakoglobin in skin carcinomas', *J Cutan Pathol*, 27: 24-9.

Takahashi, M., and T. Tezuka. 2004. 'The content of free amino acids in the stratum corneum is increased in senile xerosis', *Arch Dermatol Res*, 295: 448-52.
Takema, Y., Y. Yorimoto, M. Kawai, and G. Imokawa. 1994. 'Age-related changes in the elastic properties and thickness of human facial skin', *Br J Dermatol*, 131: 641-8.
ten Dijke, P., and H. M. Arthur. 2007. 'Extracellular control of TGFbeta signalling in vascular development and disease', *Nat Rev Mol Cell Biol*, 8: 857-69.
Tesfaigzi, J., and D. M. Carlson. 1999. 'Expression, regulation, and function of the SPR family of proteins. A review', *Cell Biochem Biophys*, 30: 243-65.
Thakoersing, V. S., G. S. Gooris, A. Mulder, M. Rietveld, A. El Ghalbzouri, and J. A. Bouwstra. 2012. 'Unraveling barrier properties of three different in-house human skin equivalents', *Tissue Eng Part C Methods*, 18: 1-11.
Tham, M., H. J. Stark, A. Jauch, C. Harwood, E. Pavez Lorie, and P. Boukamp. 2022. 'Adverse Effects of Vemurafenib on Skin Integrity: Hyperkeratosis and Skin Cancer Initiation Due to Altered MEK/ERK-Signaling and MMP Activity', *Front Oncol*, 12: 827985.
Thulabandu, V., D. Chen, and R. P. Atit. 2018. 'Dermal fibroblast in cutaneous development and healing', *Wiley Interdiscip Rev Dev Biol*, 7.
Thune, P., T. Nilsen, I. K. Hanstad, T. Gustavsen, and H. Lovig Dahl. 1988. 'The water barrier function of the skin in relation to the water content of stratum corneum, pH and skin lipids. The effect of alkaline soap and syndet on dry skin in elderly, non-atopic patients', *Acta Derm Venereol*, 68: 277-83.
Tigges, J., J. Krutmann, E. Fritsche, J. Haendeler, H. Schaal, J. W. Fischer, F. Kalfalah, H. Reinke, G. Reifenberger, K. Stuhler, N. Ventura, S. Gundermann, P. Boukamp, and F. Boege. 2014. 'The hallmarks of fibroblast ageing', *Mech Ageing Dev*, 138: 26-44.
Tomasek, J. J., G. Gabbiani, B. Hinz, C. Chaponnier, and R. A. Brown. 2002. 'Myofibroblasts and mechano-regulation of connective tissue remodelling', *Nat Rev Mol Cell Biol*, 3: 349-63.
Toutfaire, M., E. Bauwens, and F. Debacq-Chainiaux. 2017. 'The impact of cellular senescence in skin ageing: A notion of mosaic and therapeutic strategies', *Biochem Pharmacol*, 142: 1-12.
Tschumperlin, D. J. 2013. 'Fibroblasts and the ground they walk on', *Physiology (Bethesda)*, 28: 380-90.
Tyrrell, R. M., and V. E. Reeve. 2006. 'Potential protection of skin by acute UVA irradiation--from cellular to animal models', *Prog Biophys Mol Biol*, 92: 86-91.
Tzellos, T. G., I. Klagas, K. Vahtsevanos, S. Triaridis, A. Printza, A. Kyrgidis, G. Karakiulakis, C. C. Zouboulis, and E. Papakonstantinou. 2009. 'Extrinsic ageing in the human skin is associated with alterations in the expression of hyaluronic acid and its metabolizing enzymes', *Exp Dermatol*, 18: 1028-35.
Uitto, J. 1986. 'Connective tissue biochemistry of the aging dermis. Age-related alterations in collagen and elastin', *Dermatol Clin*, 4: 433-46.
Urmacher, C. 1990. 'Histology of normal skin', *Am J Surg Pathol*, 14: 671-86.
Varani, J., M. K. Dame, L. Rittie, S. E. Fligiel, S. Kang, G. J. Fisher, and J. J. Voorhees. 2006. 'Decreased collagen production in chronologically aged skin: roles of age-dependent alteration in fibroblast function and defective mechanical stimulation', *Am J Pathol*, 168: 1861-8.
Velarde, M. C., and M. Demaria. 2016. 'Targeting Senescent Cells: Possible Implications for Delaying Skin Aging: A Mini-Review', *Gerontology*, 62: 513-8.
Verrecchia, F., M. L. Chu, and A. Mauviel. 2001. 'Identification of novel TGF-beta /Smad gene targets in dermal fibroblasts using a combined cDNA microarray/promoter transactivation approach', *J Biol Chem*, 276: 17058-62.
Visse, R., and H. Nagase. 2003. 'Matrix metalloproteinases and tissue inhibitors of metalloproteinases: structure, function, and biochemistry', *Circ Res*, 92: 827-39.
Wang, F., A. Zieman, and P. A. Coulombe. 2016. 'Skin Keratins', *Methods Enzymol*, 568: 303-50.

Wang, P. W., Y. C. Hung, T. Y. Lin, J. Y. Fang, P. M. Yang, M. H. Chen, and T. L. Pan. 2019. 'Comparison of the Biological Impact of UVA and UVB upon the Skin with Functional Proteomics and Immunohistochemistry', *Antioxidants (Basel)*, 8.

Watt, F. M. 2002. 'The stem cell compartment in human interfollicular epidermis', *J Dermatol Sci*, 28: 173-80.

Webber, J., R. H. Jenkins, S. Meran, A. Phillips, and R. Steadman. 2009. 'Modulation of TGFbeta1-dependent myofibroblast differentiation by hyaluronan', *Am J Pathol*, 175: 148-60.

Weinmullner, R., B. Zbiral, A. Becirovic, E. M. Stelzer, F. Nagelreiter, M. Schosserer, I. Lammermann, L. Liendl, M. Lang, L. Terlecki-Zaniewicz, O. Andriotis, M. Mildner, B. Golabi, P. Waidhofer-Sollner, K. Schedle, G. Emsenhuber, P. J. Thurner, E. Tschachler, F. Gruber, and J. Grillari. 2020. 'Organotypic human skin culture models constructed with senescent fibroblasts show hallmarks of skin aging', *NPJ Aging Mech Dis*, 6: 4.

Wertz, P. W., D. C. Swartzendruber, K. C. Madison, and D. T. Downing. 1987. 'Composition and morphology of epidermal cyst lipids', *J Invest Dermatol*, 89: 419-25.

Wijelath, E. S., S. Rahman, M. Namekata, J. Murray, T. Nishimura, Z. Mostafavi-Pour, Y. Patel, Y. Suda, M. J. Humphries, and M. Sobel. 2006. 'Heparin-II domain of fibronectin is a vascular endothelial growth factor-binding domain: enhancement of VEGF biological activity by a singular growth factor/matrix protein synergism', *Circ Res*, 99: 853-60.

Winkler, J., A. Abisoye-Ogunniyan, K. J. Metcalf, and Z. Werb. 2020. 'Concepts of extracellular matrix remodelling in tumour progression and metastasis', *Nat Commun*, 11: 5120.

Wolf, K., S. Alexander, V. Schacht, L. M. Coussens, U. H. von Andrian, J. van Rheenen, E. Deryugina, and P. Friedl. 2009. 'Collagen-based cell migration models in vitro and in vivo', *Semin Cell Dev Biol*, 20: 931-41.

Wulf, H. C., and N. Bech-Thomsen. 1998. 'A UVB phototherapy protocol with very low dose increments as a treatment of atopic dermatitis', *Photodermatol Photoimmunol Photomed*, 14: 1-6.

Yaar, M., and B. A. Gilchrest. 2001. 'Skin aging: postulated mechanisms and consequent changes in structure and function', *Clin Geriatr Med*, 17: 617-30, v.

Yin, S., L. Cen, C. Wang, G. Zhao, J. Sun, W. Liu, Y. Cao, and L. Cui. 2010. 'Chondrogenic transdifferentiation of human dermal fibroblasts stimulated with cartilage-derived morphogenetic protein 1', *Tissue Eng Part A*, 16: 1633-43.

Young, A. R. 1987. 'The sunburn cell', *Photodermatol*, 4: 127-34.

Young, M. D., M. J. Wakefield, G. K. Smyth, and A. Oshlack. 2010. 'Gene ontology analysis for RNA-seq: accounting for selection bias', *Genome Biol*, 11: R14.

Zilberberg, L., V. Todorovic, B. Dabovic, M. Horiguchi, T. Courousse, L. Y. Sakai, and D. B. Rifkin. 2012. 'Specificity of latent TGF-beta binding protein (LTBP) incorporation into matrix: role of fibrillins and fibronectin', *J Cell Physiol*, 227: 3828-36.

List of Figures

List of Tables

List of Abbreviations

2D	Two dimensional
3D	Three dimensional
ANOVA	Analysis of variance
BCC	Basal cell carcinoma
BM	Basement membrane
Col	Collagen
cSCC	Cutaneous squamous cell carcinoma
CPD	Cyclopbutane pyrimidine dimer
ddH_2O	Double distilled water
DEJ	Dermal-epidermal junction
DMEM	Dulbecco's Modified Eagle's Medium
ECM	Extracellular matrix
EMT	Epithelial-mesenchymal-transition
EtOH	Ethanol
FBS	Fetal bovine serum
FDM	Fibroblast-derived matrix
HaCaT	human adult low calcium high temperature
H&E	hematoxylin and eosin
IRA	Near infrared
MeOH	Methanol
MMP	Matrix metalloproteinase
NHDF	Normal human dermal fibroblast
NMSC	Non-melanoma skin cancer
OTC	Organotypic culture
PBS	phosphate buffered saline
qRT-PCR	Quantitative reverse transcription polymerase chain reaction
ROS	Reactive oxygen species
SC	Stratum corneum
SE	Skin equivalent
SUN	Simulated solar radiation
TIMP	Tissue inhibitor of metalloproteinases
UVA	Ultraviolet A
UVB	Ultraviolet B
VIS	Visible light

Appendix

Table 17: ImageJ macro to calculate the epidermal proliferation rate

```
//prepare
setTool("freehand");
setSlice(3);
roiManager("Deselect");
run("Select None");
roiManager("Reset");
title=getTitle();
//select Epidermis
run("Duplicate...", " ");
run("Grays");
run("Gaussian Blur...", "sigma=10");
run("Threshold...");
setAutoThreshold("Default dark");
waitForUser("Adjust the threshold for epidermis.");
run("Analyze Particles...", "size=10000-Infinity pixel include add");
close();
roiManager("Show All");
waitForUser("Check the selection for epidermis. If it is not good select it again and add to ROImanager");
setSlice(3);
roiManager("Deselect");
run("Select None");
//analyze DAPI
setSlice(2);
run("Duplicate...", " ");
run("Grays");
run("Gaussian Blur...", "sigma=4");//change sigma to get more or less cells (smaller sigma - more cells)
run("Threshold...");
setAutoThreshold("Default dark");
waitForUser("Adjust the Threshold for DAPI");
run("Find Maxima...", "noise=2 output=[Segmented Particles] above");//change noise to get more or less cells (smaller noise - more cells)
roiManager("Select", 0);
setAutoThreshold("Default dark");
rename(title+ " DAPI count");
run("Analyze Particles...", "size=20-Infinity pixel exclude summarize add");
close();
close();
selectWindow(title);
run("Duplicate...", " ");
run("Grays");
roiManager("Show All");
waitForUser("Check the selection of DAPI");
close();
//combine dapi to count Ki67 only within DAPI which is within Epi
```

```
roiManager("Select", 0);
roiManager("Delete");
print("please wait");
roiManager("Combine");
roiManager("Reset");
roiManager("Add");
roiManager("Deselect");
run("Select None");
//analyze Ki67
setSlice(1);
run("Duplicate...", " ");
run("Subtract Background...", "rolling=50 slice");
run("Grays");
run("Median...", "radius=2");
run("Threshold...");
setAutoThreshold("Default dark");
getThreshold(min, max);
setThreshold(773, max);
titleTemp=getTitle();
waitForUser("Adjust the Threshold for Ki67 ");
selectWindow(titleTemp);
roiManager("Select", 0);
setBackgroundColor(0, 0, 0);
run("Clear Outside");
rename(title+ " Ki67 count");
run("Analyze Particles...", "size=20-Infinity pixel summarize add");//change min size to get more
or less cells
close();
//display
run("Grays");
roiManager("Show All");
roiManager("Select", 0);
```

Table 18: Differentially expressed genes that show the same response to irradiation in young and old fibroblasts

Gene Name	L2FC young SUN	L2FC young UVAB	L2FC old SUN	L2FC old UVAB	padj young SUN	padj young UVAB	padj old SUN	padj old UVAB
UP with UVA+B and SUN								
CES1	2,20	2,02	2,39	1,73	1,70E-17	3,13E-09	3,07E-05	5,98E-08
IL1RL1	3,14	3,47	2,63	2,92	5,91E-15	9,04E-10	9,35E-06	2,81E-26
GALNT15	3,15	3,32	2,43	1,96	1,52E-12	1,75E-09	3,73E-05	6,56E-09
APLN	0,99	1,07	2,05	1,23	6,92E-05	4,47E-05	2,22E-03	7,07E-04
VWCE	0,92	0,99	1,70	1,57	2,42E-03	2,53E-02	3,89E-02	8,89E-08
UP with only UVA+B								
BCL2L1	0,00	1,49	0,00	1,29	1	9,21E-07	1	1,59E-04
CDKN1A	0,00	0,66	0,00	1,00	1	1,10E-03	1	1,96E-06
LEP	0,00	2,21	0,00	0,86	1	1,20E-02	1	1,21E-02
TRABD2B	0,00	1,09	0,00	1,09	1	1,30E-02	1	3,11E-04
EIF4B	0,00	1,74	0,00	2,17	1	2,04E-02	1	4,73E-11
GDNF	0,00	1,40	0,00	1,00	1	2,34E-02	1	1,52E-02
PGAM1	0,00	0,53	0,00	0,43	1	2,34E-02	1	1,81E-02
ZNF219	0,00	0,68	0,00	0,52	1	2,53E-02	1	1,29E-02
TRNP1	0,00	0,61	0,00	0,65	1	4,02E-02	1	4,33E-02
NRXN2	0,00	1,54	0,00	1,47	1	4,42E-02	1	2,17E-04
UP with only SUN								
CTSS	8,97	0,00	9,34	0,00	1,22E-05	1	3,80E-03	1
DOWN with UVA+B and SUN								
GADD45B	-1,35	-0,55	-1,40	-0,76	5,24E-13	2,99E-02	5,21E-03	2,09E-05
MT-CYB	-1,47	-1,28	-1,69	-1,54	3,13E-09	4,08E-06	8,74E-07	6,99E-11
CDH13	-3,06	-2,99	-3,10	-2,44	1,51E-06	5,74E-04	6,53E-07	1,17E-18
MMP11	-1,31	-1,42	-2,59	-2,22	1,59E-04	2,15E-03	5,38E-09	2,39E-29
MT-ND4	-0,92	-0,73	-1,31	-1,04	5,38E-04	3,75E-02	6,30E-04	7,98E-05
CPZ	-1,33	-1,19	-2,21	-2,03	7,86E-03	3,47E-02	3,81E-02	1,23E-09
BHLHE40	-0,95	-0,74	-1,94	-1,17	9,85E-03	3,03E-02	2,34E-08	4,65E-08
MT-ND3	-0,91	-0,78	-1,18	-1,02	1,67E-02	4,71E-02	4,84E-03	1,07E-05
DOWN with only UVA+B								
RNF19B	0,00	-8,25	0,00	-1,20	1	1,48E-04	1	7,71E-04
THBD	0,00	-1,68	0,00	-1,48	1	2,43E-04	1	2,21E-02
MAFB	0,00	-0,75	0,00	-1,18	1	3,07E-03	1	5,33E-06
FHIT	0,00	-3,47	0,00	-1,88	1	1,69E-02	1	4,66E-02
TJP1	0,00	-0,97	0,00	-0,42	1	2,77E-02	1	2,73E-02
PLEKHG3	0,00	-2,56	0,00	-1,30	1	4,53E-02	1	9,06E-03
DOWN with only SUN								
IL6	-2,11	0,00	-1,81	0,00	7,67E-20	1	3,59E-02	1
ATF3	-2,52	0,00	-3,06	0,00	7,34E-16	1	5,40E-12	1
ZFP36	-1,55	0,00	-1,59	0,00	1,28E-14	1	3,23E-04	1
NR4A2	-2,47	0,00	-2,60	0,00	1,08E-12	1	7,21E-06	1
FOS	-1,24	0,00	-1,16	0,00	1,51E-06	1	1,25E-02	1
IER2	-0,93	0,00	-1,11	0,00	4,79E-06	1	2,77E-02	1
FOSB	-1,83	0,00	-2,76	0,00	6,33E-06	1	1,91E-10	1
KLF4	-1,29	0,00	-1,37	0,00	1,83E-02	1	4,06E-02	1

L2FC = log2 fold change
Padj = adjusted p-value

Eidesstattliche Erklärung

Ich versichere an Eides Statt, dass die Dissertation von mir selbständig und ohne unzulässige fremde Hilfe unter Beachtung der „Grundsätze zur Sicherung guter wissenschaftlicher Praxis an der Heinrich-Heine-Universität Düsseldorf“ erstellt worden ist.

Düsseldorf,

…….

Katharina Janke